Mechanisms of Resistance to EGFR Inhibition in HNSCC

by

Megan Ludwig

A dissertation submitted in partial fulfillment
of the requirements for the degree of
Doctor of Philosophy
(Cellular and Molecular Biology)
in the University of Michigan
2019

Doctoral Committee:

Assistant Professor Chad Brenner, Chair
Professor Thomas E Carey
Associate Professor Hui Jiang
Associate Professor Mukesh Nyati
Associate Professor Andrew Tai

Megan Ludwig

ludwigml@umich.edu

ORCID iD: 0000-0003-3133-3679

Acknowledgements

As I've learned during my course of study, it takes a team to train a graduate student. To my mentors, to my lab mates, to my friends, to my family – thank you all for your generous and unending support. I would not be the scientist or the person I am today without you.

First, to Chad. Thank you for letting me join your team. Thank you for your insight, your patience, your continual optimism, and your calm in the midst of chaos. It's been a special privilege to be your first graduate student.

I would also like to thank my committee members, Drs. Thomas Carey, Hui Jiang, Mukesh Nyati, and Andrew Tai. Dr. Carey, thank you for your encouragement, your support, and your insightful questions over the course of my training. Thank you to Dr. Jiang for your strategies and feedback on tackling data analytics, and thank you to Dr. Nyati and Dr. Tai for your thoughtful questions that moved my project forward. I walked out of committee meetings inspired with new approaches and new questions to tackle, and I greatly appreciate all of your support and guidance during my training.

Thank you to the CMB graduate program, whose diversity in research topics and event participation made for an enjoyable program. Thank you to Dr. Robert Fuller and Dr. Kathy Collins as well as the CMB support staff (Cathy Mitchell, Margarita Bekiares, Jim Musgrave, Jessica Kijek, Pat Ocelnik, and Lauren Perl) for helping me navigate the stages of graduate school.

Also, a big collective thank you to the members of the Brenner and Carey labs, past and present. Working alongside you at the bench has made science a joy. Brittany and Sue, thank you for everything you do to keep the lab running smoothly. Aditi and Apurva, thank you for being fantastic bay-mates. Nicole, Jackie, and Elizabeth, thank you for the scientific and non-scientific discussions as we collectively dealt with graduate school. Thank you to Dr. Andrew Birkeland for your clinical insights and research. Thank you to Collin and Jingyi for your insight and support during lab meetings. Thank you to the many undergraduate students who trained me as I trained them. Sai Nimmagadda, Dylan Genouw, Lindsay Remer, Juliet Gunther, Michelle Nyugen, Zechariah Diaz-Grace, Xavier Garcia, Rasika Patel, and Lydia Weykamp, thank you for all the science that you've accomplished, and I wish you the best of luck in your bright futures. I would also like to thank Dr. Heather Walline for jump-starting this project during your time at the Brenner lab and for your continued support beyond, and Dr. Todd Festerling whose continual insight and training helped develop me into the scientist I am today.

I would also like to thank my previous scientific mentors during my undergraduate training. Drs. Maria Burnatowska-Hledin and Joseph Stukey at Hope College, thank you for your teachings and trainings in both the lecture halls and labs during my time at Hope. To Dr. Eric Hendrickson at the University of Minnesota, thank you for the opportunity to learn and train in your lab, and thank you to Eu Han for training me from the beginning. I am grateful for your time and investment into my training.

Thank you to my friends for your support throughout graduate school. The happy hours and the coffee breaks and the Marvel movie nights kept me sane when the pressures were high.

Finally, last but certainly not least, thank you to my family. It's only with your encouragement and support that I have made it to where I am today.

Table of Contents

List of Tables

List of Figures

Abstract

Head and neck squamous cell carcinoma (HNSCC) remains a deadly disease with poor prognosis. Developing novel, effective combination therapies have the potential to improve patient survival. However, advancing biomarkers in conjunction with combination therapy will also be essential for efficacy so as to match treatment to the patient. In my thesis, I investigated the hypothesis that co-targeting a specific mechanism of resistance with combination therapy would be more effective than either therapy alone. I focused on identifying resistance mechanisms to cisplatin and EGFR inhibition, which are common HNSCC treatments, in UM-SCC cell lines using CRISPR/Cas9 screening libraries. This approach identified genetic knockouts that sensitized cell lines to either cisplatin or EGFR inhibition.

The results of a CRISPR/Cas9 screen nominated NOTCH pathway knockouts and specifically *NOTCH1* knockouts as capable of sensitizing cisplatin-resistance cells. Further results suggest that the combination of Notch inhibitors and cisplatin therapy are capable of overcoming cisplatin resistance, and that inactivating mutations in *NOTCH1* may be a biomarker of cisplatin sensitivity. I also used genome and kinome CRISPR libraries to identify genetic knockouts that sensitized resistant models to the EGFR inhibitors gefitinib and erlotinib. I observed that *PIK3C2A* may be an important linchpin in the PI3K pathway for mediating resistance, as well as identified an unexpected set of genes associated with KRAS signaling, nominating KRAS as a potential mediator of resistance to EGFR inhibition in HNSCC. Furthermore, my CRISPR/Cas9 screens also nominated FGF/FGFR knockouts as sensitizing cells to EGFR inhibition.

Extending these discoveries, I investigated the potential of dual EGFR and FGFR inhibition by testing multiple UM-SCC cell lines. I observed that FGFR may be a more common compensatory mechanism that previously realized, with 14/22 (63%) of cell lines undergoing cell death when challenged with combination therapy. Surprisingly, neither copy number or expression of FGFRs predicted responsiveness to the combination of EGFR and FGFR inhibition. To explore the mechanism behind this response, I generated an EGFR K/O model and showed that FGFR signaling increases when EGFR protein is lost. Evaluation of the discovery *in vivo* demonstrated that dual inhibition of EGFR and FGFR was able to significantly decrease tumor volume in a xenograft mouse model, supporting the *in vivo* relevance of this combination for HNSCC. Consistent with the literature, dual EGFR and FGFR inhibition caused weight loss in animals suggesting a high level of toxicity; thus, this data suggests that new ways to target the pathway are critical to future clinical success. Finally, to evaluate potential clinical relevance, we analyzed transcriptome profiles of tumors from patients who received the EGFR inhibitor cetuximab. We observed changes in the FGFR receptors, KRAS signaling, and PI3K-mTOR signaling, consistent with our profiling data.

Overall, my thesis work supports the hypothesis that there are specific and common compensatory pathways to EGFR inhibition and cisplatin, and that co-targeting EGFR or cisplatin with this compensatory pathway is more effective than monotherapy treatments. The CRISPR/Cas9 screens and transcriptome analysis have generated a wealth of data that can continue to be explored to develop novel, effective strategies for combination therapy. Collectively, this body of work represents a step forward in the understanding of how HNSCC tumors compensate in response to two prevalent therapies, and may provide the foundation for opportunities to advance combination therapies and improve survival of HNSCC patients.

Chapter 1 : Exploring the Potential for Targeted Therapies in LSCC and the Generation of CRISPR/Cas9 Screening Libraries

Chapter Summary

In this chapter, I review the potential for implementing targeted therapy approaches in laryngeal squamous cell carcinoma, using the laryngeal subsite as a model for head and neck squamous cell carcinoma. I discuss opportunities as well as obstacles for implementing targeted therapies in this cancer. Then, I discuss the utility and generation of CRISPR/Cas9 screening libraries, with the goal of using CRISPR/Cas9 screens to identify further opportunities for targeted therapy approaches that will be discussed in later chapters.

1.1 Changing the paradigm: the potential for targeted therapy in laryngeal squamous cell carcinoma[1]

Abstract

Laryngeal squamous cell carcinoma (LSCC) remains a highly morbid and fatal disease. Historically, it has been a model example for organ preservation and treatment stratification paradigms. Unfortunately, survival for LSCC has stagnated over the past few decades. As the era of next generation sequencing and personalized treatment for cancer approaches, LSCC may be an ideal disease for consideration of further treatment stratification and personalization. Here,

[1] This section was published in *Cancer Biology & Medicine* in collaboration with the following authors: Andrew Birkeland, Rebecca Hoesli, Paul Swiecicki, Matthew Spector, and J. Chad Brenner

we will discuss the important history of LSCC as a model system for organ preservation, unique and potentially targetable genetic signatures of LSCC, and methods for bringing stratified, personalized treatment strategies to the 21st century.

Introduction

Laryngeal squamous cell carcinoma (LSCC) remains a prevalent disease, accounting for over 150,000 new cases annually across the world(1). Previous clinical trials in LSCC demonstrated the potential for non-surgical, organ-preservation treatment options for LSCC, with similar survival rates to surgery(2, 3). While these initial organ-preserving paradigms have gradually become the predominant treatment choice for LSCC(4), no new treatment options have surfaced in the ensuing decades. For recurrent LSCC after chemotherapy, radiation, or surgery, treatments are limited. This is particularly concerning given the continued poor survival in advanced or recurrent LSCC, where 5-year survival is less than 50%(5) and has not improved in decades(6).

Whole exome and genome sequencing studies have recently provided valuable insight into dysregulated pathways and potential drivers of disease in multiple cancers, including head and neck cancers(7-10). These early studies have identified novel genetic mutations and pathway dysregulations across a variety of head and neck cancers. Importantly, LSCCs have constituted a significant portion of the tumors in these studies.

Cancer treatment is entering an exciting new era, combining the information gained from next-generation sequencing studies with targeted therapeutics to allow for models of personalized cancer care. Indeed, cancer sequencing and targeted therapy trials are being launched globally, and with some encouraging initial results(11-13). LSCC may prove to be an

ideal model for further investigation into personalized targeted therapies given its successful history in response to nonsurgical techniques, previous paradigms for treatment stratification(14), and the need to improve survival in this important cohort.

Here, we will discuss the important history of LSCC as a model system for organ preservation, current knowledge of the genomic landscapes, targeted therapies for LSCC, and potential strategies for developing stratified, personalized treatment strategies for LSCC.

Historical Treatment of LSCC

For early stage LSCC, single modality therapy (surgery or radiation) achieves cure for a majority of patients. However, patients with locally advanced disease had historically required total laryngectomy followed by adjuvant radiation as the gold standard treatment. Unfortunately, many of these surgeries are accompanied by significant morbidity and many patients are left with significant swallowing difficulties, communication difficulties, and poor cosmetic outcomes(15). Thus, in the 1990s, investigations began into equally effective but less morbid therapies.

As a result, the Veterans Affairs (VA) Laryngeal Cancer Study(2) was performed. In this prospective randomized controlled study, 332 patients with advanced LSCC were stratified between induction chemotherapy (three cycles of cisplatin and 5-FU) followed by definitive radiation versus laryngectomy followed by postoperative radiation. Patients in the chemotherapy group were assessed after two cycles of chemotherapy; those that showed clinical response to therapy went on to receive one final cycle of chemotherapy followed by radiation. Those that had no response to therapy or disease progression after two cycles went on to immediate laryngectomy and then post-operative radiation. There was no difference in two-year survival

between the chemotherapy and surgery groups, and laryngeal function was preserved in 64% of the patients in the chemotherapy group. This study established that organ preservation in LSCC was a feasible goal of treatment, while still providing equivalent overall survival.

These findings were confirmed with data from a randomized study in Europe (EORTC trial 24891)(16), where patients with cancers of the hypopharynx underwent either induction chemotherapy consisting of cisplatin and 5-FU followed by irradiation, or surgical resection followed by post-operative radiotherapy. In this study, again overall survival was equivalent, and laryngeal preservation was achieved in greater than 50% of patients after 5 years. A third study (RTOG 91-11)(17) compared concurrent chemotherapy and radiation, induction chemotherapy followed by radiation, and standard radiation therapy. This study found that laryngeal preservation was significantly higher in patients receiving concurrent chemoradiation. It is important to note this study did exclude large volume T4 tumors with cartilage invasion or extension into the base of the tongue. Finally, investigators at the University of Michigan studied the utility of a single cycle of induction chemotherapy in LSCC as stratification for further treatment in a phase II clinical trial(14). Over 75% of patients had response to induction chemotherapy, and overall larynx preservation was achieved in 70% of patients. This study verified that paradigms of treatment stratification could be utilized in LSCC.

These trials together demonstrated the efficacy of combined chemotherapy and radiation therapy in treating locally advanced LSCC while maintaining the functional status of the larynx. Additionally, they showed that treatment with induction chemotherapy did not increase complications for surgical treatment or radiotherapy administered afterwards. Finally, although there was no benefit in overall survival, a significant reduction in the rate of distant metastasis

was shown in the chemotherapy group as compared with primary surgery or radiation therapy alone(2, 16-19).

Although there was significant improvement in organ preservation gained by treatment with induction chemotherapy, unfortunately overall outcomes in LSCC remain poor. In the European study, disease free survival at 5 years remained at 25% and 27% for the chemotherapy arm and immediate surgery arm respectively(16). Additionally, patients who responded poorly to chemotherapy were likely to respond poorly to radiation[20]. As such, research began into molecular markers to predict radiosensitivity and chemosensitivity in order to better personalize therapy and more accurately predict which patients would be eligible for laryngeal preservation.

Several studies have evaluated various molecular biomarkers in an attempt to better predict a response to therapy. Malecki looked at EGFR, p53, and Ki-67, which are biomolecular markers found to be altered in patients with HNSCC. In his retrospective trial, only patients without the presence of EGFR expression were noted to have a significantly improved response to induction chemotherapy(21). In LSCC specifically, it has been recently found that levels of BAK, a gene involved in apoptosis, is associated with response to induction chemotherapy. The same study identified cyclin D1 as a predictor of LSCC overall and disease-specific survival, and over expression of EGFR as associated with risk of death(22).

These biomarker studies have led to clinical trials to evaluate novel therapies with the potential to improve outcomes in LSCC. For examples, we previously showed that AT-101, which inhibits the anti-apoptotic genes Bcl-2 and Bcl-XL, effectively blocks proliferation in LSCC models(23) and have now initiated an on-going trial specifically targeted LSCC evaluating the use of AT-101, in combination with induction chemotherapy with platinum and

docetaxel (NCT01633541). Further combinations of traditional chemotherapy, radiation and targeted therapies may be applicable for LSCC. While traditional biomarker studies have been limited in identifying additional targetable options, recent whole-genome sequencing studies have shed more light into potential key pathways in LSCC.

Genetic Landscape of LSCCs

Along with the possibility of identifying additional biomarkers of LSCCs, genomic sequencing offers the potential to identify drivers of tumorigenesis and targets for new therapy. Initial exome sequencing studies have already produced valuable insights into the underlying genetic processes, nominating multiple pathways as potential targets for LSCC treatment.

Common Mutations and Copy Number Variations

Initial exome-sequencing studies by Agrawal(7) and Stransky et al(8) contained some LSCCs in their chosen HNSCC cohort (n=2 and n=15 respectively), but the smaller sample size did not give a broad view of genetic alterations in LSCC. The Cancer Genome Atlas (TCGA) has now whole-genome sequenced 29 HNSCC tumor-normal pairs (low coverage, 30x) and whole exome sequenced 279 HNSCC tumor-normal pairs (high coverage), of which 72 are primary LSCCs(9). These LSCC samples are predominantly Caucasian (n=57, 79.2%), male (n=58, 80.6%), and older (mean age = 61). Additionally, most patients had a smoking history (n=50, 69.4%) and were diagnosed at Stage III or IV (n=55, 76.4%)(9) , with very few epidemiologically low risk patients in the cohort(24). The initial studies by Agrawal and

Stransky had similar cohort characteristics. Publicly available databases compiling clinical, mutation, and copy number data were used for the analysis of this manuscript(25, 26).

Previously, evaluating the existence of distinct mutation profiles in LSCCs from other subsites has been limited from lack of power. The significant contribution of the HNSCC cohort from the TCGA has allowed the question to begin to be addressed. Many genes that are frequently mutated are common to all HNSCC subsites such as *TP53*, *CDKN2A*, *FAT1*, and *NOTCH1* (**Table 1-1**). *CASP8*, a gene whose product plays a central role in the cell carrying out apoptosis, is frequently mutated in other HNSCCs. However, *CASP8* has significantly less mutations in LSCCs compared to the other subsites ($p<0.005$). Studies have suggested that *CASP8* mutations indicate a distinct molecular profile of SCCs(27, 28), but this subset does not seem to exist in LSCCs. Additionally, mutations in *PIK3CA* trend towards occurring more frequently in LSCCs than other subsites ($p=0.058$), and copy number amplification of 3q26 which contains *PIK3CA* is found at significantly higher frequency in LSCCs compared to other HNSCCs ($p<0.001$, **Table 1-2**). Additionally, amplifications of 3q28 and 9q34 occur at significantly higher frequency in LSCCs ($p<0.001$, $p<0.007$).

While it is clear that many of the aberrations in HNSCC are common across subsites, differences are beginning to emerge as more LSCC samples are being sequenced. By sequencing more LSCCs, we will begin to understand if these differences are due to anatomical subsite or epidemiologic variation between tumors. Likewise, as genome-wide information continues to become available, no doubt distinct subsets of molecular mechanisms will be identified.

Human Papillomavirus (HPV) in LSCC

The link between HPV status and HNSCC has been well established at some anatomical subsites(29, 30); for example, HPV appears to be a common initiating event in oropharyngeal SCCs . The oncogenic potential of high-risk HPVs in LSCCs is not as clear. Studies with larger sample sizes (where n>80) over the past thirty years have shown HPV prevalence in LSCC tumors from as low as 1% to as high as 50%(31). However, studies have also found HPV DNA in up to 19% of normal laryngeal mucosa samples(32-35), indicating that a significant portion of HPV positive LSCCs that have been reported may be latent HPV infections, and more specific techniques should be used to truly determine HPV positivity. In contrast to many of the PCR-based studies, the HNSCC TCGA project relied on multiple methods of detection including RNA-sequencing and identified only one HPV positive LSCC case (1.4%)(9). The low prevalence of HPV in this study indicates that HPV rates may have been historically overestimated in some LSCCs cohorts with similar epidemiology to the TCGA cohort, and unfortunately the low number of samples detected in LSCC will make it difficult to study the extent of the oncogenic role of HPV in LSCC until more studies are performed. This significant variance between studies is most likely due to both the method of detection and the differential rates of HPV infection in each region. For example, HPV DNA PCR assays are capable of detecting very few copies of the viral DNA and some have argued that these assays are too sensitive, able to pick up viral DNA from a transient infection rather than an integrated event[35,36].

Consequently, many additional assays have been developed that rely on detecting common downstream events of HPV biology or directly sequencing across genomic insertion sites. For example, when HPV integrates into the genome, early genes E6 and E7 are highly

expressed(36). E7 then inactivates pRb, causing increased levels of $p16^{INK4A}$ which can be detected by immunohistochemistry(37). Thus, using the downstream protein expression of p16 as a surrogate marker for HPV has become a widely acceptable method and clinically relevant method(38). Likewise, a second method of detecting HPV integration is to directly sequence the genomic breakpoints between the viral and human genomes. This method is usually cost prohibitive at this point, due to the high cost of whole genome sequencing, but may become more routine in the future. Regardless as the methods for rapid detection and location of HPV insertion sites in the genome improve, so will our understanding of the prevalence and pathogenic role for this virus in LSCC.

Translating Genetics into Targeted Therapies

The potential to improve patient survival by using genetic information to match optimal treatments can be seen in a growing number of successes in other cancers: imatinib for chronic myelogenous leukaemia(39), trastuzumab for breast cancer with *ERBB2* amplification(40), and erlotinib and gefitinib for lung cancers that express mutant *EGFR(41)*. Here, we will review a few specific molecular lesions that are altered in a large percentage of LSCC cases and have a similar potential for molecularly driven clinical trials.

PI3K Pathway

PIK3CA mutations and amplifications frequently occur in LSCCs. *PIK3CA* encodes p110α, the alpha catalytic subunit to the phosphoinositide 3-kinase (PI3K) which plays a central role in pathways involved in cell growth, survival, and metabolism(42). PI3K receives signals

from activated receptor tyrosine kinases such as EGFR and VEGFRs, and phosphorylates the lipid PIP_2 on the cell membrane to create PIP_3. AKT is then activated by PIP_3, resulting in a downstream cascade through multiple effectors including GSK-3 and mTOR (**Fig 1-1**). This pathway has been noted to be frequently overactive in other cancers including gastric, breast, and lung(43), and developing therapies targeting this pathway are underway(44).

The majority of mutations found in *PIK3CA* have been defined as 'hotspot' mutations, where the specific amino acid residue is recurrently altered in multiple tumor types(45). These hotspot mutations, such as E542K, E545K, and H1047L/R, have functional consequences of increasing the lipid activity resulting in overactive AKT signaling and downstream effector pathway activation(46). The over activation of the PI3K pathway in these cancer cells could make the cells reliant on these signals(47). For example, Garnett et al(48) found that *PIK3CA* mutations were a significant biomarker of sensitivity for several drugs targeting the PI3K pathway after screening over 600 cancer cell lines, including 23 HNSCC lines, against 130 drugs at clinical and preclinical stages. HNSCC cell lines with hotspot *PIK3CA* mutations demonstrated sensitivity to PI3K/mTOR inhibitors compared to *PIK3CA* wildtype cells, in both *in vitro*(49) and *in vivo* models(50). These preclinical results are now being tested in early clinical trials for patients with a variety of advanced cancers, including HNSCCs. In a phase I trial, patients containing *PIK3CA* mutations had significantly greater partial response rates to PI3K/AKT/mTOR therapy (6/17, 35%) than those without *PIK3CA* mutations (6/241, 6%)(51). A following early-phase trial indicated that only the H1047R mutation predicted partial response (6/16, 38%) compared to other *PIK3CA* mutations (5/50, 10%) or *PIK3CA* wildtype (23/174, 13%)(52). However, this study also noted that other hotspot *PIK3CA* mutations, such as E542K and E545K, had a strong association with *KRAS* mutations whereas the H1047R mutation did

not. As members of the Ras signaling pathway (*KRAS, HRAS)* have been known to mediate resistance to PI3K inhibition(53, 54), it is unsurprising that patients with both gene mutations may not respond to PI3K-targeting monotherapies. Notably, *KRAS* mutations are rare in HNSCCs(55-57), and there are no *KRAS* mutations present in the recent exome sequenced LSCCs(7-9). *HRAS* mutations occur with more prevalence(50), and of the 2 *HRAS* mutations in sequenced LSCCs both occur in tumors with additional *PIK3CA* hotspot mutations[11,12]. However, 68.4% (13/19) of the *PIK3CA* mutations in LSCCs are hotspot mutations without Ras mutations, and PI3K-targeted therapies could be a well-matched choice for this patient population.

In contrast, amplification of 3q26 with the *PIK3CA* gene has not been found to indicate sensitivity to PI3K-targeted therapy(48, 49). It is still unclear how the amplification of the *PIK3CA* gene affects the signaling of the PI3K pathway. While it has been shown that amplification of *PIK3CA* correlates with increased mRNA and protein expression of p110α(58), it does not necessarily lead to increased levels of phosphorylated Akt and mTOR as would be expected for increased pathway activation(49). Given the significant amplification of 3q26 in LSCCs specifically, it is crucial to understand the effects this amplification has on tumorigenesis whether *PIK3CA* or another nearby gene is the cause.

EGFR & HER2

The important role that the Epidermal Growth Factor Receptor (EGFR) plays in HNSCCs has been known for several decades(59, 60) as it has been shown to be overexpressed in >90% of HNSCCs. A tyrosine kinase receptor, EGFR belongs to the ERBB family of cell-surface receptors. Upon ligand binding to the receptor, EGFR homodimerizes or heterodimerizes with

other ERBB family receptors such as HER2 and initiates a signaling cascade(61). Potential activated pathways include Ras-MEK and PI3K/AKT/mTOR as discussed above, as well as signal transducers and activators of transcription (STATs). EGFR signaling can contribute to tumorigenesis by driving cell proliferation, evasion of apoptosis, angiogenesis, and metastasis(62).

Consistent with the molecular role of EGFR, Cetuximab, a monoclonal antibody targeting EGFR, is currently the only approved targeted molecular therapeutic for HNSCCs. The combination of cetuximab and radiation therapy has been shown to extend patient survival by 19.3 months compared to radiation alone in patients with recurrent or metastatic disease(63). However, contrasting the clear story of *EGFR* mutations in lung adenocarcinomas predicting sensitivity to EGFR-targeted therapies*(41)*, there are still no biomarkers that predict response to cetuximab.

Part of the reason for the lack of biomarkers in HNSCC as compared to lung adenocarcinomas may be due to the differential genetic lesions. On contrast to lung cancers where *EGFR* mutation is a common event, *EGFR* mutations are rare in HNSCCs (13/279, 4.7%)(9), while amplifications have been reported to vary between 10-30% (64). In HNSCC TCGA data, LSCCs had a similar frequency of amplification as other subsites at around 12% (**Table 1-2**). However, amplification of *EGFR* correlated with worse overall survival in LSCCs specifically(65). Additionally, in a phase II trial advanced LSCC patients received a single cycle of induction chemotherapy before stratification into surgery and radiation or chemoradiation treatments. Here, EGFR expression predicted increased risk of death(22). While there is no evidence for any biological difference in EGFR signaling between HNSCC subsites, the

prognostic role of EGFR in LSCCs specifically suggests an especially critical role of this receptor and pathway.

Activating similar pathways is the HER2 receptor which heterodimerizes with EGFR as well as other members of the ERBB family. While *HER2* amplifications seem rare (3/72, 4.2%)(9), experiments in LSCC cell lines have shown response to anti-HER2 therapy in models with HER2 over-expression(66). Targeting HER2 in this distinct subset of patients looks promising as research continues, and significant improvements to patient survival might be made through focusing on targeting this pathway for LSCCs.

Notch Signaling

The frequency of *NOTCH1* mutations in HNSCCs was surprising when first discovered, additionally so as many of the mutations were predicted to be loss-of-function(7). Traditionally, the Notch signaling pathway has been studied in an oncogenic role as activating mutations in *NOTCH1* have been shown to significantly contribute to tumorigenesis for several malignances including chronic lympocytic leukemia (CLL)(67) and prostate cancer(68). However, solid tumors such as lung squamous cell carcinoma, cutaneous squamous cell carcinoma(69), and HNSCC display loss-of-function mutations indicative of Notch signaling have a role as a tumor suppressor.

The Notch signaling pathway is a direct cell-cell communication network, where a signaling cell displays a ligand that binds and activates the receptor on the receiving cell membrane. There are four receptors, NOTCH1-4, which upon activation are cleaved by gamma secretase, following which the intracellular domain (ICD) of the receptor is translocated to the nucleus resulting in transcriptional activation of target genes.

In keratinocytes, it has been shown that Notch activity controls cell cycle exit as well as commitment to differentiation(70), where loss of *NOTCH1* promotes tumorigenesis(71). Importantly, the loss of Notch signaling leads to an accumulation of β-catenin expression and an increase in Wnt pathway activity(72), and Wnt signaling has been shown to have an oncogenic role in multiple cancers(73). The possibility of addiction to Wnt signaling resulting from a loss of Notch signaling creates the opportunity for therapeutic intervention. Indeed, the *PORCN* inhibitor (this gene palmitoylates WNT ligands enabling their secretion into the tumor niche) called WNT974 has shown inhibition of growth of HNSCC models with loss-of-function mutations in *NOTCH1*(74). Accordingly, we have now opened a phase II clinical trial for metastatic HNSCC patients that will be enriched for NOTCH-deficient cancer to receive WNT974 (NCT02649530). As 17% of LSCCs contained mutations in *NOTCH1*, WNT974 is a potential targeted therapeutic that will be evaluated for further clinical advancement.

In contrast to inactivating NOTCH mutations, a small subset of studies have also reported that over-activation of Notch signaling can contribute to HNSCC(75). As LSCCs have a significant amplification of *NOTCH1* compared to other HNSCC subsites (p-value<0.007, **Table 1-2**), Notch signaling may also act as an oncogene for a defined subset. A role as both an oncogene and tumor suppressor suggests Notch signaling can have a bimodal effect in HNSCCs, dependent on timing and order of mutations. These roles will need to be further elucidated to directly target Notch signaling or any of its modulators.

Cyclin D1 (CCND1)

The *CCND1* gene encodes cyclin D1, a member of a highly conserved cyclin family. Cyclin D1 regulates cyclin-depending kinases (CDKs) 4 and 6 which control the G1/S phase

transition of the cell cycle. The amplification or gain of 11q13, which contains *CCND1*, is a frequent event in LSCCs specifically (36.1%, **Table 1-2**). Importantly, high expression of cyclin D1 correlated with increased risk of death in advanced LSCC patients(22). The efficacy of CDK inhibitors to prevent cell cycle progression by overexpressed cyclin D1 is an area of active investigation in LSCC. Currently, multiple clinical trials investigating CDK4/6 inhibitors in HNSCC are underway(76), where the inhibitor palbociclib has already shown efficacy in breast cancer(77). The extent of correlation between high expression of cyclin D1 and patient response to CDK inhibitors will be critical to clarifying the potential biomarker role of *CCND1* amplification status.

Immunotherapy

An additional novel treatment option for LSCC that has rapidly advanced in recent years involved immune modulating agents. Immune dysregulation and escape have been increasingly recognized as a hallmark of cancer and potential therapeutic target over the past several years(78). It is believed that the adaptive immune system recognizes and eliminates pre-malignant cells. Progressive derangements in the immune system driven by transformed cells gradually leads to immune escape and widespread tumor proliferation(79). Observed derangements include inflammatory cytokine expression and activation of inflammatory transcription factors in tumor cells(80, 81). LSCC and other subsites of HNSCC have been demonstrated to be markedly immunosuppressive via numerous mechanisms, including downregulation of antigen presenting via human leucocyte antigen (HLA) class I molecules(9, 82-84), development of T-cell tolerance to overexpressed antigens(85, 86), inhibitory cytokine

production(87, 88), and increased programmed death-ligand 1 (PD-L1)/ programmed death-1 (PD-1) expression(89-91).

Based on these preclinical findings, numerous potential targets and interventions have been proposed. Monoclonal antibodies targeting cytotoxic T-lymphocyte-associated protein-4 (CTLA-4) (ipilimumab), PD-1 (pembrolizumab), or PD-L1 (nivolumab) have been developed with the goal of manipulating mechanisms of tumor escape and eliciting an adaptive immune system response targeted towards the tumor(92). Therapy in patients refractory to standard therapy has been well-tolerated and yielded favorable response rates(93-100). However, of more excitement, there are a few patients that appear to achieve lasting complete disease response. These durable responses are being observed in patients who previously would have had a rapidly terminal disease. PD-1/PD-L1 inhibitors have now been approved for metastatic non-small cell lung cancer, renal cell cancer, and melanoma.

Given the clinical efficacy in other malignancies and the immunologic underpinnings, immunotherapy is an avenue of significant interest in LSCC. Various modalities are under development, including vaccine therapy and targeted monoclonal antibodies. Although many of these trials are ongoing, preliminary data has been presented of the Phase I/II KEYNOTE-012, where a cohort of 132 HNSCC patients with unresectable recurrent or metastatic tumors were treated with the PD-1 inhibitor pembrolizumab. This cohort was heavily pretreated with 59% of patients having received 2 or more previous lines of therapy for recurrent or metastatic disease. The overall response rate was observed to be 24.8% with an additional 24.8% achieving stable disease. At the time of the interim report, the median duration of response was not reached and 86% of responding patients appeared to have an ongoing response(101). Correlative analysis

suggested that an inflamed genotype gene expression was able to predict 6 month progression free survival and response to anti-PD-1 therapy(102).

A few trials are examining the incorporation of immunotherapy in the management of locoregional HNSCC, including LSCC. These include neoadjuvant vaccine administration (NCT02002182, NCT02609386), concomitant cetuximab and ipilimumab with intensity modulated radiation therapy (IMRT) (NCT01860430), and addition of nivolumab to concomitant cisplatin and IMRT (RTOG3504). Although the majority of trials are targeting recurrent or metastatic HNSCC (all subsites), the preliminary promise of immunotherapy in advanced and recurrent HNSCC cases suggest that LSCC patients could benefit from this novel therapeutic approach.

Overcoming Challenges for Targeted Therapy

While targeted therapies have had several clinical successes in other cancers, these are often in tumors with relatively few "actionable" aberrations. In contrast to tumors with low genetic complexity, the relatively high number genomic alterations in LSCCs coupled with the complex level of intra-tumor genetic heterogeneity will make distilling the critical pathways disrupting tumor growth difficult to identify. Moving forward, additional LSCC genetic information and models for tumors associated with both under-represented epidemiologic-risk groups and genetic landscapes are needed to improve our ability to predict the response of tumors to genetic lesion-matched therapeutics.

As mentioned above, the available genetic information for LSCC tumors is currently largely limited to previously untreated, stage III/IV tumors from Caucasian patients with a history of tobacco and/or alcohol use. Genetic information from untreated early stage (I/II) LSCC tumors would be beneficial to isolating initial aberrational events that drive tumorigenesis. Likewise, as patients are most likely to enroll in personalized medicine trials with advanced or recurrent tumors, genomic landscapes of advanced tumors following relapse from frontline therapy would be the most beneficial for designing novel interventional strategies. Unfortunately, large sequencing studies of tumors from previously treated, advanced LSCC tumors have not yet been published, with the exception of a few small cohorts demonstrating that advanced and recurrent LSCCs typically have higher numbers of genetic aberrations than untreated counterparts(10). These studies are critical because they demonstrate proof-of-principle that the genomic landscape of LSCC tumors evolve with therapeutic course. Thus, an important goal for the immediate future is to build a comprehensive understanding of the genetic and molecular interaction between the highly recurrent disruptive genomic events found at each stage of tumor progression.

Importantly, several LSCC models already exist that can be used to dissect the genetic and molecular mechanisms of LSCC pathogenesis, but these are also limited to a few epidemiologic subsets and few genetic landscapes. For example, LSCC cell line models from primary, metastatic, and recurrent tumors(103), including two pairs of primary and metastatic cell lines from the same patient(104) and an HPV-positive line(105) (**Table 1-3**). While the value of these existing cell lines is clear, more models of various stages and pre/post-treatment status consistent with normal interventional progression are still needed to fully explore therapeutic responses at various points in the normal pathogenic course.

In addition to cell lines, models in which surgically excised tissue from patients is implanted into immunocompromised mice called patient-derived xenograft (PDX) models have recently gained traction as powerful tools for assessing therapeutic responses in pre-clinical studies. In fact, HNSCC studies using PDX models in this manner have already been used to support the translation of targeted strategies into clinical trials(106), supporting the utility of these models. Early studies have indicated that HNSCC PDX models represent parental tumors by histology(107, 108), gene expression profiles(109), single-nucleotide polymorphisms(110), copy number variants(110, 111) and proteome profiles(112) and there also has not been an indication that engraftment of the tumor is biased by either genetic or clinical factors, including HNSCC subsite(113). Unfortunately the expense as well as the variable grafting rate (30-80% reported for HNSCC) is currently limiting the wide-spread use(114), but once the PDX model is established, the tumor can be propagated and expanded into additional mice for parallel, sequential, and long-term therapeutics experiments(115). Moving forward, the establishment and characterization of LSCC PDX models from both untreated and pretreated tumors will be essential for the advancement of therapeutics for different epidemiologic and genetic subsets of LSCC.

Algorithms for Integrating LSCC Organ Preservation/Treatment

As noted above, LSCC historically has been a unique and successful model for treatment selection and for organ preservation. However, with the current evolving state of genetics and targeted agents in cancer, we will need to revisit treatment algorithms for this disease.

While existing selection paradigms have been focused on objective clinical response to induction chemotherapy(14), future goals would be to identify these potential responders to

organ-preservation therapy without the need for an induction chemotherapy cycle. Through next generation sequencing studies, we have already identified specific genetic pathways that may be of interest for targeted therapy in LSCC (**Fig 1-2**). Further incorporating patient genetic information into treatment algorithms for LSCC could serve to further stratify and improve patient outcomes (**Fig 1-3**). As the cost and turnaround for targeted next generation improves, valuable time could be saved to initiation of definitive treatment, and patients could be treated more specifically and effectively.

Specific issues should be considered as treatment algorithms are adapted to include new agents and genomic sequencing. An important decision in use of targeted therapies is whether they should be used irrespective of mutational status (as cetuximab is currently used in HNSCC), or whether targeted therapies should be employed only in those patients with genetic aberrations. Additionally, protocols will need to be designed and implemented investigating these agents in different clinical scenarios (i.e. neoadjuvant vs. adjuvant, monotherapy vs. combination therapy, early vs. late stage tumors, primary vs. recurrent tumors, **Fig 1-3**). Likewise, we must consider when and where to add immunotherapy into LSCC treatment algorithms. In a similar fashion to targeted therapy, we must identify predictive biomarkers to allow for treatment stratification(116).

Another key group of LSCC patients in need of additional treatment options are those with recurrent disease after both chemoradiation and surgery. These patients have poor outcomes (5-year overall survival 49% and disease-free survival 58%; our unpublished data). Moreover, these recurrences are often untreatable, as patients will have exhausted all other avenues of treatments. Currently, there are no other available options for these patients, and their care is often palliative. Interestingly, patients with recurrent HNSCCs may have different mutational

signatures(10). Thus, identifying these patients (through predictive genetic biomarkers) and intervening with additional therapies (targeted agents, immunotherapy) earlier in their disease-course may lead to modified treatment algorithms and improve outcomes.

Currently, targeted therapy clinical trials are aimed towards recurrent and advanced stage cancers. In the future, the possibility of expanding these agents to early-stage tumors will be important. Potentially, early-stage LSCC may be more responsive to targeted therapies, given they may have a lower overall mutational burden, and fewer potential targetable dysregulated driver mutations.

As with all next-generation sequencing trials, ethical considerations must be addressed(117). Thus, future programs for personalized medicine in LSCC should have well-established guidelines for pretest counseling on disclosure of genetic information, and have genetic counselors actively involved throughout the process.

Conclusion

With the increasing implementation of next-generation sequencing and personalized medicine protocols for cancer, LSCCs may be a particularly useful and successful model disease for novel treatment paradigms. Given the long history and relative success of LSCC and organ-preservation protocols, there will be an inevitable evolution towards adopting targeted and immune modulating agents for this disease. While identification of prognostic genetic biomarkers, therapeutic targets and models to perform molecular studies specific to LSCC remains incomplete, this field is rapidly advancing. Ultimately, these novel strategies will increasingly be investigated and applied to LSCC, which will hopefully improve both organ preservation and overall survival for patients with this disease.

1.2 Generation and utilization of CRISPR/Cas9 screening libraries in mammalian cells[2]

Introduction

The adaptation of the clustered regularly interspaced short palindromic repeats (CRISPR)/Cas9 system to generate knockouts in mammalian cells has resulted in significant scientific advances. By choosing any 20 base pair sequence guide RNA (gRNA), as long as it is next to a protospacer adjacent motif (PAM) of 5'-NGG-3', to direct the Cas9 endonuclease and establish knockouts has resulted in unmatched speed and flexibility for creating these genetic models than other gene editing methods. This power and efficiency of has allowed researchers to apply this technology on a genome-wide scale that was previously infeasible using TALENs or zinc finger nucleases. Since late 2013, several CRISPR screening libraries have been developed targeting anywhere from several hundred to thousands of genes and discovering genes essential to cell proliferation, resistance to clinical treatments, and involved in processes of toxicity(118-120).

To date, the generation of genome-wide knockout libraries is the predominant application for CRISPR-Cas9 in large-scale screening, but other methods are being actively developed. CRISPR interference, or CRISPRi, has also been used to transcriptionally repress target genes. While inactive Cas9 (dCas9) alone can sterically inhibit transcription of targets, robust silencing can be achieved by fusing dCas9 with a known transcriptional repressor, such as the repressor domain of KRAB(121, 122). dCas9 fusion proteins have also been applied in large scale gene activation

[2] This section was published as a chapter in *Genome Editing and Engineering: From TALENs, ZFNs and CRISPRs to Molecular Surgery* at Cambridge University Press in collaboration with the following authors: Nicole Michmerhuizen, Rebecca Hoesli, Jacqueline Mann, Samantha Devenport, Aditi Kulkarni, Andrew Birkeland, and J. Chad Brenner.

screens(122, 123). Konermann et al optimized a CRISPR-Cas9 mediated activation method (CRISPRa) utilizing dCas9 fusions with multiple activation domains to maximize transcriptional activation (123). This strategy, combined with a 70,290 gRNA pool, was used to identify genes for which gain-of-function perturbations could confer resistance to BRAF inhibition. As predicted, known BRAF resistance pathway members, such as EGFR, were enriched following pharmacological BRAF inhibition(123). As CRISPRi/CRISPRa technology continues to develop, broader applications are envisioned, including manipulation of multiple genes in single cells in order to unveil novel interaction networks(124).

This chapter will focus on the creation and use of a CRISPR/Cas9 screening library for large scale genetic studies. Here, we discuss important considerations in design and methodology to these screens.

Methodology

Deciding library coverage

The first consideration in designing or using a CRISPR screening library is the number of genetic targets, whether genome-wide or a targeted panel. The size of the library is critical to establishing optimal parameters in future steps, such as how many cells to screen, sequencing depth, and calling statistical significance. Many recent CRISPR screens in human cells have utilized whole genome gRNA libraries targeting 7,000 to 25,000 genes(118-120, 122, 123, 125). However, it is also necessary to have multiple gRNAs targeting each gene. While the whole genome gRNAs target up to 25,000 genes, the actual library size is around 300,000 gRNAs which results in up to 10X coverage (that is, 10 unique gRNAs per target gene). Coverage of 3-6X, or 3-6 unique gRNAs for each gene is currently most common.

Designing guide RNAs

Effective gRNA design hinges first on targeting an appropriate site within the gene of interest that has as few off-target binding sites as possible. In general, a large portion of the coding region of a given gene is targetable. While the design of each gRNA/CRISPR complex can be dependent on the specific experimental needs, for effective knockouts, most gRNAs are designed to target early exons such that they induce insertions or deletions (indels) after the start codon. Targeting sequences near the 3' end of the gene is less favorable since frameshift mutations that occur near the end of a protein are less likely to alter expression (118, 126).

To improve target cleavage, the efficacy and/or stability of the gRNA sequence must be optimized (127). The protospacer adjacent motif (PAM) is a critical element to consider. The PAM sequence is directly adjacent to the 20 base pair gRNA, and generally given as a motif of 5'-NGG-3'. However, it has been noted that cytosine is favored and thymine is disfavored as the variable nucleotide in the PAM for effective gRNA design. The preference for cytosine may be a result of RNA polymerase III termination at U-rich regions (since the downstream transcript is U-rich). The gRNA nucleotide located directly adjacent to the PAM is also very important; in this site, guanine is preferred and cytosine is undesirable (126), see **Figure 1-4**. Various other changes to specific nucleotides within the gRNA sequence have also been shown to significantly affect efficacy although these requirements are not necessarily generalizable across gRNAs, gene targets, and cell types (128).

Other characteristics of the gRNA sequence are also important to consider when designing gRNAs for experiments. For example, gRNAs with a G/C content that is too high or too low are often less effective (118, 126). Additionally, if the target sequence displays high nucleosome

occupancy or is typically in the coiled (or closed) chromatin state, gRNA efficacy will suffer (129). While the gRNA features described here apply in most CRISPR applications, other more specialized characteristics differ between individual cell lines, organisms, and techniques. Ongoing work seeks to better understand these differences in order to improve the selectivity of gRNAs at their intended target sites.

Minimizing off-target effects of gRNAs

Because the gRNA does not have to match perfectly with the target DNA sequence to effectively induce genetic alterations, there is a possibility for off-target effects when using CRISPR. Even though gRNAs are often most effective when perfectly matched to the target sequence, some degree of mismatch is tolerated by the CRISPR enzyme. In fact, the distance of the mismatch from the PAM site may be one variable in determining off-target efficiency as it has been suggested that nucleotide differences generally do not decrease efficacy as substantially if they are found at sites more distant from the PAM. As might be expected, multiple mismatches decrease efficacy further than single mismatches, particularly if they are close to each other (127). In fact, gRNAs have been shown to bind to and cleave DNA regions with as many as 5 mismatches and in some cases the mutation frequency is as high at an off-target site as it is at the intended target site (130). In other genomic "hotspots," located at some centromeres and telomeres, off-target effects are especially common (131); however, attributes of these hotspot regions have not yet been fully described, and it is still relatively unclear as to how often gRNAs cause genomic alterations in off-target regions.

Consequently, when utilizing CRISPR for screening, increasing the number of guide RNAs per target should mitigate undesirable off-target effects and reduce bias since each gRNA has a

different sequence and cleavage profile (126). In order to decrease non-specific effects further, other efforts are necessary and are an active area of investigation. Shorter gRNAs, with 17 or 18 nucleotides rather than 20, have shown improved specificity, at least in human cells (132). While nickases have also been proposed to improve efficacy, this technology is currently not useful in a knockout screening format (133-135). Furthermore, although the ratio of Cas9 to gRNA is not a direct feature of gRNA design, this parameter can also be modulated to improve specificity (127). Consequently, as the field continues to evolve gRNA libraries may be modified to alter specificity and design parameters that can be adapted to meet the needs of diverse experimental questions. In order to predict which gRNAs might be functional, recent work has developed gRNA and CRISPR library design software. Many of these programs are publicly available and their early evaluation has been promising(136, 137).

Choosing gRNA and Cas9 expression system

There are multiple methods for introducing the gRNA and Cas9 endonuclease into cells, with transient or stable expression. Currently, the most common method of gRNA library expression is using lentiviral vectors. Lentiviral constructs are effective across a wide variety of cell types, and give stable long-term expression of the gRNA and/or Cas9 (138). Additionally, as lentiviral constructs integrate into the genome, the gRNA can be used as a unique identification of the knockout that was established in the cell.

Lentiviral constructs expressing a gRNA and a Cas9 together are common, but a two-vector system where Cas9 and a library of gRNAs are introduced separately has also been established, see **Figure 1-5**. The two-vector system allows for an initial selection of a stable pool of cells expressing Cas9, and then subsequent introduction of the gRNA library with a secondary means

of selection (either different antibiotic of fluorescent marker) (118, 139). It is possible that a one-vector system that contains the gRNA, Cas9, and all the needed expression machinery creates a large lentiviral construct that might be difficult to virally package. The two-vector system also has experimental flexibility, with the ability to have a stable pool of Cas9 expressing cells against a variety of smaller, targeted gRNA libraries (120). However, the one-vector system has been successfully used in a variety of cell types for a variety of screens (119, 140, 141). The disadvantage of using lentiviral vectors are that the long-term expression of the gRNA and Cas9 has unknown effects on off-target regions on the DNA or other cell functions. While short term expression has been shown to be enough to induce knockouts, it has been suggested that continual long-term expression increases the chances of off-target effects (138).

Other vector based systems, such as adeno-associated vectors or plasmid expression vectors allow for Cas9 and gRNA expression, but do not integrate. This makes it difficult to determine successful hits from the screen, as there is currently no method for identifying the gRNA or target region without a depth of next generation sequencing that is cost prohibitive and analytically infeasible. Other transient methods of expressing gRNAs or Cas9, while potentially successful in establishing a knockout, activation, or suppression cell phenotypes, result in the inability to screen for successful events and testing of a pooled library.

Introducing library into mammalian cells

Introducing the CRISPR screening library into cells is as simple as a lentiviral transduction. However, an important concern is introducing the library into the cells at a low multiplicity of infection (MOI) so that there is a low chance of multiple constructs integrating into one cell. Generally, small-scale tests are run to determine an optimal MOI (5-30%) before the conditions

are repeated for a large-scale transduction. Coverage is again a concern. For example, a library of 65,000 gRNAs can be covered at >400X if a population of 30 million cells are maintained. If the MOI is 30%, then 100 million cells need to be transduced. After lentiviral transduction, then a selective process of either antibiotics or sorting by fluorescent marker depending on vector choice is done. While the kinetics of CRISPR/Cas9 activity are largely unknown and most likely vary per cell line, generally several days are given between selection for the library pool and experimental treatment.

Experimental design

Pooled CRISPR screens can be classified as either positive or negative selection. Positive selection screens use a strong selective pressure, such as a toxin, to eliminate the majority of cells from the population, enriching for cells with genetic perturbations conferring protection from the toxin. For example, to identify genes functioning in DNA mismatch repair (MMR), Wang et al cultured cells in the presence of 6-thioguanine (6-TG), which induces cell cycle arrest via the MMR pathway. Cas9-inducible KBM7 cells were transduced with a pool of 73,000 gRNAs targeting 7031 genes, and incubated with 6-TG. Sequencing of the surviving population revealed that gRNAs targeting the four known MMR pathway components, MSH2, MSH6, MLH1, and PMS2, were greatly enriched when compared with the original library(118). This type of screen can be powerful in identifying genes that convey resistance to drugs or other death-inducing treatments.

CRISPR-Cas9 mediated knockout libraries can also be used in negative selection screens, aimed at identifying genes essential for survival under the chosen experimental condition by monitoring the population for depletion of certain gRNAs. To verify that their methods are also

appropriate for negative selection screening, Wang et al assessed representation of gRNAs in library-infected Cas9-KBM7 cells at initial seeding and after 12 cell doublings. As expected, gRNAs targeting ribosomal protein genes were dramatically depleted in the final population, demonstrating the efficacy of this strategy in identifying essential genes (118). Negative selection screens can also be used to identify targets that convey sensitivity to a low selection process, which could identify possible combinations of inhibitors for future clinical use. It is important to note that negative selection screens have additional technical concerns. For successful identification of a loss of gRNAs, then the CRISPR pool must have each gRNA represented in many cells (>300) with many gRNAs targeting the same gene. Deep sequencing coverage of the treated library is also needed to be able to successfully identify the low frequency events or drop-outs.

Experimental conclusion

At the conclusion of the experiment, each gRNA can be PCR-amplified and sequenced to identify the surviving population because of the integrated lentiviral gRNA construct. However, there are an unknown number of gRNAs and targeted genes, making it difficult to determine proper sequencing coverage for the treatment. Library size as well as choosing a positive or negative selection screens are the main considerations. Additionally, for either screen type, the gRNA coverage needs to be compared to an initial library or a non-treated pool for which the general assumption is that full coverage has been established.

Results & Discussion

Identification of significant gRNAs and genes

In most CRISPR/Cas-9 screens, the general idea is to compare two or more populations of cells being subjected to a particular condition or treatment. The effects of the condition or treatment are measured by quantifying levels of gRNAs in the different cell populations. An increase in gRNA quantity after treatment is indicates a disruption of the function of a target gene that provides some benefit to the cells. On the other hand, a decrease of gRNA numbers indicates that the disruption of the target gene function is not beneficial to the cell for survival.

Many software analysis pipelines, modules, and packages are available for computational analyses of CRISPR/Cas9 screening data sets. Although these software packages use different algorithms, their common output is a list of significant gRNAs and genes. The first step of these analysis pipelines is to obtain read counts from each of the cell population samples in the study. These read counts are then normalized to account for library size, read count distribution, read depth, and other factors. For example, the study design may need to decide if reads with one or more mismatches from gRNAs in the reference library will be used to quantify total read numbers. If there are biological or technical replicates in the experiment, variance estimation is performed to capture the variance across replicates. By incorporating the normalized read counts, variance estimation and other parameters, the statistical significance of each gRNA is calculated. These gRNAs are then ranked and the top gRNAs are chosen for further investigation of pathways and genes of interest.

Model-based Analysis of Genome-wide CRISPR-Cas9 Knockout (MAGeCK) is one of the most popular tools for analyzing data from CRISPR/Cas9 screens. MAGeCK uses the median normalization method for read count normalization followed by mean-variance estimation to

compare replicates in an experiment. Using this mean-variance estimation model, each gRNA is assigned a statistical significance. Genes are considered essential if their gRNAs are repeatedly on the top of the ranking list after applying the robust rank aggregation (RRA) algorithm. Based on RRA results, both positively and negatively selected essential genes can be identified. To identify pathways that are enriched, the same RRA algorithm is then applied to the list of top ranked essential genes (142).

MaGeCK-VISPR is an improvised version of MAGeCK with many advanced capabilities. Quality control measures are incorporated to help in assessing the quality of the experiment. Another important feature is the ability to test if genes are essential under multiple conditions at the same time. To estimate gene significance, an expectation maximization (EM) algorithm is used instead of the RRA. This EM based method can also estimate the efficiency of the gRNA knockout along with estimating gene ranking and significance. Another very beneficial feature is the ability to visualize as well as interactively explore the QC as well as analysis results. (45).

Other data analysis pipelines include the shALIGN(143) and BiNGS!SL-seq(144), both which use different R packages for the statistical data analysis. Empirical Analysis of Digital Gene Expression Data in R (edgeR) is a popular R package commonly used for various types of gene expression data such as RNA-Seq, microarrays etc. A customized workflow in edgeR can be used for analyzing data from CRISPR/Cas9 screens (145).

Comparing CRISPR libraries to siRNA & shRNA screens

The development of the CRISPR/Cas system for precise-genome editing has significantly advanced functional genomics screening; however, its import and to understand the utility of traditional functional genetics screening approaches. Previously, functional genomics studies

relied upon small interfering RNA (siRNA) and short hairpin RNA (shRNA) technologies to explore gene function through loss of function studies. Although the usage of siRNA and shRNA revolutionized the field at its introduction, the introduction of CRISPR to the field of functional genomics has provided several advantages over siRNA and shRNA techniques, but also has some limitations where siRNA and/or shRNA approaches may still be advantageous.

In one study, Feng et al showed that CRISPR techniques resulted in improved gene inactivation efficiencies as compared with shRNA(139). This translates to improved sensitivity in evaluating gene function, as a complete knockout of a gene can reveal gene effects that are not adequately demonstrated by the knockdown of expression achieved by shRNA or siRNA screens (146). CRISPR additionally has the advantage of being able to create permanent cell line pools, which can be used to perform repeated experiments to further delineate gene function (146). Likewise, high density gene saturation editing has also enabled functional genomics screens that assess biochemical activity of proteins, whereas shRNA based approaches required complex multi-step rescue approaches.

Like shRNA or siRNA, CRISPR also has the ability to reduce gene expression by recruitment of transcriptional repressors or direct transcriptional interference, as well as increase gene expression by recruiting transcription activators (146). CRISPR also has the benefit of being able to explore effects of non-transcribed genes, as it directly acts on a DNA and does not rely upon transcription or translation like siRNA and shRNA screens (146). Finally, pooled CRISPR screens are cheaper than siRNA due to the transfection agents required to carry out siRNA screens (146), but may have similar cost points to shRNA pooled screens. Functional genomic approaches leveraging plate formats and transfection assays are beginning to emerge for CRISPR technology, but these are still in the early phases of development.

Despite the advantages of CRISPR, siRNA and shRNA screens will likely remain an important tool in functional genomics screening, as siRNA and shRNA screens often provide complementary information to CRISPR, and do maintain some advantages over CRISPR. For example, siRNA and shRNA screens are still ideal for targeting essential genes, as complete knockdown of essential functioning genes will result in cell death (147). siRNA and shRNA screens also have a larger target pool than CRISPR, as they can essentially target any existing RNA. CRISPR, on the other hand, requires particular sequences in addition to the gRNA site to recruit the necessary machinery to cause double stranded breaks (147). This limits the number of cut sites in the genome; however, modified Cas9 enzymes are being rapidly developed to overcome this issue, regulate differential cut site specificity and enzyme efficiency. In fact, in the near future, we may perform pooled CRISPR screens with high density gRNA libraries and multiple different Cas9 enzymes to analyze different effects and compare off-target and on-target activities of multiple different Cas9 enzymes.

Researchers have previously gained significant experience with siRNA and shRNA screens, allowing ample time for protocol refinement and an improvement in the rate of off-target effects (OTEs) in siRNA and shRNA screens (146), but one current limitation of CRISPR-based screens are the unknown consequences of false negatives due to variations in guide RNA accuracy, and due to improved efficiency of NHEJ resulting in accurate repair of the double-stranded breaks (146). Other technical limitations that will need to be overcome include the fact that CRISPR screens require lysis of the host cell populations in order to identify the genes of interest, and thus does not allow for screening for any image-based phenotypic screen (146) and Cas9 is also constitutively active, and while this has not been shown to harm the cell, it can result in increasing OTEs (147). Finally, as mentioned above, the CRISPR screens require complete knockout of the

gene of interest, and thus if there are many copies of the gene like in cancer cells, CRISPR may not efficiently demonstrate loss of function in that gene (147). As such, knockouts of genes, such as lncRNAs, without open reading frames or genes with high copy number in the cell population remains challenging for CRISPR, but not for si/shRNA-mediated approaches.

Consequently, while we have entered an era where knockout-based functional genomics screens are viable in almost any cell population, si/shRNA screening approaches will continue to complement CRISPR-based technology. These alternative approaches can be easily leveraged for performing secondary or tertiary screens on nominated targets advancing from CRISPR screens or to simply provide companion methodology that may enhance the chances of a successful screen under particular experimental conditions (e.g. assessing the effect of genes with high copy number in cancer cell lines).

Collectively, CRISPR technology is rapidly advancing and quickly becoming a standard tool in cell and molecular biology labs across the world. Our early experience with pooled CRISPR screening and creation of individual gene knockout lines has complemented the rapidly evolving knowledge base building around the technology. It is clear that knockout screening technology will lead to new medical and translational advances that were simply not possible before Cas9 was advanced into human models, and represents a clear story of how truly basic research can make a significant impact on the greater scientific community.

Figures

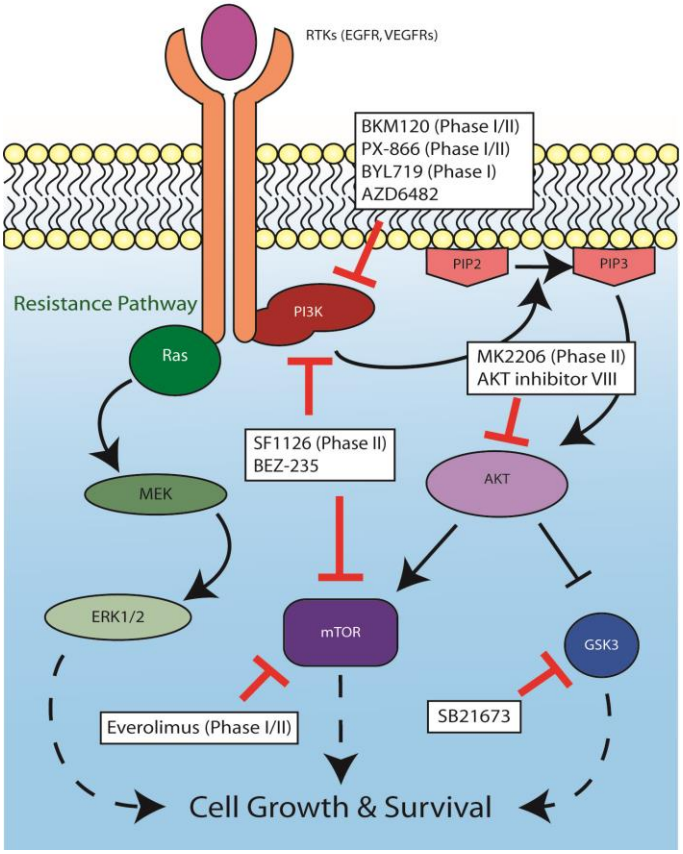

Figure 1-1. Key components of the PI3K pathway and possible therapeutics

Drugs targeting individual components are either in trials as noted, or were effective in vitro with cell lines containing PI3KCA mutations. The RAS/MEK/ERK pathway, which has been noted to play a role in resistance to PI3K-targeted therapies, is shown.

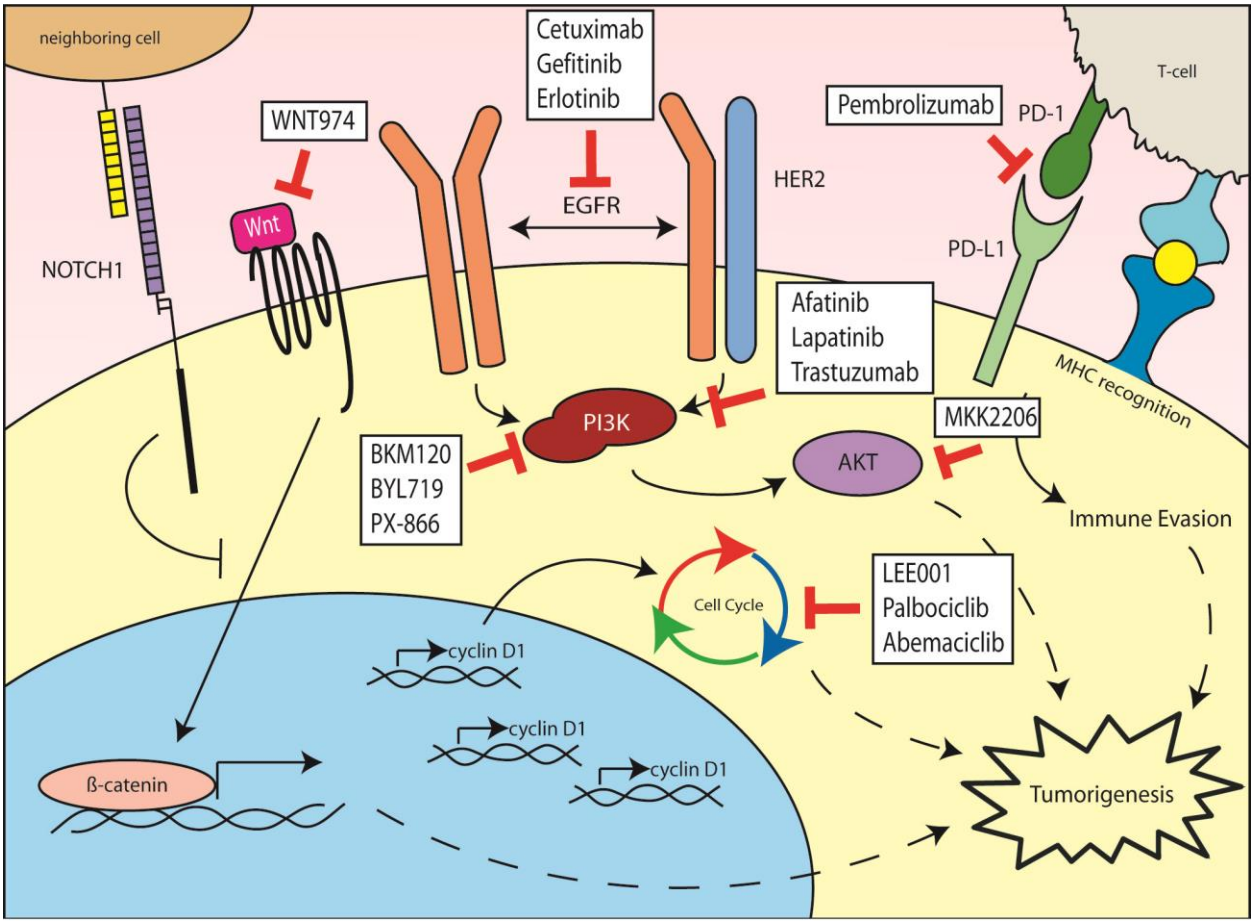

Figure 1-2. Major oncogenic mechanisms in LSCC and thereapuetic opportunities

Dysregulated pathways common to LSCCs with targeted therapies in clinical trials for HNSCCs are shown(76). WNT974 targets PORCN thereby blocking Wnt ligand secretion from neighboring cells.

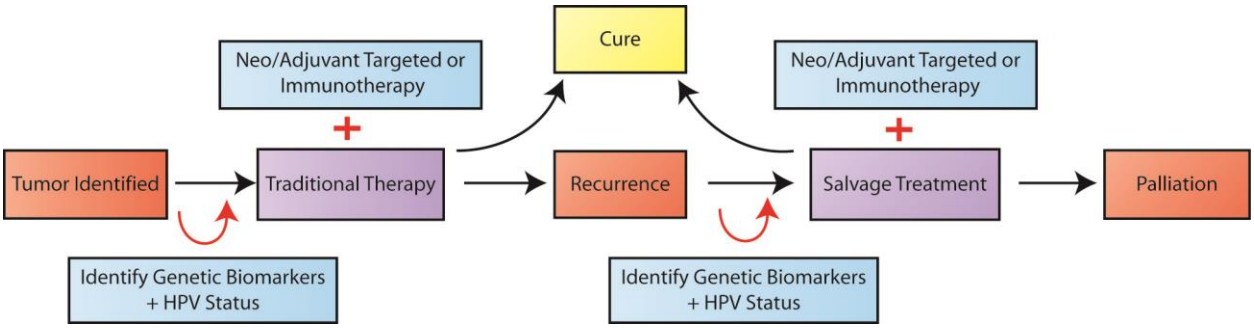

Figure 1-3. Decision algorithm for treating LSCC patients

Current practice is shown with black arrows, with traditional treatments such as surgery/radiation/chemotherapy. The red arrows incorporate HPV status and patient genetics to add targeted treatments or immunotherapy to improve cure rate.

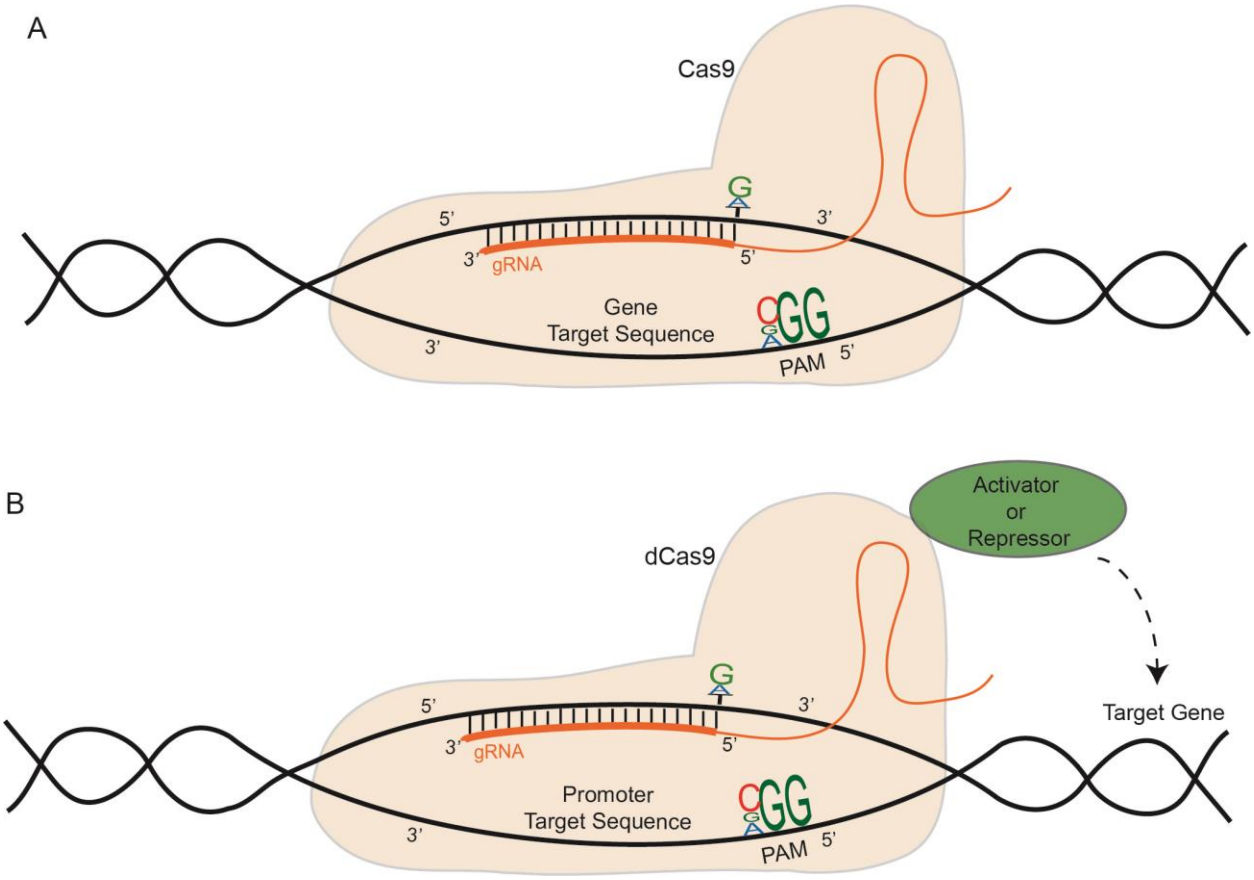

Figure 1-4. Diagram of gRNA in complex with Cas9 enzyme

Diagram of gRNA (orange) in complex with Cas9 enzyme targeting a gene to create a knockout (A). The PAM sequence, with preferred bases emphasized are marked. For CRISPRi libraries, the modified Cas9 enzyme and associated proteins are shown acting on the targeted gene (B).

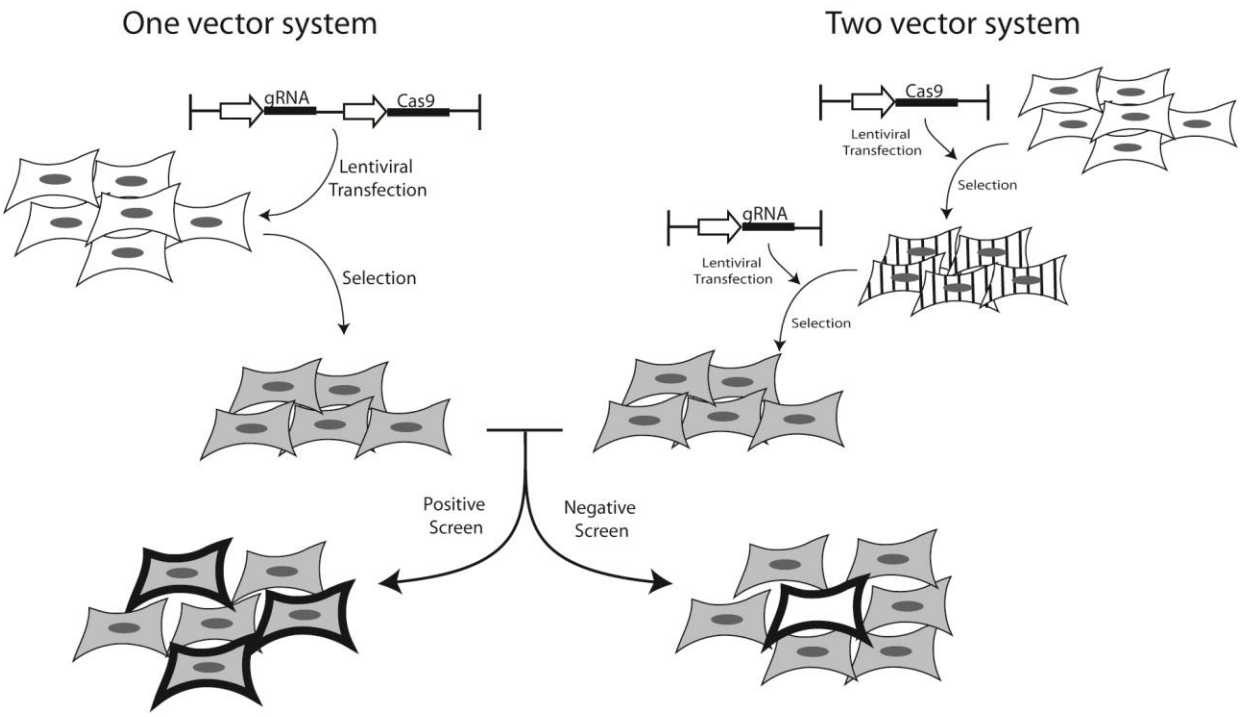

Figure 1-5. Schematic of CRISPR library generation

Overview of steps needed to introduce lentiviral CRISPR library into cells, either using a one or two vector system. After selection, the pooled library can then screened by positive selection, where the hits are observed at high frequency (circled cells), or by negative selection, where the hits are observed at low frequency or lost from the surviving population (empty circle).

Tables

Gene	TCGA n=71	Stransky n=15	Total LSCC n=88	Total (non-LSCC) n=237
TP53	64 (88.9%)	9 (60%)	75 (85.2%)	188 (79.3%)
CDKN2A	17 (23.6%)	1 (6.7%)	19 (21.6%)	53 (22.4%)
PIK3CA	18 (25%)	1 (6.7%)	19(21.6%)ǂ	31 (13.1%)
FAT1	14 (19.4%)	4 (26.7%)	18 (20.4%)	53 (22.4%)
NOTCH1	13 (18.1%)	2 (13.3%)	15 (17.0%)	44 (18.6%)
CASP8	1 (1.4%)	0 (0%)	1 (1.1%)*	29 (12.2%)

Table 1-1. Frequently mutated genes in LSCC samples

The total (non-SCC) column represents mutations from oral cavity, oral pharynx, and hypopharynx samples. Only HPV-negative samples are included. ǂ p-value =0.058, * p-value <0.005 between total LSCC and non-LSCC samples.

Cytoband (Gene)	CNV	Larynx n=72	Non-Larynx n=172
3q26 (*PIK3CA, SOX2*)	Amp	37.5%**	12.8%
11q13 (*CCND1, FGF3/4/19*)	Amp	36.1%	29.1%
9p21 (*CDKN2A/B*)	Del	31.9%	32%
3q28 (*TP63, ETV5*)	Amp	34.7%**	12.8%
8q24 (*MYC, PTK2*)	Amp	16.7%	12.2%
7p12 (*EGFR*)	Amp	12.5%	12.2%
9q34 (*NOTCH1, TRAF2*)	Amp/Del	4.2%**/1.4%	0%/0%

Table 1-2. Common copy number variations

Common copy number variations (CNV), either amplifications or deletions, in HPV negative samples of the TCGA cohort. ** p-value <0.05.

Cell Line	Age	Gender	TNM	Stage	Subsite	Type of Lesion	HPV Status
Paired:							
UMSCC-10A	57	M	T3N0M0	III	True Cord	Primary	-
UMSCC-10B	58	M	T3N1M0	III	Lymph Node	Metastasis	-
UMSCC-17A	47	F	T1N0M0	I	Supraglottis	Primary	-
UMSCC-17B	47	F	T1N0M0	I	Soft Tissue	Metastasis	-
Primary:							
UMSCC-11A	65	M	T2N2aM0	IV	Epiglottis	Primary	-
UMSCC-23	36	F	T2N0M0	II	Supraglottis	Primary	-
UMSCC-28	61	F	T1N0M0	I	True Cord	Primary	-
UMSCC-41	78	M	T2N1M0	III	Arytenoid	Primary	-
UMSCC-81B	53	M	T2N0M0	II	True Cord	Primary	-
UMSCC-105	51	M	T4N0M0	IV	True Cord	Primary	Positive
Recurrent and Metastases:							
UMSCC-12	71	M	T2N1M0	III	Larynx	Recurrence	-
UMSCC-13	60	M	T3N0M0	III	Esophagus	Recurrence	-
UMSCC-25	50	M	T3N0M0	III	Neck	Metastasis	-

Table 1-3. UM-SCC cell lines derived from LSCC patients

Patient-derived cell lines from LSCC patients at University of Michigan Comprehensive Cancer Center. Paired cell lines (-10, -17) are derived from subsequent cancers from the same patient. Appendices

Bibliography

1. Jemal A, Bray F, Center MM, Ferlay J, Ward E, Forman D. Global cancer statistics. CA Cancer J Clin. 2011;61(2):69-90. Epub 2011/02/08. doi: 10.3322/caac.20107. PubMed PMID: 21296855.
2. Induction chemotherapy plus radiation compared with surgery plus radiation in patients with advanced laryngeal cancer. The Department of Veterans Affairs Laryngeal Cancer Study Group. N Engl J Med. 1991;324(24):1685-90. Epub 1991/06/13. doi: 10.1056/nejm199106133242402. PubMed PMID: 2034244.
3. Forastiere AA, Goepfert H, Maor M, Pajak TF, Weber R, Morrison W, Glisson B, Trotti A, Ridge JA, Chao C, Peters G, Lee DJ, Leaf A, Ensley J, Cooper J. Concurrent chemotherapy and radiotherapy for organ preservation in advanced laryngeal cancer. N Engl J Med. 2003;349(22):2091-8. Epub 2003/12/03. doi: 10.1056/NEJMoa031317. PubMed PMID: 14645636.
4. Megwalu UC, Sikora AG. Survival outcomes in advanced laryngeal cancer. JAMA Otolaryngol Head Neck Surg. 2014;140(9):855-60. Epub 2014/08/22. doi: 10.1001/jamaoto.2014.1671. PubMed PMID: 25144163.
5. Edge SB, American Joint Committee on C, American Cancer S. AJCC cancer staging handbook from the AJCC cancer staging manual. New York: Springer; 2010. 1 online resource (xix, 718 p.) p.
6. Olsen KD. Reexamining the treatment of advanced laryngeal cancer. Head Neck. 2010;32(1):1-7. Epub 2009/12/03. doi: 10.1002/hed.21294. PubMed PMID: 19953627.
7. Agrawal N, Frederick MJ, Pickering CR, Bettegowda C, Chang K, Li RJ, Fakhry C, Xie TX, Zhang J, Wang J, Zhang N, El-Naggar AK, Jasser SA, Weinstein JN, Trevino L, Drummond JA, Muzny DM, Wu Y, Wood LD, Hruban RH, Westra WH, Koch WM, Califano JA, Gibbs RA, Sidransky D, Vogelstein B, Velculescu VE, Papadopoulos N, Wheeler DA, Kinzler KW, Myers JN. Exome sequencing of head and neck squamous cell carcinoma reveals inactivating mutations in NOTCH1. Science. 2011;333(6046):1154-7. Epub 2011/07/30. doi: 10.1126/science.1206923. PubMed PMID: 21798897; PMCID: 3162986.
8. Stransky N, Egloff AM, Tward AD, Kostic AD, Cibulskis K, Sivachenko A, Kryukov GV, Lawrence MS, Sougnez C, McKenna A, Shefler E, Ramos AH, Stojanov P, Carter SL, Voet D, Cortes ML, Auclair D, Berger MF, Saksena G, Guiducci C, Onofrio RC, Parkin M, Romkes M, Weissfeld JL, Seethala RR, Wang L, Rangel-Escareno C, Fernandez-Lopez JC, Hidalgo-Miranda A, Melendez-Zajgla J, Winckler W, Ardlie K, Gabriel SB, Meyerson M, Lander ES, Getz G, Golub TR, Garraway LA, Grandis JR. The mutational landscape of head and neck squamous cell carcinoma. Science. 2011;333(6046):1157-60. Epub 2011/07/30. doi: 10.1126/science.1208130. PubMed PMID: 21798893; PMCID: 3415217.
9. The Cancer Genome Atlas N. Comprehensive genomic characterization of head and neck squamous cell carcinomas. Nature. 2015;517(7536):576-82. doi: 10.1038/nature14129 http://www.nature.com/nature/journal/v517/n7536/abs/nature14129.html#supplementary-information.
10. Hedberg ML, Goh G, Chiosea SI, Bauman JE, Freilino ML, Zeng Y, Wang L, Diergaarde BB, Gooding WE, Lui VW, Herbst RS, Lifton RP, Grandis JR. Genetic landscape of metastatic

and recurrent head and neck squamous cell carcinoma. J Clin Invest. 2016;126(1):169-80. Epub 2015/12/01. doi: 10.1172/jci82066. PubMed PMID: 26619122.
11. Ingrid Breuskin CE, Ecaterina Ileana, Christophe Massard, Naima Lezghed, Ludovic Lacroix, Antoine Hollebecque, Rastislav Bahleda, Maud Ngo-Camus, Yohann Loriot, Nathalie Auger, Valerie Koubi-Pick, Thierry De Baere, Philippe Vielh, Vladimir Lazar, Marie-Cécile Le Deley, Catherine Richon, Joël Guigay, François Janot, Jean-Charles Soria, Charles Ferté, editor. MOLECULAR SCREENING FOR CANCER TREATMENT OPTIMIZATION IN HEAD AND NECK CANCER (MOSCATO 01): A PROSPECTIVE MOLECULAR TRIAGE TRIAL; INTERIM ANALYSIS OF 78 PATIENTS WITH RECURRENT OR METASTATIC HEAD AND NECK CANCERS American Head and Neck Society Translational Meeting; 2015 April 21-22, 2015; Boston, MA.
12. Beltran H, Eng K, Mosquera JM, Sigaras A, Romanel A, Rennert H, Kossai M, Pauli C, Faltas B, Fontugne J, Park K, Banfelder J, Prandi D, Madhukar N, Zhang T, Padilla J, Greco N, McNary TJ, Herrscher E, Wilkes D, MacDonald TY, Xue H, Vacic V, Emde AK, Oschwald D, Tan AY, Chen Z, Collins C, Gleave ME, Wang Y, Chakravarty D, Schiffman M, Kim R, Campagne F, Robinson BD, Nanus DM, Tagawa ST, Xiang JZ, Smogorzewska A, Demichelis F, Rickman DS, Sboner A, Elemento O, Rubin MA. Whole-Exome Sequencing of Metastatic Cancer and Biomarkers of Treatment Response. JAMA Oncol. 2015;1(4):466-74. Epub 2015/07/17. doi: 10.1001/jamaoncol.2015.1313. PubMed PMID: 26181256; PMCID: 4505739.
13. Roychowdhury S, Iyer MK, Robinson DR, Lonigro RJ, Wu YM, Cao X, Kalyana-Sundaram S, Sam L, Balbin OA, Quist MJ, Barrette T, Everett J, Siddiqui J, Kunju LP, Navone N, Araujo JC, Troncoso P, Logothetis CJ, Innis JW, Smith DC, Lao CD, Kim SY, Roberts JS, Gruber SB, Pienta KJ, Talpaz M, Chinnaiyan AM. Personalized oncology through integrative high-throughput sequencing: a pilot study. Sci Transl Med. 2011;3(111):111ra21. Epub 2011/12/03. doi: 10.1126/scitranslmed.3003161. PubMed PMID: 22133722; PMCID: 3476478.
14. Urba S, Wolf G, Eisbruch A, Worden F, Lee J, Bradford C, Teknos T, Chepeha D, Prince M, Hogikyan N, Taylor J. Single-cycle induction chemotherapy selects patients with advanced laryngeal cancer for combined chemoradiation: a new treatment paradigm. J Clin Oncol. 2006;24(4):593-8. Epub 2005/12/29. doi: 10.1200/jco.2005.01.2047. PubMed PMID: 16380415.
15. Lefebvre JL. Larynx preservation. Curr Opin Oncol. 2012;24(3):218-22. Epub 2012/03/28. doi: 10.1097/CCO.0b013e3283523c95. PubMed PMID: 22450148.
16. Lefebvre JL, Andry G, Chevalier D, Luboinski B, Collette L, Traissac L, de Raucourt D, Langendijk JA. Laryngeal preservation with induction chemotherapy for hypopharyngeal squamous cell carcinoma: 10-year results of EORTC trial 24891. Ann Oncol. 2012;23(10):2708-14. Epub 2012/04/12. doi: 10.1093/annonc/mds065. PubMed PMID: 22492697; PMCID: 3457747.
17. Forastiere AA, Zhang Q, Weber RS, Maor MH, Goepfert H, Pajak TF, Morrison W, Glisson B, Trotti A, Ridge JA, Thorstad W, Wagner H, Ensley JF, Cooper JS. Long-term results of RTOG 91-11: a comparison of three nonsurgical treatment strategies to preserve the larynx in patients with locally advanced larynx cancer. J Clin Oncol. 2013;31(7):845-52. Epub 2012/11/28. doi: 10.1200/jco.2012.43.6097. PubMed PMID: 23182993; PMCID: 3577950.
18. Denaro N, Russi EG, Lefebvre JL, Merlano MC. A systematic review of current and emerging approaches in the field of larynx preservation. Radiother Oncol. 2014;110(1):16-24. Epub 2013/10/22. doi: 10.1016/j.radonc.2013.08.016. PubMed PMID: 24139733.
19. Vainshtein JM, Wu VF, Spector ME, Bradford CR, Wolf GT, Worden FP. Chemoselection: a paradigm for optimization of organ preservation in locally advanced larynx

cancer. Expert Rev Anticancer Ther. 2013;13(9):1053-64. Epub 2013/09/24. doi: 10.1586/14737140.2013.829646. PubMed PMID: 24053204; PMCID: 4264982.
20. Cummings CW, Flint P. Cummings otolaryngology--head & neck surgery. Philadelphia, Penn.: Elsevier Mosby; 2010.
21. Malecki K, Glinski B, Mucha-Malecka A, Rys J, Kruczak A, Roszkowski K, Urbanska-Gasiorowska M, Hetnal M. Prognostic and predictive significance of p53, EGFr, Ki-67 in larynx preservation treatment. Rep Pract Oncol Radiother. 2010;15(4):87-92. Epub 2010/01/01. doi: 10.1016/j.rpor.2010.06.001. PubMed PMID: 24376930; PMCID: 3863202.
22. Bradford CR, Kumar B, Bellile E, Lee J, Taylor J, D'Silva N, Cordell K, Kleer C, Kupfer R, Kumar P, Urba S, Worden F, Eisbruch A, Wolf GT, Teknos TN, Prince ME, Chepeha DB, Hogikyan ND, Moyer JS, Carey TE. Biomarkers in advanced larynx cancer. Laryngoscope. 2014;124(1):179-87. Epub 2013/06/19. doi: 10.1002/lary.24245. PubMed PMID: 23775802; PMCID: 4123871.
23. Sikora MJ, Bauer JA, Verhaegen M, Belbin TJ, Prystowsky MB, Taylor JC, Brenner JC, Wang S, Soengas MS, Bradford CR, Carey TE. Anti-oxidant treatment enhances anti-tumor cytotoxicity of (-)-gossypol. Cancer Biol Ther. 2008;7(5):767-76. Epub 2008/04/01. PubMed PMID: 18376141; PMCID: 4157391.
24. Tillman BN, Yanik M, Birkeland AC, Liu C, Hovelson DH, Cani AK, Palanisamy N, Carskadon S, Carey TE, Bradford CR, Tomlins SA, McHugh JB, Spector ME, Brenner JC. Targeted sequencing of an epidemiologically low risk patient defines Fibroblast Growth Factor Receptor family aberrations as a putative driver of head and neck squamous cell carcinoma. Head & Neck. 2015;In press.
25. Cerami E, Gao J, Dogrusoz U, Gross BE, Sumer SO, Aksoy BA, Jacobsen A, Byrne CJ, Heuer ML, Larsson E, Antipin Y, Reva B, Goldberg AP, Sander C, Schultz N. The cBio Cancer Genomics Portal: An Open Platform for Exploring Multidimensional Cancer Genomics Data. Cancer Discovery. 2012;2(5):401-4. doi: 10.1158/2159-8290.cd-12-0095.
26. Gao J, Aksoy BA, Dogrusoz U, Dresdner G, Gross B, Sumer SO, Sun Y, Jacobsen A, Sinha R, Larsson E, Cerami E, Sander C, Schultz N. Integrative analysis of complex cancer genomics and clinical profiles using the cBioPortal. Sci Signal. 2013;6(269):pl1. Epub 2013/04/04. doi: 10.1126/scisignal.2004088. PubMed PMID: 23550210; PMCID: 4160307.
27. Pickering CR, Zhang J, Yoo SY, Bengtsson L, Moorthy S, Neskey DM, Zhao M, Ortega Alves MV, Chang K, Drummond J, Cortez E, Xie TX, Zhang D, Chung W, Issa JP, Zweidler-McKay PA, Wu X, El-Naggar AK, Weinstein JN, Wang J, Muzny DM, Gibbs RA, Wheeler DA, Myers JN, Frederick MJ. Integrative genomic characterization of oral squamous cell carcinoma identifies frequent somatic drivers. Cancer Discov. 2013;3(7):770-81. Epub 2013/04/27. doi: 10.1158/2159-8290.cd-12-0537. PubMed PMID: 23619168; PMCID: 3858325.
28. Mutational landscape of gingivo-buccal oral squamous cell carcinoma reveals new recurrently-mutated genes and molecular subgroups. Nat Commun. 2013;4:2873. Epub 2013/12/03. doi: 10.1038/ncomms3873. PubMed PMID: 24292195; PMCID: 3863896.
29. Fakhry C, Westra WH, Li S, Cmelak A, Ridge JA, Pinto H, Forastiere A, Gillison ML. Improved Survival of Patients With Human Papillomavirus–Positive Head and Neck Squamous Cell Carcinoma in a Prospective Clinical Trial. Journal of the National Cancer Institute. 2008;100(4):261-9. doi: 10.1093/jnci/djn011.
30. Vokes EE, Agrawal N, Seiwert TY. HPV-Associated Head and Neck Cancer. Journal of the National Cancer Institute. 2015;107(12). doi: 10.1093/jnci/djv344.

31. Torrente MC, Rodrigo JP, Haigentz M, Jr., Dikkers FG, Rinaldo A, Takes RP, Olofsson J, Ferlito A. Human papillomavirus infections in laryngeal cancer. Head Neck. 2011;33(4):581-6. Epub 2010/09/18. doi: 10.1002/hed.21421. PubMed PMID: 20848441.
32. Garcia-Milian R, Hernandez H, Panade L, Rodriguez C, Gonzalez N, Valenzuela C, Arana MD, Perea SE. Detection and typing of human papillomavirus DNA in benign and malignant tumours of laryngeal epithelium. Acta Otolaryngol. 1998;118(5):754-8. Epub 1998/12/05. PubMed PMID: 9840518.
33. Fukushima K, Ogura H, Watanabe S, Yabe Y, Masuda Y. Human papillomavirus type 16 DNA detected by the polymerase chain reaction in non-cancer tissues of the head and neck. Eur Arch Otorhinolaryngol. 1994;251(2):109-12. Epub 1994/01/01. PubMed PMID: 8024757.
34. Rihkanen H, Peltomaa J, Syrjanen S. Prevalence of human papillomavirus (HPV) DNA in vocal cords without laryngeal papillomas. Acta Otolaryngol. 1994;114(3):348-51. Epub 1994/05/01. PubMed PMID: 8073869.
35. Smith EM, Summersgill KF, Allen J, Hoffman HT, McCulloch T, Turek LP, Haugen TH. Human papillomavirus and risk of laryngeal cancer. Ann Otol Rhinol Laryngol. 2000;109(11):1069-76. Epub 2000/11/23. PubMed PMID: 11090000.
36. Wiest T, Schwarz E, Enders C, Flechtenmacher C, Bosch FX. Involvement of intact HPV16 E6/E7 gene expression in head and neck cancers with unaltered p53 status and perturbed pRb cell cycle control. Oncogene. 2002;21(10):1510-7. Epub 2002/03/16. doi: 10.1038/sj.onc.1205214. PubMed PMID: 11896579.
37. zur Hausen H. Papillomaviruses and cancer: from basic studies to clinical application. Nat Rev Cancer. 2002;2(5):342-50.
38. Robinson M, Sloan P, Shaw R. Refining the diagnosis of oropharyngeal squamous cell carcinoma using human papillomavirus testing. Oral Oncol. 2010;46(7):492-6. Epub 2010/03/17. doi: 10.1016/j.oraloncology.2010.02.013. PubMed PMID: 20227331.
39. Druker BJ, Talpaz M, Resta DJ, Peng B, Buchdunger E, Ford JM, Lydon NB, Kantarjian H, Capdeville R, Ohno-Jones S, Sawyers CL. Efficacy and Safety of a Specific Inhibitor of the BCR-ABL Tyrosine Kinase in Chronic Myeloid Leukemia. New England Journal of Medicine. 2001;344(14):1031-7. doi: doi:10.1056/NEJM200104053441401. PubMed PMID: 11287972.
40. Vogel CL, Cobleigh MA, Tripathy D, Gutheil JC, Harris LN, Fehrenbacher L, Slamon DJ, Murphy M, Novotny WF, Burchmore M, Shak S, Stewart SJ, Press M. Efficacy and safety of trastuzumab as a single agent in first-line treatment of HER2-overexpressing metastatic breast cancer. J Clin Oncol. 2002;20(3):719-26. Epub 2002/02/01. PubMed PMID: 11821453.
41. Lynch TJ, Bell DW, Sordella R, Gurubhagavatula S, Okimoto RA, Brannigan BW, Harris PL, Haserlat SM, Supko JG, Haluska FG, Louis DN, Christiani DC, Settleman J, Haber DA. Activating Mutations in the Epidermal Growth Factor Receptor Underlying Responsiveness of Non–Small-Cell Lung Cancer to Gefitinib. New England Journal of Medicine. 2004;350(21):2129-39. doi: doi:10.1056/NEJMoa040938. PubMed PMID: 15118073.
42. Engelman JA, Luo J, Cantley LC. The evolution of phosphatidylinositol 3-kinases as regulators of growth and metabolism. Nat Rev Genet. 2006;7(8):606-19. Epub 2006/07/19. doi: 10.1038/nrg1879. PubMed PMID: 16847462.
43. Samuels Y, Wang Z, Bardelli A, Silliman N, Ptak J, Szabo S, Yan H, Gazdar A, Powell SM, Riggins GJ, Willson JK, Markowitz S, Kinzler KW, Vogelstein B, Velculescu VE. High frequency of mutations of the PIK3CA gene in human cancers. Science. 2004;304(5670):554. Epub 2004/03/16. doi: 10.1126/science.1096502. PubMed PMID: 15016963.

44. Engelman JA. Targeting PI3K signalling in cancer: opportunities, challenges and limitations. Nat Rev Cancer. 2009;9(8):550-62.
45. Chang MT, Asthana S, Gao SP, Lee BH, Chapman JS, Kandoth C, Gao J, Socci ND, Solit DB, Olshen AB, Schultz N, Taylor BS. Identifying recurrent mutations in cancer reveals widespread lineage diversity and mutational specificity. Nat Biotechnol. 2015. Epub 2015/12/01. doi: 10.1038/nbt.3391. PubMed PMID: 26619011.
46. Kang S, Bader AG, Vogt PK. Phosphatidylinositol 3-kinase mutations identified in human cancer are oncogenic. Proc Natl Acad Sci U S A. 2005;102(3):802-7. Epub 2005/01/14. doi: 10.1073/pnas.0408864102. PubMed PMID: 15647370; PMCID: 545580.
47. Torti D, Trusolino L. Oncogene addiction as a foundational rationale for targeted anti-cancer therapy: promises and perils. EMBO Molecular Medicine. 2011;3(11):623-36. doi: 10.1002/emmm.201100176. PubMed PMID: PMC3377106.
48. Garnett MJ, Edelman EJ, Heidorn SJ, Greenman CD, Dastur A, Lau KW, Greninger P, Thompson IR, Luo X, Soares J, Liu Q, Iorio F, Surdez D, Chen L, Milano RJ, Bignell GR, Tam AT, Davies H, Stevenson JA, Barthorpe S, Lutz SR, Kogera F, Lawrence K, McLaren-Douglas A, Mitropoulos X, Mironenko T, Thi H, Richardson L, Zhou W, Jewitt F, Zhang T, O'Brien P, Boisvert JL, Price S, Hur W, Yang W, Deng X, Butler A, Choi HG, Chang JW, Baselga J, Stamenkovic I, Engelman JA, Sharma SV, Delattre O, Saez-Rodriguez J, Gray NS, Settleman J, Futreal PA, Haber DA, Stratton MR, Ramaswamy S, McDermott U, Benes CH. Systematic identification of genomic markers of drug sensitivity in cancer cells. Nature. 2012;483(7391):570-5. Epub 2012/03/31. doi: 10.1038/nature11005. PubMed PMID: 22460902; PMCID: 3349233.
49. Mazumdar T, Byers LA, Ng PK, Mills GB, Peng S, Diao L, Fan YH, Stemke-Hale K, Heymach JV, Myers JN, Glisson BS, Johnson FM. A comprehensive evaluation of biomarkers predictive of response to PI3K inhibitors and of resistance mechanisms in head and neck squamous cell carcinoma. Mol Cancer Ther. 2014;13(11):2738-50. Epub 2014/09/07. doi: 10.1158/1535-7163.mct-13-1090. PubMed PMID: 25193510; PMCID: 4221385.
50. Lui VW, Hedberg ML, Li H, Vangara BS, Pendleton K, Zeng Y, Lu Y, Zhang Q, Du Y, Gilbert BR, Freilino M, Sauerwein S, Peyser ND, Xiao D, Diergaarde B, Wang L, Chiosea S, Seethala R, Johnson JT, Kim S, Duvvuri U, Ferris RL, Romkes M, Nukui T, Kwok-Shing Ng P, Garraway LA, Hammerman PS, Mills GB, Grandis JR. Frequent mutation of the PI3K pathway in head and neck cancer defines predictive biomarkers. Cancer Discov. 2013;3(7):761-9. Epub 2013/04/27. doi: 10.1158/2159-8290.cd-13-0103. PubMed PMID: 23619167; PMCID: 3710532.
51. Janku F, Tsimberidou AM, Garrido-Laguna I, Wang X, Luthra R, Hong DS, Naing A, Falchook GS, Moroney JW, Piha-Paul SA, Wheler JJ, Moulder SL, Fu S, Kurzrock R. PIK3CA mutations in patients with advanced cancers treated with PI3K/AKT/mTOR axis inhibitors. Mol Cancer Ther. 2011;10(3):558-65. Epub 2011/01/11. doi: 10.1158/1535-7163.mct-10-0994. PubMed PMID: 21216929; PMCID: 3072168.
52. Janku F, Wheler JJ, Naing A, Falchook GS, Hong DS, Stepanek VM, Fu S, Piha-Paul SA, Lee JJ, Luthra R, Tsimberidou AM, Kurzrock R. PIK3CA mutation H1047R is associated with response to PI3K/AKT/mTOR signaling pathway inhibitors in early-phase clinical trials. Cancer Res. 2013;73(1):276-84. Epub 2012/10/16. doi: 10.1158/0008-5472.can-12-1726. PubMed PMID: 23066039; PMCID: 3537862.
53. Engelman JA, Chen L, Tan X, Crosby K, Guimaraes AR, Upadhyay R, Maira M, McNamara K, Perera SA, Song Y, Chirieac LR, Kaur R, Lightbown A, Simendinger J, Li T, Padera RF, Garcia-Echeverria C, Weissleder R, Mahmood U, Cantley LC, Wong KK. Effective

use of PI3K and MEK inhibitors to treat mutant Kras G12D and PIK3CA H1047R murine lung cancers. Nat Med. 2008;14(12):1351-6. Epub 2008/11/26. doi: 10.1038/nm.1890. PubMed PMID: 19029981; PMCID: 2683415.
54. Ihle NT, Lemos R, Jr., Wipf P, Yacoub A, Mitchell C, Siwak D, Mills GB, Dent P, Kirkpatrick DL, Powis G. Mutations in the phosphatidylinositol-3-kinase pathway predict for antitumor activity of the inhibitor PX-866 whereas oncogenic Ras is a dominant predictor for resistance. Cancer Res. 2009;69(1):143-50. Epub 2009/01/02. doi: 10.1158/0008-5472.can-07-6656. PubMed PMID: 19117997; PMCID: 2613546.
55. Yarbrough WG, Shores C, Witsell DL, Weissler MC, Fidler ME, Gilmer TM. ras mutations and expression in head and neck squamous cell carcinomas. Laryngoscope. 1994;104(11 Pt 1):1337-47. Epub 1994/11/01. doi: 10.1288/00005537-199411000-00005. PubMed PMID: 7968162.
56. Matsuda H, Konishi N, Hiasa Y, Hayashi I, Tsuzuki T, Tao M, Kitahori Y, Yoshioka N, Kirita T, Sugimura M. Alterations of p16/CDKN2, p53 and ras genes in oral squamous cell carcinomas and premalignant lesions. J Oral Pathol Med. 1996;25(5):232-8. Epub 1996/05/01. PubMed PMID: 8835820.
57. Bissada E, Abboud O, Abou Chacra Z, Guertin L, Weng X, Nguyen-Tan PF, Tabet JC, Thibaudeau E, Lambert L, Audet ML, Fortin B, Soulieres D. Prevalence of K-RAS Codons 12 and 13 Mutations in Locally Advanced Head and Neck Squamous Cell Carcinoma and Impact on Clinical Outcomes. Int J Otolaryngol. 2013;2013:848021. Epub 2013/06/06. doi: 10.1155/2013/848021. PubMed PMID: 23737793; PMCID: 3657450.
58. Woenckhaus J, Steger K, Werner E, Fenic I, Gamerdinger U, Dreyer T, Stahl U. Genomic gain of PIK3CA and increased expression of p110alpha are associated with progression of dysplasia into invasive squamous cell carcinoma. The Journal of Pathology. 2002;198(3):335-42. doi: 10.1002/path.1207.
59. Ozanne B, Richards CS, Hendler F, Burns D, Gusterson B. Over-expression of the EGF receptor is a hallmark of squamous cell carcinomas. J Pathol. 1986;149(1):9-14. Epub 1986/05/01. doi: 10.1002/path.1711490104. PubMed PMID: 2425067.
60. Grandis JR, Tweardy DJ. Elevated levels of transforming growth factor alpha and epidermal growth factor receptor messenger RNA are early markers of carcinogenesis in head and neck cancer. Cancer Res. 1993;53(15):3579-84. Epub 1993/08/01. PubMed PMID: 8339264.
61. Hynes NE, Lane HA. ERBB receptors and cancer: the complexity of targeted inhibitors. Nat Rev Cancer. 2005;5(5):341-54. Epub 2005/05/03. doi: 10.1038/nrc1609. PubMed PMID: 15864276.
62. Holbro T, Civenni G, Hynes NE. The ErbB receptors and their role in cancer progression. Exp Cell Res. 2003;284(1):99-110. Epub 2003/03/22. PubMed PMID: 12648469.
63. Bonner JA, Harari PM, Giralt J, Azarnia N, Shin DM, Cohen RB, Jones CU, Sur R, Raben D, Jassem J, Ove R, Kies MS, Baselga J, Youssoufian H, Amellal N, Rowinsky EK, Ang KK. Radiotherapy plus cetuximab for squamous-cell carcinoma of the head and neck. N Engl J Med. 2006;354(6):567-78. Epub 2006/02/10. doi: 10.1056/NEJMoa053422. PubMed PMID: 16467544.
64. Leemans CR, Braakhuis BJ, Brakenhoff RH. The molecular biology of head and neck cancer. Nat Rev Cancer. 2011;11(1):9-22. Epub 2010/12/17. doi: 10.1038/nrc2982. PubMed PMID: 21160525.
65. Birkeland AC, Ludwig ML, Meraj TS, Brenner JC, Prince ME. The Tip of the Iceberg: Clinical Implications of Genomic Sequencing Projects in Head and Neck Cancer. Cancers

(Basel). 2015;7(4):2094-109. Epub 2015/10/28. doi: 10.3390/cancers7040879. PubMed PMID: 26506389.
66. Birkeland AC, Yanik M, Tillman BN, Scott MV, Foltin SK, Mann JE, Michmerhuizen NL, Ludwig ML, Sandelski MM, Komarck CM, Carey TE, Prince M, Bradford CR, McHugh JB, Spector ME, Brenner JC. Identification of Targetable HER2 Aberrations in Head and Neck Squamous Cell Carcinoma. JAMA Oncol. 2015;*In press*.
67. Fabbri G, Rasi S, Rossi D, Trifonov V, Khiabanian H, Ma J, Grunn A, Fangazio M, Capello D, Monti S, Cresta S, Gargiulo E, Forconi F, Guarini A, Arcaini L, Paulli M, Laurenti L, Larocca LM, Marasca R, Gattei V, Oscier D, Bertoni F, Mullighan CG, Foa R, Pasqualucci L, Rabadan R, Dalla-Favera R, Gaidano G. Analysis of the chronic lymphocytic leukemia coding genome: role of NOTCH1 mutational activation. J Exp Med. 2011;208(7):1389-401. Epub 2011/06/15. doi: 10.1084/jem.20110921. PubMed PMID: 21670202; PMCID: 3135373.
68. Santagata S, Demichelis F, Riva A, Varambally S, Hofer MD, Kutok JL, Kim R, Tang J, Montie JE, Chinnaiyan AM, Rubin MA, Aster JC. JAGGED1 expression is associated with prostate cancer metastasis and recurrence. Cancer Res. 2004;64(19):6854-7. Epub 2004/10/07. doi: 10.1158/0008-5472.can-04-2500. PubMed PMID: 15466172.
69. Wang NJ, Sanborn Z, Arnett KL, Bayston LJ, Liao W, Proby CM, Leigh IM, Collisson EA, Gordon PB, Jakkula L, Pennypacker S, Zou Y, Sharma M, North JP, Vemula SS, Mauro TM, Neuhaus IM, Leboit PE, Hur JS, Park K, Huh N, Kwok PY, Arron ST, Massion PP, Bale AE, Haussler D, Cleaver JE, Gray JW, Spellman PT, South AP, Aster JC, Blacklow SC, Cho RJ. Loss-of-function mutations in Notch receptors in cutaneous and lung squamous cell carcinoma. Proc Natl Acad Sci U S A. 2011;108(43):17761-6. Epub 2011/10/19. doi: 10.1073/pnas.1114669108. PubMed PMID: 22006338; PMCID: 3203814.
70. Nickoloff BJ, Qin JZ, Chaturvedi V, Denning MF, Bonish B, Miele L. Jagged-1 mediated activation of notch signaling induces complete maturation of human keratinocytes through NF-kappaB and PPARgamma. Cell Death Differ. 2002;9(8):842-55. Epub 2002/07/11. doi: 10.1038/sj.cdd.4401036. PubMed PMID: 12107827.
71. Nicolas M, Wolfer A, Raj K, Kummer JA, Mill P, van Noort M, Hui CC, Clevers H, Dotto GP, Radtke F. Notch1 functions as a tumor suppressor in mouse skin. Nat Genet. 2003;33(3):416-21. Epub 2003/02/19. doi: 10.1038/ng1099. PubMed PMID: 12590261.
72. Kwon C, Cheng P, King IN, Andersen P, Shenje L, Nigam V, Srivastava D. Notch post-translationally regulates [beta]-catenin protein in stem and progenitor cells. Nat Cell Biol. 2011;13(10):1244-51. doi: http://www.nature.com/ncb/journal/v13/n10/abs/ncb2313.html#supplementary-information.
73. Polakis P. Wnt signaling in cancer. Cold Spring Harb Perspect Biol. 2012;4(5). Epub 2012/03/23. doi: 10.1101/cshperspect.a008052. PubMed PMID: 22438566; PMCID: 3331705.
74. Liu J, Pan S, Hsieh MH, Ng N, Sun F, Wang T, Kasibhatla S, Schuller AG, Li AG, Cheng D, Li J, Tompkins C, Pferdekamper A, Steffy A, Cheng J, Kowal C, Phung V, Guo G, Wang Y, Graham MP, Flynn S, Brenner JC, Li C, Villarroel MC, Schultz PG, Wu X, McNamara P, Sellers WR, Petruzzelli L, Boral AL, Seidel HM, McLaughlin ME, Che J, Carey TE, Vanasse G, Harris JL. Targeting Wnt-driven cancer through the inhibition of Porcupine by LGK974. Proc Natl Acad Sci U S A. 2013;110(50):20224-9. Epub 2013/11/28. doi: 10.1073/pnas.1314239110. PubMed PMID: 24277854; PMCID: 3864356.
75. Sun W, Gaykalova DA, Ochs MF, Mambo E, Arnaoutakis D, Liu Y, Loyo M, Agrawal N, Howard J, Li R, Ahn S, Fertig E, Sidransky D, Houghton J, Buddavarapu K, Sanford T, Choudhary A, Darden W, Adai A, Latham G, Bishop J, Sharma R, Westra WH, Hennessey P,

Chung CH, Califano JA. Activation of the NOTCH pathway in head and neck cancer. Cancer Res. 2014;74(4):1091-104. Epub 2013/12/20. doi: 10.1158/0008-5472.can-13-1259. PubMed PMID: 24351288; PMCID: 3944644.
76. Birkeland AC, Brenner JC. Personalizing Medicine in Head and Neck Squamous Cell Carcinoma: The Rationale for Combination Therapies. Medical Research Archives. 2015(3).
77. Finn RS, Crown JP, Lang I, Boer K, Bondarenko IM, Kulyk SO, Ettl J, Patel R, Pinter T, Schmidt M, Shparyk Y, Thummala AR, Voytko NL, Fowst C, Huang X, Kim ST, Randolph S, Slamon DJ. The cyclin-dependent kinase 4/6 inhibitor palbociclib in combination with letrozole versus letrozole alone as first-line treatment of oestrogen receptor-positive, HER2-negative, advanced breast cancer (PALOMA-1/TRIO-18): a randomised phase 2 study. The Lancet Oncology.16(1):25-35. doi: 10.1016/s1470-2045(14)71159-3.
78. Hanahan D, Weinberg RA. Hallmarks of cancer: the next generation. Cell. 2011;144(5):646-74. doi: 10.1016/j.cell.2011.02.013. PubMed PMID: 21376230.
79. Dunn GP, Bruce AT, Ikeda H, Old LJ, Schreiber RD. Cancer immunoediting: from immunosurveillance to tumor escape. Nature immunology. 2002;3(11):991-8. doi: 10.1038/ni1102-991. PubMed PMID: 12407406.
80. Leibowitz MS, Andrade Filho PA, Ferrone S, Ferris RL. Deficiency of activated STAT1 in head and neck cancer cells mediates TAP1-dependent escape from cytotoxic T lymphocytes. Cancer immunology, immunotherapy : CII. 2011;60(4):525-35. doi: 10.1007/s00262-010-0961-7. PubMed PMID: 21207025; PMCID: 3426276.
81. Leibowitz MS, Srivastava RM, Andrade Filho PA, Egloff AM, Wang L, Seethala RR, Ferrone S, Ferris RL. SHP2 is overexpressed and inhibits pSTAT1-mediated APM component expression, T-cell attracting chemokine secretion, and CTL recognition in head and neck cancer cells. Clinical cancer research : an official journal of the American Association for Cancer Research. 2013;19(4):798-808. doi: 10.1158/1078-0432.CCR-12-1517. PubMed PMID: 23363816; PMCID: 3578140.
82. Mizukami Y, Kono K, Maruyama T, Watanabe M, Kawaguchi Y, Kamimura K, Fujii H. Downregulation of HLA Class I molecules in the tumour is associated with a poor prognosis in patients with oesophageal squamous cell carcinoma. British journal of cancer. 2008;99(9):1462-7. doi: 10.1038/sj.bjc.6604715. PubMed PMID: 18841157; PMCID: 2579690.
83. Ogino T, Shigyo H, Ishii H, Katayama A, Miyokawa N, Harabuchi Y, Ferrone S. HLA class I antigen down-regulation in primary laryngeal squamous cell carcinoma lesions as a poor prognostic marker. Cancer Res. 2006;66(18):9281-9. doi: 10.1158/0008-5472.CAN-06-0488. PubMed PMID: 16982773.
84. Ferris RL, Whiteside TL, Ferrone S. Immune escape associated with functional defects in antigen-processing machinery in head and neck cancer. Clinical cancer research : an official journal of the American Association for Cancer Research. 2006;12(13):3890-5. doi: 10.1158/1078-0432.CCR-05-2750. PubMed PMID: 16818683.
85. Pak AS, Wright MA, Matthews JP, Collins SL, Petruzzelli GJ, Young MR. Mechanisms of immune suppression in patients with head and neck cancer: presence of CD34(+) cells which suppress immune functions within cancers that secrete granulocyte-macrophage colony-stimulating factor. Clinical cancer research : an official journal of the American Association for Cancer Research. 1995;1(1):95-103. PubMed PMID: 9815891.
86. Ostrand-Rosenberg S, Sinha P. Myeloid-derived suppressor cells: linking inflammation and cancer. Journal of immunology. 2009;182(8):4499-506. doi: 10.4049/jimmunol.0802740. PubMed PMID: 19342621; PMCID: 2810498.

87. Jebreel A, Mistry D, Loke D, Dunn G, Hough V, Oliver K, Stafford N, Greenman J. Investigation of interleukin 10, 12 and 18 levels in patients with head and neck cancer. The Journal of laryngology and otology. 2007;121(3):246-52. doi: 10.1017/S0022215106002428. PubMed PMID: 17040593.
88. Cheng F, Wang HW, Cuenca A, Huang M, Ghansah T, Brayer J, Kerr WG, Takeda K, Akira S, Schoenberger SP, Yu H, Jove R, Sotomayor EM. A critical role for Stat3 signaling in immune tolerance. Immunity. 2003;19(3):425-36. PubMed PMID: 14499117.
89. Lyford-Pike S, Peng S, Young GD, Taube JM, Westra WH, Akpeng B, Bruno TC, Richmon JD, Wang H, Bishop JA, Chen L, Drake CG, Topalian SL, Pardoll DM, Pai SI. Evidence for a role of the PD-1:PD-L1 pathway in immune resistance of HPV-associated head and neck squamous cell carcinoma. Cancer Res. 2013;73(6):1733-41. doi: 10.1158/0008-5472.CAN-12-2384. PubMed PMID: 23288508; PMCID: 3602406.
90. Badoual C, Hans S, Merillon N, Van Ryswick C, Ravel P, Benhamouda N, Levionnois E, Nizard M, Si-Mohamed A, Besnier N, Gey A, Rotem-Yehudar R, Pere H, Tran T, Guerin CL, Chauvat A, Dransart E, Alanio C, Albert S, Barry B, Sandoval F, Quintin-Colonna F, Bruneval P, Fridman WH, Lemoine FM, Oudard S, Johannes L, Olive D, Brasnu D, Tartour E. PD-1-expressing tumor-infiltrating T cells are a favorable prognostic biomarker in HPV-associated head and neck cancer. Cancer Res. 2013;73(1):128-38. doi: 10.1158/0008-5472.CAN-12-2606. PubMed PMID: 23135914.
91. Jie HB, Schuler PJ, Lee SC, Srivastava RM, Argiris A, Ferrone S, Whiteside TL, Ferris RL. CTLA-4(+) Regulatory T Cells Increased in Cetuximab-Treated Head and Neck Cancer Patients Suppress NK Cell Cytotoxicity and Correlate with Poor Prognosis. Cancer Res. 2015;75(11):2200-10. doi: 10.1158/0008-5472.CAN-14-2788. PubMed PMID: 25832655; PMCID: 4452385.
92. Ramsay AG. Immune checkpoint blockade immunotherapy to activate anti-tumour T-cell immunity. British journal of haematology. 2013;162(3):313-25. doi: 10.1111/bjh.12380. PubMed PMID: 23691926.
93. Gettinger SN, Horn L, Gandhi L, Spigel DR, Antonia SJ, Rizvi NA, Powderly JD, Heist RS, Carvajal RD, Jackman DM, Sequist LV, Smith DC, Leming P, Carbone DP, Pinder-Schenck MC, Topalian SL, Hodi FS, Sosman JA, Sznol M, McDermott DF, Pardoll DM, Sankar V, Ahlers CM, Salvati M, Wigginton JM, Hellmann MD, Kollia GD, Gupta AK, Brahmer JR. Overall Survival and Long-Term Safety of Nivolumab (Anti-Programmed Death 1 Antibody, BMS-936558, ONO-4538) in Patients With Previously Treated Advanced Non-Small-Cell Lung Cancer. J Clin Oncol. 2015;33(18):2004-12. doi: 10.1200/JCO.2014.58.3708. PubMed PMID: 25897158; PMCID: 4672027.
94. Larkin J, Chiarion-Sileni V, Gonzalez R, Grob JJ, Cowey CL, Lao CD, Schadendorf D, Dummer R, Smylie M, Rutkowski P, Ferrucci PF, Hill A, Wagstaff J, Carlino MS, Haanen JB, Maio M, Marquez-Rodas I, McArthur GA, Ascierto PA, Long GV, Callahan MK, Postow MA, Grossmann K, Sznol M, Dreno B, Bastholt L, Yang A, Rollin LM, Horak C, Hodi FS, Wolchok JD. Combined Nivolumab and Ipilimumab or Monotherapy in Untreated Melanoma. N Engl J Med. 2015;373(1):23-34. doi: 10.1056/NEJMoa1504030. PubMed PMID: 26027431.
95. Weber JS, D'Angelo SP, Minor D, Hodi FS, Gutzmer R, Neyns B, Hoeller C, Khushalani NI, Miller WH, Jr., Lao CD, Linette GP, Thomas L, Lorigan P, Grossmann KF, Hassel JC, Maio M, Sznol M, Ascierto PA, Mohr P, Chmielowski B, Bryce A, Svane IM, Grob JJ, Krackhardt AM, Horak C, Lambert A, Yang AS, Larkin J. Nivolumab versus chemotherapy in patients with advanced melanoma who progressed after anti-CTLA-4 treatment (CheckMate 037): a

randomised, controlled, open-label, phase 3 trial. The Lancet Oncology. 2015;16(4):375-84. doi: 10.1016/S1470-2045(15)70076-8. PubMed PMID: 25795410.
96. Ribas A, Puzanov I, Dummer R, Schadendorf D, Hamid O, Robert C, Hodi FS, Schachter J, Pavlick AC, Lewis KD, Cranmer LD, Blank CU, O'Day SJ, Ascierto PA, Salama AK, Margolin KA, Loquai C, Eigentler TK, Gangadhar TC, Carlino MS, Agarwala SS, Moschos SJ, Sosman JA, Goldinger SM, Shapira-Frommer R, Gonzalez R, Kirkwood JM, Wolchok JD, Eggermont A, Li XN, Zhou W, Zernhelt AM, Lis J, Ebbinghaus S, Kang SP, Daud A. Pembrolizumab versus investigator-choice chemotherapy for ipilimumab-refractory melanoma (KEYNOTE-002): a randomised, controlled, phase 2 trial. The Lancet Oncology. 2015;16(8):908-18. doi: 10.1016/S1470-2045(15)00083-2. PubMed PMID: 26115796.
97. Brahmer J, Reckamp KL, Baas P, Crino L, Eberhardt WE, Poddubskaya E, Antonia S, Pluzanski A, Vokes EE, Holgado E, Waterhouse D, Ready N, Gainor J, Aren Frontera O, Havel L, Steins M, Garassino MC, Aerts JG, Domine M, Paz-Ares L, Reck M, Baudelet C, Harbison CT, Lestini B, Spigel DR. Nivolumab versus Docetaxel in Advanced Squamous-Cell Non-Small-Cell Lung Cancer. N Engl J Med. 2015;373(2):123-35. doi: 10.1056/NEJMoa1504627. PubMed PMID: 26028407; PMCID: 4681400.
98. Garon EB, Rizvi NA, Hui R, Leighl N, Balmanoukian AS, Eder JP, Patnaik A, Aggarwal C, Gubens M, Horn L, Carcereny E, Ahn MJ, Felip E, Lee JS, Hellmann MD, Hamid O, Goldman JW, Soria JC, Dolled-Filhart M, Rutledge RZ, Zhang J, Lunceford JK, Rangwala R, Lubiniecki GM, Roach C, Emancipator K, Gandhi L, Investigators K-. Pembrolizumab for the Treatment of Non-Small-Cell Lung Cancer. N Engl J Med. 2015. doi: 10.1056/NEJMoa1501824. PubMed PMID: 25891174.
99. Motzer RJ, Escudier B, McDermott DF, George S, Hammers HJ, Srinivas S, Tykodi SS, Sosman JA, Procopio G, Plimack ER, Castellano D, Choueiri TK, Gurney H, Donskov F, Bono P, Wagstaff J, Gauler TC, Ueda T, Tomita Y, Schutz FA, Kollmannsberger C, Larkin J, Ravaud A, Simon JS, Xu LA, Waxman IM, Sharma P, CheckMate I. Nivolumab versus Everolimus in Advanced Renal-Cell Carcinoma. N Engl J Med. 2015;373(19):1803-13. doi: 10.1056/NEJMoa1510665. PubMed PMID: 26406148.
100. Robert C, Schachter J, Long GV, Arance A, Grob JJ, Mortier L, Daud A, Carlino MS, McNeil C, Lotem M, Larkin J, Lorigan P, Neyns B, Blank CU, Hamid O, Mateus C, Shapira-Frommer R, Kosh M, Zhou H, Ibrahim N, Ebbinghaus S, Ribas A, investigators K-. Pembrolizumab versus Ipilimumab in Advanced Melanoma. N Engl J Med. 2015. doi: 10.1056/NEJMoa1503093. PubMed PMID: 25891173.
101. Seiwert TG, S., Mehra R., et al. Antitumor activity and safety of pembrolizumab in patients (pts) with advanced squamous cell carcinoma of the head and neck (scchn): Preliminary results from keynote-012 expansion cohort. J Clin Oncol. 2015;22(suppl; abstr LBA6008).
102. Seiwert TW, J. Eder, J. et. al. Inflamed-phenotype gene expression signatures to predict benefit from the anti-pd-1 antibody pembrolizumab in pd-l1+ head and neck cancer patients. J Clin Oncol. 2015;33(suppl; abstr 6017).
103. Brenner JC, Graham MP, Kumar B, Saunders LM, Kupfer R, Lyons RH, Bradford CR, Carey TE. Genotyping of 73 UM-SCC head and neck squamous cell carcinoma cell lines. Head & Neck. 2010;32(4):417-26. doi: 10.1002/hed.21198. PubMed PMID: PMC3292176.
104. Carey TE, Van Dyke DL, Worsham MJ, Bradford CR, Babu VR, Schwartz DR, Hsu S, Baker SR. Characterization of human laryngeal primary and metastatic squamous cell carcinoma cell lines UM-SCC-17A and UM-SCC-17B. Cancer Res. 1989;49(21):6098-107. Epub 1989/11/01. PubMed PMID: 2790823.

105. Chinn SB, Walline HM, McHugh JB, Prince ME, Carey TE. Prevalence of a HPV Laryngeal Squamous Cell Carcinoma and a Novel Cell Line. Otolaryngology -- Head and Neck Surgery. 2012;147(2 suppl):P173-P4. doi: 10.1177/0194599812451426a154.
106. Tentler JJ, Tan AC, Weekes CD, Jimeno A, Leong S, Pitts TM, Arcaroli JJ, Messersmith WA, Eckhardt SG. Patient-derived tumour xenografts as models for oncology drug development. Nat Rev Clin Oncol. 2012;9(6):338-50. Epub 2012/04/18. doi: 10.1038/nrclinonc.2012.61. PubMed PMID: 22508028; PMCID: 3928688.
107. DeRose YS, Wang G, Lin YC, Bernard PS, Buys SS, Ebbert MT, Factor R, Matsen C, Milash BA, Nelson E, Neumayer L, Randall RL, Stijleman IJ, Welm BE, Welm AL. Tumor grafts derived from women with breast cancer authentically reflect tumor pathology, growth, metastasis and disease outcomes. Nat Med. 2011;17(11):1514-20. Epub 2011/10/25. doi: 10.1038/nm.2454. PubMed PMID: 22019887; PMCID: 3553601.
108. Loukopoulos P, Kanetaka K, Takamura M, Shibata T, Sakamoto M, Hirohashi S. Orthotopic transplantation models of pancreatic adenocarcinoma derived from cell lines and primary tumors and displaying varying metastatic activity. Pancreas. 2004;29(3):193-203. Epub 2004/09/16. PubMed PMID: 15367885.
109. Zhao X, Liu Z, Yu L, Zhang Y, Baxter P, Voicu H, Gurusiddappa S, Luan J, Su JM, Leung HC, Li XN. Global gene expression profiling confirms the molecular fidelity of primary tumor-based orthotopic xenograft mouse models of medulloblastoma. Neuro Oncol. 2012;14(5):574-83. Epub 2012/03/31. doi: 10.1093/neuonc/nos061. PubMed PMID: 22459127; PMCID: 3337308.
110. McEvoy J, Ulyanov A, Brennan R, Wu G, Pounds S, Zhang J, Dyer MA. Analysis of MDM2 and MDM4 single nucleotide polymorphisms, mRNA splicing and protein expression in retinoblastoma. PLoS One. 2012;7(8):e42739. Epub 2012/08/24. doi: 10.1371/journal.pone.0042739. PubMed PMID: 22916154; PMCID: 3423419.
111. Morton CL, Houghton PJ. Establishment of human tumor xenografts in immunodeficient mice. Nat Protoc. 2007;2(2):247-50. Epub 2007/04/05. doi: 10.1038/nprot.2007.25. PubMed PMID: 17406581.
112. Li H, Wheeler S, Park YS, Ju Z, Thomas SM, Fichera M, Egloff AM, Lui VW, Duvvuri U, Bauman JE, Mills GB, Grandis JR. Proteomic Characterization of Head and Neck Cancer Patient-Derived Xenografts. Mol Cancer Res. 2015. Epub 2015/12/20. doi: 10.1158/1541-7786.mcr-15-0354. PubMed PMID: 26685214.
113. Chen J, Milo GE, Shuler CF, Schuller DE. Xenograft growth and histodifferentiation of squamous cell carcinomas of the pharynx and larynx. Oral Surg Oral Med Oral Pathol Oral Radiol Endod. 1996;81(2):197-202. Epub 1996/02/01. PubMed PMID: 8665315.
114. Siolas D, Hannon GJ. Patient-derived tumor xenografts: transforming clinical samples into mouse models. Cancer Res. 2013;73(17):5315-9. Epub 2013/06/05. doi: 10.1158/0008-5472.can-13-1069. PubMed PMID: 23733750; PMCID: 3766500.
115. Lodhia KA, Hadley AM, Haluska P, Scott CL. Prioritizing therapeutic targets using patient-derived xenograft models. Biochimica et Biophysica Acta (BBA) - Reviews on Cancer. 2015;1855(2):223-34. doi: http://dx.doi.org/10.1016/j.bbcan.2015.03.002.
116. Tanguy Y. Seiwert BB, Jared Weiss, Joseph Paul Eder, Jennifer Yearley, Erin Murphy, Michael Nebozhyn, Terri McClanahan, Mark Ayers, Jared K. Lunceford, Ranee Mehra, Karl Heath, Jonathan D. Cheng, Laura Q. Chow; The University of Chicago, Chicago, IL; Yale Cancer Center, Yale School of Medicine, New Haven, CT; Lineberger Comprehensive Cancer Center, University of North Carolina, Chapel Hill, NC; Merck & Co., Inc., Kenilworth, NJ; Fox

Chase Cancer Center, Philadelphia, PA; Department of Medicine, Division of Oncology, University of Washington, Seattle, WA, editor. Inflamed-phenotype gene expression signatures to predict benefit from the anti-PD-1 antibody pembrolizumab in PD-L1+ head and neck cancer patients. 2015 ASCO Annual Meeting; 2015: J Clin Oncol 33, 2015 (suppl; abstr 6017).
117. Birkeland AC, Uhlmann WR, Brenner JC, Shuman AG. Getting personal: Head and neck cancer management in the era of genomic medicine. Head Neck. 2015. Epub 2015/05/23. doi: 10.1002/hed.24132. PubMed PMID: 25995036.
118. Wang T, Wei JJ, Sabatini DM, Lander ES. Genetic screens in human cells using the CRISPR-Cas9 system. Science. 2014;343(6166):80-4. Epub 2013/12/18. doi: 10.1126/science.1246981. PubMed PMID: 24336569; PMCID: 3972032.
119. Shalem O, Sanjana NE, Hartenian E, Shi X, Scott DA, Mikkelsen TS, Heckl D, Ebert BL, Root DE, Doench JG, Zhang F. Genome-scale CRISPR-Cas9 knockout screening in human cells. Science. 2014;343(6166):84-7. Epub 2013/12/18. doi: 10.1126/science.1247005. PubMed PMID: 24336571; PMCID: 4089965.
120. Zhou Y, Zhu S, Cai C, Yuan P, Li C, Huang Y, Wei W. High-throughput screening of a CRISPR/Cas9 library for functional genomics in human cells. Nature. 2014;509(7501):487-91. Epub 2014/04/11. doi: 10.1038/nature13166. PubMed PMID: 24717434.
121. Gilbert LA, Larson MH, Morsut L, Liu Z, Brar GA, Torres SE, Stern-Ginossar N, Brandman O, Whitehead EH, Doudna JA, Lim WA, Weissman JS, Qi LS. CRISPR-mediated modular RNA-guided regulation of transcription in eukaryotes. Cell. 2013;154(2):442-51. Epub 2013/07/16. doi: 10.1016/j.cell.2013.06.044. PubMed PMID: 23849981; PMCID: 3770145.
122. Gilbert LA, Horlbeck MA, Adamson B, Villalta JE, Chen Y, Whitehead EH, Guimaraes C, Panning B, Ploegh HL, Bassik MC, Qi LS, Kampmann M, Weissman JS. Genome-Scale CRISPR-Mediated Control of Gene Repression and Activation. Cell. 2014;159(3):647-61. Epub 2014/10/14. doi: 10.1016/j.cell.2014.09.029. PubMed PMID: 25307932; PMCID: Pmc4253859.
123. Konermann S, Brigham MD, Trevino AE, Joung J, Abudayyeh OO, Barcena C, Hsu PD, Habib N, Gootenberg JS, Nishimasu H, Nureki O, Zhang F. Genome-scale transcriptional activation by an engineered CRISPR-Cas9 complex. Nature. 2015;517(7536):583-8. Epub 2014/12/11. doi: 10.1038/nature14136. PubMed PMID: 25494202; PMCID: 4420636.
124. Zalatan JG, Lee ME, Almeida R, Gilbert LA, Whitehead EH, La Russa M, Tsai JC, Weissman JS, Dueber JE, Qi LS, Lim WA. Engineering complex synthetic transcriptional programs with CRISPR RNA scaffolds. Cell. 2015;160(1-2):339-50. Epub 2014/12/24. doi: 10.1016/j.cell.2014.11.052. PubMed PMID: 25533786; PMCID: 4297522.
125. Shalem O, Sanjana NE, Zhang F. High-throughput functional genomics using CRISPR-Cas9. Nat Rev Genet. 2015;16(5):299-311. Epub 2015/04/10. doi: 10.1038/nrg3899. PubMed PMID: 25854182; PMCID: Pmc4503232.
126. Doench JG, Hartenian E, Graham DB, Tothova Z, Hegde M, Smith I, Sullender M, Ebert BL, Xavier RJ, Root DE. Rational design of highly active sgRNAs for CRISPR-Cas9-mediated gene inactivation. Nat Biotechnol. 2014;32(12):1262-7. Epub 2014/09/04. doi: 10.1038/nbt.3026. PubMed PMID: 25184501; PMCID: Pmc4262738.
127. Hsu PD, Scott DA, Weinstein JA, Ran FA, Konermann S, Agarwala V, Li Y, Fine EJ, Wu X, Shalem O, Cradick TJ, Marraffini LA, Bao G, Zhang F. DNA targeting specificity of RNA-guided Cas9 nucleases. Nat Biotechnol. 2013;31(9):827-32. Epub 2013/07/23. doi: 10.1038/nbt.2647. PubMed PMID: 23873081; PMCID: Pmc3969858.

128. Mohr SE, Hu Y, Ewen-Campen B, Housden BE, Viswanatha R, Perrimon N. CRISPR guide RNA design for research applications. The FEBS Journal. 2016:n/a-n/a. doi: 10.1111/febs.13777.
129. Smith JD, Suresh S, Schlecht U, Wu M, Wagih O, Peltz G, Davis RW, Steinmetz LM, Parts L, St Onge RP. Quantitative CRISPR interference screens in yeast identify chemical-genetic interactions and new rules for guide RNA design. Genome biology. 2016;17:45. Epub 2016/03/10. doi: 10.1186/s13059-016-0900-9. PubMed PMID: 26956608; PMCID: Pmc4784398.
130. Fu Y, Foden JA, Khayter C, Maeder ML, Reyon D, Joung JK, Sander JD. High-frequency off-target mutagenesis induced by CRISPR-Cas nucleases in human cells. Nat Biotechnol. 2013;31(9):822-6. Epub 2013/06/25. doi: 10.1038/nbt.2623. PubMed PMID: 23792628; PMCID: Pmc3773023.
131. Tsai SQ, Zheng Z, Nguyen NT, Liebers M, Topkar VV, Thapar V, Wyvekens N, Khayter C, Iafrate AJ, Le LP, Aryee MJ, Joung JK. GUIDE-seq enables genome-wide profiling of off-target cleavage by CRISPR-Cas nucleases. Nat Biotechnol. 2015;33(2):187-97. Epub 2014/12/17. doi: 10.1038/nbt.3117. PubMed PMID: 25513782; PMCID: Pmc4320685.
132. Fu Y, Sander JD, Reyon D, Cascio VM, Joung JK. Improving CRISPR-Cas nuclease specificity using truncated guide RNAs. Nat Biotechnol. 2014;32(3):279-84. Epub 2014/01/28. doi: 10.1038/nbt.2808. PubMed PMID: 24463574; PMCID: Pmc3988262.
133. Ran FA, Hsu PD, Lin CY, Gootenberg JS, Konermann S, Trevino AE, Scott DA, Inoue A, Matoba S, Zhang Y, Zhang F. Double nicking by RNA-guided CRISPR Cas9 for enhanced genome editing specificity. Cell. 2013;154(6):1380-9. Epub 2013/09/03. doi: 10.1016/j.cell.2013.08.021. PubMed PMID: 23992846; PMCID: Pmc3856256.
134. Mali P, Aach J, Stranges PB, Esvelt KM, Moosburner M, Kosuri S, Yang L, Church GM. CAS9 transcriptional activators for target specificity screening and paired nickases for cooperative genome engineering. Nat Biotechnol. 2013;31(9):833-8. Epub 2013/08/03. doi: 10.1038/nbt.2675. PubMed PMID: 23907171; PMCID: Pmc3818127.
135. Cho SW, Kim S, Kim Y, Kweon J, Kim HS, Bae S, Kim JS. Analysis of off-target effects of CRISPR/Cas-derived RNA-guided endonucleases and nickases. Genome research. 2014;24(1):132-41. Epub 2013/11/21. doi: 10.1101/gr.162339.113. PubMed PMID: 24253446; PMCID: Pmc3875854.
136. Heigwer F, Zhan T, Breinig M, Winter J, Brugemann D, Leible S, Boutros M. CRISPR library designer (CLD): software for multispecies design of single guide RNA libraries. Genome biology. 2016;17:55. Epub 2016/03/26. doi: 10.1186/s13059-016-0915-2. PubMed PMID: 27013184; PMCID: Pmc4807595.
137. Xie S, Shen B, Zhang C, Huang X, Zhang Y. sgRNAcas9: a software package for designing CRISPR sgRNA and evaluating potential off-target cleavage sites. PLoS One. 2014;9(6):e100448. Epub 2014/06/24. doi: 10.1371/journal.pone.0100448. PubMed PMID: 24956386; PMCID: Pmc4067335.
138. Agrotis A, Ketteler R. A new age in functional genomics using CRISPR/Cas9 in arrayed library screening. Frontiers in Genetics. 2015;6:300. doi: 10.3389/fgene.2015.00300. PubMed PMID: PMC4585242.
139. Koike-Yusa H, Li Y, Tan EP, Velasco-Herrera Mdel C, Yusa K. Genome-wide recessive genetic screening in mammalian cells with a lentiviral CRISPR-guide RNA library. Nat Biotechnol. 2014;32(3):267-73. Epub 2014/02/19. doi: 10.1038/nbt.2800. PubMed PMID: 24535568.

140. Wu Y, Zhou L, Wang X, Lu J, Zhang R, Liang X, Wang L, Deng W, Zeng YX, Huang H, Kang T. A genome-scale CRISPR-Cas9 screening method for protein stability reveals novel regulators of Cdc25A. Cell Discov. 2016;2:16014. Epub 2016/07/28. doi: 10.1038/celldisc.2016.14. PubMed PMID: 27462461; PMCID: 4877570.
141. Wallace J, Hu R, Mosbruger TL, Dahlem TJ, Stephens WZ, Rao DS, Round JL, O'Connell RM. Genome-Wide CRISPR-Cas9 Screen Identifies MicroRNAs That Regulate Myeloid Leukemia Cell Growth. PLoS One. 2016;11(4):e0153689. Epub 2016/04/16. doi: 10.1371/journal.pone.0153689. PubMed PMID: 27081855; PMCID: 4833428.
142. Li W, Xu H, Xiao T, Cong L, Love MI, Zhang F, Irizarry RA, Liu JS, Brown M, Liu XS. MAGeCK enables robust identification of essential genes from genome-scale CRISPR/Cas9 knockout screens. Genome biology. 2014;15(12):554. Epub 2014/12/06. doi: 10.1186/s13059-014-0554-4. PubMed PMID: 25476604; PMCID: 4290824.
143. Sims D, Mendes-Pereira AM, Frankum J, Burgess D, Cerone MA, Lombardelli C, Mitsopoulos C, Hakas J, Murugaesu N, Isacke CM, Fenwick K, Assiotis I, Kozarewa I, Zvelebil M, Ashworth A, Lord CJ. High-throughput RNA interference screening using pooled shRNA libraries and next generation sequencing. Genome biology. 2011;12(10):R104. doi: 10.1186/gb-2011-12-10-r104. PubMed PMID: 22018332; PMCID: PMC3333774.
144. Kim J, Tan AC. BiNGS!SL-seq: a bioinformatics pipeline for the analysis and interpretation of deep sequencing genome-wide synthetic lethal screen. Methods in molecular biology (Clifton, NJ). 2012;802:389-98. Epub 2011/12/02. doi: 10.1007/978-1-61779-400-1_26. PubMed PMID: 22130895.
145. Dai Z, Sheridan JM, Gearing LJ, Moore DL, Su S, Wormald S, Wilcox S, O'Connor L, Dickins RA, Blewitt ME, Ritchie ME. edgeR: a versatile tool for the analysis of shRNA-seq and CRISPR-Cas9 genetic screens. F1000Research. 2014;3. doi: 10.12688/f1000research.3928.2. PubMed PMID: 24860646; PMCID: PMC4023662.
146. Wade M. High-Throughput Silencing Using the CRISPR-Cas9 System: A Review of the Benefits and Challenges. J Biomol Screen. 2015. Epub 2015/05/24. doi: 10.1177/1087057115587916. PubMed PMID: 26001564.
147. Taylor J, Woodcock S. A Perspective on the Future of High-Throughput RNAi Screening: Will CRISPR Cut Out the Competition or Can RNAi Help Guide the Way? J Biomol Screen. 2015;20(8):1040-51. Epub 2015/06/07. doi: 10.1177/1087057115590069. PubMed PMID: 26048892.

Chapter 2: The Genomic Landscape of UM-SCC Oral Cavity Squamous Cell Carcinoma Cell Lines

Abstract

Objectives: We sought to describe the genetic complexity of 14 UM-SCC oral cavity cancer cell lines that have remained uncharacterized despite being used as model systems for decades.

Materials and Methods: We performed exome sequencing on 14 oral cavity UM-SCC cell lines and denote the mutational profile of each line. We used a SNP array to profile the multiple copy number variations of each cell line and use immunoblotting to compare alterations to protein expression of commonly amplified genes (*EGFR, PIK3CA, etc.)*. RNA sequencing was performed to characterize the expression of genes with copy number alterations.

Results: The cell lines displayed a highly complex network of genetic aberrations that was consistent with alterations identified in the HNSCC TCGA project including *PIK3CA* amplification, *CDKN2A* deletion, as well as *TP53* and *CASP8* mutations, enabling genetic stratification of each cell line in the panel. Copy number FISH and spectral karyotyping analysis demonstrate that cell lines retain chromosomal heterogeneity.

Conclusions: Collectively, we developed an important resource for future oral cavity HNSCC cell line studies and highlight the complexity of genomic aberrations in cell lines.[3]

Introduction

Head and neck squamous cell carcinomas (HNSCCs) are the sixth most common cancer worldwide and consist of malignant tumors of the oral cavity, oropharynx, hypopharynx, and larynx (1), which are thought to arise due to a variety of etiologic factors including tobacco-exposure, alcohol consumption and high risk human papilloma virus (HPV) infection. Importantly, clinical outcome and treatment course vary by anatomic site with 5-year survival rates ranging from 40-80% depending on stage, subsite, and HPV status. As such, it is important to build models representing each specific HNSCC subsite in order to model differences between subsites. This is especially true for HNSCCs of the oral cavity, which are the most common HNSCCs, have less than 60% overall survival at 5 years (2), and are not currently associated with a high rate of HPV infection. With the results of The Cancer Genome Atlas (3) and other genomic sequencing studies (4-7), the mutational landscape of primary untreated HNSCCs is beginning to be characterized (8). However, there is still a need for follow-up *in vitro* studies to investigate key regulatory pathways, confirm malignant drivers, and discriminate potential therapeutic targets in genetically characterized models.

Indeed, it is clear from early precision medicine literature that the effectiveness of "matched" or "companion" therapies (*e.g.* those that target specific molecular lesions such as Imatinib and *BCR-ABL* gene fusions) can be tissue type specific, which may be due to the

[3] This chapter was published in *Oral Oncology* and completed in collaboration with the following authors: Aditi Kulkarni, Andrew Birkeland, Nicole Michmerhuizen, Susan Foltin, Jacqueline Mann, Rebecca Hoesli, Samantha Devenport, Brittany Jewell, Andrew Shuman, Matthew Spector, Thomas E. Carey, Hui Jiang, and J. Chad Brenner.

inherent genetic complexity or unique compensatory pathways of each cancer type (9). In order to assess potential compensatory pathways for advancing matched therapies across different tissues, cell line models have historically have been valuable tools for investigating the role of focused genetic alterations in tumor behavior and response to therapy, especially for HNSCC (10-13). In particular, the University of Michigan has created a repository of HNSCC cell lines (UM-SCC) (14), which have been extensively used for *in vitro* and *in vivo* modeling of HNSCCs (15). Despite the extensive use of UM-SCCs in the literature and characterization of some lines using cytogenetics and loss of heterozygosity assessments (16-18), full genetic characterization of these cell lines has not yet been performed. Given the potential for wide phenotypic variations based on genetic mutations (19) as well as the move towards genetics based personalized medicine approaches (20-22), it is increasingly important to understand the genetic architecture of cell lines used for *in vitro* studies. While studies have started characterizing the genetic implications of therapeutic response in other cell line models (19, 23-25), this analysis has been limited in HNSCC.

Accordingly, whole exome characterization of UM-SCC cell lines is critical to accurately understand critical pathways and mechanistic factors that may be involved in UM-SCC phenotypes and therapeutic response to advancing precision therapies. In this study, we sought to catalog the mutational landscape of oral cavity UM-SCC cell lines. To identify genetic subsets of the disease that are well- or under-represented by our models, we then classified UM-SCCs based on disruptive genomic events and compared the mutational and copy number profiles in our panel with those of other HNSCC cell lines and primary HNSCCs. Ultimately, characterization of UM-SCCs can potentially identify tumor drivers in cell line models, and

genetic biomarkers for applicability to specific targeted therapies (12) in translational models of HNSCCs.

Materials and Methods

UM-SCC models. Cell lines were derived and characterized in the Head and Neck Oncology laboratory at the University of Michigan after consent of the patient donors (14). The oral cavity cell lines studied in this report were selected from this panel. Cell lines were grown in DMEM with 10% FBS, 7µg/mL penicillin/streptomycin and 1% Non-essential amino acids in 5% CO_2 incubator. Cell lines were maintained in exponential growth phase and whole genomic DNA was isolated using the Qiagen DNeasy kit according to manufacturer's instructions. All cell lines were genotyped as previously described (14).

Exome Sequencing. Exome Capture Library Construction was done using the Roche NimbleGen V2 (44.1 Mbp) Exome Enrichment Kit as described (12) or by using the Roche NimbleGen V3. Paired-end sequencing (2 × 100 bp) of the captured exons was carried out on an Illumina Genome Analyzer IIx Platform. Paired-end sequencing (2 × 150 bp) for NimbleGen V3 libraries on an Illumina HiSEQ 4000 at the University of Michigan DNA sequencing core according to standard protocol.

Variant Calling. Read quality was assessed using FastQC (26). Reads were aligned to hg19 reference genome using BWA v0.7.8 (27). Mapping was followed by marking duplicates using PicardTools v1.79 (Broad Institute). INDEL realignment and base quality score recalibration was done using GATK v3.2-2 (28). Variant calling was performed using the HaplotypeCaller and

Genotype GVCFs following the GATK best practices workflow guideline (29) for jointly calling variants across all samples. To filter low quality calls, Variant Quality Score Recalibration (VQSR) was applied to the variant call set. Since the suggested sample size for applying VQSR is 30, samples from the 1000 genomes project (30) were combined along with our cell lines to reach this sample size. Varseq v1.4.0 (Golden Helix, Inc., Bozeman, MT) was used to annotate and filter the variants of interest. Filters were set to eliminate false positive variant calls due to sequencing artifacts. The variants were required to have 5 or more reads supporting the alternate allele and be found in less than 1% in a normal population according to the 1000 genomes project (30). Additional annotations were included to annotate each alterations with COSMIC and dbSNP, which are provided in the supplement. Intronic and intergenic variants were filtered out with the exception of the variants in splice donor or accepter regions.

Sanger Sequencing Validation. Genomic DNA was isolated following Gentra PureGene protocol (Qiagen) and PCR amplified with Platinum Taq DNA Polymerase High Fidelity (Invitrogen) according to manufacturer's instructions. Primer sequences for *CASP8* are listed in SFig2. PCR products were cloned out using pCR8 TOPO vector (Invitrogen) and submitted for Sanger sequencing at the University of Michigan DNA Sequencing Core on the 3730XL DNA Sequencer (Applied Biosystems). Sequences were aligned using the DNASTAR Lasergene software suite.

Copy Number Analysis. The OncoScan FFPE Assay Kit (Affymetrix) was used to analyze copy number variations in our samples. Due to a lack of matched normal samples for the cell lines, a common issue for most cell lines in culture, the kit uses an internal pooled normal sample as a

comparison to make copy number variation calls. CEL files generated from the kit were combined using the OncoScan Console software to generate OSCHP files. These OSCHP files were then analyzed using the TuScan algorithm of the Nexus Express for OncoScan Software. We also used keratinocyte DNA (ATCC® PCS-200-011) to generate additional OncoScan results as an additional control. We noted that in case of some homozygous deletion calls (CN=0), the B-Allele Frequency plot did not agree with the copy number estimate made by the TuScan algorithm. To provide more accurate copy number calls, we used the presence or absence of exome sequencing reads to validate complete loss of the gene. In cases that we observed a copy number call of zero but the presence of exome sequencing reads, we modified the copy number in **Table 2-6** to one copy, noted with an asterisk.

Western blot Analysis. Western blot analysis was performed as previously described (31). Briefly, UM-SCC cell lines at 70-80% confluency were rinsed with PBS and lysed in buffer (150 mM NaCl, 10% Glycerol, 1% NP40, 0.1% Triton X-100, 1 mM PIPES, 1 mM MgCl, 50 mM Tris) containing protease and phosphatase inhibitors (Thermo 186129, 1861277) as described (32). See **Table 2-7** for primary and secondary antibodies used.

Spectral Karyotyping, Cell lines in exponential growth phase were treated with Colcemid to capture metaphases. SKY images of UM-SCC-69 and UM-SCC-92 were then prepared and imaged by the Molecular Cytogenetic Core at Albert Einstein College of Medicine using Applied Spectral Imaging's protocol for DNA spectral karyotyping hybridization and detection.

Fluorescent In-Situ Hybridization. Cell lines UM-SCC-92 ad UM-SCC-97 were treated with Colcemid to arrest cells in metaphase as previously described by our group (31). Slides were prepared and then probed for EGFR or RB1 with respective chromosome controls (Empire Genomics). Representative images were taken on Leica SP8 confocal.

RNA Sequencing and Bioinformatic Analysis. RNA isolated with the Qiagen Allprep kit was submit to the University of Michigan DNA Sequencing core and processed using the Illumina HiSeq 4000 by paired end 75nt sequencing. Libraries were prepared according to manufacturer's protocols with the Illumina Total RNA kit. Read quality was assessed for each cohort using FastQC (v0.11.5). No quality issues were detected in the sample set. Read alignment was performed using STAR (v2.5.3a) according to the two-step alignment protocol recommended in the user manual. Cufflinks (v2.2.1) was used to compute FPKM and values were loaded into MEV for visualization of relative expression between models.

Results

We first performed exome sequencing on 14 UM-SCC cell lines from patients with oral cavity SCC. This patient cohort consists of a mix of seven men and seven women with stage II through stage IV oral cavity cancers arising at a variety of oral cavity sites. Six patients (4 female, 2 male) were under age 40 (range 26-39yrs) and eight patients (5 male, 3 female) were 58 years of age or older (range 58-76) (**Table 2-1**). Our analysis found a large mutational load with over 1300 non-synonymous variants per cell line (**Fig 2-1**, **Table 2-2**, **Table 2-3**), but as with many cell line studies was limited by a lack of normal controls for each cell line model accounting for the large number of mutation calls relative to those in tumor samples from the TCGA.

Nonetheless, we characterized common aberrations found in oral cavity HNSCC tumors in the data set. Similar to TCGA HNSCC tumor studies, we found high frequencies of mutations in 13/14 (93%) affecting *TP53*, 6/14 (43%), affecting *NOTCH1*, and 5/14 (36%) affecting *CDKN2A* (**Fig 2-2**). Mutations found in other oral cavity lines from a previous study (25) are in provided **Fig 2-3**. In our panel, we observed a range of mutations occurring in the coding regions and in splice sites as well as several frameshift alterations in common tumor suppressor genes like *NOTCH1* and *CASP8*. We validated a set of these mutations by Sanger sequencing for *CASP8* and *CDKN2A* (**Fig 2-4**). To then define copy number alterations in these models, we performed high density SNP arrays on all 14 oral cavity cell lines. Analysis of all 14 cell lines by summing copy number alterations at each specific SNP probe site demonstrated copy number common in oral cavity HNSCC. These include amplifications of chromosome 3q, 11q13 and 20, and loss of 3p, 8p, and 18q (**Fig 2-5A**). Genome wide analysis was performed for each cell line and demonstrated numerous differences in each cell line model (**Fig 2-6**), and held true when compared to an additional keratinocyte control (**Fig 2-7**). At the gene level, we identified frequent focal copy number variations in several canonical HNSCC genes, including amplifications of *EGFR* and deletions of *CDKN2A*. The copy number calls of our panel in relation to a list of commonly altered genes in HNSCC as identified from TCGA is shown in **Fig 2-5B**, and shows complex copy number profiles for each of our cell lines.

To then associate copy number outliers with protein expression in the cell line panel, we performed Western blot analysis on several proposed HNSCC oncogenic drivers with substantial copy number alterations across the panel. We observed that cell lines with the highest copy number amplification of *EGFR*, UM-SCC-59 and -69, also had the highest protein expression (**Fig 2-5C**). In contrast, *PIK3CA* copy number did not result in dramatic variance of the

functional protein p110α. As *PIK3CA* is contained within the larger 3q amplicon, and focal *PIK3CA* amplifications are rare in HNSCC tumors, these data suggest that 3q amplification is not necessarily a marker for *PIK3CA* protein overexpression in the cell line models. Importantly, signaling downstream of these common tyrosine kinase aberrations through AKT, ERK, and MEK pathways were present in all cell lines assessed (**Fig 2-5C**). Accordingly, p53 expression is generally associated with mutations as wild type p53 is degraded by MDM2 in normal culture conditions. Our protein expression data was consistent with this postulate as the wild type cell line and those with splice site mutations did not express p53 protein. Similarly, the RNAseq data further validated our copy number calls from above as cell lines with at least one copy of *CDKN2A,* such as UM-SCC-43, -110 expressed *CDKN2A,* and cell lines with no copies of *CDKN2A* (UM-SCC-49, -55) did not express the gene (**Fig 2-8**).

Surprisingly, the copy number analysis revealed that some chromosomes had uneven distributions in each cell line. For example, in UM-SCC-92, *EGFR* located on chromosome 7 was found an average of 2.33 times suggesting that some cells may contain 3 copies or more and others just 2 or fewer copies. Similarly, UM-SCC-69 contained 15.67 copies of EGFR. Given the apparent mixed chromosome content of some cell lines, it is likely that the cell lines contain heterogeneous populations with genetic diversity within each cell line population. We postulate that within the populations, driving genetic lesions will be found in all cells while passenger mutations would reside in only sub-populations. Thus, we analyzed the chromosomal content and fusion status of two representative cell lines from our collection, UM-SCC-69 and UM-SCC-92, by spectral karyotyping to determine the distribution on chromosome content between individual cells in each model (**Fig 2-5D**). This analysis demonstrated that UM-SCC-69 cells contained an average of 129 chromosomes, while UM-SCC-92 contained 71 chromosomes.

These data were also consistent with the complexity of copy number data from the SNP arrays. For example, while most cells analyzed from the UM-SCC-92 population contained 3 copies of chromosome 1, 2/10 cells had 4 copies, 1/10 cells had 2 copies, and 2/10 cells harbored unique translocations of chromosome 1 to chromosomes 9 and 15, respectively t(1;9;15)(**Table 2-4, 2-5**). We also identified a recurrent chromosome 5 to 17 translocation t(5;17) that was present in 10/10 UM-SCC-92 cells, though we did not identify any additional translocations that were present in all cells from the population in UM-SCC-69. This suggests that no initiating translocations were responsible for transformation of this model, though we did identify highly recurrent translocations in both models such as t(17,1) in 6/10 UM-SCC-69 cells and t(7,8) in 9/10 UM-SCC-92 cells. In addition, we performed FISH to evaluate the potential heterogeneity of two genes, *EGFR* and *RB1*, in two of our cells lines and found that we indeed had cells with differing copy numbers of genes, suggesting heterogeneity persisting in the cell lines (**Fig 2-9**). Collectively, these data support the concept that the UM-SCC cell lines contain heterogeneous populations of tumor cells even after several passages in long term cell culture.

With this understanding, we then summarized the overall representation of genetic events in our cell line panel as compared to the representation of events in the HNSCC TCGA data. This demonstrated that the disruptive genomic events found in our UM-SCC oral cavity collection represent a highly complex genetic distribution than is generally not found in primary untreated tumors, but could be more consistent with advanced HNSCC cases. In analyzing key pathways of oncogenesis similar to TCGA, we found that while there are some commonalities across all models (*PIK3CA*, *E2F1*, and *TP63* amplifications were common) most events are a mixture of possible gain or loss of function aberration (**Fig 2-10**). For example, the tumor

suppressor *FAT1*, an inhibitor of Wnt/β-catenin signaling, is found to be amplified, deleted, or mutated across multiple cell lines.

Discussion

The UM-SCC cell line panel was developed over the past 40 years at the University of Michigan from over 100 different donors (14, 33-37) and has available citations dating back to 1983. Here, we have characterized the molecular landscape of 14 of the most highly utilized oral cavity UM-SCC models. In the precision medicine era, comprehensive genetic sub-stratification of known driver mutations is critical in order to identify how and where to strategically plan targeted therapies (38). *In vitro* experiments with cell lines are critical to identifying genetic profiles and connecting subsets to therapeutic responses. Until now, however, genetic characterization of the UM-SCC cell line panel has been limited despite their wide-ranging use as models for HNSCCs.

An important finding of this study is the limited genetic diversity observed amongst the existing cell line panel as compared to global distributions of common genetic drivers. For example, *PIK3CA* alterations in HNSCC range from 0-70% globally depending on cohort (39), but occur in 100% of our models. In contrast, we and others have recently described activating genetic alterations to *ERBB2* (HER2) and *FGFR1* that occur in both epidemiologically low risk and high risk HNSCC populations (31, 40-44); interestingly, these genes harbored activating genetic alterations in 10/14 and 3/14 cell lines, respectively. This data suggests a need to continue deriving cell lines representative of different ethnic and genetic sub-groups to more accurately model the complexity of genetic alterations observed in oral cavity HNSCC.

Moving forward, studies of genetic heterogeneity and tumor evolution are becoming increasingly prevalent as sequencing and single cell technologies become more tenable. The data generated in this report suggest that the UM-SCC cell lines retain a high level of genetic heterogeneity which has both advantages and disadvantages for *in vitro* experiments. The use of CRISPR technology to knockout multiple alleles of a gene, for example, could produce clones that may not represent the whole cell line population. In short term experiments, genetic heterogeneity is unlikely to play a major role in outcomes, which may be hypothesized to relate to the primary driver mutations with which each cell line is characterized. However, in long-term culture experiments, such as selection of therapy resistant clones, genetic heterogeneity of the cell lines may play a profound effect similar to the *in vivo* clonal evolution of tumors following treatment. Further follow up from single cell analysis techniques (45, 46) could be very interesting in exploring this cell line heterogeneity we observed, especially over time. Nonetheless, these consequences of the genetic heterogeneity in the HNSCC remain to be explored, though previous work has shown that cell lines reflect the cytogenetic changes that are present in the tumor tissue from which they were developed (47, 48).

The data collected here suggest that many of the highly recurrent aberrations found in the HNSCC TCGA project are well represented in the UM-SCC oral cavity cell line panel. Interestingly, the distribution of mutations is distinctive. Whereas most primary untreated HNSCC tumors contain a single aberration in multiple pathways (*e.g. EGFR* amplification OR *PIK3CA* amplification plus *CDKN2A* deletion OR *CCND1* (Cyclin D1) amplification), the majority of cell lines harbor multiple aberrations in a single pathway (*e.g. EGFR* amplification AND *PIK3CA* amplification plus *CDKN2A* deletion AND *CCND1* (Cyclin D1) amplification). Whether this is associated with selection of successful adaptation to *in vitro* culture or represents

the evolution of the tumor within the patient is unknown, but suggests that the cell lines represent a highly complex and genetically distinct subset of HNSCC tumors. This subset may be of particular use in representing responses in a more metastatic setting, in which the tumor may have acquired additional mutations, than of modeling the phenotypes of primary patient tumors. Sequencing patients in a metastatic setting, and understanding the genomic landscape of those tumors, will be particularly interesting in comparison. Despite this observation of mutation accumulation, a subset of cell lines such as UM-SCC-108, contain fewer established "driver" aberrations than other models and begin to add to the genetic diversity of the panel.

Collectively, this panel of UM-SCC oral cavity cell lines has immense utility for studies of HNSCC as evidenced by the vast array of publications from labs around the world over the past four decades. We report comprehensive genetic characterizations on the models that can be leveraged to validate cell line identity and just as importantly to put individual studies in the context of genetic alterations. Our study shows that UM-SCC oral cavity cell lines contain models with an array of genetic alterations that are commonly found in HNSCC, and suggests that the field may benefit from the derivation of additional models with unique genetics. As we strive towards improved personalized medicine protocols for HNSCC patients, the cell lines continue to represent important models for discovery of both HNSCC pathogenesis and therapeutic protocols that aim to improve overall survival.

Acknowledgements

The authors thank Drs. Carol R Bradford and Mark EP Prince for their support on this project and manuscript.

Figures

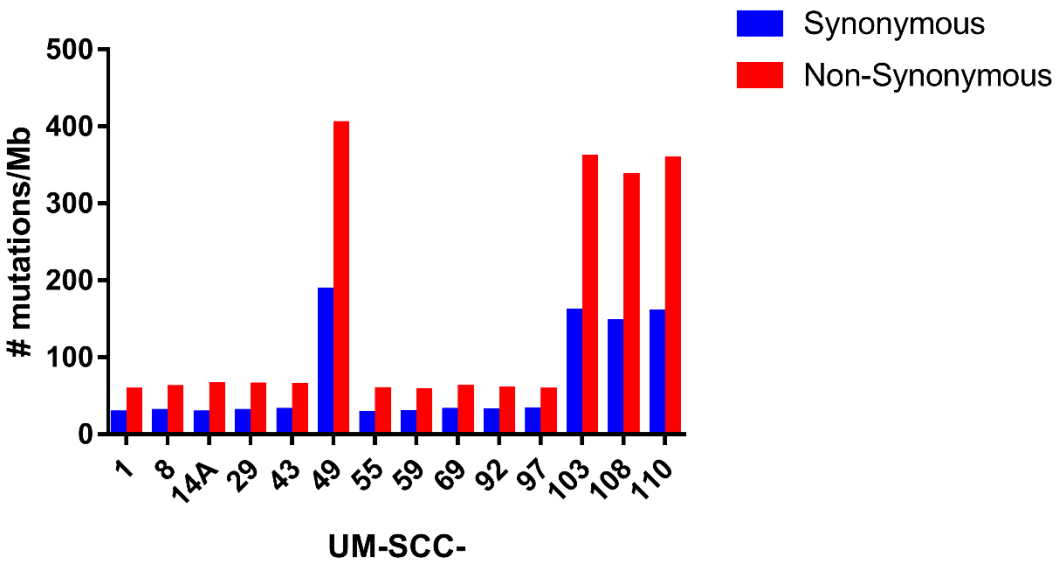

Figure 2-1. Mutation load in UM-SCC lines

For each UM-SCCC cell line, exome sequencing identified many synonymous (blue) and non-synonymous (mutations). The total number of mutations for each category is normalized by dividing over the sequencing target regions in megabase (Mb).

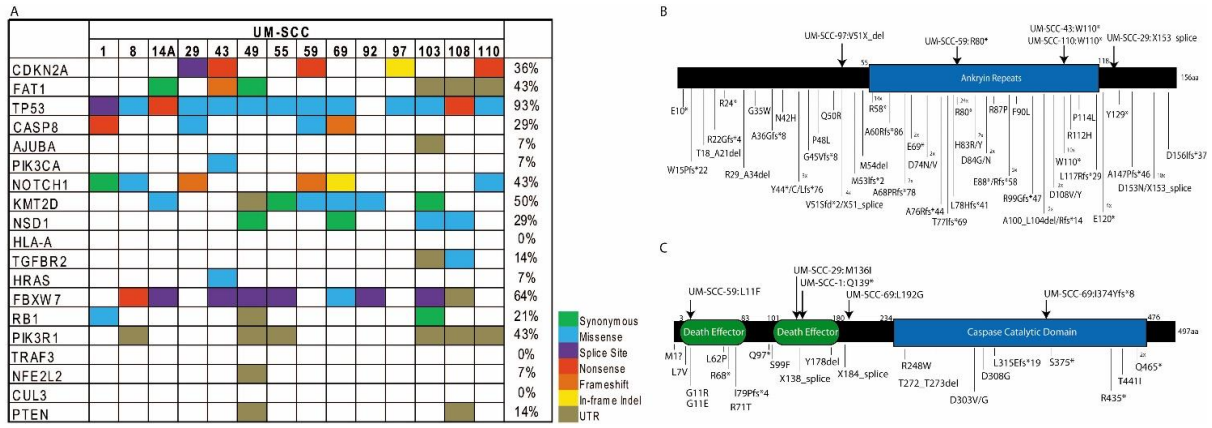

Figure 2-2. Single nucleotide variants identified in the UM-SCC oral cavity cell line panel

(A) Mutations in oral cavity UM-SCC cell lines were annotated by color code as indicated as called from Nimblegen capture-based exome sequencing. The mutation list contains the common single nucleotide variants identified in the HNSCC TCGA project, and the percentage of cell lines with mutation in each gene is shown on the right. Schematics were created to show the distribution of mutations found in **(B)** *CDKN2A* or **(C)** *CASP8* in the UM-SCC oral cavity cell lines (top) or in the HNSCC TCGA data set (bottom). Numbers next to individual mutations indicate the number of independent tissue samples in which each specific mutation was identified if it was recurrently mutated.

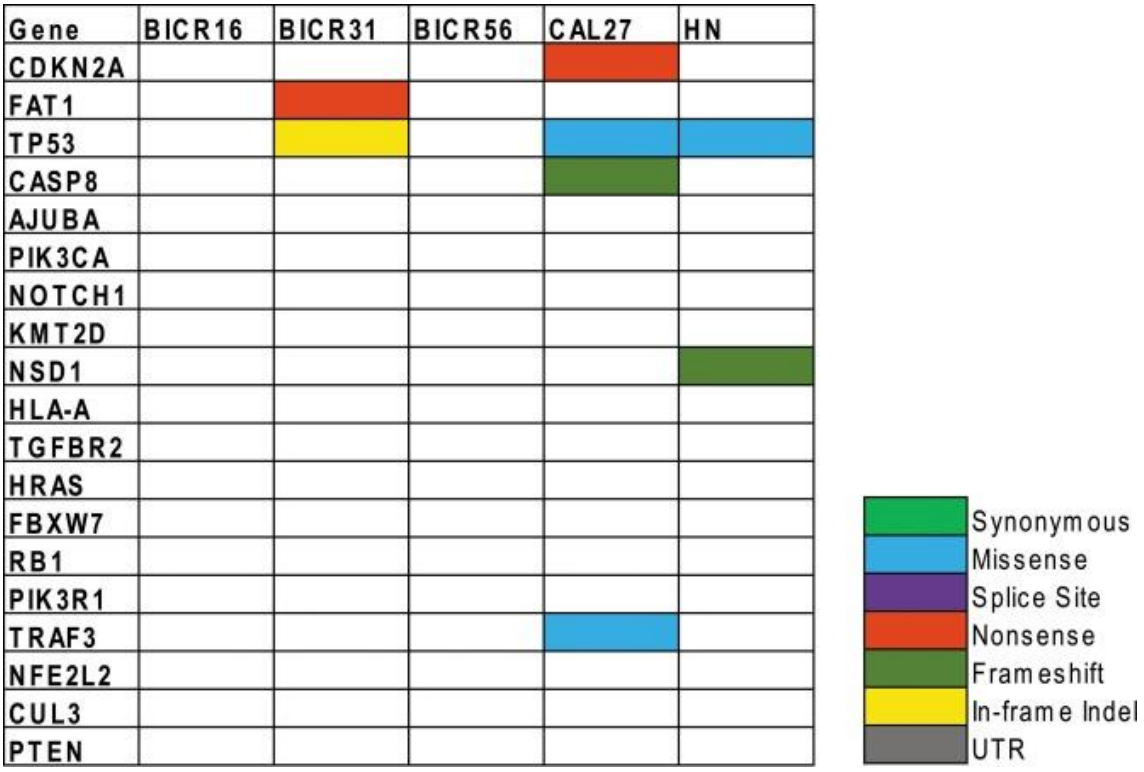

Figure 2-3. Single nucleotide variants for non-UM-SCC oral cavity cell lines

Mutation calls for other publicly availably oral cavity cell lines. The genes chosen are the same in Figure 1-2 for comparison.

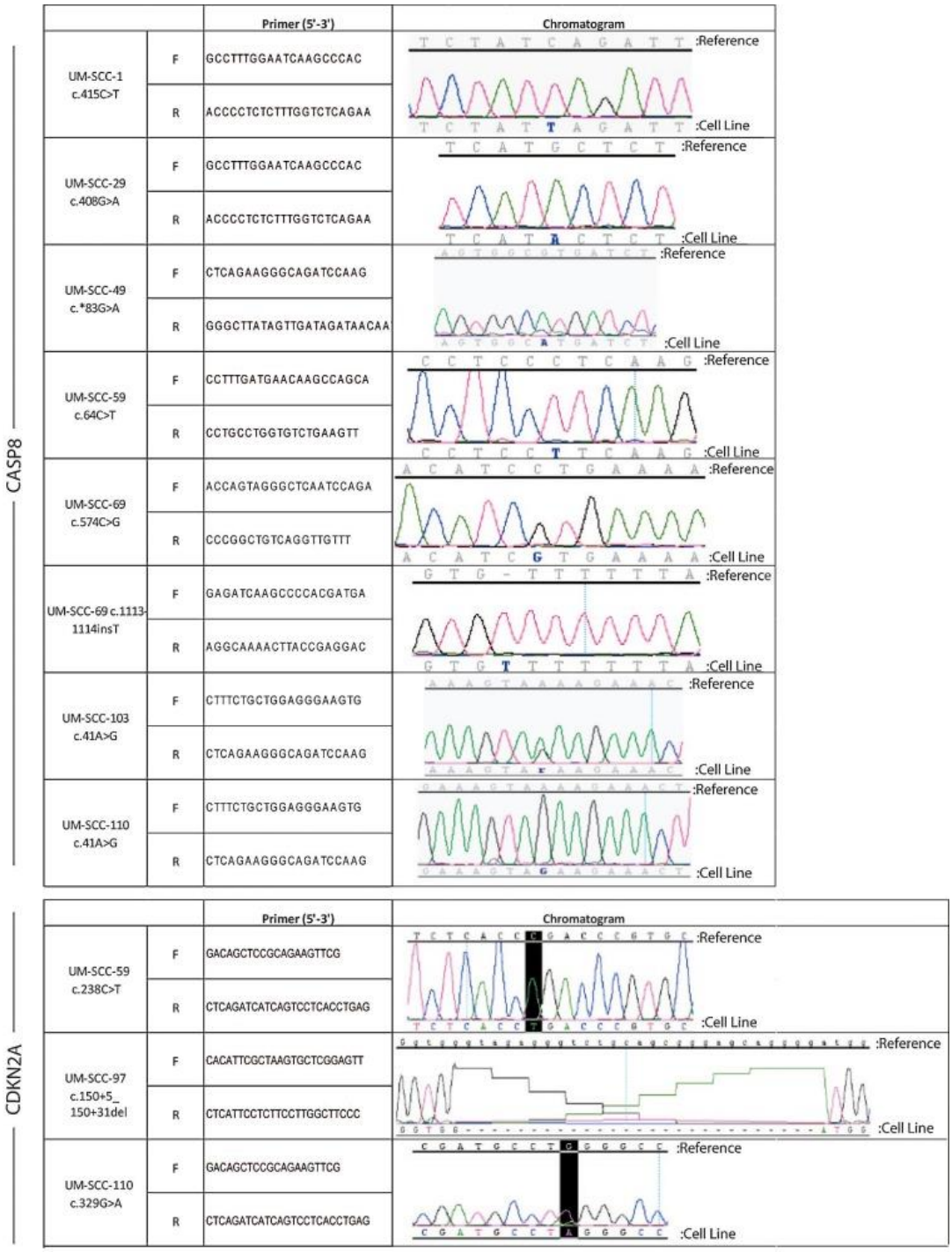

Figure 2-4. Sanger sequencing validation of mutations

Sanger sequencing validation of *CASP8* and *CDKN2A* mutations. The UM-SCC cell line and identified genetic mutation is shown in the left column. The primer sequences and a section of the chromatograms from aligning PCR products with wildtype *CASP8* are shown. Only the mutation-containing allele is shown, with the altered base shown in blue.

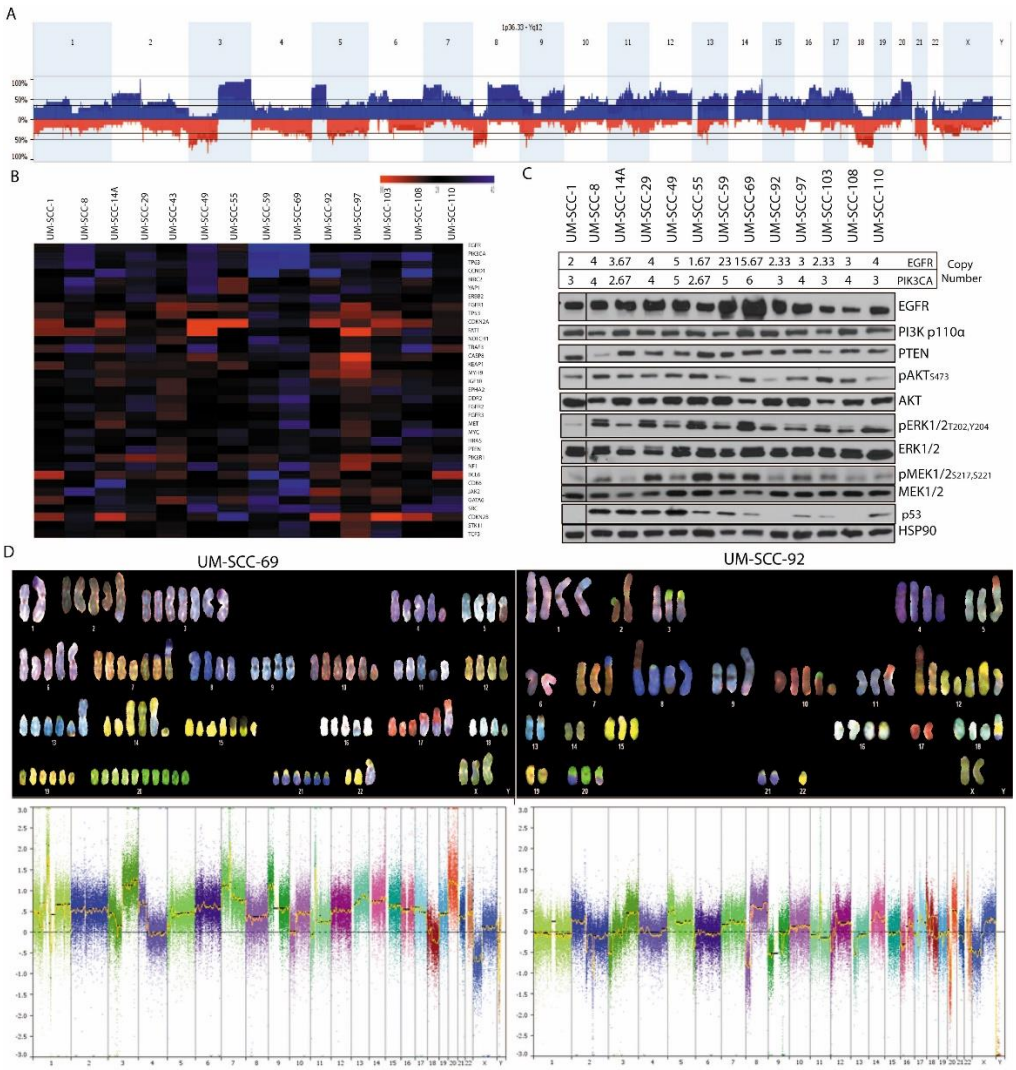

Figure 2-5. Genetic heterogeneity of UM-SCC oral cavity cell lines characterized by copy number alterations

(A) Genomic DNA from low passage cell lines was analyzed with high density SNP arrays and compared to a commercially available pooled control. Copy number alterations were called using Affymetrix software and average copy number calls were annotated. This panel shows a summary of genetic alterations summed across the entire UM-SCC oral cavity cell line panel. Amplifications (blue) and deletions (red) were annotated. **(B)** Copy number variations of genes commonly altered in the HNSCC TCGA project are shown for each of the oral cavity cell lines using the probe medians. **(C)** Protein isolated from the cell line panel was used to perform Western blot analysis for several highly recurrent genetic drivers that are amplified in the cell lines including *EGFR*, *PIK3CA* and their downstream effectors as indicated. Estimated copy number values by the TuScan algorithm for *EGFR* and *PIK3CA* are shown above the Western blots. Representative blots are shown for each image. **(D)** Spectral Karyotyping (SKY) of UM-SCC-69 and UM-SCC-92 cells (top panel) and respective high density copy number plots from SNP array data (bottom panel). We performed SKY analysis on 10 individual cells from both cell lines and a representative image is shown for each line.

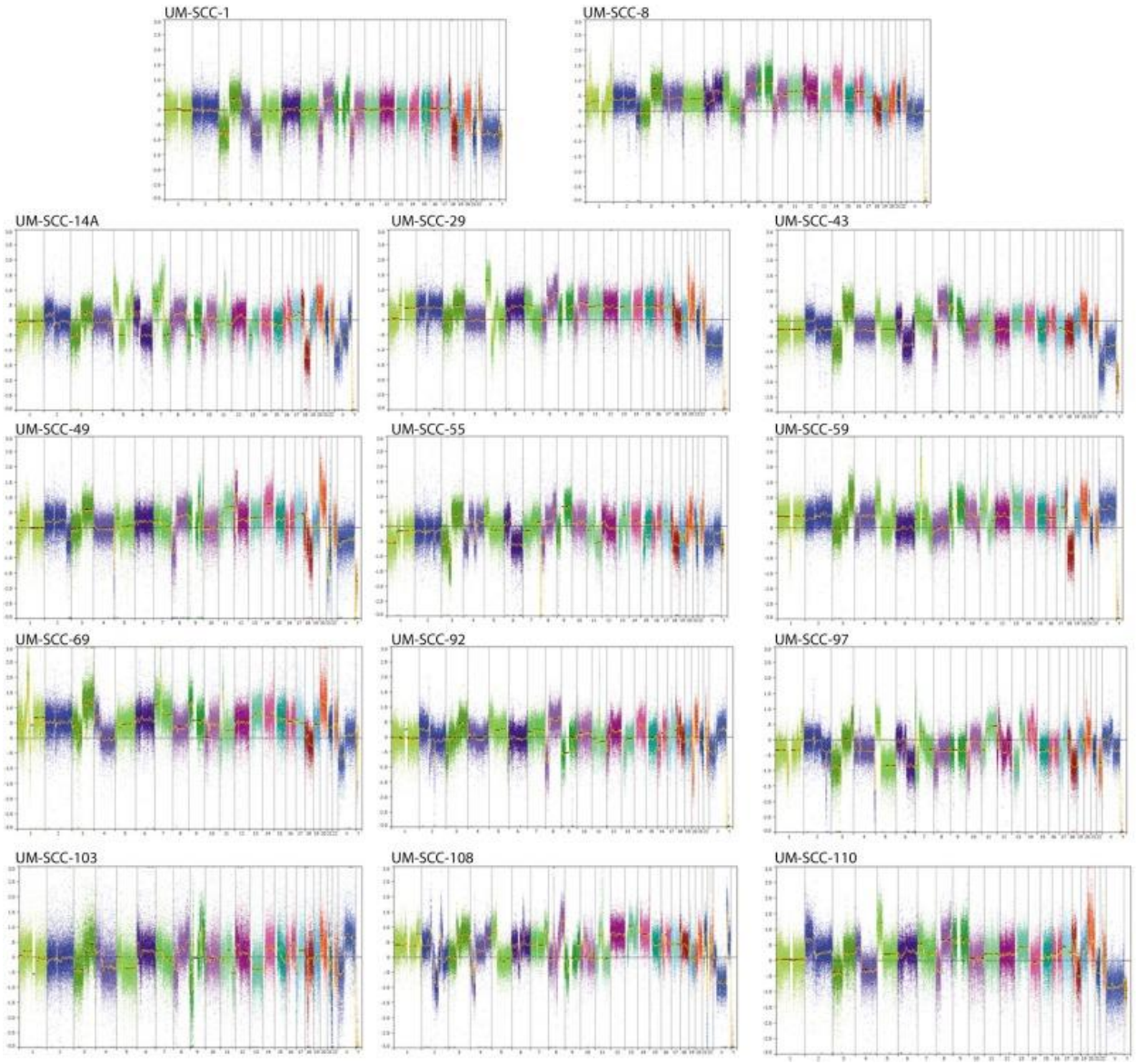

Figure 2-6. Genome-wdie view of copy number alterations for oral cavity UM-SCC cell lines

Genome-wide view of copy number alterations for each UM-SCC cell line. Each plot depicts the intensities of the probes from OncoScan. The zero centered on the y-axis of each plot represents a neutral copy number, with amplifications and deletions depicted above and below.

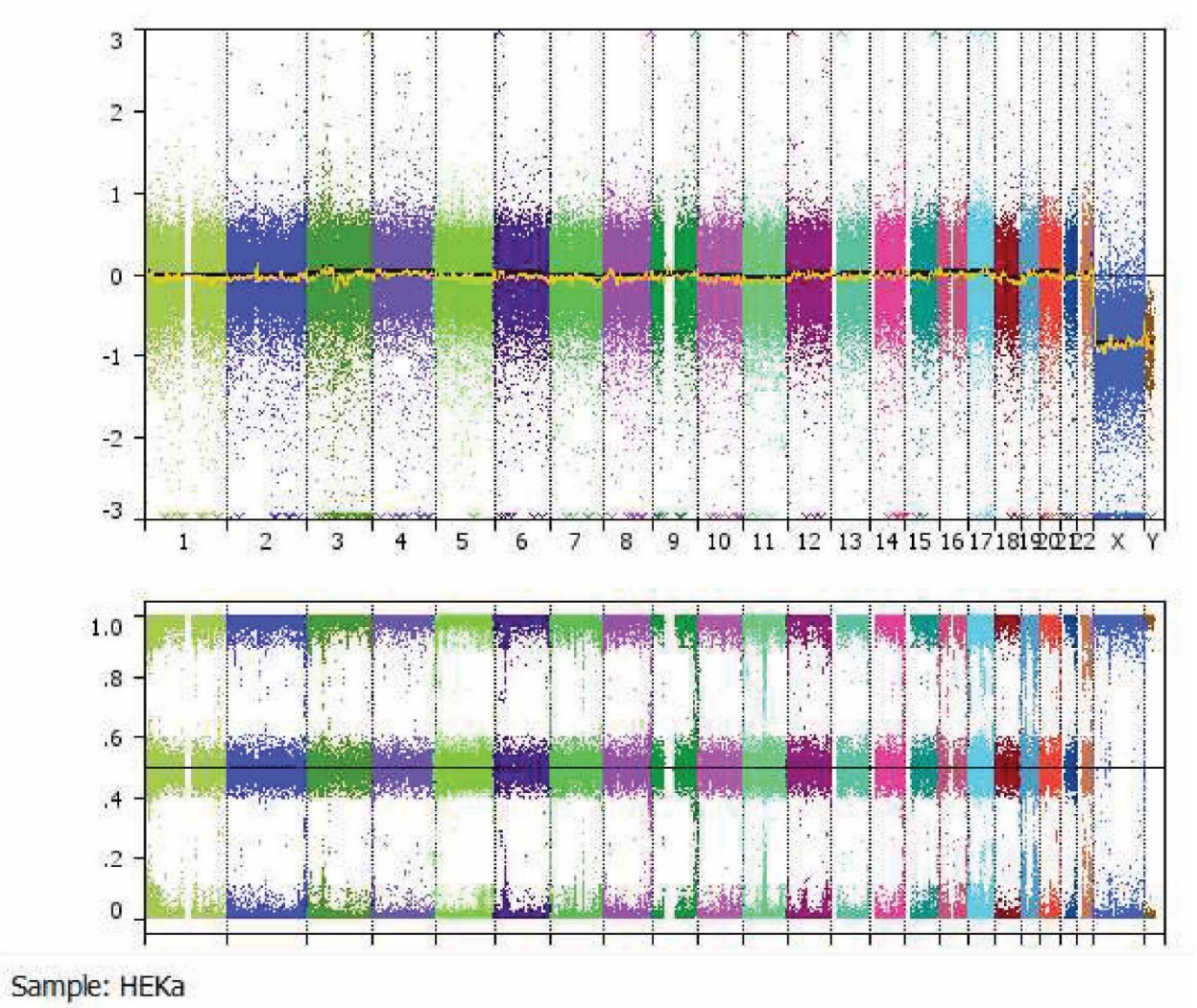

Figure 2-7. Copy number calls from normalized keratinocytes HEKa

Genome-wide view of copy number alterations normalized keratinocytes HEKa . Plot depicts the intensities of the probes from OncoScan. The zero centered on the y-axis of each plot represents a neutral copy number, with amplifications and deletions depicted above and below.

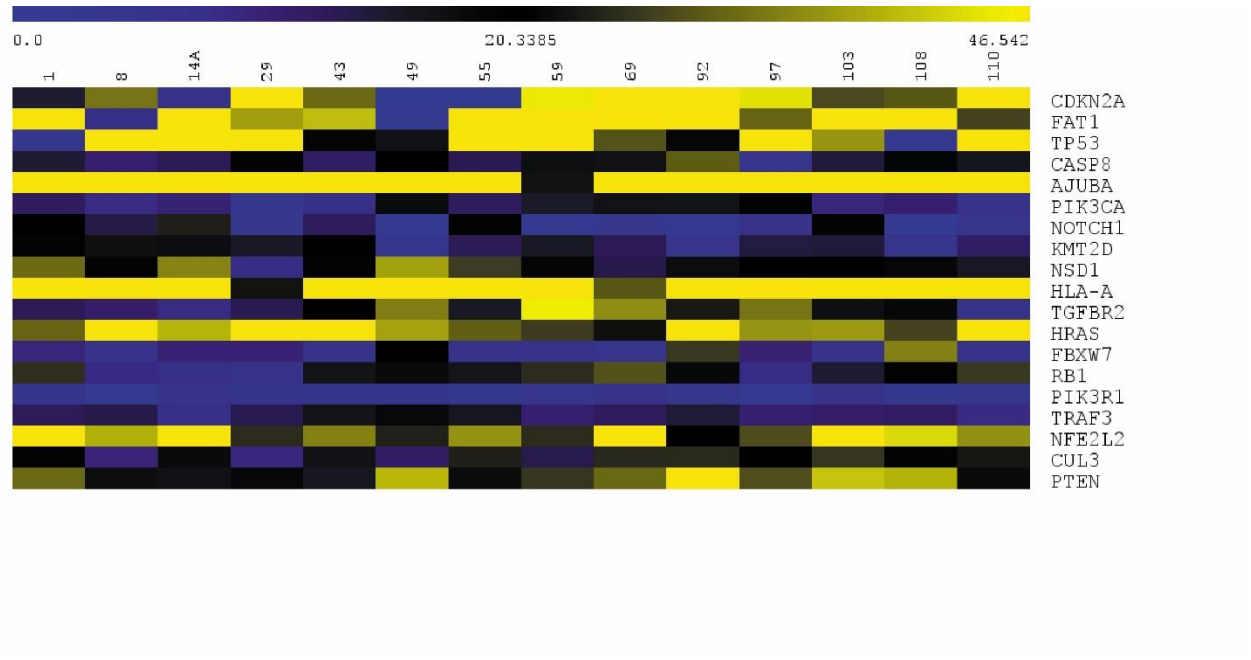

Figure 2-8. Expression of TCGA related genes in the UM-SCC oral cavity cell lines

Heatmap of FPKM values for genes of interest that are displayed across each row, with the cell lines across the top.

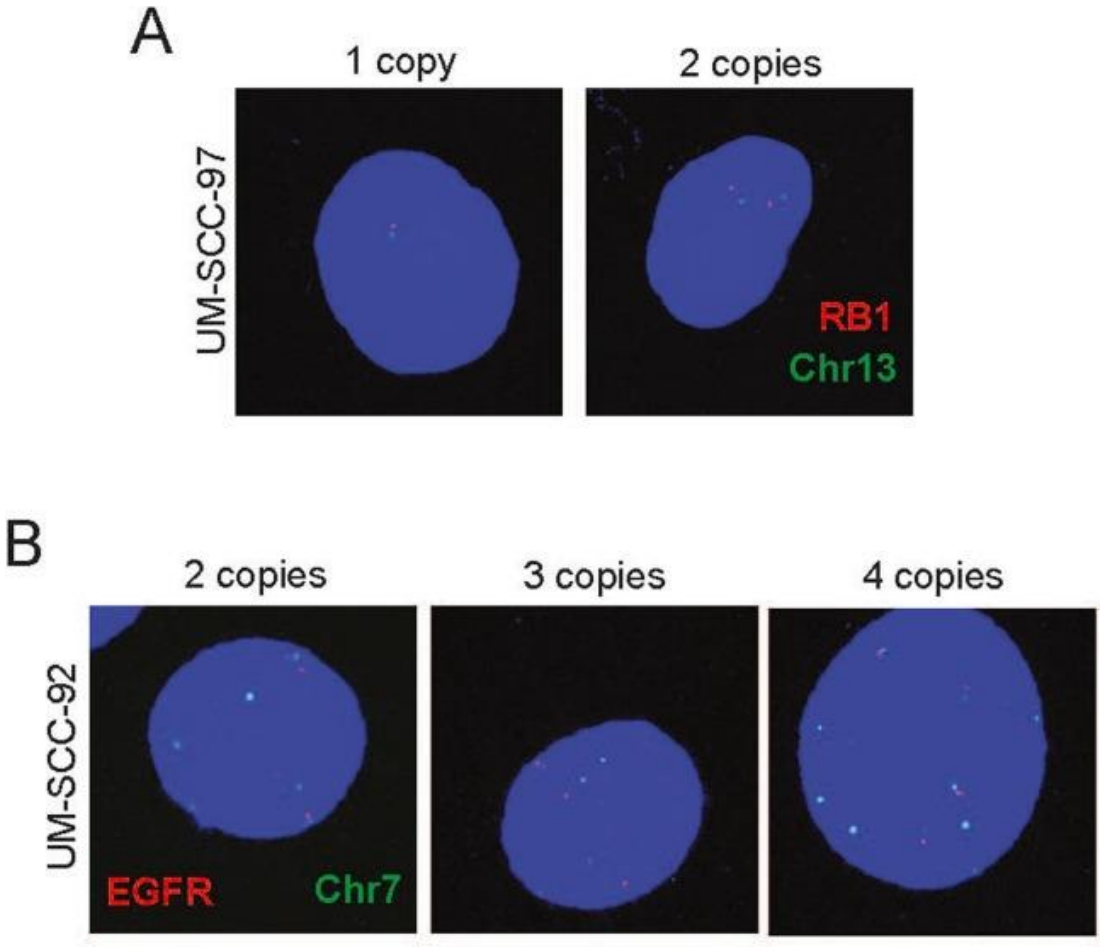

Figure 2-9. FISH confirmation of cell line heterogeneity

Images from FISH for *RB1* in UM-SCC-97 (A) and *EGFR* in UM-SCC-92 (B) with respective chromosomal controls. For both lines, the gene is red, the chromosome in green, and DAPI in blue, showing representative images of cells with varying copies of genes.

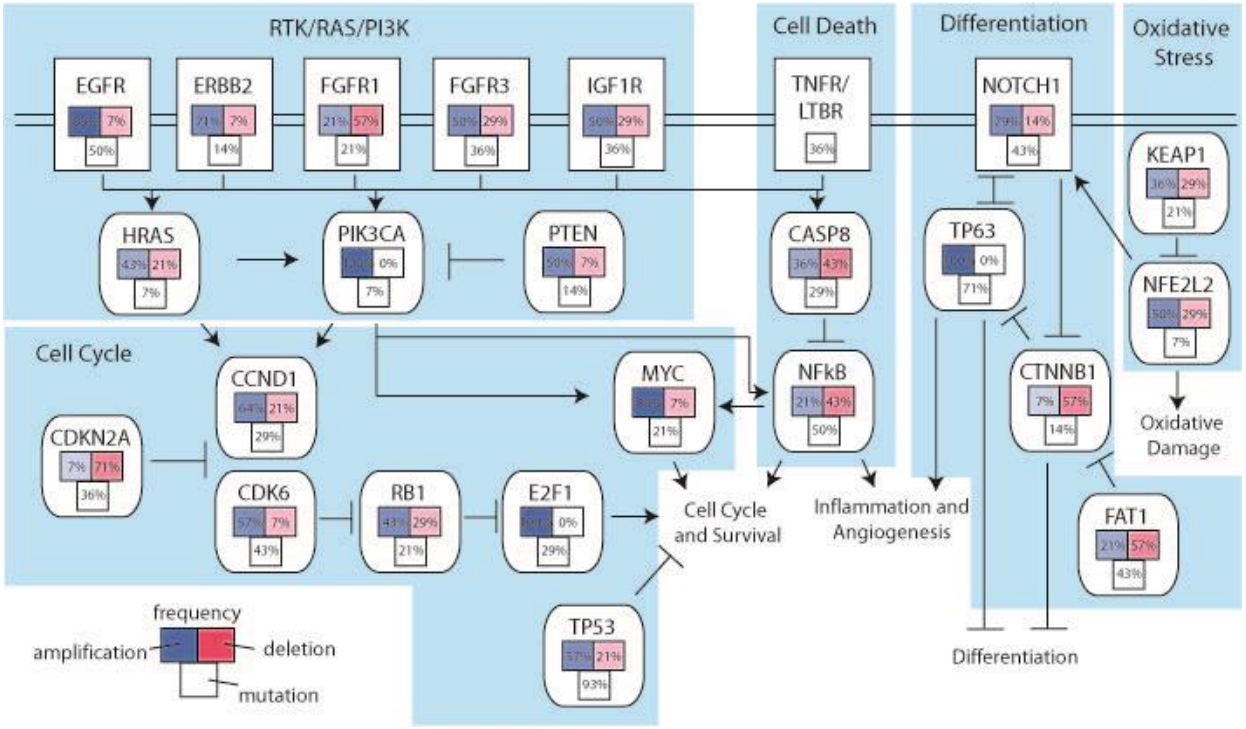

Figure 2-10. Summary of the oncogenic pathways genetically disrupted in the UM-SCC oral cavity cell line panel

Alterations (mutations and copy number alterations) in common oncogenic pathways in the UM-SCC oral cavity cell lines were broken down by pathway classification, *e.g.* Cell Cycle pathway, Receptor Tyrosine Kinases, etc. as in the HNSCC TCGA project. Color shades indicate the frequency of alterations to each pathway, as either potential activating or inactivating alterations.

Tables

Cell Line	Age	Gender	Race	Clinical TNM	Grade	Stage	Subsite	Type of Lesion	Previous Tx	Smoking	Alcohol	Postoperative Tx?	Recurrence?
UMSCC-1	73	M	-	T2N0M0	Moderately Differentiated	II	Floor of mouth	Recurrence	S,RT	Heavy	Rare	No	Yes (local)
UMSCC-8	76	F	White	T2N1M0	Moderately to Well Differentiated	III	Alveolar Ridge	Recurrence	RT	50 pack-year	None	No	No
UMSCC-14A	58	F	White	T1N0M0	Moderately to Poorly Differentiated	I	Floor of mouth	Recurrence	S,S,RT,S	30 pack-year	Occasional	No	Yes (local)
UMSCC-29	66	M	White	T3N2aM0	Well Differentiated	IV	Alveolar Ridge	Persistent primary	CX	Tobacco (heavy)	Heavy	RT	Yes (metastatic)
UM-SCC-43	73	M	-	-	-	-	Hard Palate	Primary (lymph node)	None	-	-	-	-
UMSCC-49	63	M	Black	T3N1M0	Moderately to Well Differentiated	III	Tongue	Primary	None	10 pack-year	Occasional	RT	Yes (persistence)
UMSCC-55	65	M	White	T2N0M0	-	II	Floor of mouth	Primary	None	90 pack-year	Heavy	Left hemimandibulectomy for ORN	Yes (Tonsillar fossa)
UMSCC-59	71	F	White	T3N2bM0	-	IV	Tongue	Primary	None	None	None	RT	-
UMSCC-69	35	M	-	T4N0M0	Moderately to Well Differentiated	IV	Hard Palate	Persistent primary	CX	50 pack-year	Heavy	RT	-
UMSCC-92	38	F	White	T2N0M0	-	II	Tongue	Second Primary	None	None	None	No	No
UMSCC-97	38	F	White	T2N0M0	-	II	Tongue	Primary	None	None	Rare	No	Yes (local)
UMSCC-103	26	F	White	T4N2bM0	Well Differentiated	IV	Tongue	Primary	None	Former (6-pack years)	None	CX	Yes (local, regional)
UMSCC-108	30	F	Asian	rT4N0M0 (T3N1)	Moderately Differentiated	IV	Tongue	Second Primary	CX,RT	None	None	Palliative chemo	Yes
UMSCC-110	39	M	White	T3N0M0	Moderately Differentiated	III	Tongue	Primary	None	44 pack-year	Heavy	RT	Yes

Table 2-1. Clinical statistics of patients from which the oral cavity SCC cell lines were derived.

https://www.sciencedirect.com/science/article/pii/S1368837518303993?via%3Dihub#m0030

Table 2-2. Genomic variants in UM-SCC lines, part one

The list of genomic variants is too large to put into this thesis. Please see link above for ability to download and view this spreadsheet, noted as **supplementary data 1**.

https://www.sciencedirect.com/science/article/pii/S1368837518303993?via%3Dihub#m0030

Table 2-3. Genomic variants in UM-SCC cell lines, part two

The list of genomic variants is too large to put into this thesis. Please see link above for ability to download and view this spreadsheet, noted as **supplementary data 2**.

UM-SCC-69

Cell	1	2	3	4	5	6	7	8	9	10
Chr. No.	122	140	118	134	131	120	130	133	130	131
Chr. 1	3, t(1;Y)	4, 2t(1;Y)	3, 2del(1)(1;Y)	5, t(1;11), t(1;Y), t(1;7)	9, del(1), t(1;x;15), 2t(1;Y), del(1), t(1;x)	2, t(1;Y)	3, t(1;Y), t(Y;1;3)	4, del(1)(1;7), t(1;7)	3, t(1;11), t(1;11)	6, del(1)(1;10), del(1), 3t(1;Y)
Chr. 2	6, del(2)(2;6), del(2)	6, t(2;7), t(2;3)	3, del(2)	5, 2t(2;9)	4, t(2;3)	5, t(2;3)	6, t(2;9)	3, t(2;20)	4, t(2;11), t(2;4)	7, t(2;7)
Chr. 3	7, t(3;Y), t(3;X), t(3;?)	6, t(3;12)	6, t(3;Y)	6	6, del(3)	7, t(3;Y), t(3;?)	5	8	6, t(3;Y)	5
Chr. 4	4, del(4)(4;?)	4, del(4)(4;5)	3	6, del(4)(4;21), t(4;14)	6, 2del(4)(4;Y), del(4)	5, del(4)(4;18), del(4)(4;10)	4, del(4)(4;6)	5, del(4), t(10;4;Y)	4, del(4)(4;18)	4, t(4;3)
Chr. 5	4, del(5)(5;15), dup(5?)	5, dup(5)	11, del(5)(5;4), del(5)(5;2), dup(5), 3del(5)(5;12), t(5;16)	4	8, del(5)(5;4), del(5), t(5;14), del(5)	4, t(5;10)	6, del(5)(5;4), t(5;7)	9, del(5), del(5)(5;4), t(5;15), del(5)(5;1)	5, dup(5), t(5;4)	4, del(5)
Chr. 6	7, t(6;14)	8, t(6;14), t(6;17)	5	6	3	5, t(6;10), t(6;1), t(6;1)	9, del(6)(6;Y), t(6;7)	8, t(6;4), del(6), del(6), t(6;15)	7, 2t(6;19)	4
Chr. 7	3	8, 3t(7;Y)	1	6, t(7;Y), t(7;15), del(7)	4, t(7;Y)	6, 2 t(7;Y), t(7;Y), t(7;12)	8, t(7;15) 2t(7;Y)	9, del(7)(7;10), t(7;Y), t(7;15)	9, 3t(7;Y), t(7;22)	3
Chr. 8	4, t(9;8;14)	5	5, t(8;14)	4	4, t(8;14)	4, t(14;8;9)	4, t(9;8;14)	5	4	5
Chr. 9	6, del(9)(9;2), del(9)(9;2), del(9)(9;15)	7, dup(9), t(9;3)	2	7, del(9)	5, del(9)	4	5, t(11;9), t(Y;1;9)	5, del(9)	9, dup(9), t(9;x;18)	8, 2del(9)
Chr. 10	4, t(10;9)	6, del(10)(10;1), t(10;9), del(10)(10;15)	3	6, t(10;4), t(10;4)	8, t(10;5), 3del(10)	6, del(10)	10, t(10Y), t(10;11), t(10;Y), 2t(10;19), dup(10)	7, del(10), t(10;4)	5, t(10;Y)	11, t(10;7), t(10;Y), t(Y;22;10), t(10;6)
Chr. 11	3	6, del(11)	6	5	4	5, del(11)	6	6, del(11)	7, 3dup(11)	5
Chr. 12	7	8, 2dup(12), del(12)	8, 2t(12;Y)	7, t(12;14;15), t(1;12)	7, t(12;Y)	4	6, Rob(12), del(12), t(12;10)	5, t(12;4)	6, t(12;10)	8, t(12;22), t(12;Y)
Chr. 13	6, t(13;2)	10, dup(13)	6, t(13;2)	7	8, t(13;3), dup(13)	6, Rob(13;9), t(13;19)	7, t(13;10), Rob(13)	7, t(13;Y)	7	6
Chr. 14	7, 2t(14;2), dup(14)	4	5	5	7, dup(14)	6, 2Rob(14), del(14), Rob(14;18)	3, t(14;15)	6, t(14;4), t(14;17)	6, t(14;12), t(14;2), t(14;2)	2, t(14;20)
Chr. 15	5	2, t(15;5)	5, 3t(15;2)	8, t(15;7), dup(15), t(15;16), t(Y;1;15)	1, t(15;7)	7, 2Rob(15;10)	5, t(15;10)	9, t(15;4), t(15;10), t(15;10), t(15;16)	5	2
Chr. 16	4, t(16;19)	5	7, del(16), 2t(16;7), t(16;7),	5	4	5	5, t(2;16)	4, t(16;15)	5, t(16;13)	7, t(16;X)

Chr. 17	5, 2t(17;1)	6, t(17;7), t(17;1), t(17;6)	6, 2t(17;6), t(17;9)	7, t(17;5), 2t(17;6), t(17;4)	6, t(17;1)	6, 2t(17;1), t(17;1;Y)	6, t(17;6), t(6;17;3)	6, 2t(17;1)	6, 2t(17;6), t(16;14)	11, 2t(17;Y), dup(17), 2t(17;1)
Chr. 18	4	6, del(18)	2, del(18)	3	4	4, del(18)	4, del(18)	4, t(18;10)	5, del(18), t(18;10;17)	4, t(18;4), del(18)
Chr. 19	5, t(19;5	5	5	3	6	6	2	6	3	2
Chr. 20	10, t(20;1)	10, t(20;1)	9	10	11	10	10	9	11	10, t(20;11)
Chr. 21	7	7	7	6	6	6	6	3	8	6
Chr. 22	5	7, 2t(22;7)	3	4	4, t(22;4)	3, t(22;1)	5	1	3	6, 2t(22;19)
Chr. X	1	3	4, t(x;5)	4	4	3, dup(X)?	3, dup(X)	1	2, del(X)	2
Chr. Y	1	1	1	1	1	0	1	3, Rob(Y)	0	1
Markers	4		1	2						

Table 2-4. Karyotyping results from UM-SCC-69

UM-SCC-92

Cell	1	2	3	4	5	6	7	8	9	10
Chr. No.	70	72	73	73	72	74	71	58	71	74
Chr. 1	4, t(1;9)	2	3	4	3	3	3	3	3, t(1;15)	3
Chr. 2	2, del(2)(2;20)	2, t(2;12)	3, del(2)(2;20)	4, t(2;8), 2del(2)(2;20)	4, t(2;22), t(2;8), del(2)(2;8)	4, t(2;8), 2del(2)(2;20)	4, 2del(2)(2;20), del(2)(2;12)	1	3, 2del(2)(2;20)	3, 2del(2)(2;20)
Chr. 3	3, del(3)(3;10), 2del(3)(3;20)	2	2	4, t(3;11), 2del(3)(3;8)	4, del(3)(3;8), del(3)(3;11), del(3)(3;20),t(3;9)	3, 2del(3)(3;20)	3, t(3;9), del(3)(3;20), del(3)(3;11)	1	0	4, t(3;9), t(3;9), t(3;17)
Chr. 4	4, del(4)	4, t(4;17), del(4)	4, del(4)(4;20)	4, del(4)	4, del(4), del(4)(4;20)	4, del(4)	4, del(4)	2, del(4)	4, t(4;9)	4, del(4)
Chr. 5	3, t(5;17)	4, del(5)(5;12), del(5)(5;17), Ins(17)	5, t(5;17), del(5)(5;14), del(5)(5;17)	6, t(5;6), del(5), t(5;17), t(5;17), del(5)(5;14)	5, 2del(5), 2t(5;17)	4, del(5), 2t(5;17)	4, 2t(5;17), del(5)	5, del(5), t(5;17), t(5;17), del(5)	4, 2t(5;17), del(5)	5, del(5)(5;14), t(5;17), t(5;9;17), del(5)
Chr. 6	2, t(6;11)	2	3, t(6;3)	2, t(6;3), del(6)	3, del(6)	4, del(6), t(5;15;6)	3, del(6)	3	4, t(6;17)	2
Chr. 7	3, t(7;8)	3, t(7;8)	3, t(7;8)	4, t(7;8), del(7)	3, t(7;8)	4, t(7;2), t(7;8)	3, t(7;8)	2, t(7;8)	6, t(7;8), 2t(7;3)	3, t(7;21)
Chr. 8	4, t(8;2), t(8;7), t(8;20?)	4, t(8;2), t(8;2)	4, t(8;5), t(8;12), del(8)	4, t(8;19), t(9;8;11), t(8;10)	3, t(8;5), del(8)(8;7)	3, t(8;6)	4, t(8;9), t(8;7), t(8;2)	3, dup(8), t(8;6)	4, t(8;11), t(8;4), dup(8), t(8;15)	4, del(8)(8;7), t(8;2;3)
Chr. 9	3, dup(9)(9;1)	2, t(9;1)	2	2	2	2	2	2	2, t(9;18;16)	2
Chr. 10	5, del(10)(10;20)	4, t(10;20)	4	3	3	4,t(10;17)	4, del(10)	2	2	3
Chr. 11	3, t(11;17)	5, dup(11)	3, t(11;5)	2, del(11)	3, t(11;6)	4, t(11;3), t(11;6)	2, dup(11)	3	6, t(11;12), t(11;20;18), t(11;20)	2
Chr. 12	7, t(12;2), t(12;22), t(12;19), t(12;5;18), del(12)	6, t(12;22), t(12;15), t(12;15), del(12)	2	3, t(12;2)	2	2	2	3, t(12;2)	3, t(12;10)	3, t(12;2)
Chr. 13	2, t(14?;13)	2	2	2	2	2	2	2	3, t(13;22)	2
Chr. 14	2	2, t(14;20)	3, t(14;22), t(14;22)	4, t(14;19), t(14;12), t(14;22)	4, t(14;5), t(14;19)	5, t(14;22), t(14;19), t(14;7), t(14;5)	3, 2t(14;15)	4, t(14;15), t(14;18), t(14;19)	2	4, t(14;22), t(14;15), t(14;19)
Chr. 15	3	3	2	3, t(15;5)	3	3	2	2	5, del(15), t(15;18;	4, t(15;16)

									7), t(15;16)	
Chr. 16	4, t(16;14), t(16;18)	4, del(16)(16;18), del(16)(16;12)	4, t(16;?), dup(16)	3, t(16;15)	3, del(16)(16;18)	4, del(16)(16;12), t(16;18)	4, t(16;18), t(16;5)	1	4, t(16;12), t(16;15;5)	3
Chr. 17	2	3, t(17;11)	3, t(17;3)	3, t(17;3)	3, t(17;3)	2	3, t(17;3)	1, t(17;10;3)	2, t(17;11)	3, t(17;6), t(17;3)
Chr. 18	4, t(18;22;8)	4, t(18;22;8)	4, t(18;16), t(18;22;8)	4, t(18;22;8). t(18;16)	4, t(18;22;8)	3	4, t(18;22;8)	4, t(5;18)	3, t(18;22;8), t(18;16)	4, t(18;22;8)
Chr. 19	2	2	2	2	3	3, t(19;15)	3	3	2	3
Chr. 20	3, t(20;8), t(20;3)	5, t(20;11), t(20;8), t(20;11), t(20;4)	4, t(20;8), t(20;3), t(20;8)	3, 2t(20;4)	2, t(20;4)	3, t(20;11), t(20;21)	4, 2t(20;21), t(20;3)	4, 2t(20;3), t(20;21)	2, t(20;3)	5, 2t(20;3), 2t(20;21)
Chr. 21	2	2	3	2	2	3	2	2	4, t(21;20)	2
Chr. 22	1	2	2	1	2, t(22;14)	1	2, t(22;14)	1	1	1
Chr. X	2	3, del(X)	4, 2del(X)	4, 2del(X)	4, 2del(X)	4, 2del(X)	4, 2del(X)	4, 2del(X)	2	4, 2del(X)
Chr. Y	0	0	0	0	0	0	0	0	0	0
Markers			2		1					1

Table 2-5. Karotyping results from UM-SCC-92

	UM-SCC													
	1	8	14A	29	43	49	55	59	69	92	97	103	108	110
EGFR	2	4	3.67	4	3,2.5	5	1.67	23	15.67	2.33	3	2.33	3	4
PIK3CA	3	4	2.67	4	3	5	2.67	5	6	3	4	3	4	3
TP63	3	4	2.67	4	3	5	2.67	5	6	3	4	3	3	3
CCND1	1	3	5.33	4	2	5	1.67	12	2.33	12	3	1.67	11	2
BIRC2	2	4	1.67	4	3	5	1.33	3	2.33	1.67	4	2.33	2	3
YAP1	2	4	1.67	4	3	5	1.33	3	2.33	1.67	4	2.33	2	3
ERBB2	2	3	2.33	5	1	4	2.33	4	3	4	2	2.33	2	4
FGFR1	1	2	2.67,2,2.33	2	1*	1*	1.33	1.5	2.67	3.67	1*	1.33	2	1
TP53	2	3	2.33	4	1	3	2	4	3.33	2	1	1.33	3	3
CDKN2A	0,1	0,3	1	2	2	0	0.33	4	2,3.33	1.33	1	0.67	1	1
FAT1	1	1	1.33	2	1	1*	2.33	3	2	2	1*	1.33	3	1
NOTCH1	3	5	2	4	1	2.5	3	4	3.33	2,2.33	1	2.33	3	3
TRAF3	2	4	1.67	4	2	6	2.33	3	4	2.67	2	2.67	4	2
CASP8	2	3	2	4	1	1	1.67	3	3.33	1.67	1*	2	1.5	4
KEAP1	1	3	1.67	2	2	2	1.33	3	3	2	1*	2	3	3
MYH9	3	3	2	2	2	2	2	2	3	1.33	1*	1.67	3,2	2
IGF1R	2	3	1.67	4	1	3	2	3	3.67	2	1	1.67	3	3
EPHA2	2	3	1.67	2	1	2	1.33	3	3	2	1	2	3	2
DDR2	2	2	2	4	1	2	1.67	3	3.67	2	1	1.67	3	2
FGFR2	2	3	2.33	4	1	2	2.33	2	3	2.33	2	2	2	2
FGFR3	2	3	1.33	4,3	1	2	1.67	2	3.33	3	1	2.67,2	2.5	3
MET	2	2.5	1.33	2	2	3	2.33	3	4	2.33	1	2	3	2.5
MYC	3	4	2.67	7	4	4	3.33	2	2.67	3.67	1	3.33	6	8
HRAS	2	2.5	2	3	1	3	2	4	2.67	2	1	1.67	2.5	2
PTEN	2	3	2.33	5	1	2	2.33	3	3	2.33	2	2	2	2
PIK3R1	2	3	1.33	1*	1	1	1.67	1.5	3	2.33	1*	1.33	1.5	3
NF1	2	3	2.33	4	1	4	2.33	2	3.33	1.33	1*	2.33	2	3
BCL6	3	4	2.67	4	3	5	2.67	5	6	3	4	3	3	3
CDK6	2	2.5	5	2	2	2	2.33	3	5	2.33	1	2	3	3
JAK2	2	4	3	3	4	3	1.67	3	5	1.33	1	1.33	1.5	5
GATA6	2	3	3	4	1	5	2	5	2	2	2	1.67	3	6
SRC	2	3	3	4	3	7	3	4	4	3	3	2.33	4	9
CDKN2B	1	3	1	2	2	4	0	4	3.33	1.33	1	0.67	1	1
STK11	1	2	2	2	1,2	2	2	3	3	2	1	2	2	2
TCF3	1	3	2	2	1	2.5	2	3	3	2	1	2	2	2
RB1	2	2,3	1.33	4	2	3,4	1.67	3,4	3,4	1.67,2	1*	1.33	5	4

Table 2-6. Estimated copy numbers for UM-SCC oral cavity cell line panel

Estimated copy numbers as noted by the TuScan algorithm for cell lines for panel of genes. For copy numbers with a comma, multiple values were reported over the course of the gene. For cell lines with a copy number of 1*, the TuScan algorithm estimated a complete deletion (CN=0), however, we observed those genes had exome sequencing reads. We felt it more accurate to report a one copy loss rather than a complete deletion in those cases.

Primary	Company	Catalog #
EGFR	OriGene	TA312545
PI3K p110α	Cell Signaling	4249
PTEN	Cell Signaling	9559
pAKT (S473)	Cell Signaling	40605
AKT	Cell Signaling	46855
pERK1/2 (T202, Y204)	Cell Signaling	4370
ERK1/2	Cell Signaling	4695
pMEK1/2 (S217, S221)	Cell Signaling	9121
MEK1/2	Cell Signaling	8727
p53	Neo Markers	MS-187-P0
HSP90	Cell Signaling	4877
pRb (S807, S811)	Cell Signaling	8516
pRb (S780)	Cell Signaling	8180
pRb (S795)	Cell Signaling	9301
Rb	Cell Signaling	9313
Beta-actin	Cell Signaling	4970
Secondary		
anti-rabbit	Jackson ImmunoResearch	711-035-152
anti-mouse	Jackson ImmunoResearch	115-035-166

Table 2-7. Antibody information

Bibliography

1. Jemal A, Bray F, Center MM, Ferlay J, Ward E, Forman D. Global cancer statistics. CA Cancer J Clin. 2011;61(2):69-90. Epub 2011/02/08. doi: 10.3322/caac.20107. PubMed PMID: 21296855.
2. National Cancer Institute: Surveillance E, and End Results (SEER) Program. Oral Cancer 5-Year Survival Rates by Race, Gender, and Stage of Diagnosis 2006. Available from: http://www.nidcr.nih.gov/DataStatistics/FindDataByTopic/OralCancer/OralCancer5YearSurvivalRates.htm.
3. The Cancer Genome Atlas N. Comprehensive genomic characterization of head and neck squamous cell carcinomas. Nature. 2015;517(7536):576-82. doi: 10.1038/nature14129 http://www.nature.com/nature/journal/v517/n7536/abs/nature14129.html#supplementary-information.
4. Stransky N, Egloff AM, Tward AD, Kostic AD, Cibulskis K, Sivachenko A, Kryukov GV, Lawrence MS, Sougnez C, McKenna A, Shefler E, Ramos AH, Stojanov P, Carter SL, Voet D, Cortes ML, Auclair D, Berger MF, Saksena G, Guiducci C, Onofrio RC, Parkin M, Romkes M, Weissfeld JL, Seethala RR, Wang L, Rangel-Escareno C, Fernandez-Lopez JC, Hidalgo-Miranda A, Melendez-Zajgla J, Winckler W, Ardlie K, Gabriel SB, Meyerson M, Lander ES, Getz G, Golub TR, Garraway LA, Grandis JR. The mutational landscape of head and neck squamous cell carcinoma. Science. 2011;333(6046):1157-60. Epub 2011/07/30. doi: 10.1126/science.1208130. PubMed PMID: 21798893; PMCID: 3415217.
5. Agrawal N, Frederick MJ, Pickering CR, Bettegowda C, Chang K, Li RJ, Fakhry C, Xie TX, Zhang J, Wang J, Zhang N, El-Naggar AK, Jasser SA, Weinstein JN, Trevino L, Drummond JA, Muzny DM, Wu Y, Wood LD, Hruban RH, Westra WH, Koch WM, Califano JA, Gibbs RA, Sidransky D, Vogelstein B, Velculescu VE, Papadopoulos N, Wheeler DA, Kinzler KW, Myers JN. Exome sequencing of head and neck squamous cell carcinoma reveals inactivating mutations in NOTCH1. Science. 2011;333(6046):1154-7. Epub 2011/07/30. doi: 10.1126/science.1206923. PubMed PMID: 21798897; PMCID: 3162986.
6. Mountzios G, Rampias T, Psyrri A. The mutational spectrum of squamous-cell carcinoma of the head and neck: targetable genetic events and clinical impact. Ann Oncol. 2014;25(10):1889-900. doi: 10.1093/annonc/mdu143. PubMed PMID: 24718888.
7. Seiwert TY, Zuo Z, Keck MK, Khattri A, Pedamallu CS, Stricker T, Brown C, Pugh TJ, Stojanov P, Cho J, Lawrence MS, Getz G, Bragelmann J, DeBoer R, Weichselbaum RR, Langerman A, Portugal L, Blair E, Stenson K, Lingen MW, Cohen EE, Vokes EE, White KP, Hammerman PS. Integrative and comparative genomic analysis of HPV-positive and HPV-negative head and neck squamous cell carcinomas. Clinical cancer research : an official journal of the American Association for Cancer Research. 2015;21(3):632-41. Epub 2014/07/25. doi: 10.1158/1078-0432.ccr-13-3310. PubMed PMID: 25056374; PMCID: 4305034.
8. Giefing M, Wierzbicka M, Szyfter K, Brenner JC, Braakhuis BJ, Brakenhoff RH, Bradford CR, Sorensen JA, Rinaldo A, Rodrigo JP, Takes RP, Ferlito A. Moving towards personalised therapy in head and neck squamous cell carcinoma through analysis of next generation sequencing data. European journal of cancer. 2016;55:147-57. doi: 10.1016/j.ejca.2015.10.070. PubMed PMID: 26851381; PMCID: 4761501.
9. Birkeland AC, Ludwig ML, Meraj TS, Brenner JC, Prince ME. The Tip of the Iceberg: Clinical Implications of Genomic Sequencing Projects in Head and Neck Cancer. Cancers

(Basel). 2015;7(4):2094-109. Epub 2015/10/28. doi: 10.3390/cancers7040879. PubMed PMID: 26506389.
10. Grenman R, Carey TE, McClatchey KD, Wagner JG, Pekkola-Heino K, Schwartz DR, Wolf GT, Lacivita LP, Ho L, Baker SR, et al. In vitro radiation resistance among cell lines established from patients with squamous cell carcinoma of the head and neck. Cancer. 1991;67(11):2741-7. Epub 1991/06/01. PubMed PMID: 2025837.
11. Bradford CR, Zhu S, Ogawa H, Ogawa T, Ubell M, Narayan A, Johnson G, Wolf GT, Fisher SG, Carey TE. P53 mutation correlates with cisplatin sensitivity in head and neck squamous cell carcinoma lines. Head Neck. 2003;25(8):654-61. Epub 2003/07/29. doi: 10.1002/hed.10274. PubMed PMID: 12884349.
12. Liu J, Pan S, Hsieh MH, Ng N, Sun F, Wang T, Kasibhatla S, Schuller AG, Li AG, Cheng D, Li J, Tompkins C, Pferdekamper A, Steffy A, Cheng J, Kowal C, Phung V, Guo G, Wang Y, Graham MP, Flynn S, Brenner JC, Li C, Villarroel MC, Schultz PG, Wu X, McNamara P, Sellers WR, Petruzzelli L, Boral AL, Seidel HM, McLaughlin ME, Che J, Carey TE, Vanasse G, Harris JL. Targeting Wnt-driven cancer through the inhibition of Porcupine by LGK974. Proc Natl Acad Sci U S A. 2013;110(50):20224-9. Epub 2013/11/28. doi: 10.1073/pnas.1314239110. PubMed PMID: 24277854; PMCID: 3864356.
13. Akervall J, Guo X, Qian CN, Schoumans J, Leeser B, Kort E, Cole A, Resau J, Bradford C, Carey T, Wennerberg J, Anderson H, Tennvall J, Teh BT. Genetic and expression profiles of squamous cell carcinoma of the head and neck correlate with cisplatin sensitivity and resistance in cell lines and patients. Clinical cancer research : an official journal of the American Association for Cancer Research. 2004;10(24):8204-13. Epub 2004/12/30. doi: 10.1158/1078-0432.ccr-04-0722. PubMed PMID: 15623595.
14. Brenner JC, Graham MP, Kumar B, Saunders LM, Kupfer R, Lyons RH, Bradford CR, Carey TE. Genotyping of 73 UM-SCC head and neck squamous cell carcinoma cell lines. Head Neck. 2010;32(4):417-26. doi: 10.1002/hed.21198. PubMed PMID: 19760794; PMCID: 3292176.
15. Wolter KG, Wang SJ, Henson BS, Wang S, Griffith KA, Kumar B, Chen J, Carey TE, Bradford CR, D'Silva NJ. (-)-gossypol inhibits growth and promotes apoptosis of human head and neck squamous cell carcinoma in vivo. Neoplasia. 2006;8(3):163-72. Epub 2006/04/14. doi: 10.1593/neo.05691. PubMed PMID: 16611409; PMCID: 1578526.
16. Jones JW, Raval JR, Beals TF, Worsham MJ, Van Dyke DL, Esclamado RM, Wolf GT, Bradford CR, Miller T, Carey TE. Frequent loss of heterozygosity on chromosome arm 18q in squamous cell carcinomas. Identification of 2 regions of loss--18q11.1-q12.3 and 18q21.1-q23. Archives of otolaryngology--head & neck surgery. 1997;123(6):610-4. PubMed PMID: 9193222.
17. Van Dyke DL, Worsham MJ, Benninger MS, Krause CJ, Baker SR, Wolf GT, Drumheller T, Tilley BC, Carey TE. Recurrent cytogenetic abnormalities in squamous cell carcinomas of the head and neck region. Genes, chromosomes & cancer. 1994;9(3):192-206. PubMed PMID: 7515662.
18. Carey TE, Vandyke DL, Worsham MJ. Nonrandom Chromosome-Aberrations and Clonal Populations in Head and Neck-Cancer. Anticancer Res. 1993;13(6b):2561-7. PubMed PMID: WOS:A1993NE37200033.
19. Garnett MJ, Edelman EJ, Heidorn SJ, Greenman CD, Dastur A, Lau KW, Greninger P, Thompson IR, Luo X, Soares J, Liu Q, Iorio F, Surdez D, Chen L, Milano RJ, Bignell GR, Tam AT, Davies H, Stevenson JA, Barthorpe S, Lutz SR, Kogera F, Lawrence K, McLaren-Douglas A, Mitropoulos X, Mironenko T, Thi H, Richardson L, Zhou W, Jewitt F, Zhang T, O'Brien P,

Boisvert JL, Price S, Hur W, Yang W, Deng X, Butler A, Choi HG, Chang JW, Baselga J, Stamenkovic I, Engelman JA, Sharma SV, Delattre O, Saez-Rodriguez J, Gray NS, Settleman J, Futreal PA, Haber DA, Stratton MR, Ramaswamy S, McDermott U, Benes CH. Systematic identification of genomic markers of drug sensitivity in cancer cells. Nature. 2012;483(7391):570-5. Epub 2012/03/31. doi: 10.1038/nature11005. PubMed PMID: 22460902; PMCID: 3349233.
20. Birkeland AC, Brenner JC. Personalizing Medicine in Head and Neck Squamous Cell Carcinoma: The Rationale for Combination Therapies. Medical research archives. 2015;3. doi: 10.18103/mra.v0i3.77. PubMed PMID: 26913293; PMCID: 4762450.
21. Birkeland AC, Ludwig ML, Spector ME, Brenner JC. The potential for tumor suppressor gene therapy in head and neck cancer. Discovery medicine. 2016;21(113):41-7. PubMed PMID: 26896601; PMCID: 4772772.
22. Birkeland AC, Uhlmann WR, Brenner JC, Shuman AG. Getting personal: Head and neck cancer management in the era of genomic medicine. Head Neck. 2015. Epub 2015/05/23. doi: 10.1002/hed.24132. PubMed PMID: 25995036.
23. Barretina J, Caponigro G, Stransky N, Venkatesan K, Margolin AA, Kim S, Wilson CJ, Lehar J, Kryukov GV, Sonkin D, Reddy A, Liu M, Murray L, Berger MF, Monahan JE, Morais P, Meltzer J, Korejwa A, Jane-Valbuena J, Mapa FA, Thibault J, Bric-Furlong E, Raman P, Shipway A, Engels IH, Cheng J, Yu GK, Yu J, Aspesi P, Jr., de Silva M, Jagtap K, Jones MD, Wang L, Hatton C, Palescandolo E, Gupta S, Mahan S, Sougnez C, Onofrio RC, Liefeld T, MacConaill L, Winckler W, Reich M, Li N, Mesirov JP, Gabriel SB, Getz G, Ardlie K, Chan V, Myer VE, Weber BL, Porter J, Warmuth M, Finan P, Harris JL, Meyerson M, Golub TR, Morrissey MP, Sellers WR, Schlegel R, Garraway LA. The Cancer Cell Line Encyclopedia enables predictive modelling of anticancer drug sensitivity. Nature. 2012;483(7391):603-7. Epub 2012/03/31. doi: 10.1038/nature11003. PubMed PMID: 22460905; PMCID: 3320027.
24. Greshock J, Bachman KE, Degenhardt YY, Jing J, Wen YH, Eastman S, McNeil E, Moy C, Wegrzyn R, Auger K, Hardwicke MA, Wooster R. Molecular target class is predictive of in vitro response profile. Cancer Res. 2010;70(9):3677-86. Epub 2010/04/22. doi: 10.1158/0008-5472.can-09-3788. PubMed PMID: 20406975.
25. Li H, Wawrose JS, Gooding WE, Garraway LA, Lui VW, Peyser ND, Grandis JR. Genomic analysis of head and neck squamous cell carcinoma cell lines and human tumors: a rational approach to preclinical model selection. Mol Cancer Res. 2014;12(4):571-82. doi: 10.1158/1541-7786.MCR-13-0396. PubMed PMID: 24425785; PMCID: 3989421.
26. Andrews S. FastQC A Quality Control tool for High Throughput Sequence Data. http://wwwbioinformaticsbabrahamacuk/projects/fastqc/. doi: citeulike-article-id:11583827.
27. Li H, Durbin R. Fast and accurate short read alignment with Burrows-Wheeler transform. Bioinformatics. 2009;25(14):1754-60. Epub 2009/05/20. doi: 10.1093/bioinformatics/btp324. PubMed PMID: 19451168; PMCID: 2705234.
28. McKenna A, Hanna M, Banks E, Sivachenko A, Cibulskis K, Kernytsky A, Garimella K, Altshuler D, Gabriel S, Daly M, DePristo MA. The Genome Analysis Toolkit: a MapReduce framework for analyzing next-generation DNA sequencing data. Genome research. 2010;20(9):1297-303. Epub 2010/07/21. doi: 10.1101/gr.107524.110. PubMed PMID: 20644199; PMCID: 2928508.
29. DePristo MA, Banks E, Poplin R, Garimella KV, Maguire JR, Hartl C, Philippakis AA, del Angel G, Rivas MA, Hanna M, McKenna A, Fennell TJ, Kernytsky AM, Sivachenko AY, Cibulskis K, Gabriel SB, Altshuler D, Daly MJ. A framework for variation discovery and

genotyping using next-generation DNA sequencing data. Nat Genet. 2011;43(5):491-8. Epub 2011/04/12. doi: 10.1038/ng.806. PubMed PMID: 21478889; PMCID: 3083463.
30. The Genomes Project C. A global reference for human genetic variation. Nature. 2015;526(7571):68-74. doi: 10.1038/nature15393 http://www.nature.com/nature/journal/v526/n7571/abs/nature15393.html#supplementary-information.
31. Tillman BN, Yanik M, Birkeland AC, Liu CJ, Hovelson DH, Cani AK, Palanisamy N, Carskadon S, Carey TE, Bradford CR, Tomlins SA, McHugh JB, Spector ME, Chad Brenner J. Fibroblast growth factor family aberrations as a putative driver of head and neck squamous cell carcinoma in an epidemiologically low-risk patient as defined by targeted sequencing. Head Neck. 2016;38 Suppl 1:E1646-52. doi: 10.1002/hed.24292. PubMed PMID: 26849095; PMCID: 4844767.
32. Michmerhuizen N.M. LE, Kulkarni A., Brenner J.C. Differential Compensation mechanisms Define Resistance to PI3K inhibitors in PIK3CA amplified HNSCC. Oto Head and Neck Surgery. 2016(NIHMS799178).
33. Owen JH, Hauff SJ, Tang AL, Graham MP, Czerwinski MJ, Kaddoura M, Papagerakis S, Bradford CR, Carey TE, Prince ME. UM-SCC-103: a unique tongue cancer cell line that recapitulates the tumorigenic stem cell population of the primary tumor. Ann Otol Rhinol Laryngol. 2014;123(9):662-72. doi: 10.1177/0003489414531910. PubMed PMID: 24816422; PMCID: 4153472.
34. Carey TE, Van Dyke DL, Worsham MJ, Bradford CR, Babu VR, Schwartz DR, Hsu S, Baker SR. Characterization of human laryngeal primary and metastatic squamous cell carcinoma cell lines UM-SCC-17A and UM-SCC-17B. Cancer Res. 1989;49(21):6098-107. Epub 1989/11/01. PubMed PMID: 2790823.
35. Grenman R, Virolainen E, Shapira A, Carey T. In vitro effects of tamoxifen on UM-SCC head and neck cancer cell lines: correlation with the estrogen and progesterone receptor content. International journal of cancer. 1987;39(1):77-81. PubMed PMID: 3793272.
36. Shapira A, Virolainen E, Jameson JJ, Ossakow SJ, Carey TE. Growth inhibition of laryngeal UM-SCC cell lines by tamoxifen. Comparison with effects on the MCF-7 breast cancer cell line. Archives of otolaryngology--head & neck surgery. 1986;112(11):1151-8. PubMed PMID: 3755989.
37. Krause CJ, Carey TE, Ott RW, Hurbis C, McClatchey KD, Regezi JA. Human squamous cell carcinoma. Establishment and characterization of new permanent cell lines. Archives of otolaryngology. 1981;107(11):703-10. PubMed PMID: 7295166.
38. Ludwig ML, Birkeland AC, Hoesli R, Swiecicki P, Spector ME, Brenner JC. Changing the paradigm: the potential for targeted therapy in laryngeal squamous cell carcinoma. Cancer biology & medicine. 2016;13(1):87-100. doi: 10.28092/j.issn.2095-3941.2016.0010. PubMed PMID: 27144065; PMCID: 4850131.
39. Michmerhuizen NL, Birkeland AC, Bradford CR, Brenner JC. Genetic determinants in head and neck squamous cell carcinoma and their influence on global personalized medicine. Genes & cancer. 2016;7(5-6):182-200. doi: 10.18632/genesandcancer.110. PubMed PMID: 27551333.
40. Birkeland AC, Yanik M, Tillman BN, Scott MV, Foltin SK, Mann JE, Michmerhuizen NL, Ludwig ML, Sandelski MM, Komarck CM, Carey TE, Prince ME, Bradford CR, McHugh JB, Spector ME, Brenner JC. Identification of Targetable ERBB2 Aberrations in Head and Neck

Squamous Cell Carcinoma. JAMA Otolaryngol Head Neck Surg. 2016. doi: 10.1001/jamaoto.2016.0335. PubMed PMID: 27077364.
41. Pollock NI, Grandis JR. HER2 as a Therapeutic Target in Head and Neck Squamous Cell Carcinoma. Clinical cancer research : an official journal of the American Association for Cancer Research. 2014. doi: 10.1158/1078-0432.CCR-14-1432. PubMed PMID: 25424855.
42. Koole K, Brunen D, van Kempen PM, Noorlag R, de Bree R, Lieftink C, van Es RJ, Bernards R, Willems SM. FGFR1 Is a Potential Prognostic Biomarker and Therapeutic Target in Head and Neck Squamous Cell Carcinoma. Clinical cancer research : an official journal of the American Association for Cancer Research. 2016;22(15):3884-93. doi: 10.1158/1078-0432.CCR-15-1874. PubMed PMID: 26936917.
43. Goke F, Franzen A, Hinz TK, Marek LA, Yoon P, Sharma R, Bode M, von Maessenhausen A, Lankat-Buttgereit B, Goke A, Golletz C, Kirsten R, Boehm D, Vogel W, Kleczko EK, Eagles JR, Hirsch FR, Van Bremen T, Bootz F, Schroeck A, Kim J, Tan AC, Jimeno A, Heasley LE, Perner S. FGFR1 Expression Levels Predict BGJ398 Sensitivity of FGFR1-Dependent Head and Neck Squamous Cell Cancers. Clinical cancer research : an official journal of the American Association for Cancer Research. 2015;21(19):4356-64. doi: 10.1158/1078-0432.CCR-14-3357. PubMed PMID: 26015511; PMCID: 4592392.
44. von Massenhausen A, Franzen A, Heasley L, Perner S. FGFR1 as a novel prognostic and predictive biomarker in squamous cell cancers of the lung and the head and neck area. Annals of translational medicine. 2013;1(3):23. doi: 10.3978/j.issn.2305-5839.2013.06.08. PubMed PMID: 25332967; PMCID: 4200677.
45. Navin N, Kendall J, Troge J, Andrews P, Rodgers L, McIndoo J, Cook K, Stepansky A, Levy D, Esposito D, Muthuswamy L, Krasnitz A, McCombie WR, Hicks J, Wigler M. Tumour evolution inferred by single-cell sequencing. Nature. 2011;472:90. doi: 10.1038/nature09807 https://www.nature.com/articles/nature09807#supplementary-information.
46. Puram SV, Tirosh I, Parikh AS, Patel AP, Yizhak K, Gillespie S, Rodman C, Luo CL, Mroz EA, Emerick KS, Deschler DG, Varvares MA, Mylvaganam R, Rozenblatt-Rosen O, Rocco JW, Faquin WC, Lin DT, Regev A, Bernstein BE. Single-Cell Transcriptomic Analysis of Primary and Metastatic Tumor Ecosystems in Head and Neck Cancer. Cell. 2017;171(7):1611-24.e24. Epub 2017/12/05. doi: 10.1016/j.cell.2017.10.044. PubMed PMID: 29198524; PMCID: PMC5878932.
47. Worsham MJ, Van Dyke DL, Grenman SE, Grenman R, Hopkins MP, Roberts JA, Gasser KM, Schwartz DR, Carey TE. Consistent chromosome abnormalities in squamous cell carcinoma of the vulva. Genes, chromosomes & cancer. 1991;3(6):420-32. Epub 1991/11/01. PubMed PMID: 1777413.
48. Worsham MJ, Wolman SR, Carey TE, Zarbo RJ, Benninger MS, Van Dyke DL. Chromosomal aberrations identified in culture of squamous carcinomas are confirmed by fluorescence in situ hybridisation. Mol Pathol. 1999;52(1):42-6. Epub 1999/08/10. PubMed PMID: 10439839; PMCID: 395670.

Chapter 3: Using CRISPR/Cas9 Screening Libraries to Identify Mechanisms of Resistance to HNSCC Therapeutics

Abstract

Head and neck squamous cell carcinoma remains a deadly disease with poor prognosis. Developing novel, effective combination therapies can improve patient survival. To identify genes that mediate resistance to HNSCC therapies and are therefore prime targets for combination therapy, we developed CRISPR libraries in multiple UM-SCC lines. Using the CRISPR screens, we identified that loss of *NOTCH1* and inhibition of Notch signaling drove sensitivity to cisplatin treatment, nominating Notch inhibitors and cisplatin therapy as an effective combination treatment. We also used our genome and kinome CRISPR libraries to identify genetic knockouts that created sensitivity to the EGFR inhibitors gefitinib and erlotinib. We observed that the gene *PIK3C2A* may be an important linchpin in the PI3K pathway for mediating resistance to EGFR inhibition, and that *FGFR3* and FGF signaling may be a compensatory mechanism to EGFR signaling such that dual EGFR and FGFR inhibition may be an effective therapy in HNSCC.

Introduction

Patients with head and neck squamous cell carcinoma (HNSCC) have seen limited improvement in overall survival despite advances in standard therapies such as surgery, radiation, and chemotherapy (1). Likewise, while recent advances in immunotherapy have the potential to make significant improvements in HNSCC (2), not all patients will benefit, as only

10-15% of patients respond to the therapy (3). A promising option is combination therapy, meaning a treatment plan that includes two or more agents, which is a staple of cancer therapy. Where monotherapy treatment can often fail, a multi-dimensional therapy plan can be effective to reduce toxicity and cancer recurrence (4). However, the discovery of effective combinations remains a limiting factor.

The adaptation of the CRISPR/Cas9 genetic engineering platform for mammalian systems has allowed for a new approach to discover effective drivers of drug resistance, making the generation of arrays of genetic knockouts more feasible. Upon challenging a CRISPR library with a therapy, we can screen hundreds of genes simultaneously to identify genetic knockouts that create sensitivity to the treatment and nominate potential targets for combination therapy (5-7). Cisplatin is likely candidate to be one of the combination arms, as cisplatin is frequently used in HNSCC and specifically for recurrent and metastatic cases (8). Cisplatin crosslinks DNA which makes the process of DNA repair impossible, leading to activation of apoptosis mechanisms and resulting in cell death for quickly dividing cells (9). However, only 10-25% of patients will respond to cisplatin therapy (10), with few therapeutic options after failure. Resistance to cisplatin therapy remains an unfortunately common challenge in HNSCC (11).

An additional therapeutic treatment for HNSCC is the epidermal growth factor receptor (EGFR) inhibitor cetuximab. Cetuximab is a monoclonal antibody that binds and inhibits EGFR, and was approved for treatment in HNSCC in 2006 when the combination of cetuximab and radiation improved patient survival over radiation alone (12). However, cetuximab has limited effectiveness as monotherapy (13), despite that the majority of patients with HNSCC exhibit EGFR overexpression (14, 15). Indeed, there are no biomarkers of response to cetuximab treatment, and even patients that initially respond eventually recur.

Because of recurrence, several resistance mechanisms for EGFR inhibition have already been nominated. Activation of MET has been noted to cause resistance to cetuximab (16), potentially through the reactivation of the PI3K pathway (17). The PI3K pathway is frequently altered in HNSCC, specifically PIK3CA, either through activating mutations or gene amplification (18). However, while dual inhibition of EGFR and PI3K is currently ongoing in clinical trials, initial results from the pan-PI3K inhibitor PX-866 with cetuximab showed no improvement to patient survival (19). To improve efficacy, it will be important to use biomarkers to nominate specific compensatory pathways within a tumor to better rationalize combinational approaches.

In this chapter, we sought to identify mechanisms of resistance to cisplatin and EGFR inhibition using CRISPR libraries. We generated genome-wide and kinome-wide CRISPR libraries in UM-SCC cell line models that are resistant to cisplatin and EGFR inhibition, and then screened for genetic knockouts that generated sensitivity to these therapies. Here, we used the tyrosine kinase inhibitors (TKIs) gefitinib and erlotinib to inhibit EGFR. While gefitinib and erlotinib have had limited effectiveness in HNSCC, the TKIs have had *in vitro* activity (20). As gefitinib and erlotinib have had success in other EGFR-driven cancers (21-23), we propose that resistance mechanisms prevent these EGFR TKIs from being effective in HNSCC. In identifying these resistance mechanisms with our CRISPR screen, we expect to nominate combinational therapy approaches that can be applicable to TKIs and the EGFR inhibition activity through cetuximab.

Methods

Cell Culture. Cell lines were cultured in Dulbecco's Modified Eagle's Medium (DMEM) (Invitrogen #11965) containing 10% fetal bovine serum (FBS, Sigma), 1% NEAA (Invitrogen 15140122) and 7 µL/mL penicillin-streptomycin (Invitrogen 15140122) in a humidified atmosphere of 5% CO_2 at 37°C. Cells were tested for mycoplasma contamination using the MycoAlert detection kit (Lonza).

UM-SCC lines were transduced with the Human GeCKO CRISPR knockout pooled library, either version 1 (Addgene plasmid #49535) or version 2 (Addgene plasmid #52961) which were both gifts from Feng Zhang, or the Human Kinase Lentiviral CRISPR Pool (Sigma Aldrich HKCRISPR) (**Fig 3-1**). Conditions for transduction were established for a multiplicity of infection (MOI) of 0.3. After 7 days of puromycin selection, the cells were expanded and seeded per treatment. To preserve at least 300x coverage, 30 million cells were seeded per treatment for the GeCKO libraries while only 3 million cells per treatment were needed for the Kinase Library. At the end of treatment, genomic DNA was extracted from the remaining cells using Gentra Puregene Cell Kit (Qiagen).

Cisplatin treatment: Cells were dosed with 0.125 µM cisplatin (Selleckchem S1166) or DMSO (Sigma Aldrich) for 24 hours, once a week for two weeks.

Gefitinib and erlotinib treatment: Cells were dosed with 1 µM gefitinib (Selleckchem S1025) or 1 µM erlotinib (Selleckchem S7786) in triplicate. For the Kinase Library samples, the DMSO control was also in triplicate, while the GeCKO Library samples had one DMSO control treatment.

GeCKO Library Preparation. To preserve coverage of the GeCKO library, 130 µg of genomic DNA was used to PCR amplify the gRNA sequence using the Herculase ii Fusion DNA Polymerase (Agilent # 600675). 13 reactions with 10 µg input DNA were amplified with the following primers:

PCR #1 Fwd: AATGGACTATCATATGCTTACCGTAACTTGAAAGTATTTCG

PCR #2 Rev: GGTCTTGAAAGGAGTGGGAATTGGCTCCGGTGCCCGTCAG

The 13 reactions were combined, and then 5 µL were used to set up the second round PCR reactions with the following primers:

PCR #2 Fwd:

AATGATACGGCGACCACCGAGATCTACACTCTTTCCCTACACGACGCTCTTCCGATC

T(1-9bp stagger)AAGTAGAGtcttgtggaaaggacgaaacaccg

PCR #2 Rev:

CAAGCAGAAGACGGCATACGAGATTCGCCTTAGTGACTGGAGTTCAGACGTGTGCT

CTTCCGATCTataacggactagccttattttaac

Uppercase sequence represents Illumina adapters. The forward primer has the TruSeq Universal Adapter, and the reverse primer consists of Illumina P7, 8bp index, and multiplexing PCR primer 2.0. The underlined sequence represents an 8bp barcode. Lowercase letters are the priming sites for the lentiviral construct.

The PCR product was gel extracted and purified using Gel Extraction PCR Purification Kit (Qiagen) before submission to the University of Michigan DNA Sequencing Core for sequencing with Illumina MiSeq V3 Kit for cisplatin samples or Illumina HiSeq 2500 High-Output with V4 Kit with gefitinib and erlotinib treated samples.

Kinase Library Preparation. To preserve coverage of the Kinase Library, 12 µg of DNA was used to PCR amplify the gRNA sequence using the Herculase ii Fusion DNA Polymerase (Agilent # 600675). 2 reactions with 6 µg input DNA was amplified with the following primers:

PCR #1 Forward : AATGGACTATCATATGCTTACCGTAACTTGAAAGTATTTCG

PCR #2 Reverse: CTCGATTAATTAAGGTTGCTCACTTGTCGACTAATGC

The two reactions were then combined, and 5 µL were used to set up the second round of PCR reactions. PCR #2 primers are same as listed above in the GeCKO Library Preparation section, as this adds on Illumina adaptor sequences and barcodes.

The PCR products were gel extracted and purified using Gel Extraction PCR Purification Kit (Qiagen). Samples were then submitted to the University of Michigan DNA Sequencing Core for sequencing with Illumina MiSeq V3 Kit.

Analysis of CRISPR libraries. Reads were demultiplexed by barcode and then mapped to the corresponding reference library using an in-house python script. gRNA counts were input into Model-based Analysis of Genome-wide CRISPR/Cas9 knockouts (MAGeCK, v0.5.2) (24). MAGeCK algorithms calculated significant gRNAs and genes, and genes with an α-RRA score of ≤0.05 were advanced to GSEA analysis. GSEA was then performed using the Molecular Signatures Database (v5.1) with the GSEA3.0.jar module to identify overlap with “Hallmark”, “C3_motif”, “Go-BP” and “Oncogene” gene set databases. Analysis was performed with 1000 permutations and gene sets with false discovery rate of less than 0.05 were considered significant (max of 20 gene sets per reference database) as described [PMIDs:16199517, 12808457] and advanced for network analysis of representative and recurrent gene sets using the Cytoscape_v3.7.1 desktop module.

EGFR resistance analysis. Gefitinib IC50 values for non-UM-SCC cell lines were downloaded from The Genomics of Drug Sensitivity in Cancer Project (cancerrxgene.org) (25-27), using data version 17.3.

Venn diagrams. Venn diagrams were modified from the output of Galaxy's Venn Diagram program (28).

Generation of Clonal Knockout Lines. UM-SCC-49 was transduced with a lentiviral CRISPR construct targeting *NOTCH1 (*Sigma Aldrich, HS0000408729) and after antibiotic and GFP selection, individual clones were isolated. MARVELD3 and FGFR3 gRNA sequences were ordered as TrueGuide Modified Synthetic crRNA (ThermoFisher Scientific) and prepared according to manufacturer recommendations. The gRNAs were co-delivered with TrueCut Cas9 Protein v2 (ThermoFisher, A36496) using Lipofectamine CRISPRMAX Cas9 transfection reagents (ThermoFisher, CMAX00003) and then individual clones were isolated.
Individual clones were screened for knockout by sanger sequencing. DNA was extracted from clones (Qiagen, Gentra Puregene Cell Kit) and the gRNA region amplified by PCR using Platinum HiFi Taq (Invitrogen). Primers for amplification are in **Table 3-1**. PCR products were then ligated into pCR8 vector (ThermoFisher, K250020), transformed, and plasmid DNA extracted from individual colonies (Qiagen, QIAprep Spin Miniprep Kit) and submitted for sanger sequencing at the University of Michigan DNA Sequencing Core. Sequences were aligned using the DNASTAR Lasergene software suite.

Immunoblotting. Western blot analysis was performed as previously described (29, 30). Briefly, UM-SCC cell lines at 70-80% confluency were rinsed with PBS and lysed in buffer (150 mM NaCl, 10% Glycerol, 1% NP40, 0.1% Triton X-100, 1 mM PIPES, 1 mM MgCl, 50 mM Tris) containing protease and phosphatase inhibitors (Thermo 186129, 1861277) as described (31). See **Table 3-2** for primary and secondary antibodies used.

Clonogenic Cell Survival. Cells received cisplatin for 24 hours. Cells were then plated in triplicate and allowed to grow for two weeks, before being fixed and stained with 6% glutaraldehyde/0.5% crystal violet. Colonies with greater than 50 cells were counted and percent survival was calculated as number of colonies divided by number of plated cells. Survival fraction was calculated by dividing treatment cells by untreated controls.

Cell viability assays. 2,000 cells per well were seeded in 384-well microplates using a Multiflo liquid handling dispensing system. After 24 hours, cells were treated with compound or DMSO in a 10-point two-fold dilution series in quadruplicate. 96-well plates were prepared with compounds in 200X concentration and then diluted to 10X concentration in media in a second 96-well plate using the Agilent Bravo Automated Liquid Handling Platform and VWorks Automation Control Software. These compounds were then used to treat the cells with the desired drug concentration, again using liquid handling robotics. Cells were stained with resazurin (Sigma) in PBS for 12-24 hours before fluorescent signal intensity was quantified 72 hours after treatment using the Cytation3 fluorescence plate reader enabled with automatic stacking at excitation and emission wavelengths of 540 and 612 nm, respectively. All

compounds were purchased from Selleck Chemicals. 10 mM aliquots were stored -80 °C. Each compound was subjected to no more than 5 freeze-thaw cycles.

Trypan blue assays. 32,000 cells were seeded in 24-well plates. After 24 hours, cells were treated with compound or DMSO. All compounds were purchased from Selleck Chemicals. After 72 hours, cells were harvested and counted with trypan blue reagent (Invitrogen) using the Countess II Automated Cell Counter (ThermoFisher). Statistical analysis on trypan data was conducted by using a t-test to compare between wildtype and knockout cell lines and with Bonferroni correction to adjust p-value for multiple comparisons. For statistical analysis on comparing a dual inhibition treatment to the vehicle or monotherapy treatments, linear regression with interaction was used with Bonferroni correction to adjust p-value.

Transcript analysis by qPCR. Cells were rinsed with PBS and then preserved in Qiazol (Qiagen) at -80°C until RNA extraction was performed using RNeasy Spin Kit (Qiagen) according to manufacturer recommendations. cDNA templates were then synthesized using random primers and SuperScript III Reverse Transcriptase (Invitrogen) according to manufacturer recommendations. Primers used for qPCR analysis are listed in **Table 3-3**. Amplification by qPCR was performed with Quantitech Sybr Green (Qiagen) on QuantStudio5 (Applied Biosystems) under the cycling conditions recommended by manufacturer.

Results

With our goal being to nominate potential combination therapies that can block resistance to prioritized therapies, we chose a negative selection screening model for the CRISPR library

screens. The schematic in **Figure 3-2** outlines the creation, expansion, and experimental design to identify genetic knockouts that result in sensitivity to the treatment, and as such nominates potential dual therapy combinations for effective cell death. To test out our hypothesis that genetic knockouts in the CRISPR library could drive sensitivity to a monotherapy, we chose to use cisplatin due to its prevalence in treatment for head and neck cancer and the relative resistance of UM-SCC-49 cells to cisplatin monotherapy.

Thus, we transduced UM-SCC-49 cells with the GeCKO v2A CRISPR library, then selected and expanded this pool before treating with cisplatin or vehicle control. The low dose of cisplatin every 7 days was chosen based on minimal impact to wildtype UM-SCC-49 cells (**Figure 3-3**). At the end of treatment, we isolated genomic DNA from the remaining cell pools and used Next Generation Sequencing (NGS) to sequence the gRNAs. We observed that over 80% of the original GeCKO v2A library was represented in both control and treatment populations (**Fig 3-4**).

We then compared the gRNA sequences from the cisplatin treatment to the vehicle control using the MAGeCK algorithm for CRISPR knockout screens (24). This analysis pipeline identified gRNAs (**Fig 3-5A**) and genes (**Fig 3-5B**) that were significantly depleted in the cisplatin treatment compared to the control. We then advanced significant genes (p-value $\leq$ 0.005) for GSEA analysis which nominated several pathways as candidate drivers of cisplatin resistance (**Fig 3-5C**). To our surprise, the most significant pathway enriched in the gene set was the Notch signaling pathway. Genetic knockouts in the Notch signaling pathway targeting genes such as *NOTCH1*, *SSPO, NCOR1*, *MARK2,* and *MYCBP* were underrepresented in the UM-SCC-49 GeCKO pool following cisplatin treatment. Previous studies in ovarian cancer (32) and

colorectal cancer (33) have found that inhibition of the Notch signaling pathway sensitized cells to cisplatin, which gave us confidence that our screening method provided valid targets.

We then went on to further validate that a genetic knockout in the Notch signaling pathway would sensitize UM-SCC-49 cells to cisplatin. We used CRISPR/Cas9 to knockout *NOTCH1* in UM-SCC-49, where the gRNA was targeted to exon 25 as shown in **Fig 3-6A**. The resulting deletions in both alleles of *NOTCH1* resulted in no detectable expression of Notch1 protein in the *NOTCH1* knockout (K/O) (**Fig 3-6B**). There are moderate decreases in expression of downstream effectors such as Hes1, Hey1, and c-Myc. It is also interesting to note the increase in Notch2 expression, potentially to compensate for the knockout of *NOTCH1*. Then, we wanted to test if the NOTCH1 K/O cell line was more sensitive to cisplatin than wildtype UM-SCC-49 cells as expected from the results of the CRISPR library screen. Clonogenic assays showed that the NOTCH1 K/O cell line is more sensitive to cisplatin than the wildtype UM-SCC-49 cells and we observed a similar sensitivity in the NOTCH1 K/O as when Notch signaling is inhibited by the γ-secretase inhibitor DAPT (**Fig 3-6C**).

With the successful identification of a genetic knockout that sensitized a UM-SCC model to cisplatin, we then moved on to test the hypothesis that genetic knockouts could drive sensitivity to EGFR inhibition. In addition to the UM-SCC-49 model, we also transduced GeCKO libraries into two additional cell lines resistant to EGFR inhibition, UM-SCC-58 and -108 (**Fig 3-7**), and then challenged all three GeCKO pools with gefitinib or erlotinib alongside vehicle controls. We maintained a broad coverage of library diversity across libraries and treatments with the exception of UM-SCC-49 GeCKO v2A that was treated with erlotinib (**Fig 3-8**). As the loss of ~50% coverage applies to both the vehicle control and erlotinib treatments, we suspect that the coverage was lost before seeding the library pool for treatment. While part of

the diversity of the library was lost, we continued the analysis for the knockouts that were maintained in the library pool.

We expected that the similar mechanism of actions between gefitinib and erlotinib would produce similar hits and so first looked at the overlap between these inhibitors. For UM-SCC-49, the gefitinib treatment had 1,877 genes as significant and erlotinib treatment had 969 genes (p-value ≤ 0.05). This difference in number of hits called, almost two-fold, is most likely due to the loss of diversity in the erlotinib libraries. However, there were still 132 genes that overlapped in the gefitinib and erlotinib treated libraries in UM-SCC-49. UM-SCC-108 had 1,887 genes called as significant for gefitinib and 1,658 genes for erlotinib (p-value ≤ 0.05) with 539 genes overlapping between these two treatments. UM-SCC-58 had 1,908 significant genes in the gefitinib treatment and 2,050 genes for the erlotinib treatment (p-value ≤ 0.05), with 310 genes overlapping. To further prioritize targets, we then looked for genes that overlapped between the cell lines (**Fig 3-9**). To our surprise, few genes were found to be the same across cell lines. Two genes, *TSPAN7* and *CYP39A1*, were found in UM-SCC-49 and UM-SCC-108 libraries. Four genes, *BBS9, RHO, NARF*, and *ZCCHC14*, were found in both UM-SCC-49 and UM-SCC-58 libraries, and 9 genes, *ZNF449*, *CALCR*, *NUBPL CYP2C18*, *DEK*, *AKZF1*, *AURKB*, *FAM19A5*, and *DPY19L4* were found in both UM-SCC-58 and UM-SCC-108 libraries. There were no genes in common between all three cell lines for both the gefitinib and erlotinib treatments. We saw similarly low numbers of overlap when analyzing only gefitinib or only erlotinib results between all three lines (**Fig 3-10**).

As we identified few genes in common between all GeCKO screens, we sought to use a parallel strategy to add additional statistical support to the candidates advanced for validation. Thus, we then acquired the Human Kinase CRISPR Knockout Library. The number of gene

targets for knockout is smaller than the GeCKO libraries, but allowed for more gRNAs per gene to provide more statistical power in analysis (**Table 3-4**). We transduced the cell lines UM-SCC-49, -97, and -108 with this Kinase library and repeated the pool expansion for treatment with vehicle control, gefitinib or erlotinib with the same doses of inhibitor and conditions as the GeCKO screen above. After sequencing the surviving cell population, we again analyzed the diversity content of the library which was maintained at above 80% coverage for the majority of conditions (**Fig 3-11**).

We then used the MAGeCK algorithm to identify significant gRNA and gene depletion in the gefitinib or erlotinib treatments compared to their respective controls. For UM-SCC-49, 111 genes were significantly depleted in the gefitinib treatment and 116 genes in the erlotinib treatment (p-value ≤ 0.05), with 65 genes in common between both treatments. UM-SCC-108 had 109 significant genes in the gefitinib treatment and 113 genes in the erlotinib treatment (p-value ≤ 0.05), with 31 genes overlapping. UM-SCC-97 had 155 significant genes for gefitinib and 119 genes for Erlotinib (p-value ≤ 0.05), with 72 genes in common. There were 9 genes in common between UM-SCC-49 and UM-SCC-97 (*PHKG2, PINK1, PIP4K2B, CAMK1D, RAB32, SLK, TRIM33, CDKL1, MAP3K8),* 3 genes in common between UM-SCC-49 and UM-SCC-108 (*CDK5R1, ULK4, PDK4),* and 3 genes in common between UM-SCC-108 and UM-SCC-97 (*RPS6KB1, BTK, CDK12).* The gene *PIK3C2A* was the only gene called as significant for both gefitinib and erlotinib treatments across all three lines (**Fig 3-12).** We also noted 8 genes overlapping between the gefitinib treatments across all three cell lines (*PIK3C2A, MIP, PINK1, CAMK1D, KIAA1804, TRIM33, CAMK1G, FRK*), and 3 for the erlotinib treatments (*PIK3C2A, PDXK, TNK1)* (**Fig 3-13**).

We next performed gene set enrichment analysis to evaluate similar pathways between the gefitinib and erlotinib treatments across the three lines. As expected, the PI3K/mTOR/FOXO4 pathway was enriched, as the PI3K pathway is a frequent combinational target with EGFR inhibition (31, 34-36) (**Fig 3-14A**). We also noted enrichment for several transcription factors (*SP1, MAX, PAX4)* and, interestingly, the Notch signaling pathway. Surprisingly, we also noted enrichment in the KRAS pathway, suggesting that KRAS signaling may play more of a role in resistance to EGFR inhibition than previously thought for HNSCCs. We then looked at gene enrichment in the GeCKO libraries, where the KRAS pathway was also enriched (**Fig 3-14B**). Similar to the results of the Kinase libraries, transcriptional regulation and PI3K and Notch signaling pathways were also enriched. In addition, the GeCKO libraries nominated cell death and DNA damage pathways, WNT signaling, cell cycle genes, interferon gamma and TGF-beta pathways, and genes involved in estrogen response. GSEA outputs for the individual cell line and inhibitor treatments for the Kinase and GeCKO libraries are in **Table 3-6, 3-7**.

From this analysis, we nominated 6 candidate genes to generate individual CRISPR/Cas9 knockout clones for further validation of their role in compensatory EGFR inhibitor resistance (**Table 3-5**). We chose *PIK3C2A* as it was a significant hit in all six of the Human Kinase libraries and represented a potential mechanism of activation of the PI3K/mTOR gene set node. Further, we chose to focus on highly recurrent kinases identified in the screens as we postulated that these may represent more easily druggable targets including both *CDK12* and *PINK1,* which were depleted in 5/6 of the Kinase screens, *PDXK,* depleted in 4/6 of the Kinase screens including all the erlotinib treatments, and *MARVELD3,* depleted in 3/6 screens including both UM-SCC-49 Kinase screens. We also prioritized *FGFR3* which was found in both UM-SCC-49

treatments, as FGFR signaling has been noted as a promising target for HNSCC (37, 38). *PINK1* and *PDXK* were also significant hits in 2 and 1 of the GeCKO screens respectively, further supporting the potential role for these kinases in EGFR inhibitor resistance.

At the time of writing this dissertation, only knockout clones for *FGFR3* and *MARVELD3* were successfully isolated in the UM-SCC-49 model. The MARVELD3 K/O clone displayed loss-of-function deletions in each of the three *MARVELD3* alleles in UM-SCC-49 (**Fig 3-15A**). However, the MARVELD3 K/O cell line did not display any additional sensitivity to the EGFR inhibitors gefitinib or erlotinib compared to the UM-SCC-49 wildtype cell line after 72 hours (**Fig 3-15B**). We successfully engineered two independent *FGFR3* knockout clones, though both clones contain the same 7bp deletion in one allele (**Fig 3-16A**). Interestingly, FGFR3 K/O #2 contains an allele with a 7bp deletion and 192bp insertion in which the insertion matches an intronic region in *SLC4A4* before resuming *FGFR3* sequence. Both FGFR3 K/O clone #1 and #2 display a significant sensitivity to gefitinib after 72 hours ($p\text{-value} \leq 0.05$, $p\text{-value} \leq 0.01$) as compared to UM-SCC-49 wildtype (**Fig 3-16B**). We also challenged UM-SCC-49 and the FGFR3 K/O clones with a pan-FGFR inhibitor in combination with EGFR inhibition. As no specific FGFR3 inhibitors were available, we choose a pan-FGFR inhibitor with two goals in mind. First, we postulated that if FGFR3 was the main driver of sensitivity to EGFR inhibitors and there was no additional compensation from FGFR1 or FGFR2, then the FGFR3 K/O clones would display no additional sensitivity to a pan-FGFR inhibitor. Second, we postulated that the combination of EGFR and FGFR3 (and/or pan-FGFR inhibition) may lead to cell death in UM-SCC-49 wildtype which could nominate the dual inhibition of EGFR and FGFR as an effective therapeutic combination. **Fig 3-16B** also shows that while neither UM-SCC-49 WT or the FGFR3 K/O clones are sensitive to the pan-FGFR inhibitor as a monotherapy, all the cell lines

undergo cell death with the combination of the pan-FGFR inhibitor and EGFR inhibitor. Furthermore, both FGFR3 K/O clones have significantly more cell death with the combination of EGFR and pan-FGFR inhibition (p-value ≤ 0.01), indicating that there may be additional compensation from FGFR1 and FGFR2. However, under normal cell growth conditions the FGFR1 and FGFR2 transcripts are not upregulated in either of the FGFR3 K/O clones (**Fig 3-16C**).

Discussion

Here, we present the results of two CRISPR screening libraries used in negative selection screens with UM-SCC cell lines as well as the subsequent validation of prioritized candidates from each screen. Our results nominate candidate genes that potentially drive resistance to two common HNSCC therapies. Because a large number of patients are treated with cisplatin and will eventually develop resistance to the therapy (10, 11), we first focused on identifying knockouts that sensitized cisplatin-resistant cells to the therapy. Our genome-wide CRISPR screen identified the Notch signaling pathway as the most significant pathway that, when inhibited, was sensitive to cisplatin. Importantly, these data are consistent with previous results in other models (32, 33), and this finding is particularly interesting for HNSCC given the prevalence of inactivating NOTCH mutations (39, 40). In addition, others have found that higher expressions of Notch1 correlated with cisplatin resistance (41, 42).

Given this relationship between NOTCH signaling and cisplatin resistance, we went on to validate our findings by generating a syngeneic *NOTCH1* knockout model. Our targeted knockout model corroborated the results of our CRISPR screen, showing that knocking out *NOTCH1* alone was enough to induce sensitivity to cisplatin. While we observed moderate

changes in the Notch signaling pathway after knocking out *NOTCH1*, both in downstream effectors and the Notch2 receptor, these responses did not compensate for the lack of Notch1. Indeed, the *NOTCH1* knockout model had a similar sensitivity to cisplatin as the DAPT treatment which would have inhibited all 4 of the Notch receptors. Findings from Lee et al. in other HNSCC models suggest that inhibiting Notch1 leads to a reduction of cancer stem cell traits which augments sensitivity to cisplatin (43), which is one potential mechanism consistent with our observation.

Our results nominate Notch inhibitors as potential combination therapies alongside cisplatin treatment. Unfortunately, this combination is unlikely to be feasible in translation. Gamma-secretase inhibitors (GSIs) have undergone clinical trials, most notably for patients with activating Notch mutations in T-ALL (44, 45), and have dose limiting gastrointestinal toxicity from inhibition of Notch signaling (46). Additionally, a GSI clinical trial for Alzheimer's patients led to the occurrence of both basal cell and squamous cell carcinoma (47). While the inhibition of Notch signaling may sensitize HNSCCs to cisplatin, the current therapeutic options to inhibit the Notch pathway are not clinically beneficial to make this combination an effective therapeutic option.

Our other 12 CRISPR screens, 6 of which were genome-wide and 6 of which targeted the kinome, were setup to nominate genes and pathways that would sensitize HNSCC to EGFR inhibition. While the small molecule inhibitors gefitinib and erlotinib are not currently approved for HNSCCs, we postulated that these EGFR inhibitors may be effective in combination with another therapy. Our 6 genome-wide screen nominated hundreds of genes that could sensitize our HNSCC models to gefitinib or erlotinib. Unfortunately, very few of these genes overlapped between the three cell line models which made it difficult to prioritize targets for validation. We

then acquired the kinome library, which given its more limited target size in comparison to the genome-wide library, allowed for more gRNAs per gene without becoming technically infeasible. With the additional statistical power, the kinome library provided more confidence in choosing targets for validation. For example, the gene *PIK3C2A* was significantly depleted in all six of the kinome screens. While *PIK3C2A* was not significantly depleted in any of the genome-wide screens, the kinome screens nominated *PIK3C2A* as a potentially important node for the PI3K pathway's contribution to resistance to EGFR inhibition.

Concordantly, our analysis of critical pathways that contribute to resistance to EGFR inhibition nominated the PI3K/mTOR/FOXO4 pathway for both the genome-wide and kinome screens. More surprising, the results of both screens also nominate the Notch signaling pathway as a potential resistance mechanism to EGFR inhibition. However, we anticipate the same difficulties as discussed above in advancing a combination with Notch inhibitors. Of particular interest to us was the significant depletion of genes in the KRAS pathway across both genome-wide and kinome screens. While the KRAS pathway is a known resistance mechanism to EGFR inhibition in other cancers such as colon (48) and lung (49, 50), it is frequently due to activating mutations in KRAS. However, KRAS activating mutations are rare in HNSCC (18) and are not present in the UM-SCC cell lines used in the screens (30). The result of the KRAS pathway may speak more generally to Ras activity, though again these UM-SCC cell lines do not have activating mutations in *KRAS*, *HRAS*, or *NRAS*.

From our CRISPR screens we nominated six genes for further validation. At the time of writing this dissertation, we successfully isolated clonal CRISPR knockout lines for *FGFR3* and *MARVELD3*. From the results of the CRISPR screen, we expected these knockout lines to show greater sensitivity to EGFR inhibition than the parental wildtype cell line. However, the

MARVELD3 K/O clone did not display sensitivity. As the CRISPR screen was conducted with multiple doses of EGFR inhibitor over the course of two weeks, it is possible that the MARVELD3 K/O cell line may have a greater sensitivity to EGFR inhibition that is not observable over the course of three days. A longer term experiment, such as dosing for two weeks and monitoring cell proliferation as well as cell viability, would be informative on any potential sensitivity that the MARVELD3 K/O clone may have. However, both FGFR3 K/O clones showed a statistically significant sensitivity to EGFR inhibition over a shorter 3-day experiment, and the UM-SCC-49 wildtype cell line underwent cell death in response to dual EGFR and FGFR inhibition. Interestingly, the combination of EGFR and FGFR inhibition has shown effectiveness in a model without *FGFR1* amplification, a frequently used biomarker for possible response to this therapy.

In summary, we used multiple CRISPR screens to identify genetic knockouts that may drive sensitivity to HNSCC therapies. Our results nominated the Notch signaling pathway and specifically *NOTCH1* as a co-target with cisplatin therapy, suggesting that the combination of Notch inhibition and cisplatin could be clinically beneficial for HNSCC if and when therapeutics targeting Notch have decreased side-effects. When using EGFR inhibitors, our results identified *FGFR3* and the FGF signaling pathway as a potential compensatory pathway. The combination of EGFR and FGFR inhibition has shown promise in other cancer types, and we propose that this dual inhibition may also be efficacious in HNSCC.

Acknowledgements

Thank you to A. Kulkarni for the bioinformatics work on the CRISPR screen and A. Birkeland on the generation of the NOTCH1 K/O model and follow-up immunoblotting and clonogenic assays. Thank you to N. Michmerhuizen and S. Foltin for the resazurin cell viability assays. Thank you to S. Foltin and E. Gensterblum-Miller for assistance in screening clones for the MARVELD3 and FGFR3 K/O models, and to C. Brenner for the GSEA analysis. Thank you to J. Zhai and H. Jiang for statistical analysis.

Figures

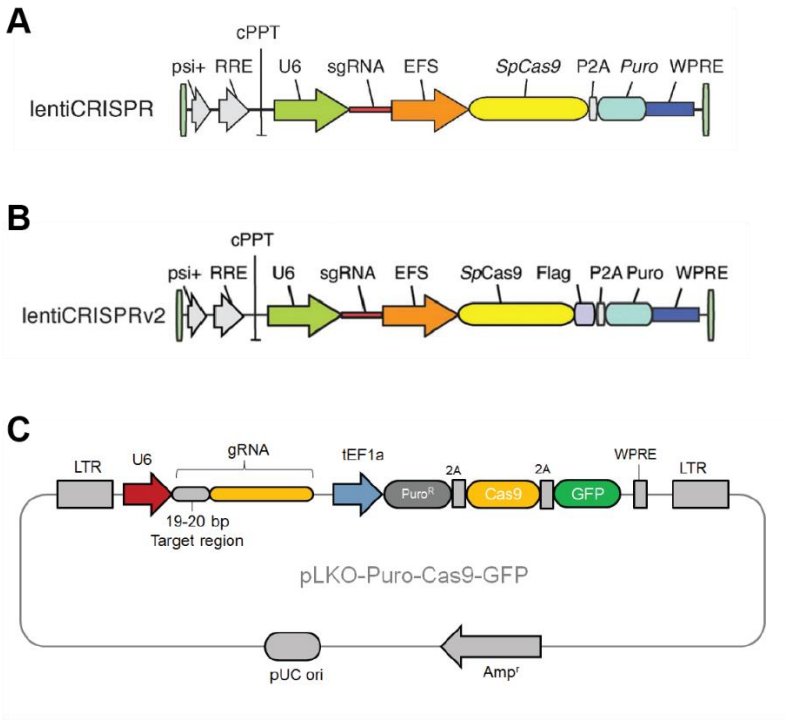

Figure 3-1. CRISPR library constructs

Schematics of lentiviral vectors used in CRISPR screens. **A)** GeCKO version 1 **B)** GeCKO version 2 **C)** Human Kinase Library

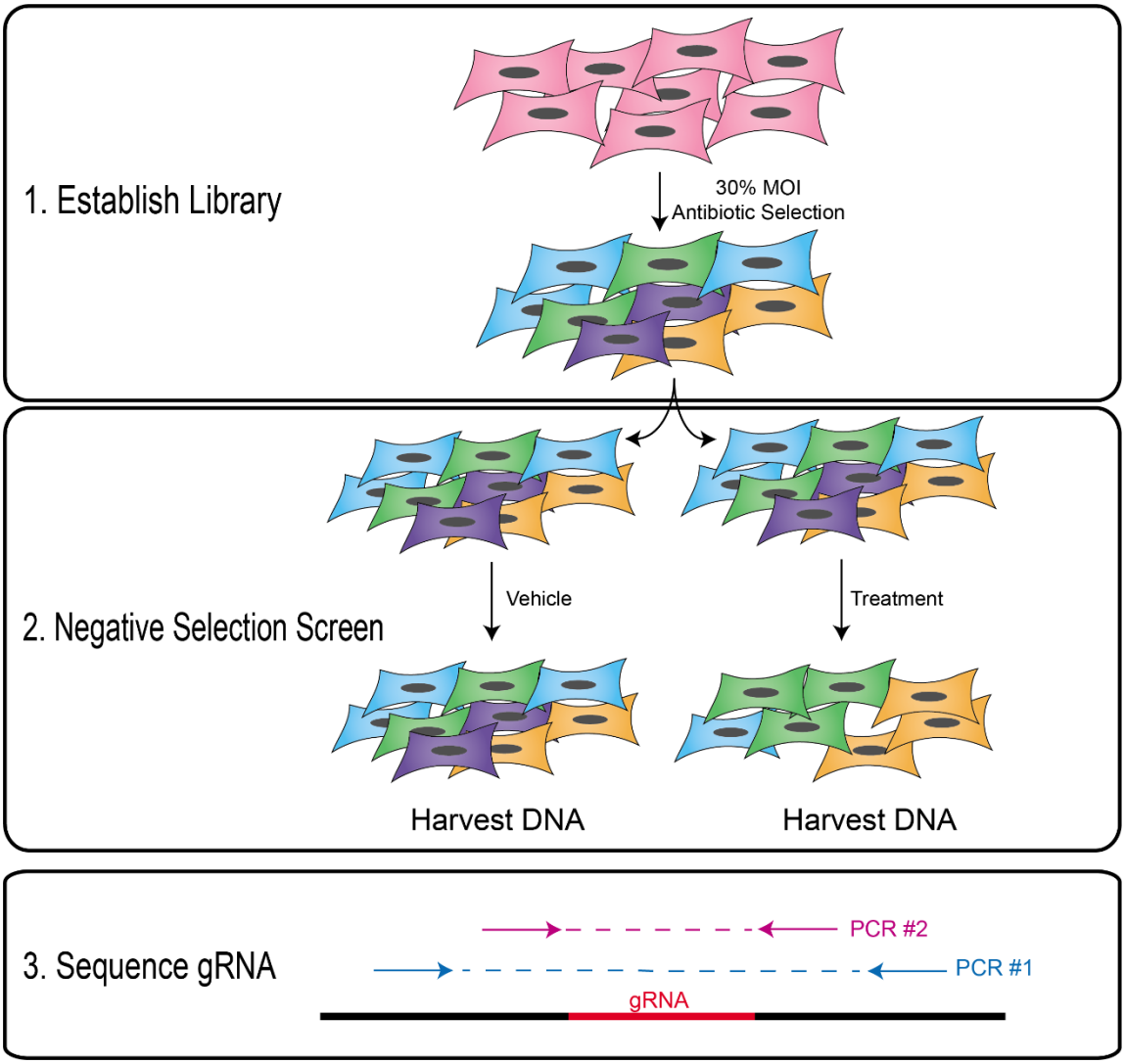

Figure 3-2. Workflow schematic of the CRISPR library screen

Schematic of negative selection screen from CRISPR library. First a library is established, taking a wildtype cell line and adding the lentiviral library at 30% MOI and then undergoing antibiotic selection. Here, different knockouts from gRNAs are represented in different colors. Then the CRISPR library pool is expanded and split for treatment, either vehicle control or compound. At the end of treatment, DNA is harvested from the surviving populations, and next generation sequencing libraries are prepared using a nested PCR setup around the gRNA.

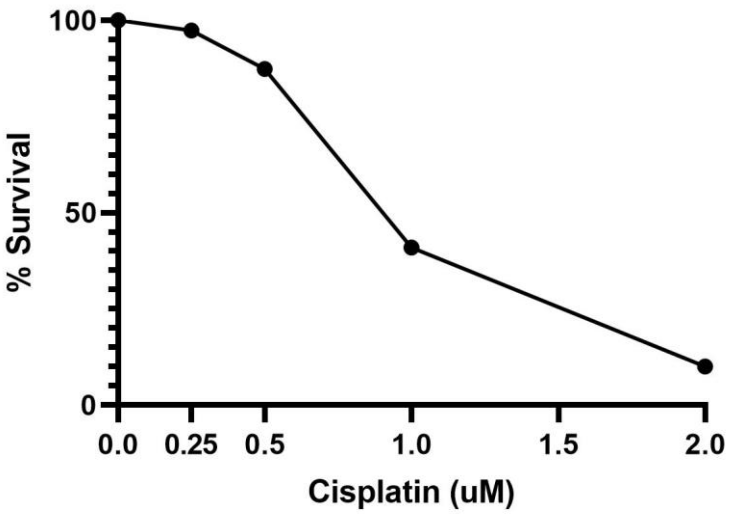

Figure 3-3. Response of UM-SCC-49 to cisplatin

Percent survival of the UM-SCC-49 cell line after treatment with cisplatin as determined by clonogenic assay. Each dot represents a dosage tested, with a line drawn for interpretation.

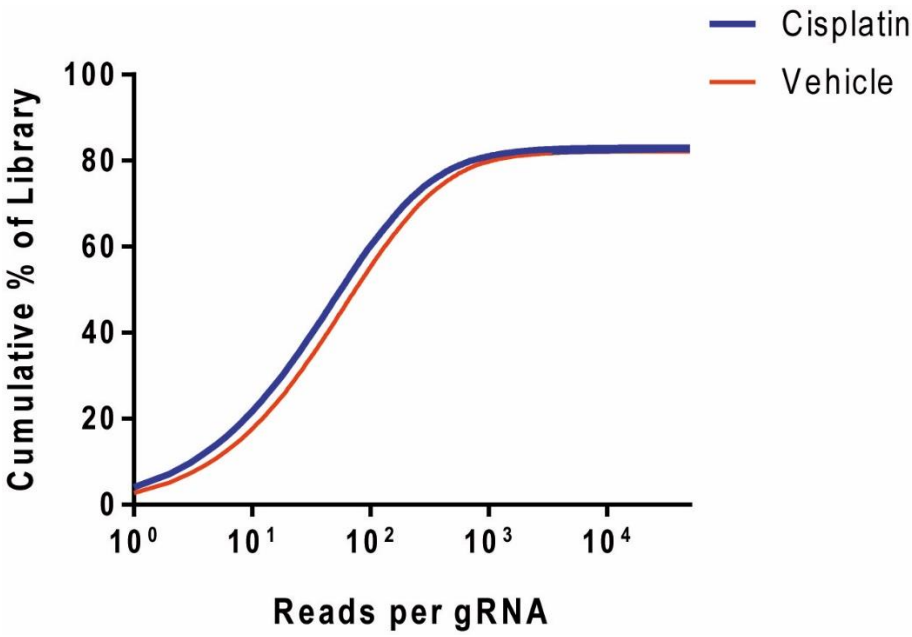

Figure 3-4. Library coverage plots for cisplatin and vehicle treated libraries

Cumulative percentage of library coverage for UM-SCC-49 GeCKO v2A treated with vehicle or cisplatin. The incline of the curve from 20-80% of cumulative total represents the bulk of the library has an average of 100 reads representing each gRNA, indicating good depth of sequencing. Few gRNAs either have very few reads (<10) or very high reads (>1000).

A.

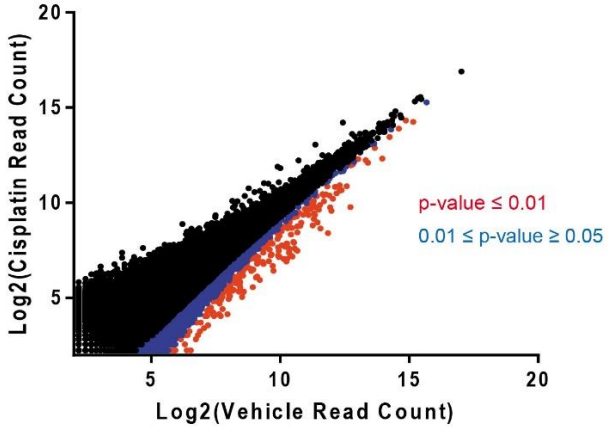

B.

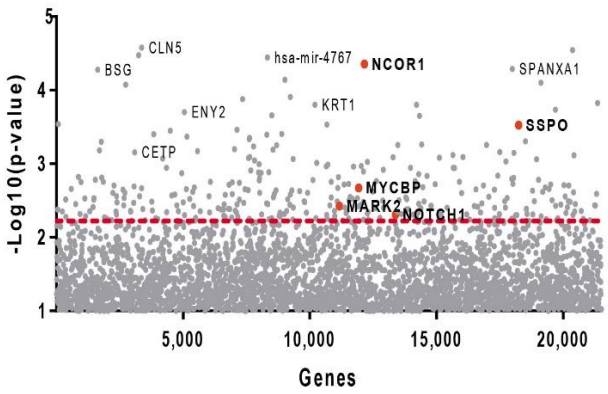

C.

Pathway	Genes	p-value	FDR
NOTCH signaling	*NOTCH1, SSPO, NCOR1, MARK2, MYCBP*	1.94E-06	2.58E-03
mTOR signaling	*SSPO, RAC1, CCNE1, ULK1*	9.77E-05	3.63E-02
LIS1 in neuronal migration and development	*RAC1, CDK5R1, VLDLR*	1.23E-04	3.63E-02
E2F Network	*CCNE1, RBL1, DHFR, E2F6*	1.28E-04	3.63E-02
Reelin signaling pathway	*CDK5R1, VLDLR, MAP2K7*	1.36E-04	3.63E-02

Figure 3-5. Cisplatin CRISPR screen nominates Notch signaling pathway

A) gRNA read counts plotted for vehicle verses control treatment. gRNAs in blue indicate a significant depletion ($0.01 \leq$ p-value ≥ 0.05) and gRNAs in red indicate a significant depletion with p-value ≤ 0.01. B) The –log10(p-value) for each gene is plotted, where the p-value represents the significance of depletion in the cisplatin treatment as compared to the vehicle control. A dotted line representing a p-value cut off of 0.005 is shown, where everything above the line has a p-value ≤ 0.005. Significantly depleted genes in the Notch pathway are bolded and values colored red. C) GSEA results from genes with a p-value ≤ 0.005, where the enriched pathway and significantly depleted genes are noted as well as p-value and FDR from the GSEA analysis.

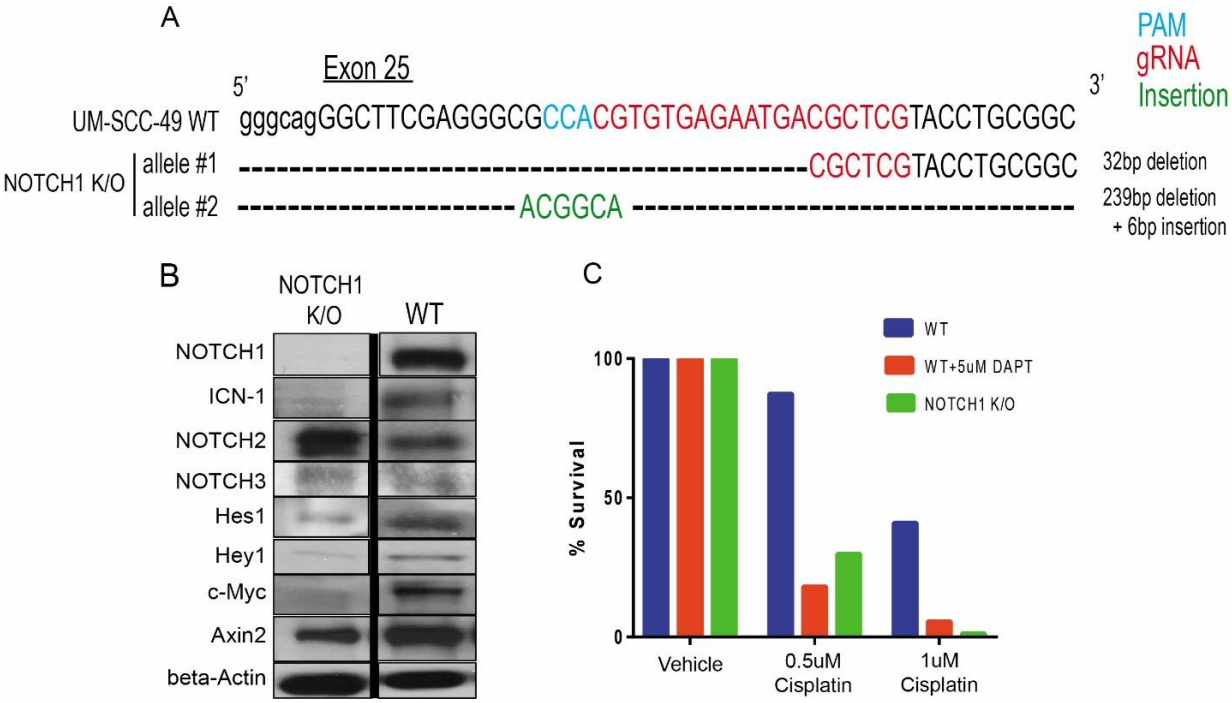

Figure 3-6. Response of NOTCH1 K/O model to cisplatin

A) Schematic of sanger sequencing results from NOTCH1 K/O, showing a 32bp deletion and 239bp deletion + 6bp insertion for both allelic copies of *NOTCH1*. The gRNA (red) and PAM sequence (blue) were in exon 25 of *NOTCH1*. B) Western blot images of UM-SCC-49 line (WT) and NOTCH1 K/O. C) Bar graph shows percent survival of UM-SCC-49 WT (blue), UM-SCC-49 WT plus 5uM DAPT treatment (red), and NOTCH1 K/O (green) across vehicle or cisplatin treatment.

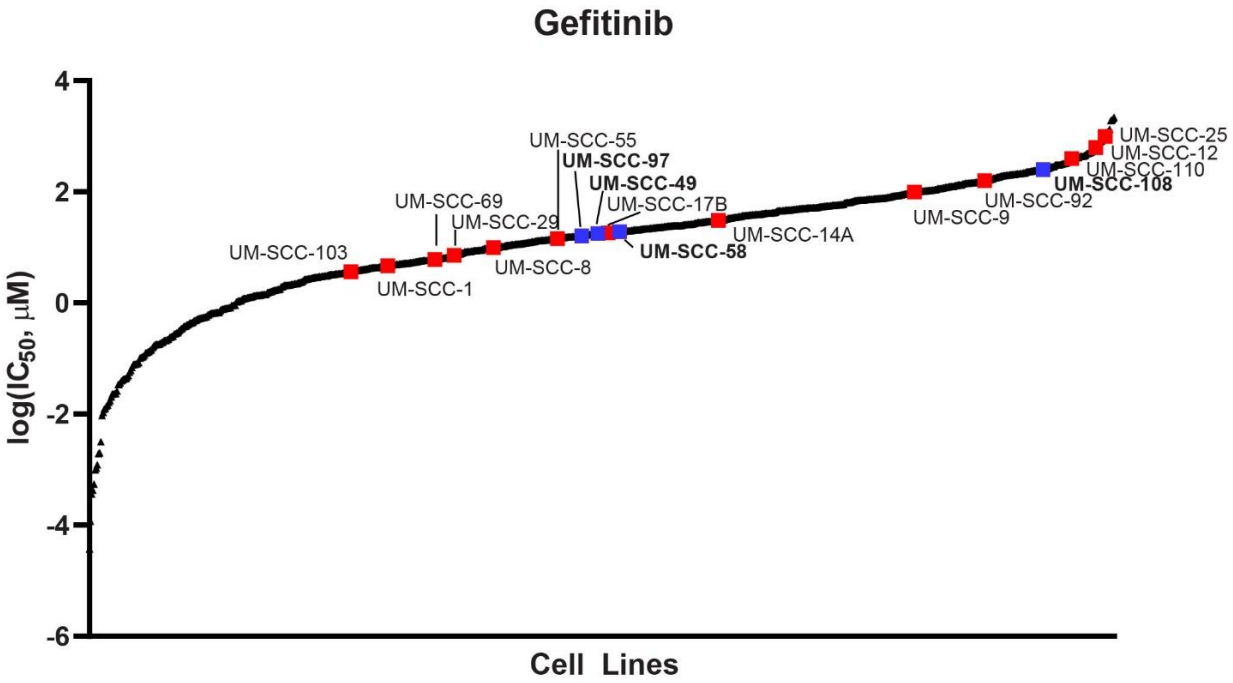

Figure 3-7. UM-SCC resistance to EGFR inhibitor gefitinib

Responses of cell lines to the EGFR inhibitor gefitinib, plotting log10 of the IC_{50} value in μM. Black dots are from cell line responses downloaded from The Genomics of Drug Sensitivity in Cancer Project. UM-SCC cell lines are in red as tested by cell viability assays using resazurin. IC_{50} values were determined from the mean and standard deviation of at least quadruplicate measurements for each treatment and cell line. Cell lines used for CRISPR screening are noted in blue.

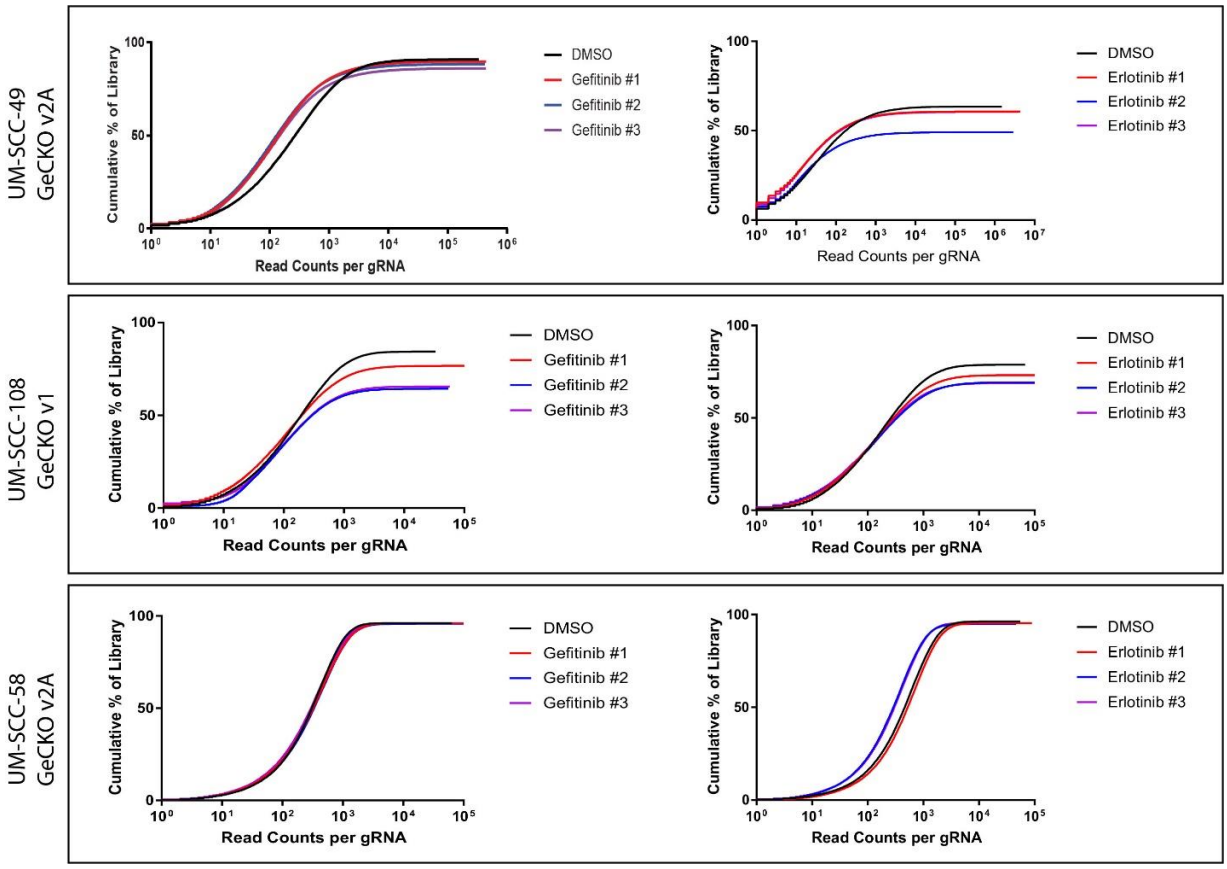

Figure 3-8. Library coverage plots for GeCKO libraries

Coverage plots for each replicate of the GeCKO library CRISPR screens for each cell line tested. Read counts per each gRNA are across the x-axis. Notably, there are few gRNAs with low read counts (<10) or high read counts (>1000), as indicated by the strong incline ~100 reads. The vehicle control DMSO is in black, with the replicates of the drug treatments in red, blue, and purple.

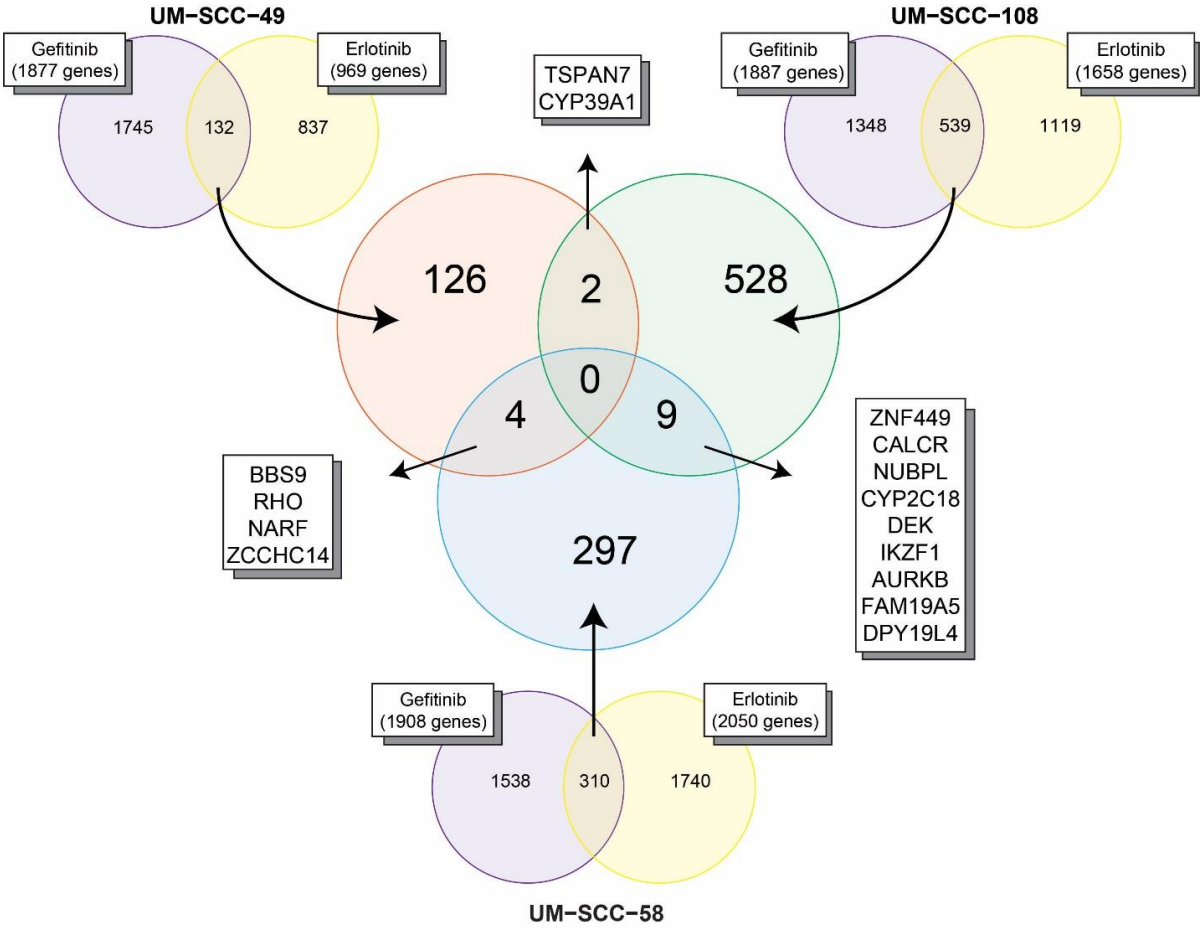

Figure 3-9. Overlap of GeCKO libraries

Venn diagram of overlap of the significantly depleted genes (p-value ≤ 0.05) for each GeCKO screen as indicated.

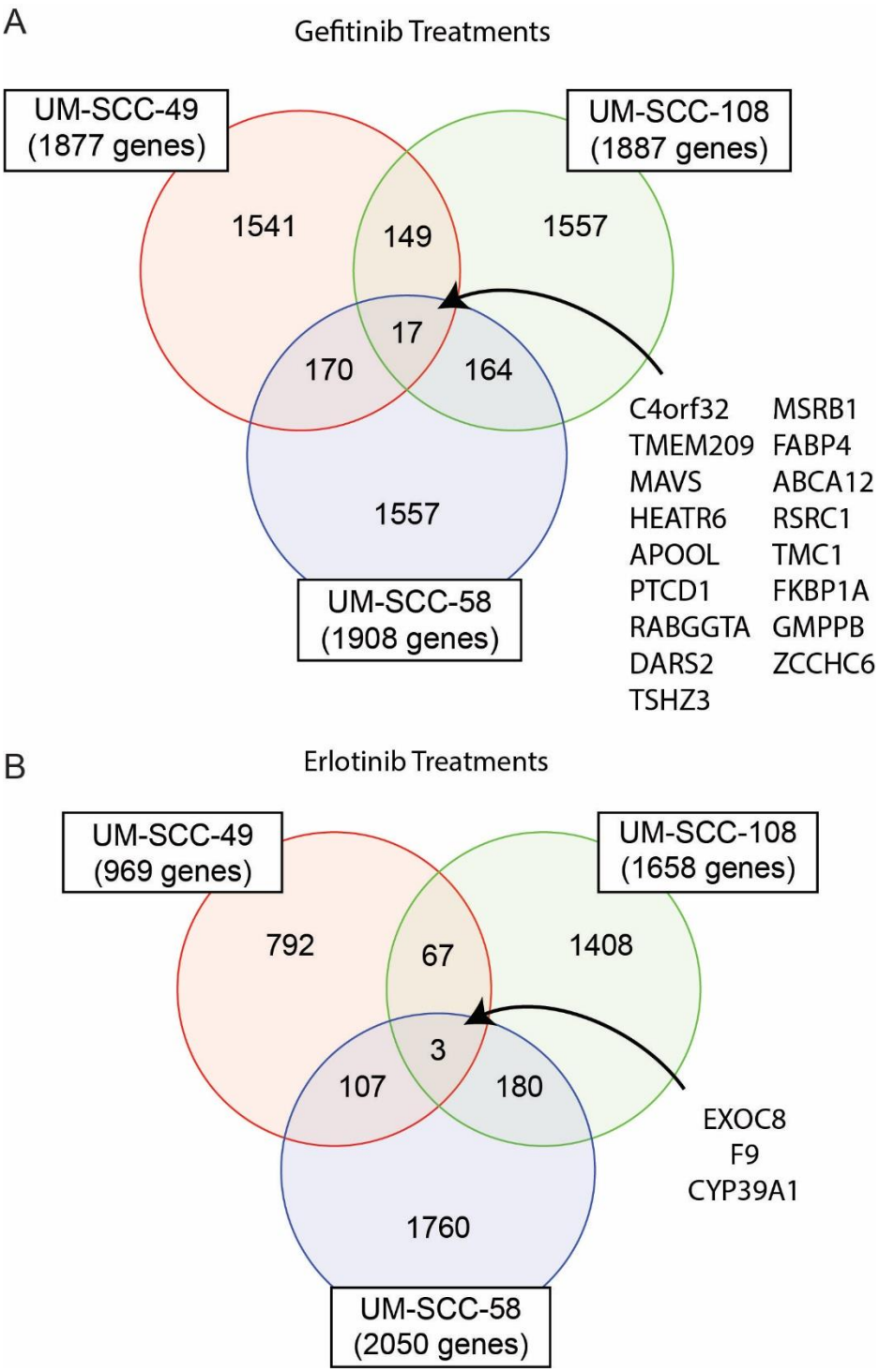

Figure 3-10. Overlap of GeCKO library for each inhibitor

Venn diagrams showing the overlap of significantly depleted genes (p-value ≤ 0.05) between cell lines for gefitinib (A) or erlotinib (B) treatments for the GeCKO library.

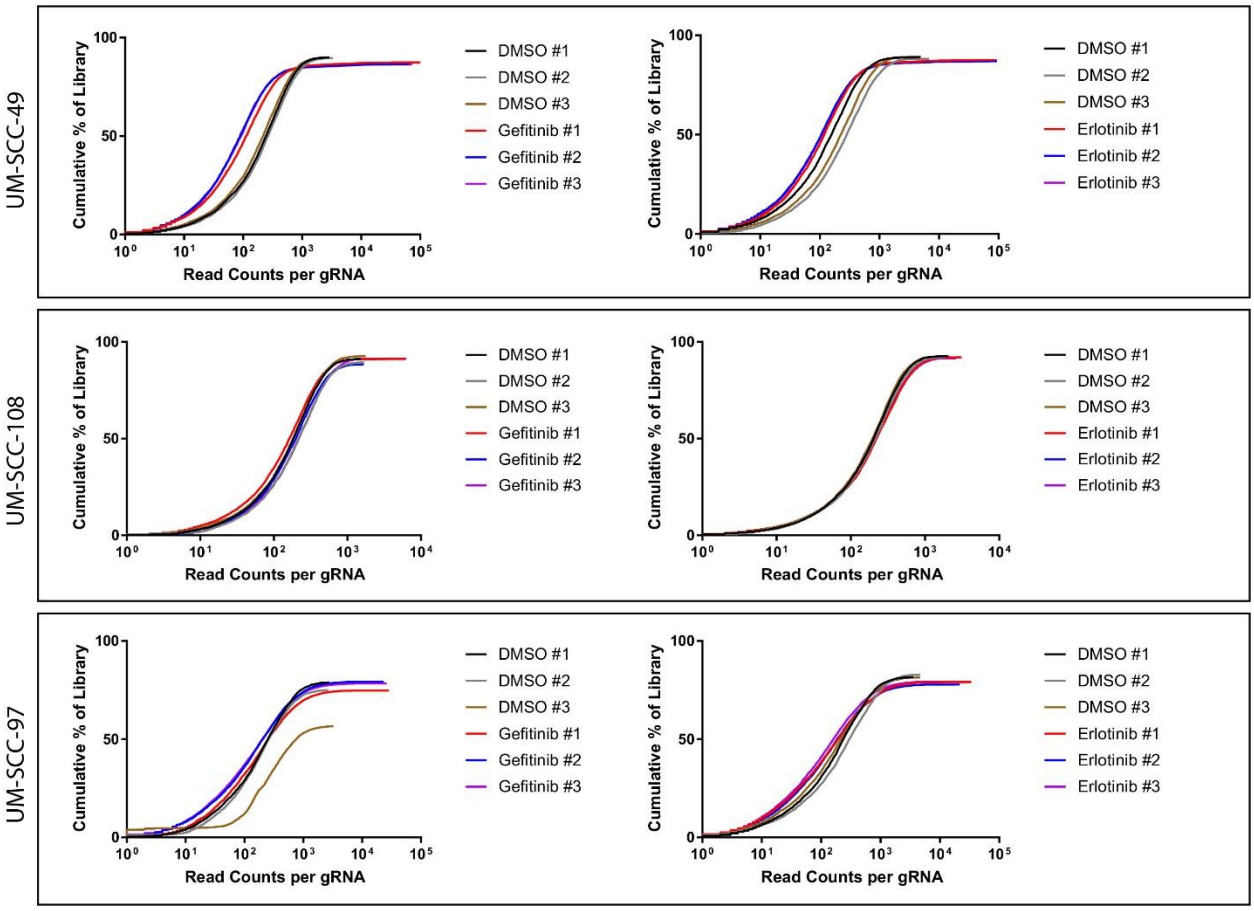

Figure 3-11. Library coverage for Kinase libraries

Coverage plots for each replicate of the Kinase library CRISPR screens for each cell line tested. Read counts per each gRNA are across the x-axis. Notably, there are few gRNAs with low read counts (<10) or high read counts (>1000), as indicated by the strong incline ~100 reads. The vehicle control DMSO is in black, with the replicates of the drug treatments in red, blue, and purple.

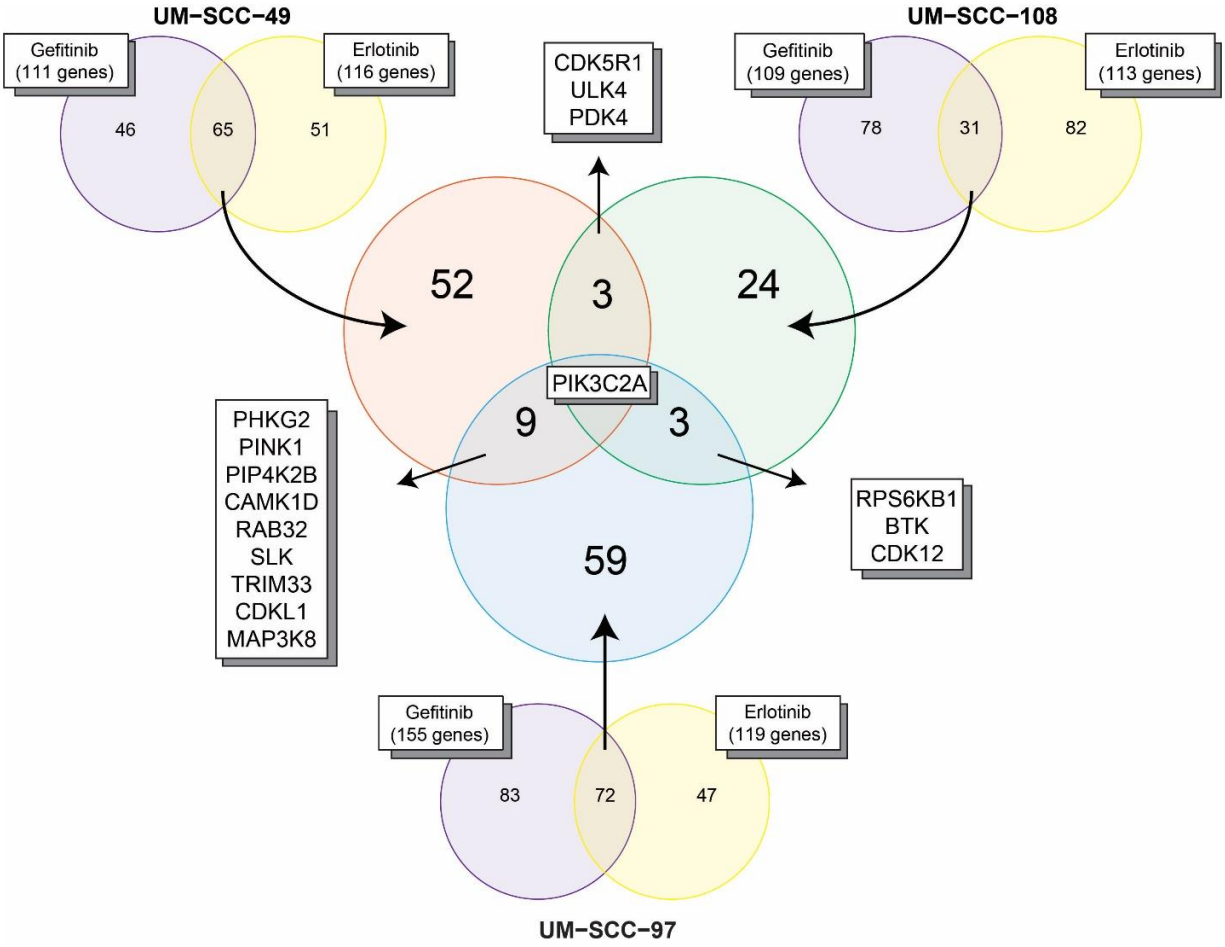

Figure 3-12. Overlap of Kinase CRISPR library

Venn diagram of overlap of the significantly depleted genes (p-value ≤ 0.05) for each Kinase screen as indicated.

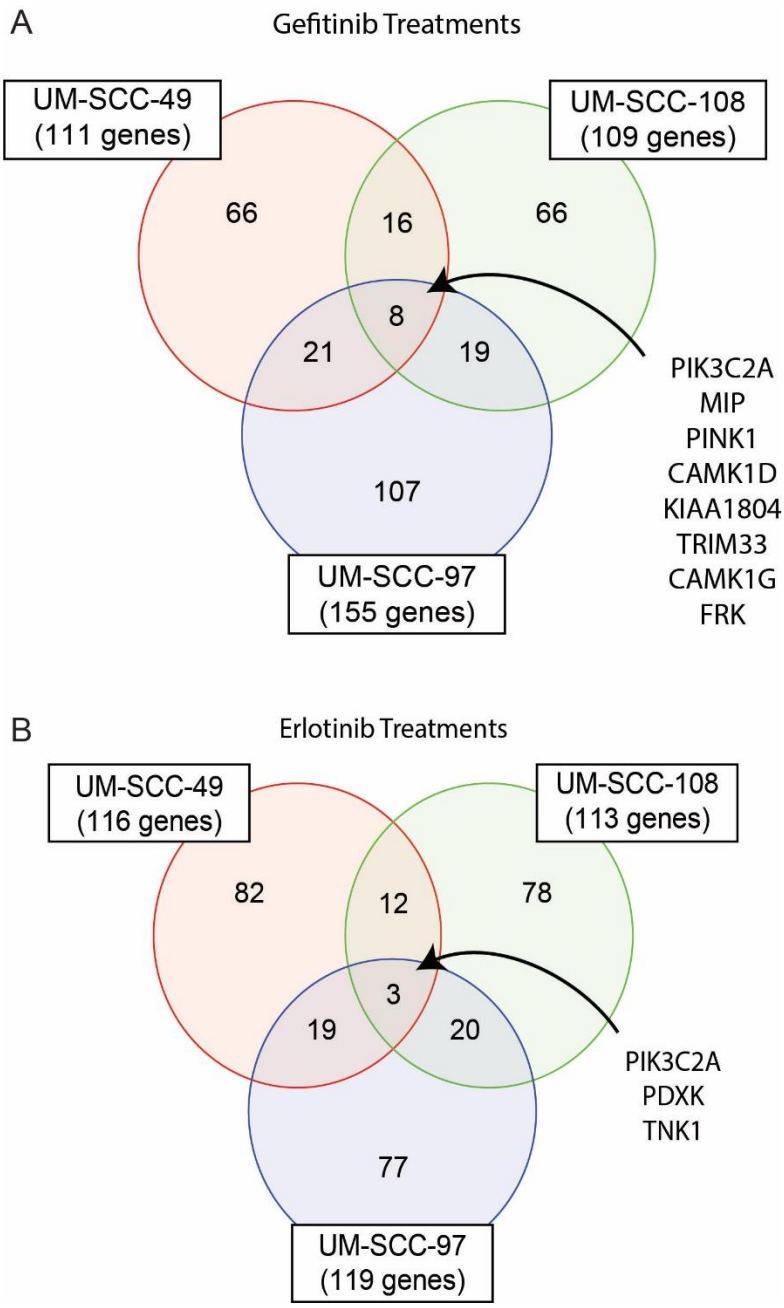

Figure 3-13. Overlap of Kinase CRISPR library for each inhibitor

Venn diagrams showing the overlap of significantly depleted genes (p-value ≤ 0.05) between cell lines for gefitinib (A) or erlotinib (B) treatments for the Kinase library.

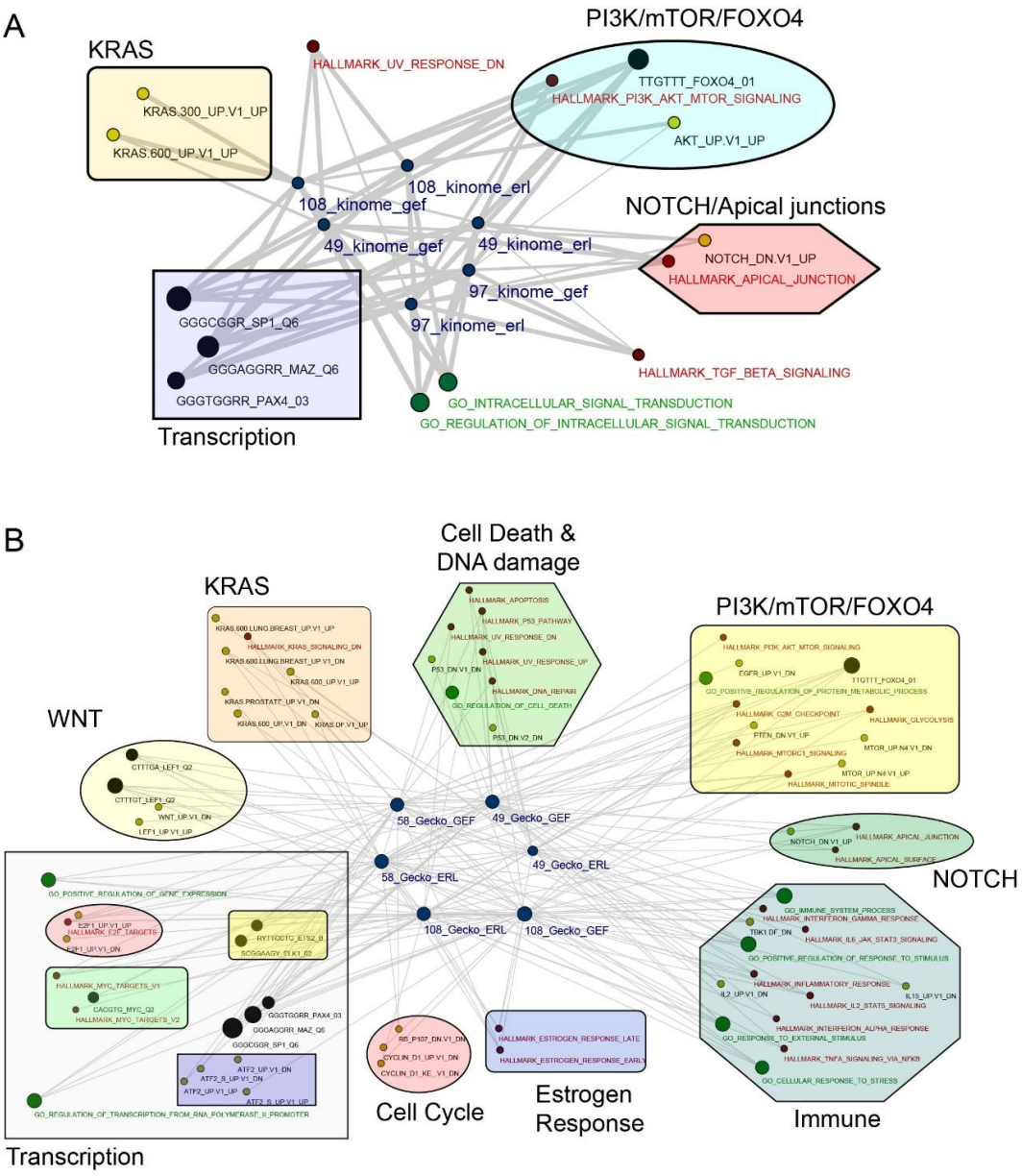

Figure 3-14. Gene set enrichment analysis of Kinase and GeCKO CRISPR screens

Cytoscape network plot shows significant enrichments of gene sets identified in each of the 6 CRISPR kinome screens (A) or GeCKO screens (B) (with each gene set represented by blue circular nodes) with annotated gene sets downloaded from the molecular signatures data bases v5.1 (red nodes = “Hallmark” gene sets, black nodes = “Motif” gene sets, green nodes = “Go-biological process” gene sets and yellow nodes = “Oncogene” gene sets). The size of each node is proportional to the number of genes in the gene set. Lines connecting each node are proportional to the significance of overlap between the gene sets, determined by false discovery rate (FDR), with more significant interactions represented by thicker edge weights. All interactions shown have FDR < 0.05. Recurrent and selected concepts are grouped within the transparent geometric shapes to highlight network concepts identified by the analysis.

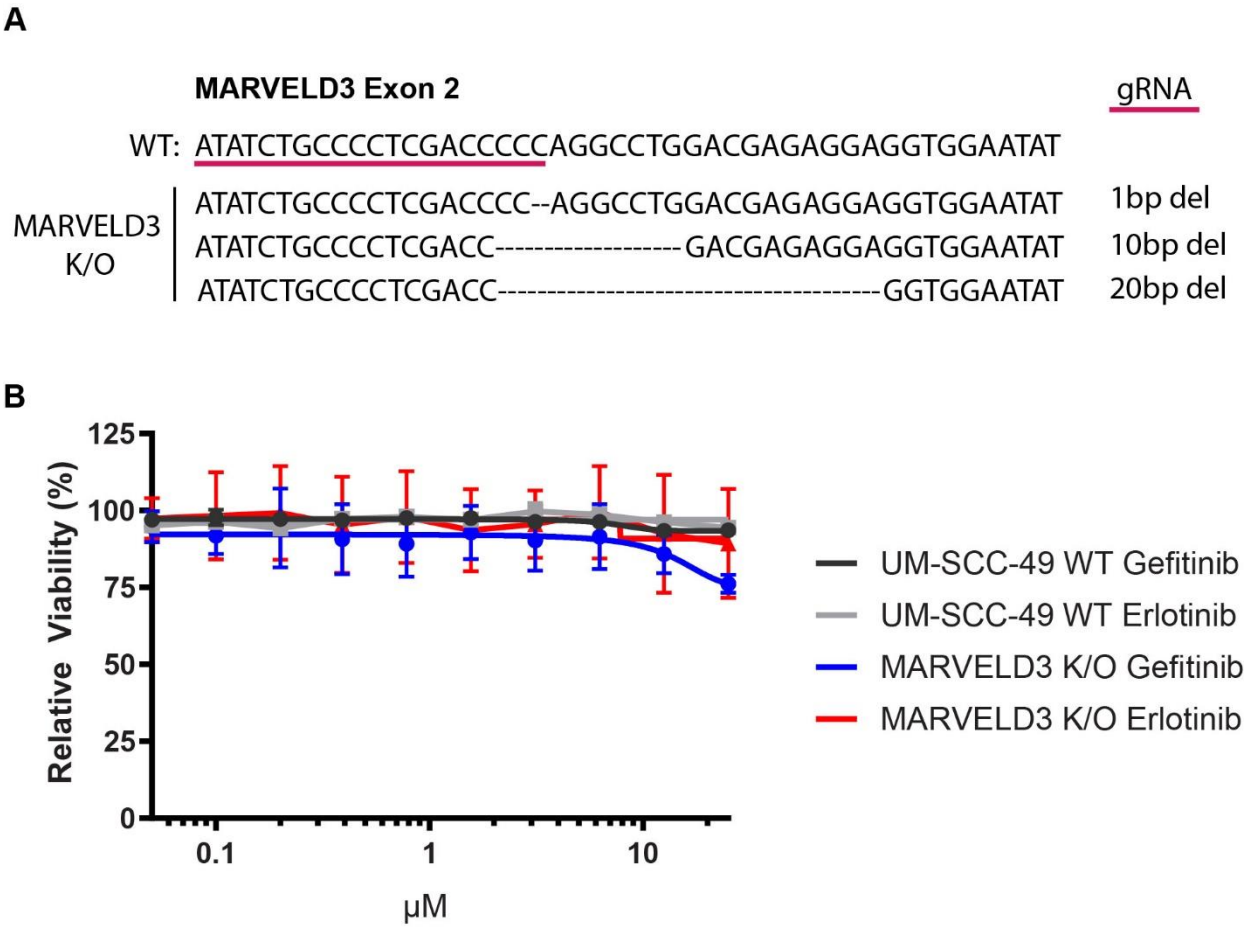

Figure 3-15. Response of MARVELD3 K/O clone to EGFR inhibition

A) Schematic of sanger sequencing results from MARVELD3 K/O clone as compared to wildtype (WT) sequence. The gRNA sequence is underlined in red, targeted to exon 2 of *MARVELD3*. UM-SCC-49 has 3 copies of *MARVELD3*, and the MARVELD3 K/O has 1bp, 10bp, and 20bp deletions. B) Cell viability response of UM-SCC-49 wildtype or MARVELD3 K/O cell lines to the EGFR inhibitors gefitinib or erlotinib. Error bars indicate standard deviation.

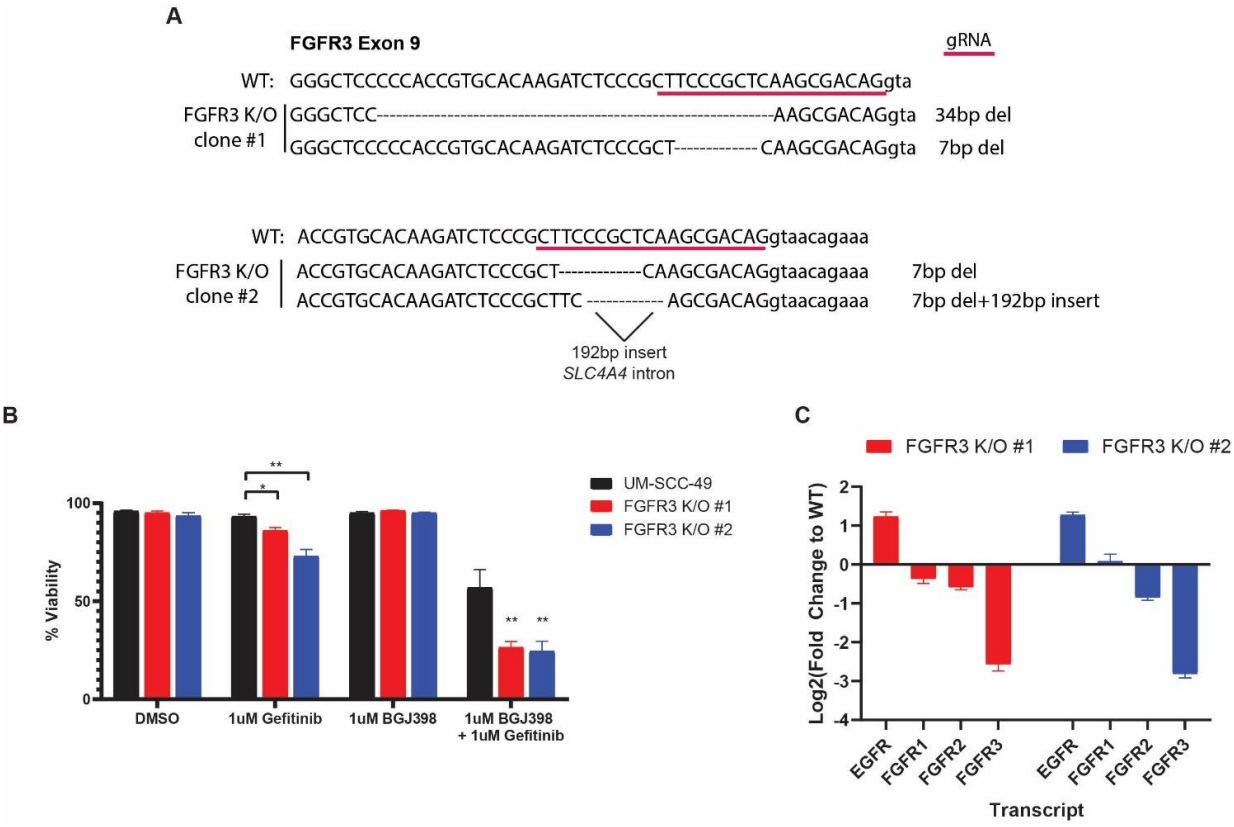

Figure 3-16. Response of FGFR3 K/O clones to EGFR inhibition

A) Schematic representation of sanger sequencing data from FGFR3 K/O clones as compared to wildtype (WT) sequence. The gRNA is underlined in red, targeted to exon 9 of *FGFR3*. FGFR3 clone #1 has a 34bp and 7bp deletion, and FGFR3 clone #2 has a 7bp deletion and a 192bp insertion of intronic *SLC4A4* sequence + 7bp deletion for a combined resulted insertion of 185bp. B) Cell viability as determined by trypan blue assay for UM-SCC-49 (black), FGFR3 K/O clone #1 (red) or FGFR3 K/O clone #2 (blue) at 72hour timepoint. Asterisks denote p-value (*p-value ≤ 0.05, **p-value ≤0.01) according to statistical analysis detailed in methods section. C) Transcript expression levels as detected by qPCR as compared to the fold change of UM-SCC-49 wildtype cells. FGFR3 K/O clone #1 is in red and FGFR3 K/O clone #2 is in blue.

Tables

Primer	Direction	Sequence (5'-3')
NOTCH1 K/O	Fwd	CTTGGCTTTGTGGTT
	Rev	GTCCAGGATGTGGCACAAG
MARVELD3 K/O	Fwd	ACAGCATCTGTCACGTGGTT
	Rev	TCAAACAGCCTGCAAAACGG
FGFR3 K/O	Fwd	CGTTACTGACTGCGAGACCC
	Rev	GTTTCGTGCCCCAAAGTACC

Table 3-1. Genomic primers

Genomic primers used for sanger sequencing of CRISPR knockout clones as indicated.

Antibody Target	Catalog #
NOTCH1	CST 3608
ICN-1	CST 4147
NOTCH2	CST 5732
NOTCH3	CST 5276
Hes1	CST 11988
c-Myc	CST 5605
Axin2	CST 2151
Beta-actin	CST 4970
Anti-Rabbit Secondary	Jackson Research 111-035-045
Anti-Mouse Secondary	Jackson Research 715-035-151

Table 3-2. Antibodies

List of antibodies used in chapter 3 for immunoblotting.

Gene	Direction	Sequence (5'-3')
EGFR	Fwd	TGTGCCCACTACATTGACGG
	Rev	CGGGATCTTAGGCCCATTCG
FGFR1	Fwd	AAAGGAGGATCGAGCTCACTG
	Rev	CCAGGGCTGGGCTTGTTCA
FGFR2	Fwd	TTGCCCAGTGTCAGCTTATCT
	Rev	AACAGTTTCGGCTGAGTCCA
FGFR3	Fwd	GCGCTAACACCACCGACA
	Rev	AGCTCCTCTCGGCTGG
HPRT	Fwd	AGATGGTCAAGGTCGCAAGC
	Rev	ATGACACAAACATGATTCAAATCCC
RPL19	Fwd	AAATCGCCAATGCCAACTCC
	Rev	CCGCTTACCTATGCCCATGT
ACTIN	Fwd	GCCGCCAGCTCACCAT
	Rev	AATCCTTCTGACCCATGCCC

Table 3-3. qPCR primers

Primers for quantifying transcript by qPCR.

	GeCKO v1	GeCKOv2 (A or B)	Kinase
Gene targets	18,080	19,050	684
miRNA targets	0	1,864	0
gRNA/gene	~3-4	3	~9
Cells/treatment	30 million	30 million	3 million

Table 3-4. CRISPR library statistics

Table depicting the number of targets, gRNAs, and recommended cells plated per treatment for each of the three CRISPR libraries used.

	Kinase Libraries							GeCKO Libraries					
	UM-SCC-49		UM-SCC-108		UM-SCC-97			UM-SCC-49		UM-SCC-108		UM-SCC-58	
	gefitinib	erlotinib	gefitinib	erlotinib	gefitinib	erlotinib		gefitinib	erlotinib	gefitinib	erlotinib	gefitinib	erlotinib
PIK3C2A	0.0005	0.0019	0.0006	0.0324	0.0282	0.0244		0.5458	0.9953	0.3398	0.1086	0.6822	0.0914
CDK12	0.0565	0.1755	0.0361	0.0026	0.0340	0.0301		0.0767	-	0.7889	0.3910	0.2189	0.1416
PINK1	0.0102	0.0215	0.0355	0.3252	0.0298	0.0014		0.6011	0.0353	0.1162	0.6672	0.8318	0.0458
PDXK	0.1184	0.0223	0.0767	0.0006	0.0063	0.0405		0.9624	-	0.0719	0.0131	0.1262	0.4262
MARVELD3	0.0008	0.0028	0.1082	0.0068	0.1848	0.4968		0.2190	0.7358	0.9380	0.9406	0.2563	0.4117
FGFR3	0.0110	0.0150	0.1758	0.2505	0.8514	0.9566		0.8124	0.4790	0.0789	0.1088	0.0691	0.3059

Table 3-5. Significance of six nominated genes across all library screens

Table of p-values from MAGeCK output by gene for both Kinase and GeCKO library screens. P-values that are ≤ 0.05 are colored green.

Node	Node Size	Gene Set Name	# Genes in Gene Set (K)	FDR q-value
49_kinome_erl	116	GO_PHOSPHORYLATION	1228	7.08E-147
49_kinome_erl	116	GO_PHOSPHATE_CONTAINING_COMPOUND_METABOLIC_PROCESS	1977	5.28E-125
49_kinome_erl	116	GO_PROTEIN_PHOSPHORYLATION	944	2.34E-108
49_kinome_erl	116	GO_PROTEIN_AUTOPHOSPHORYLATION	192	5.52E-57
49_kinome_erl	116	GO_PEPTIDYL_AMINO_ACID_MODIFICATION	841	6.18E-43
49_kinome_erl	116	GO_INTRACELLULAR_SIGNAL_TRANSDUCTION	1572	3.75E-35
49_kinome_erl	116	GO_REGULATION_OF_PHOSPHORUS_METABOLIC_PROCESS	1618	4.11E-32
49_kinome_erl	116	GO_PEPTIDYL_TYROSINE_MODIFICATION	186	1.42E-31
49_kinome_erl	116	GO_ENZYME_LINKED_RECEPTOR_PROTEIN_SIGNALING_PATHWAY	689	4.53E-30
49_kinome_erl	116	GO_POSITIVE_REGULATION_OF_PHOSPHORUS_METABOLIC_PROCESS	1036	1.37E-29
49_kinome_erl	116	GO_POSITIVE_REGULATION_OF_KINASE_ACTIVITY	482	5.43E-29
49_kinome_erl	116	GO_REGULATION_OF_PROTEIN_MODIFICATION_PROCESS	1710	1.06E-27
49_kinome_erl	116	GO_REGULATION_OF_KINASE_ACTIVITY	776	3.50E-27
49_kinome_erl	116	GO_TRANSMEMBRANE_RECEPTOR_PROTEIN_TYROSINE_KINASE_SIGNALING_PATHWAY	498	3.50E-27
49_kinome_erl	116	GO_REGULATION_OF_INTRACELLULAR_SIGNAL_TRANSDUCTION	1656	3.64E-27
49_kinome_erl	116	GO_POSITIVE_REGULATION_OF_TRANSFERASE_ACTIVITY	616	4.33E-26
49_kinome_erl	116	GO_POSITIVE_REGULATION_OF_PROTEIN_MODIFICATION_PROCESS	1135	7.23E-26
49_kinome_erl	116	GO_POSITIVE_REGULATION_OF_PROTEIN_METABOLIC_PROCESS	1492	2.10E-25
49_kinome_erl	116	GO_SIGNAL_TRANSDUCTION_BY_PROTEIN_PHOSPHORYLATION	404	3.44E-25
49_kinome_erl	116	GO_PEPTIDYL_SERINE_MODIFICATION	148	6.66E-25
49_kinome_gef	111	GO_PHOSPHORYLATION	1228	3.78E-134
49_kinome_gef	111	GO_PHOSPHATE_CONTAINING_COMPOUND_METABOLIC_PROCESS	1977	4.70E-116
49_kinome_gef	111	GO_PROTEIN_PHOSPHORYLATION	944	4.46E-111
49_kinome_gef	111	GO_PROTEIN_AUTOPHOSPHORYLATION	192	1.14E-55
49_kinome_gef	111	GO_PEPTIDYL_AMINO_ACID_MODIFICATION	841	5.88E-44
49_kinome_gef	111	GO_PEPTIDYL_TYROSINE_MODIFICATION	186	8.49E-36
49_kinome_gef	111	GO_INTRACELLULAR_SIGNAL_TRANSDUCTION	1572	5.59E-35
49_kinome_gef	111	GO_REGULATION_OF_PHOSPHORUS_METABOLIC_PROCESS	1618	2.09E-29
49_kinome_gef	111	GO_REGULATION_OF_INTRACELLULAR_SIGNAL_TRANSDUCTION	1656	4.72E-29
49_kinome_gef	111	GO_POSITIVE_REGULATION_OF_PHOSPHORUS_METABOLIC_PROCESS	1036	1.01E-27
49_kinome_gef	111	GO_ENZYME_LINKED_RECEPTOR_PROTEIN_SIGNALING_PATHWAY	689	1.50E-26
49_kinome_gef	111	GO_REGULATION_OF_PROTEIN_MODIFICATION_PROCESS	1710	3.11E-26
49_kinome_gef	111	GO_SIGNAL_TRANSDUCTION_BY_PROTEIN_PHOSPHORYLATION	404	1.52E-25
49_kinome_gef	111	GO_POSITIVE_REGULATION_OF_PROTEIN_MODIFICATION_PROCESS	1135	2.92E-25
49_kinome_gef	111	GO_POSITIVE_REGULATION_OF_KINASE_ACTIVITY	482	3.55E-25
49_kinome_gef	111	GO_TRANSMEMBRANE_RECEPTOR_PROTEIN_TYROSINE_KINASE_SIGNALING_PATHWAY	498	7.73E-25
49_kinome_gef	111	GO_POSITIVE_REGULATION_OF_CELL_COMMUNICATION	1532	1.36E-24
49_kinome_gef	111	GO_REGULATION_OF_MAPK_CASCADE	660	1.69E-24
49_kinome_gef	111	GO_POSITIVE_REGULATION_OF_RESPONSE_TO_STIMULUS	1929	1.82E-24
49_kinome_gef	111	GO_POSITIVE_REGULATION_OF_TRANSFERASE_ACTIVITY	616	5.87E-24
97_kinome_erl	119	GO_PHOSPHORYLATION	1228	4.71E-149
97_kinome_erl	119	GO_PHOSPHATE_CONTAINING_COMPOUND_METABOLIC_PROCESS	1977	1.00E-133
97_kinome_erl	119	GO_PROTEIN_PHOSPHORYLATION	944	2.35E-117
97_kinome_erl	119	GO_PROTEIN_AUTOPHOSPHORYLATION	192	2.86E-36
97_kinome_erl	119	GO_INTRACELLULAR_SIGNAL_TRANSDUCTION	1572	3.51E-33
97_kinome_erl	119	GO_PEPTIDYL_AMINO_ACID_MODIFICATION	841	2.31E-25
97_kinome_erl	119	GO_REGULATION_OF_PROTEIN_MODIFICATION_PROCESS	1710	3.34E-19
97_kinome_erl	119	GO_REGULATION_OF_PHOSPHORUS_METABOLIC_PROCESS	1618	5.65E-19
97_kinome_erl	119	GO_PEPTIDYL_SERINE_MODIFICATION	148	5.81E-19
97_kinome_erl	119	GO_REGULATION_OF_INTRACELLULAR_SIGNAL_TRANSDUCTION	1656	1.01E-17
97_kinome_erl	119	GO_PEPTIDYL_TYROSINE_MODIFICATION	186	8.34E-16
97_kinome_erl	119	GO_POSITIVE_REGULATION_OF_MOLECULAR_FUNCTION	1791	8.49E-16
97_kinome_erl	119	GO_REGULATION_OF_KINASE_ACTIVITY	776	2.01E-15
97_kinome_erl	119	GO_REGULATION_OF_CELL_DEATH	1472	2.94E-15
97_kinome_erl	119	GO_POSITIVE_REGULATION_OF_RESPONSE_TO_STIMULUS	1929	5.73E-15
97_kinome_erl	119	GO_POSITIVE_REGULATION_OF_PHOSPHORUS_METABOLIC_PROCESS	1036	6.18E-15
97_kinome_erl	119	GO_SIGNAL_TRANSDUCTION_BY_PROTEIN_PHOSPHORYLATION	404	7.22E-15
97_kinome_erl	119	GO_REGULATION_OF_CELL_CYCLE	949	9.11E-15

97_kinome_erl	119	GO_REGULATION_OF_MAPK_CASCADE	660	1.06E-14
97_kinome_erl	119	GO_POSITIVE_REGULATION_OF_PROTEIN_METABOLIC_PROCESS	1492	2.85E-14
97_kinome_gef	155	GO_PHOSPHORYLATION	1228	1.77E-190
97_kinome_gef	155	GO_PHOSPHATE_CONTAINING_COMPOUND_METABOLIC_PROCESS	1977	5.54E-166
97_kinome_gef	155	GO_PROTEIN_PHOSPHORYLATION	944	3.37E-151
97_kinome_gef	155	GO_PROTEIN_AUTOPHOSPHORYLATION	192	1.31E-51
97_kinome_gef	155	GO_INTRACELLULAR_SIGNAL_TRANSDUCTION	1572	1.46E-42
97_kinome_gef	155	GO_PEPTIDYL_AMINO_ACID_MODIFICATION	841	3.87E-42
97_kinome_gef	155	GO_PEPTIDYL_TYROSINE_MODIFICATION	186	5.48E-30
97_kinome_gef	155	GO_POSITIVE_REGULATION_OF_MOLECULAR_FUNCTION	1791	4.58E-25
97_kinome_gef	155	GO_REGULATION_OF_PHOSPHORUS_METABOLIC_PROCESS	1618	8.07E-24
97_kinome_gef	155	GO_PEPTIDYL_SERINE_MODIFICATION	148	8.55E-24
97_kinome_gef	155	GO_REGULATION_OF_PROTEIN_MODIFICATION_PROCESS	1710	5.91E-22
97_kinome_gef	155	GO_REGULATION_OF_INTRACELLULAR_SIGNAL_TRANSDUCTION	1656	1.48E-19
97_kinome_gef	155	GO_REGULATION_OF_KINASE_ACTIVITY	776	2.49E-19
97_kinome_gef	155	GO_REGULATION_OF_TRANSFERASE_ACTIVITY	946	3.53E-19
97_kinome_gef	155	GO_POSITIVE_REGULATION_OF_RESPONSE_TO_STIMULUS	1929	3.61E-19
97_kinome_gef	155	GO_POSITIVE_REGULATION_OF_PHOSPHORUS_METABOLIC_PROCESS	1036	3.67E-19
97_kinome_gef	155	GO_POSITIVE_REGULATION_OF_CATALYTIC_ACTIVITY	1518	4.65E-19
97_kinome_gef	155	GO_ENZYME_LINKED_RECEPTOR_PROTEIN_SIGNALING_PATHWAY	689	1.58E-18
97_kinome_gef	155	GO_ORGANOPHOSPHATE_METABOLIC_PROCESS	885	6.13E-18
97_kinome_gef	155	GO_REGULATION_OF_CELL_CYCLE	949	3.83E-17
108_kinome_erl	118	GO_PHOSPHORYLATION	1228	1.06E-139
108_kinome_erl	118	GO_PHOSPHATE_CONTAINING_COMPOUND_METABOLIC_PROCESS	1977	5.18E-128
108_kinome_erl	118	GO_PROTEIN_PHOSPHORYLATION	944	7.82E-108
108_kinome_erl	118	GO_PROTEIN_AUTOPHOSPHORYLATION	192	5.99E-47
108_kinome_erl	118	GO_PEPTIDYL_AMINO_ACID_MODIFICATION	841	1.53E-43
108_kinome_erl	118	GO_INTRACELLULAR_SIGNAL_TRANSDUCTION	1572	1.19E-30
108_kinome_erl	118	GO_PEPTIDYL_TYROSINE_MODIFICATION	186	6.08E-30
108_kinome_erl	118	GO_REGULATION_OF_PHOSPHORUS_METABOLIC_PROCESS	1618	1.29E-26
108_kinome_erl	118	GO_REGULATION_OF_PROTEIN_MODIFICATION_PROCESS	1710	9.29E-26
108_kinome_erl	118	GO_TRANSMEMBRANE_RECEPTOR_PROTEIN_TYROSINE_KINASE_SIGNALING_PATHWAY	498	5.82E-23
108_kinome_erl	118	GO_ENZYME_LINKED_RECEPTOR_PROTEIN_SIGNALING_PATHWAY	689	3.45E-22
108_kinome_erl	118	GO_REGULATION_OF_CELL_DEATH	1472	3.82E-20
108_kinome_erl	118	GO_PEPTIDYL_SERINE_MODIFICATION	148	1.68E-19
108_kinome_erl	118	GO_REGULATION_OF_INTRACELLULAR_SIGNAL_TRANSDUCTION	1656	1.21E-18
108_kinome_erl	118	GO_REGULATION_OF_KINASE_ACTIVITY	776	1.89E-18
108_kinome_erl	118	GO_REGULATION_OF_TRANSFERASE_ACTIVITY	946	1.28E-17
108_kinome_erl	118	GO_REGULATION_OF_MAPK_CASCADE	660	1.28E-17
108_kinome_erl	118	GO_NEGATIVE_REGULATION_OF_CELL_DEATH	872	2.54E-17
108_kinome_erl	118	GO_REGULATION_OF_PROTEIN_SERINE_THREONINE_KINASE_ACTIVITY	470	1.74E-15
108_kinome_erl	118	GO_SIGNAL_TRANSDUCTION_BY_PROTEIN_PHOSPHORYLATION	404	2.35E-15
108_kinome_gef	109	GO_PHOSPHORYLATION	1228	1.18E-128
108_kinome_gef	109	GO_PHOSPHATE_CONTAINING_COMPOUND_METABOLIC_PROCESS	1977	1.25E-115
108_kinome_gef	109	GO_PROTEIN_PHOSPHORYLATION	944	4.71E-110
108_kinome_gef	109	GO_PROTEIN_AUTOPHOSPHORYLATION	192	2.13E-41
108_kinome_gef	109	GO_INTRACELLULAR_SIGNAL_TRANSDUCTION	1572	1.02E-40
108_kinome_gef	109	GO_PEPTIDYL_AMINO_ACID_MODIFICATION	841	9.38E-37
108_kinome_gef	109	GO_PEPTIDYL_TYROSINE_MODIFICATION	186	1.80E-28
108_kinome_gef	109	GO_REGULATION_OF_PHOSPHORUS_METABOLIC_PROCESS	1618	2.50E-27
108_kinome_gef	109	GO_REGULATION_OF_KINASE_ACTIVITY	776	1.38E-26
108_kinome_gef	109	GO_REGULATION_OF_PROTEIN_MODIFICATION_PROCESS	1710	1.63E-26
108_kinome_gef	109	GO_REGULATION_OF_INTRACELLULAR_SIGNAL_TRANSDUCTION	1656	6.89E-26
108_kinome_gef	109	GO_REGULATION_OF_TRANSFERASE_ACTIVITY	946	2.00E-25
108_kinome_gef	109	GO_PEPTIDYL_SERINE_MODIFICATION	148	2.88E-25
108_kinome_gef	109	GO_POSITIVE_REGULATION_OF_PROTEIN_METABOLIC_PROCESS	1492	4.77E-24
108_kinome_gef	109	GO_POSITIVE_REGULATION_OF_PHOSPHORUS_METABOLIC_PROCESS	1036	1.43E-20
108_kinome_gef	109	GO_POSITIVE_REGULATION_OF_KINASE_ACTIVITY	482	1.29E-19
108_kinome_gef	109	GO_POSITIVE_REGULATION_OF_PROTEIN_MODIFICATION_PROCESS	1135	1.55E-19
108_kinome_gef	109	GO_POSITIVE_REGULATION_OF_TRANSFERASE_ACTIVITY	616	1.09E-18
108_kinome_gef	109	GO_REGULATION_OF_PROTEIN_SERINE_THREONINE_KINASE_ACTIVITY	470	1.60E-18
108_kinome_gef	109	GO_ACTIVATION_OF_PROTEIN_KINASE_ACTIVITY	279	1.63E-18
49_kinome_erl	116	HALLMARK_PI3K_AKT_MTOR_SIGNALING	105	1.49E-05
49_kinome_erl	116	HALLMARK_APICAL_JUNCTION	200	3.14E-04
49_kinome_erl	116	HALLMARK_SPERMATOGENESIS	135	6.59E-03

49_kinome_erl	116	HALLMARK_ALLOGRAFT_REJECTION	200	1.42E-02
49_kinome_erl	116	HALLMARK_COMPLEMENT	200	1.42E-02
49_kinome_erl	116	HALLMARK_MYOGENESIS	200	1.42E-02
49_kinome_erl	116	HALLMARK_ANDROGEN_RESPONSE	101	1.56E-02
49_kinome_erl	116	HALLMARK_PANCREAS_BETA_CELLS	40	2.89E-02
49_kinome_erl	116	HALLMARK_UV_RESPONSE_UP	158	4.15E-02
49_kinome_erl	116	HALLMARK_TGF_BETA_SIGNALING	54	4.15E-02
49_kinome_erl	116	HALLMARK_G2M_CHECKPOINT	200	4.49E-02
49_kinome_erl	116	HALLMARK_HYPOXIA	200	4.49E-02
49_kinome_erl	116	HALLMARK_INFLAMMATORY_RESPONSE	200	4.49E-02
49_kinome_erl	116	HALLMARK_KRAS_SIGNALING_DN	200	4.49E-02
49_kinome_erl	116	HALLMARK_P53_PATHWAY	200	4.49E-02
49_kinome_erl	116	HALLMARK_TNFA_SIGNALING_VIA_NFKB	200	4.49E-02
49_kinome_gef	111	HALLMARK_COMPLEMENT	200	3.08E-05
49_kinome_gef	111	HALLMARK_PI3K_AKT_MTOR_SIGNALING	105	1.50E-04
49_kinome_gef	111	HALLMARK_SPERMATOGENESIS	135	3.38E-04
49_kinome_gef	111	HALLMARK_UV_RESPONSE_DN	144	3.46E-04
49_kinome_gef	111	HALLMARK_APICAL_JUNCTION	200	1.31E-03
49_kinome_gef	111	HALLMARK_TGF_BETA_SIGNALING	54	2.59E-03
49_kinome_gef	111	HALLMARK_INFLAMMATORY_RESPONSE	200	1.04E-02
49_kinome_gef	111	HALLMARK_REACTIVE_OXIGEN_SPECIES_PATHWAY	49	3.75E-02
49_kinome_gef	111	HALLMARK_UV_RESPONSE_UP	158	3.75E-02
97_kinome_erl	119	HALLMARK_HYPOXIA	200	7.27E-04
97_kinome_erl	119	HALLMARK_APICAL_JUNCTION	200	2.27E-03
97_kinome_erl	119	HALLMARK_E2F_TARGETS	200	2.27E-03
97_kinome_erl	119	HALLMARK_IL2_STAT5_SIGNALING	200	2.27E-03
97_kinome_erl	119	HALLMARK_TGF_BETA_SIGNALING	54	3.81E-03
97_kinome_erl	119	HALLMARK_IL6_JAK_STAT3_SIGNALING	87	1.17E-02
97_kinome_erl	119	HALLMARK_GLYCOLYSIS	200	1.17E-02
97_kinome_erl	119	HALLMARK_MITOTIC_SPINDLE	200	1.17E-02
97_kinome_erl	119	HALLMARK_PI3K_AKT_MTOR_SIGNALING	105	1.45E-02
97_kinome_erl	119	HALLMARK_UV_RESPONSE_DN	144	3.16E-02
97_kinome_erl	119	HALLMARK_APOPTOSIS	161	3.90E-02
97_kinome_gef	155	HALLMARK_HYPOXIA	200	3.21E-03
97_kinome_gef	155	HALLMARK_IL6_JAK_STAT3_SIGNALING	87	5.57E-03
97_kinome_gef	155	HALLMARK_E2F_TARGETS	200	7.65E-03
97_kinome_gef	155	HALLMARK_G2M_CHECKPOINT	200	7.65E-03
97_kinome_gef	155	HALLMARK_TGF_BETA_SIGNALING	54	8.23E-03
97_kinome_gef	155	HALLMARK_MYC_TARGETS_V2	58	8.45E-03
97_kinome_gef	155	HALLMARK_APICAL_JUNCTION	200	2.20E-02
97_kinome_gef	155	HALLMARK_COMPLEMENT	200	2.20E-02
97_kinome_gef	155	HALLMARK_GLYCOLYSIS	200	2.20E-02
97_kinome_gef	155	HALLMARK_IL2_STAT5_SIGNALING	200	2.20E-02
97_kinome_gef	155	HALLMARK_MYOGENESIS	200	2.20E-02
97_kinome_gef	155	HALLMARK_PANCREAS_BETA_CELLS	40	3.38E-02
108_kinome_erl	118	HALLMARK_PI3K_AKT_MTOR_SIGNALING	105	1.19E-08
108_kinome_erl	118	HALLMARK_UV_RESPONSE_DN	144	7.53E-04
108_kinome_erl	118	HALLMARK_ESTROGEN_RESPONSE_LATE	200	1.55E-02
108_kinome_erl	118	HALLMARK_MITOTIC_SPINDLE	200	1.55E-02
108_kinome_erl	118	HALLMARK_MYOGENESIS	200	1.55E-02
108_kinome_gef	109	HALLMARK_PI3K_AKT_MTOR_SIGNALING	105	2.74E-04
108_kinome_gef	109	HALLMARK_UV_RESPONSE_DN	144	9.96E-03
108_kinome_gef	109	HALLMARK_GLYCOLYSIS	200	1.13E-02
108_kinome_gef	109	HALLMARK_HEME_METABOLISM	200	1.13E-02
108_kinome_gef	109	HALLMARK_KRAS_SIGNALING_DN	200	1.13E-02
108_kinome_gef	109	HALLMARK_MYOGENESIS	200	1.13E-02
108_kinome_gef	109	HALLMARK_ANDROGEN_RESPONSE	101	1.30E-02
49_kinome_erl	116	CAGGTG_E12_Q6	2485	4.13E-07
49_kinome_erl	116	GGGAGGRR_MAZ_Q6	2274	9.17E-07
49_kinome_erl	116	GGGCGGR_SP1_Q6	2940	4.51E-06
49_kinome_erl	116	HNF4ALPHA_Q6	271	6.94E-06
49_kinome_erl	116	PAX4_01	262	6.26E-05
49_kinome_erl	116	AATGTGA_MIR23A_MIR23B	419	1.80E-04
49_kinome_erl	116	CACTTTG_MIR520G_MIR520H	237	3.06E-04
49_kinome_erl	116	GCACTTT_MIR175P_MIR20A_MIR106A_MIR106B_MIR20B_MIR519D	595	3.06E-04
49_kinome_erl	116	RTAAACA_FREAC2_01	919	3.56E-04

49_kinome_erl	116	TTGTTT_FOXO4_01	2061	3.56E-04
49_kinome_erl	116	HNF4_DR1_Q3	261	3.58E-04
49_kinome_erl	116	GGGTGGRR_PAX4_03	1294	3.58E-04
49_kinome_erl	116	HNF4_01	269	3.79E-04
49_kinome_erl	116	CCTGTGA_MIR513	125	1.03E-03
49_kinome_erl	116	TGTTTGY_HNF3_Q6	738	1.06E-03
49_kinome_erl	116	RYTTCCTG_ETS2_B	1085	1.07E-03
49_kinome_erl	116	AGCACTT_MIR93_MIR302A_MIR302B_MIR302C_MIR302D_MIR372_MIR373_MIR520E_MIR520A_MIR526B_MIR520B_MIR520C_MIR520D	343	1.31E-03
49_kinome_erl	116	CTGAGCC_MIR24	231	1.31E-03
49_kinome_erl	116	AAGTCCA_MIR422B_MIR422A	71	1.45E-03
49_kinome_erl	116	PEA3_Q6	255	1.80E-03
49_kinome_gef	111	CAGGTG_E12_Q6	2485	2.60E-08
49_kinome_gef	111	TTGTTT_FOXO4_01	2061	2.95E-07
49_kinome_gef	111	GGGAGGRR_MAZ_Q6	2274	1.27E-06
49_kinome_gef	111	GGGCGGR_SP1_Q6	2940	5.72E-06
49_kinome_gef	111	AACTTT_UNKNOWN	1890	2.24E-05
49_kinome_gef	111	PAX4_01	262	3.72E-05
49_kinome_gef	111	CTGCAGY_UNKNOWN	765	3.89E-05
49_kinome_gef	111	RTAAACA_FREAC2_01	919	3.89E-05
49_kinome_gef	111	MEF2_Q6_01	244	2.15E-04
49_kinome_gef	111	PEA3_Q6	255	2.54E-04
49_kinome_gef	111	ATF4_Q2	258	2.54E-04
49_kinome_gef	111	HNF4ALPHA_Q6	271	2.85E-04
49_kinome_gef	111	E2F_Q2	176	2.85E-04
49_kinome_gef	111	GTGACGY_E4F1_Q6	658	2.85E-04
49_kinome_gef	111	TGTTTGY_HNF3_Q6	738	7.18E-04
49_kinome_gef	111	GCACTTT_MIR175P_MIR20A_MIR106A_MIR106B_MIR20B_MIR519D	595	7.62E-04
49_kinome_gef	111	TGCTGCT_MIR15A_MIR16_MIR15B_MIR195_MIR424_MIR497	601	7.62E-04
49_kinome_gef	111	GTGCAAA_MIR507	131	7.62E-04
49_kinome_gef	111	RNGTGGGC_UNKNOWN	766	7.62E-04
49_kinome_gef	111	AAGCCAT_MIR135A_MIR135B	335	7.62E-04
97_kinome_erl	119	CTTTGT_LEF1_Q2	1972	5.78E-06
97_kinome_erl	119	PAX2_02	258	7.89E-06
97_kinome_erl	119	GGGCGGR_SP1_Q6	2940	7.89E-06
97_kinome_erl	119	TTGTTT_FOXO4_01	2061	1.45E-05
97_kinome_erl	119	AACTTT_UNKNOWN	1890	1.45E-05
97_kinome_erl	119	RTAAACA_FREAC2_01	919	1.75E-05
97_kinome_erl	119	TTAYRTAA_E4BP4_01	265	5.93E-05
97_kinome_erl	119	GGGTGGRR_PAX4_03	1294	1.44E-04
97_kinome_erl	119	GGGAGGRR_MAZ_Q6	2274	1.47E-04
97_kinome_erl	119	SP3_Q3	245	3.17E-04
97_kinome_erl	119	CAGGTG_E12_Q6	2485	4.55E-04
97_kinome_erl	119	TTANTCA_UNKNOWN	952	4.82E-04
97_kinome_erl	119	OLF1_01	272	4.82E-04
97_kinome_erl	119	TGACATY_UNKNOWN	665	5.81E-04
97_kinome_erl	119	E4BP4_01	223	1.49E-03
97_kinome_erl	119	RNGTGGGC_UNKNOWN	766	1.50E-03
97_kinome_erl	119	E2F1DP1_01	235	1.50E-03
97_kinome_erl	119	E2F1DP2_01	235	1.50E-03
97_kinome_erl	119	E2F4DP2_01	235	1.50E-03
97_kinome_erl	119	E2F_02	235	1.50E-03
97_kinome_gef	155	GGGCGGR_SP1_Q6	2940	1.88E-09
97_kinome_gef	155	GGGTGGRR_PAX4_03	1294	1.29E-06
97_kinome_gef	155	GGGAGGRR_MAZ_Q6	2274	3.24E-06
97_kinome_gef	155	CAGGTG_E12_Q6	2485	3.83E-06
97_kinome_gef	155	AACTTT_UNKNOWN	1890	1.68E-05
97_kinome_gef	155	TTGTTT_FOXO4_01	2061	1.68E-05
97_kinome_gef	155	RYTTCCTG_ETS2_B	1085	2.14E-05
97_kinome_gef	155	TTAYRTAA_E4BP4_01	265	3.47E-05
97_kinome_gef	155	CTATGCA_MIR153	216	6.71E-05
97_kinome_gef	155	CTTTGT_LEF1_Q2	1972	6.71E-05
97_kinome_gef	155	TTANTCA_UNKNOWN	952	6.71E-05
97_kinome_gef	155	GCACTTT_MIR175P_MIR20A_MIR106A_MIR106B_MIR20B_MIR519D	595	6.71E-05
97_kinome_gef	155	TGCACTT_MIR519C_MIR519B_MIR519A	448	2.10E-04
97_kinome_gef	155	OLF1_01	272	2.40E-04

97_kinome_gef	155	CCTGTGA_MIR513	125	2.40E-04
97_kinome_gef	155	CTTTGA_LEF1_Q2	1232	2.40E-04
97_kinome_gef	155	TGTTTAC_MIR30A5P_MIR30C_MIR30D_MIR30B_MIR30E5P	579	2.40E-04
97_kinome_gef	155	RGAGGAARY_PU1_Q6	502	3.90E-04
97_kinome_gef	155	TATAAA_TATA_01	1296	3.90E-04
97_kinome_gef	155	E4BP4_01	223	4.75E-04
108_kinome_erl	118	TTGTTT_FOXO4_01	2061	1.48E-07
108_kinome_erl	118	GGGTGGRR_PAX4_03	1294	8.23E-06
108_kinome_erl	118	GGGCGGR_SP1_Q6	2940	1.11E-05
108_kinome_erl	118	AATGTGA_MIR23A_MIR23B	419	1.87E-05
108_kinome_erl	118	TGACAGNY_MEIS1_01	827	1.87E-05
108_kinome_erl	118	CAGGTG_E12_Q6	2485	1.87E-05
108_kinome_erl	118	TGCACTT_MIR519C_MIR519B_MIR519A	448	1.87E-05
108_kinome_erl	118	AACTTT_UNKNOWN	1890	1.87E-05
108_kinome_erl	118	TGAATGT_MIR181A_MIR181B_MIR181C_MIR181D	484	3.35E-05
108_kinome_erl	118	ATTCTTT_MIR186	272	3.40E-05
108_kinome_erl	118	TTANTCA_UNKNOWN	952	5.17E-05
108_kinome_erl	118	CTTTGCA_MIR527	235	1.42E-04
108_kinome_erl	118	TGCTGCT_MIR15A_MIR16_MIR15B_MIR195_MIR424_MIR497	601	1.62E-04
108_kinome_erl	118	CAATGCA_MIR33	92	2.04E-04
108_kinome_erl	118	PAX2_02	258	2.10E-04
108_kinome_erl	118	TTGCACT_MIR130A_MIR301_MIR130B	403	3.91E-04
108_kinome_erl	118	TACTTGA_MIR26A_MIR26B	300	4.91E-04
108_kinome_erl	118	CEBP_C	200	4.91E-04
108_kinome_erl	118	GGGAGGRR_MAZ_Q6	2274	4.91E-04
108_kinome_erl	118	ACAGGGT_MIR10A_MIR10B	123	5.89E-04
108_kinome_gef	109	GGGCGGR_SP1_Q6	2940	5.34E-07
108_kinome_gef	109	YTATTTTNR_MEF2_02	697	5.34E-07
108_kinome_gef	109	CAGGTG_E12_Q6	2485	9.23E-07
108_kinome_gef	109	AACTTT_UNKNOWN	1890	3.92E-06
108_kinome_gef	109	GGGAGGRR_MAZ_Q6	2274	1.34E-05
108_kinome_gef	109	MEF2_Q6_01	244	1.88E-05
108_kinome_gef	109	TGAATGT_MIR181A_MIR181B_MIR181C_MIR181D	484	2.71E-05
108_kinome_gef	109	TCCCCAC_MIR491	57	2.71E-05
108_kinome_gef	109	CACTTTG_MIR520G_MIR520H	237	1.42E-04
108_kinome_gef	109	TTGTTT_FOXO4_01	2061	1.42E-04
108_kinome_gef	109	PTF1BETA_Q6	244	1.47E-04
108_kinome_gef	109	MYOD_Q6	245	1.47E-04
108_kinome_gef	109	HNF4_01_B	253	1.68E-04
108_kinome_gef	109	ACCAAAG_MIR9	499	1.90E-04
108_kinome_gef	109	AP1_Q6_01	264	1.92E-04
108_kinome_gef	109	HNF4_01	269	2.04E-04
108_kinome_gef	109	RTAAACA_FREAC2_01	919	5.44E-04
108_kinome_gef	109	TATAAA_TATA_01	1296	5.44E-04
108_kinome_gef	109	RSRFC4_Q2	214	5.44E-04
108_kinome_gef	109	GCACTTT_MIR175P_MIR20A_MIR106A_MIR106B_MIR20B_MIR519D	595	5.44E-04
49_kinome_erl	116	CYCLIN_D1_KE_.V1_DN	194	2.00E-03
49_kinome_erl	116	CYCLIN_D1_KE_.V1_UP	190	8.18E-03
49_kinome_erl	116	RAPA_EARLY_UP.V1_DN	191	8.18E-03
49_kinome_erl	116	CRX_DN.V1_UP	136	1.92E-02
49_kinome_erl	116	KRAS.600_UP.V1_UP	287	2.85E-02
49_kinome_erl	116	STK33_NOMO_DN	292	2.85E-02
49_kinome_erl	116	ESC_J1_UP_EARLY.V1_UP	183	2.88E-02
49_kinome_erl	116	CYCLIN_D1_UP.V1_DN	191	2.88E-02
49_kinome_erl	116	NOTCH_DN.V1_UP	193	2.88E-02
49_kinome_erl	116	PIGF_UP.V1_DN	194	2.88E-02
49_kinome_gef	111	CYCLIN_D1_KE_.V1_DN	194	1.55E-03
49_kinome_gef	111	STK33_DN	289	5.10E-03
49_kinome_gef	111	STK33_NOMO_DN	292	5.10E-03
49_kinome_gef	111	IL2_UP.V1_UP	192	5.11E-03
49_kinome_gef	111	KRAS.600_UP.V1_UP	287	2.40E-02
49_kinome_gef	111	ESC_J1_UP_EARLY.V1_UP	183	2.40E-02
49_kinome_gef	111	SRC_UP.V1_UP	188	2.40E-02
49_kinome_gef	111	CYCLIN_D1_KE_.V1_UP	190	2.40E-02
49_kinome_gef	111	CYCLIN_D1_UP.V1_DN	191	2.40E-02
49_kinome_gef	111	NOTCH_DN.V1_UP	193	2.40E-02

97_kinome_erl	119	TBK1.DN.48HRS_UP	50	1.12E-03
97_kinome_erl	119	DCA_UP.V1_DN	193	1.12E-03
97_kinome_erl	119	TBK1.DF_DN	287	6.82E-03
97_kinome_erl	119	JNK_DN.V1_DN	191	6.92E-03
97_kinome_erl	119	PDGF_ERK_DN.V1_UP	147	2.27E-02
97_kinome_erl	119	CSR_LATE_UP.V1_UP	172	2.99E-02
97_kinome_erl	119	CYCLIN_D1_KE_.V1_UP	190	2.99E-02
97_kinome_erl	119	IL15_UP.V1_UP	192	2.99E-02
97_kinome_erl	119	JNK_DN.V1_UP	192	2.99E-02
97_kinome_erl	119	NOTCH_DN.V1_UP	193	2.99E-02
97_kinome_erl	119	MTOR_UP.N4.V1_UP	196	2.99E-02
97_kinome_gef	155	JNK_DN.V1_UP	192	4.99E-03
97_kinome_gef	155	PRC2_EED_UP.V1_DN	193	4.99E-03
97_kinome_gef	155	BMI1_DN_MEL18_DN.V1_UP	145	8.78E-03
97_kinome_gef	155	RB_P130_DN.V1_UP	133	4.32E-02
97_kinome_gef	155	RB_DN.V1_UP	137	4.32E-02
97_kinome_gef	155	ATM_DN.V1_DN	149	4.32E-02
97_kinome_gef	155	PKCA_DN.V1_DN	167	4.32E-02
97_kinome_gef	155	AKT_UP.V1_UP	172	4.32E-02
97_kinome_gef	155	TBK1.DF_DN	287	4.32E-02
97_kinome_gef	155	TBK1.DF_UP	290	4.32E-02
97_kinome_gef	155	SNF5_DN.V1_UP	177	4.32E-02
97_kinome_gef	155	E2F1_UP.V1_UP	189	4.32E-02
97_kinome_gef	155	CYCLIN_D1_KE_.V1_UP	190	4.32E-02
97_kinome_gef	155	JNK_DN.V1_DN	191	4.32E-02
97_kinome_gef	155	IL15_UP.V1_UP	192	4.32E-02
97_kinome_gef	155	IL2_UP.V1_UP	192	4.32E-02
97_kinome_gef	155	VEGF_A_UP.V1_DN	193	4.32E-02
97_kinome_gef	155	CYCLIN_D1_KE_.V1_DN	194	4.32E-02
97_kinome_gef	155	PIGF_UP.V1_DN	194	4.32E-02
97_kinome_gef	155	CAHOY_OLIGODENDROCUTIC	100	4.53E-02
108_kinome_erl	118	TBK1.DF_UP	290	1.24E-04
108_kinome_erl	118	TGFB_UP.V1_UP	192	8.10E-04
108_kinome_erl	118	AKT_UP.V1_UP	172	4.28E-03
108_kinome_erl	118	AKT_UP_MTOR_DN.V1_UP	184	4.28E-03
108_kinome_erl	118	EIF4E_UP	100	4.28E-03
108_kinome_erl	118	RAPA_EARLY_UP.V1_DN	191	3.88E-02
108_kinome_erl	118	MEK_UP.V1_UP	196	3.88E-02
108_kinome_gef	109	KRAS.600_UP.V1_UP	287	1.13E-03
108_kinome_gef	109	KRAS.300_UP.V1_UP	146	2.56E-03
108_kinome_gef	109	TBK1.DF_DN	287	4.19E-03
108_kinome_gef	109	LEF1_UP.V1_UP	195	5.04E-03
108_kinome_gef	109	KRAS.600_UP.V1_DN	289	2.45E-02
108_kinome_gef	109	AKT_UP.V1_UP	172	2.45E-02
108_kinome_gef	109	ESC_J1_UP_EARLY.V1_UP	183	2.64E-02

Table 3-6. Gene sets enriched in individual Kinase library screens

Gene set enrichment analysis was performed with significant genes from each kinome screen to identify significant overlap with gene sets in the “Hallmark”, “Motif”, “Go-Biological Process” and “Oncogene” databases with the molecular signatures database v5.1. Pivotal input variables used for network analysis in Cytoscape are shown. Node is the sample in the following format: ‘cell line_library_drug’. Node Size is the number of input genes from the sample. Gene Set Name is the pathway enriched, with # of Genes in Gene Set being the number of genes in the GSEA pathway being tested.

Node	Node Size	Gene Set Name	# Genes in Gene Set (K)	FDR q-value
108_Gecko_GEF	1823	GO_NEGATIVE_REGULATION_OF_CELL_COMMUNICATION	1192	7.61E-32
108_Gecko_GEF	1823	GO_NEGATIVE_REGULATION_OF_RESPONSE_TO_STIMULUS	1360	5.05E-31
108_Gecko_GEF	1823	GO_RESPONSE_TO_EXTERNAL_STIMULUS	1821	2.90E-30
108_Gecko_GEF	1823	GO_POSITIVE_REGULATION_OF_MOLECULAR_FUNCTION	1791	2.90E-30
108_Gecko_GEF	1823	GO_POSITIVE_REGULATION_OF_GENE_EXPRESSION	1733	8.92E-30
108_Gecko_GEF	1823	GO_CELLULAR_RESPONSE_TO_ORGANIC_SUBSTANCE	1848	1.19E-29
108_Gecko_GEF	1823	GO_POSITIVE_REGULATION_OF_BIOSYNTHETIC_PROCESS	1805	1.19E-29
108_Gecko_GEF	1823	GO_PHOSPHATE_CONTAINING_COMPOUND_METABOLIC_PROCESS	1977	1.19E-29
108_Gecko_GEF	1823	GO_REGULATION_OF_INTRACELLULAR_SIGNAL_TRANSDUCTION	1656	1.42E-29
108_Gecko_GEF	1823	GO_REGULATION_OF_TRANSCRIPTION_FROM_RNA_POLYMERASE_II_PROMOTER	1784	1.67E-28
108_Gecko_GEF	1823	GO_REGULATION_OF_CELL_PROLIFERATION	1496	1.44E-25
108_Gecko_GEF	1823	GO_REGULATION_OF_TRANSPORT	1804	2.85E-25
108_Gecko_GEF	1823	GO_CATABOLIC_PROCESS	1773	2.85E-25
108_Gecko_GEF	1823	GO_POSITIVE_REGULATION_OF_RESPONSE_TO_STIMULUS	1929	5.49E-25
108_Gecko_GEF	1823	GO_IMMUNE_SYSTEM_PROCESS	1984	7.47E-25
108_Gecko_GEF	1823	GO_RESPONSE_TO_ENDOGENOUS_STIMULUS	1450	8.77E-25
108_Gecko_GEF	1823	GO_POSITIVE_REGULATION_OF_CATALYTIC_ACTIVITY	1518	1.32E-24
108_Gecko_GEF	1823	GO_CELLULAR_RESPONSE_TO_STRESS	1565	3.75E-24
108_Gecko_GEF	1823	GO_NEGATIVE_REGULATION_OF_GENE_EXPRESSION	1493	5.22E-24
108_Gecko_GEF	1823	GO_SMALL_MOLECULE_METABOLIC_PROCESS	1767	7.43E-24
108_Gecko_ERL	1587	GO_POSITIVE_REGULATION_OF_MOLECULAR_FUNCTION	1791	1.49E-40
108_Gecko_ERL	1587	GO_CELLULAR_RESPONSE_TO_ORGANIC_SUBSTANCE	1848	1.51E-33
108_Gecko_ERL	1587	GO_IMMUNE_SYSTEM_PROCESS	1984	1.00E-32
108_Gecko_ERL	1587	GO_REGULATION_OF_PROTEIN_MODIFICATION_PROCESS	1710	7.23E-32
108_Gecko_ERL	1587	GO_POSITIVE_REGULATION_OF_CATALYTIC_ACTIVITY	1518	3.22E-31
108_Gecko_ERL	1587	GO_RESPONSE_TO_ENDOGENOUS_STIMULUS	1450	7.48E-31
108_Gecko_ERL	1587	GO_PHOSPHATE_CONTAINING_COMPOUND_METABOLIC_PROCESS	1977	8.21E-31
108_Gecko_ERL	1587	GO_POSITIVE_REGULATION_OF_RESPONSE_TO_STIMULUS	1929	9.57E-31
108_Gecko_ERL	1587	GO_REGULATION_OF_RESPONSE_TO_STRESS	1468	1.99E-30
108_Gecko_ERL	1587	GO_POSITIVE_REGULATION_OF_BIOSYNTHETIC_PROCESS	1805	1.99E-29
108_Gecko_ERL	1587	GO_MOVEMENT_OF_CELL_OR_SUBCELLULAR_COMPONENT	1275	7.36E-29
108_Gecko_ERL	1587	GO_RESPONSE_TO_EXTERNAL_STIMULUS	1821	1.46E-28
108_Gecko_ERL	1587	GO_POSITIVE_REGULATION_OF_GENE_EXPRESSION	1733	1.14E-26
108_Gecko_ERL	1587	GO_CATABOLIC_PROCESS	1773	1.35E-26
108_Gecko_ERL	1587	GO_CELLULAR_RESPONSE_TO_STRESS	1565	1.35E-26
108_Gecko_ERL	1587	GO_REGULATION_OF_PHOSPHORUS_METABOLIC_PROCESS	1618	1.41E-26
108_Gecko_ERL	1587	GO_NEGATIVE_REGULATION_OF_RESPONSE_TO_STIMULUS	1360	3.11E-26
108_Gecko_ERL	1587	GO_POSITIVE_REGULATION_OF_CELL_COMMUNICATION	1532	1.21E-25
108_Gecko_ERL	1587	GO_REGULATION_OF_TRANSCRIPTION_FROM_RNA_POLYMERASE_II_PROMOTER	1784	1.86E-25
108_Gecko_ERL	1587	GO_CELL_DEVELOPMENT	1426	2.65E-25
58_Gecko_GEF	1554	GO_RNA_PROCESSING	835	3.88E-36
58_Gecko_GEF	1554	GO_MRNA_METABOLIC_PROCESS	611	2.67E-29
58_Gecko_GEF	1554	GO_ORGANONITROGEN_COMPOUND_METABOLIC_PROCESS	1796	9.25E-28
58_Gecko_GEF	1554	GO_CATABOLIC_PROCESS	1773	4.76E-27
58_Gecko_GEF	1554	GO_CELLULAR_CATABOLIC_PROCESS	1322	1.10E-25
58_Gecko_GEF	1554	GO_PROTEIN_LOCALIZATION	1805	2.12E-25
58_Gecko_GEF	1554	GO_INTRACELLULAR_SIGNAL_TRANSDUCTION	1572	5.08E-25
58_Gecko_GEF	1554	GO_POSITIVE_REGULATION_OF_MOLECULAR_FUNCTION	1791	5.21E-24
58_Gecko_GEF	1554	GO_PHOSPHATE_CONTAINING_COMPOUND_METABOLIC_PROCESS	1977	1.40E-23
58_Gecko_GEF	1554	GO_POSITIVE_REGULATION_OF_RESPONSE_TO_STIMULUS	1929	5.34E-23
58_Gecko_GEF	1554	GO_ESTABLISHMENT_OF_PROTEIN_LOCALIZATION	1423	5.34E-23
58_Gecko_GEF	1554	GO_SMALL_MOLECULE_METABOLIC_PROCESS	1767	6.04E-23
58_Gecko_GEF	1554	GO_POSITIVE_REGULATION_OF_CATALYTIC_ACTIVITY	1518	7.05E-23
58_Gecko_GEF	1554	GO_CELLULAR_RESPONSE_TO_STRESS	1565	1.32E-22
58_Gecko_GEF	1554	GO_ESTABLISHMENT_OF_LOCALIZATION_IN_CELL	1676	4.14E-22
58_Gecko_GEF	1554	GO_CELLULAR_RESPONSE_TO_ORGANIC_SUBSTANCE	1848	5.27E-22
58_Gecko_GEF	1554	GO_POSITIVE_REGULATION_OF_PROTEIN_METABOLIC_PROCESS	1492	8.86E-22
58_Gecko_GEF	1554	GO_RNA_SPLICING	367	1.12E-21

58_Gecko_GEF	1554	GO_MACROMOLECULAR_COMPLEX_ASSEMBLY	1398	1.73E-21
58_Gecko_GEF	1554	GO_MACROMOLECULE_CATABOLIC_PROCESS	926	5.51E-21
58_Gecko_ERL	1656	GO_POSITIVE_REGULATION_OF_MOLECULAR_FUNCTION	1791	1.11E-34
58_Gecko_ERL	1656	GO_CELLULAR_RESPONSE_TO_STRESS	1565	1.66E-33
58_Gecko_ERL	1656	GO_PHOSPHATE_CONTAINING_COMPOUND_METABOLIC_PROCESS	1977	1.87E-31
58_Gecko_ERL	1656	GO_REGULATION_OF_TRANSPORT	1804	8.84E-30
58_Gecko_ERL	1656	GO_POSITIVE_REGULATION_OF_GENE_EXPRESSION	1733	1.57E-28
58_Gecko_ERL	1656	GO_POSITIVE_REGULATION_OF_BIOSYNTHETIC_PROCESS	1805	1.84E-28
58_Gecko_ERL	1656	GO_RESPONSE_TO_EXTERNAL_STIMULUS	1821	4.52E-28
58_Gecko_ERL	1656	GO_IMMUNE_SYSTEM_PROCESS	1984	7.09E-28
58_Gecko_ERL	1656	GO_POSITIVE_REGULATION_OF_CATALYTIC_ACTIVITY	1518	7.89E-28
58_Gecko_ERL	1656	GO_INTRACELLULAR_SIGNAL_TRANSDUCTION	1572	3.22E-27
58_Gecko_ERL	1656	GO_REGULATION_OF_TRANSCRIPTION_FROM_RNA_POLYMERASE_II_PROMOTER	1784	6.32E-27
58_Gecko_ERL	1656	GO_NEUROGENESIS	1402	1.62E-26
58_Gecko_ERL	1656	GO_SYSTEM_PROCESS	1785	4.98E-26
58_Gecko_ERL	1656	GO_PROTEIN_LOCALIZATION	1805	5.54E-26
58_Gecko_ERL	1656	GO_POSITIVE_REGULATION_OF_RESPONSE_TO_STIMULUS	1929	1.76E-25
58_Gecko_ERL	1656	GO_REGULATION_OF_PROTEIN_MODIFICATION_PROCESS	1710	2.28E-25
58_Gecko_ERL	1656	GO_REGULATION_OF_PHOSPHORUS_METABOLIC_PROCESS	1618	1.15E-24
58_Gecko_ERL	1656	GO_REGULATION_OF_RESPONSE_TO_STRESS	1468	1.15E-24
58_Gecko_ERL	1656	GO_REGULATION_OF_HYDROLASE_ACTIVITY	1327	1.66E-24
58_Gecko_ERL	1656	GO_POSITIVE_REGULATION_OF_PROTEIN_METABOLIC_PROCESS	1492	1.71E-24
49_Gecko_GEF	1579	GO_CATABOLIC_PROCESS	1773	1.27E-29
49_Gecko_GEF	1579	GO_NEGATIVE_REGULATION_OF_NITROGEN_COMPOUND_METABOLIC_PROCESS	1517	6.47E-28
49_Gecko_GEF	1579	GO_PROTEIN_LOCALIZATION	1805	1.02E-26
49_Gecko_GEF	1579	GO_REGULATION_OF_INTRACELLULAR_SIGNAL_TRANSDUCTION	1656	3.58E-26
49_Gecko_GEF	1579	GO_PHOSPHATE_CONTAINING_COMPOUND_METABOLIC_PROCESS	1977	3.58E-26
49_Gecko_GEF	1579	GO_IMMUNE_SYSTEM_PROCESS	1984	3.70E-25
49_Gecko_GEF	1579	GO_SMALL_MOLECULE_METABOLIC_PROCESS	1767	9.05E-25
49_Gecko_GEF	1579	GO_REGULATION_OF_TRANSCRIPTION_FROM_RNA_POLYMERASE_II_PROMOTER	1784	1.85E-23
49_Gecko_GEF	1579	GO_POSITIVE_REGULATION_OF_RESPONSE_TO_STIMULUS	1929	4.35E-23
49_Gecko_GEF	1579	GO_NEGATIVE_REGULATION_OF_GENE_EXPRESSION	1493	8.61E-23
49_Gecko_GEF	1579	GO_INTRACELLULAR_SIGNAL_TRANSDUCTION	1572	3.97E-22
49_Gecko_GEF	1579	GO_ORGANONITROGEN_COMPOUND_METABOLIC_PROCESS	1796	5.55E-22
49_Gecko_GEF	1579	GO_REGULATION_OF_RESPONSE_TO_STRESS	1468	1.13E-21
49_Gecko_GEF	1579	GO_CELLULAR_CATABOLIC_PROCESS	1322	2.05E-21
49_Gecko_GEF	1579	GO_CELLULAR_RESPONSE_TO_ORGANIC_SUBSTANCE	1848	7.59E-21
49_Gecko_GEF	1579	GO_RESPONSE_TO_EXTERNAL_STIMULUS	1821	1.23E-20
49_Gecko_GEF	1579	GO_POSITIVE_REGULATION_OF_CELL_COMMUNICATION	1532	1.42E-20
49_Gecko_GEF	1579	GO_POSITIVE_REGULATION_OF_GENE_EXPRESSION	1733	3.84E-20
49_Gecko_GEF	1579	GO_REGULATION_OF_CELL_DEATH	1472	7.26E-20
49_Gecko_GEF	1579	GO_REGULATION_OF_TRANSPORT	1804	7.75E-20
49_Gecko_ERL	806	GO_TISSUE_DEVELOPMENT	1518	8.99E-24
49_Gecko_ERL	806	GO_PHOSPHATE_CONTAINING_COMPOUND_METABOLIC_PROCESS	1977	2.20E-23
49_Gecko_ERL	806	GO_POSITIVE_REGULATION_OF_MOLECULAR_FUNCTION	1791	6.66E-17
49_Gecko_ERL	806	GO_RESPONSE_TO_EXTERNAL_STIMULUS	1821	1.54E-15
49_Gecko_ERL	806	GO_REGULATION_OF_CELL_DEATH	1472	1.80E-15
49_Gecko_ERL	806	GO_PHOSPHORYLATION	1228	1.82E-15
49_Gecko_ERL	806	GO_SYSTEM_PROCESS	1785	2.57E-15
49_Gecko_ERL	806	GO_POSITIVE_REGULATION_OF_RESPONSE_TO_STIMULUS	1929	2.99E-15
49_Gecko_ERL	806	GO_MOVEMENT_OF_CELL_OR_SUBCELLULAR_COMPONENT	1275	8.77E-15
49_Gecko_ERL	806	GO_PROTEIN_PHOSPHORYLATION	944	2.79E-14
49_Gecko_ERL	806	GO_POSITIVE_REGULATION_OF_CATALYTIC_ACTIVITY	1518	5.12E-14
49_Gecko_ERL	806	GO_REPRODUCTION	1297	5.58E-14
49_Gecko_ERL	806	GO_ORGANONITROGEN_COMPOUND_METABOLIC_PROCESS	1796	5.94E-14
49_Gecko_ERL	806	GO_SINGLE_ORGANISM_BIOSYNTHETIC_PROCESS	1340	7.38E-14
49_Gecko_ERL	806	GO_LIPID_METABOLIC_PROCESS	1158	8.85E-14
49_Gecko_ERL	806	GO_VESICLE_MEDIATED_TRANSPORT	1239	1.76E-13
49_Gecko_ERL	806	GO_EMBRYO_DEVELOPMENT	894	3.75E-13
49_Gecko_ERL	806	GO_IMMUNE_SYSTEM_PROCESS	1984	5.50E-13
49_Gecko_ERL	806	GO_CELLULAR_RESPONSE_TO_ORGANIC_SUBSTANCE	1848	6.13E-13
49_Gecko_ERL	806	GO_EPITHELIUM_DEVELOPMENT	945	8.58E-13
108_Gecko_GEF	1823	HALLMARK_TNFA_SIGNALING_VIA_NFKB	200	9.24E-08

108_Gecko_GEF	1823	HALLMARK_E2F_TARGETS	200	0.0000029 9
108_Gecko_GEF	1823	HALLMARK_APICAL_JUNCTION	200	0.0000156
108_Gecko_GEF	1823	HALLMARK_MYC_TARGETS_V1	200	0.0000156
108_Gecko_GEF	1823	HALLMARK_P53_PATHWAY	200	0.0000156
108_Gecko_GEF	1823	HALLMARK_EPITHELIAL_MESENCHYMAL_TRANSITION	200	0.0000375
108_Gecko_GEF	1823	HALLMARK_HYPOXIA	200	0.0000375
108_Gecko_GEF	1823	HALLMARK_UNFOLDED_PROTEIN_RESPONSE	113	0.0000645
108_Gecko_GEF	1823	HALLMARK_COMPLEMENT	200	0.0000767
108_Gecko_GEF	1823	HALLMARK_G2M_CHECKPOINT	200	0.0000767
108_Gecko_GEF	1823	HALLMARK_IL2_STAT5_SIGNALING	200	0.0000767
108_Gecko_GEF	1823	HALLMARK_INTERFERON_ALPHA_RESPONSE	97	0.000121
108_Gecko_GEF	1823	HALLMARK_INFLAMMATORY_RESPONSE	200	0.000173
108_Gecko_GEF	1823	HALLMARK_KRAS_SIGNALING_DN	200	0.000173
108_Gecko_GEF	1823	HALLMARK_MITOTIC_SPINDLE	200	0.000173
108_Gecko_GEF	1823	HALLMARK_SPERMATOGENESIS	135	0.000296
108_Gecko_GEF	1823	HALLMARK_ESTROGEN_RESPONSE_EARLY	200	0.000371
108_Gecko_GEF	1823	HALLMARK_ESTROGEN_RESPONSE_LATE	200	0.000371
108_Gecko_GEF	1823	HALLMARK_GLYCOLYSIS	200	0.000371
108_Gecko_GEF	1823	HALLMARK_INTERFERON_GAMMA_RESPONSE	200	0.000371
108_Gecko_ERL	1587	HALLMARK_FATTY_ACID_METABOLISM	158	2.07E-09
108_Gecko_ERL	1587	HALLMARK_E2F_TARGETS	200	8.15E-07
108_Gecko_ERL	1587	HALLMARK_ESTROGEN_RESPONSE_LATE	200	2.21E-06
108_Gecko_ERL	1587	HALLMARK_COMPLEMENT	200	2.87E-06
108_Gecko_ERL	1587	HALLMARK_IL2_STAT5_SIGNALING	200	2.87E-06
108_Gecko_ERL	1587	HALLMARK_INTERFERON_GAMMA_RESPONSE	200	2.87E-06
108_Gecko_ERL	1587	HALLMARK_MYC_TARGETS_V1	200	2.87E-06
108_Gecko_ERL	1587	HALLMARK_P53_PATHWAY	200	2.87E-06
108_Gecko_ERL	1587	HALLMARK_TNFA_SIGNALING_VIA_NFKB	200	2.87E-06
108_Gecko_ERL	1587	HALLMARK_ADIPOGENESIS	200	9.58E-06
108_Gecko_ERL	1587	HALLMARK_MYC_TARGETS_V2	58	1.87E-05
108_Gecko_ERL	1587	HALLMARK_ESTROGEN_RESPONSE_EARLY	200	2.42E-05
108_Gecko_ERL	1587	HALLMARK_G2M_CHECKPOINT	200	2.42E-05
108_Gecko_ERL	1587	HALLMARK_HEME_METABOLISM	200	2.42E-05
108_Gecko_ERL	1587	HALLMARK_APICAL_JUNCTION	200	7.58E-05
108_Gecko_ERL	1587	HALLMARK_BILE_ACID_METABOLISM	112	1.03E-04
108_Gecko_ERL	1587	HALLMARK_UV_RESPONSE_DN	144	1.20E-04
108_Gecko_ERL	1587	HALLMARK_CHOLESTEROL_HOMEOSTASIS	74	1.27E-04
108_Gecko_ERL	1587	HALLMARK_MYOGENESIS	200	1.81E-04
108_Gecko_ERL	1587	HALLMARK_XENOBIOTIC_METABOLISM	200	1.81E-04
58_Gecko_GEF	1554	HALLMARK_E2F_TARGETS	200	1.80E-05
58_Gecko_GEF	1554	HALLMARK_DNA_REPAIR	150	2.10E-05
58_Gecko_GEF	1554	HALLMARK_MYOGENESIS	200	2.27E-05
58_Gecko_GEF	1554	HALLMARK_UNFOLDED_PROTEIN_RESPONSE	113	8.18E-05
58_Gecko_GEF	1554	HALLMARK_G2M_CHECKPOINT	200	3.93E-04
58_Gecko_GEF	1554	HALLMARK_MYC_TARGETS_V1	200	3.93E-04
58_Gecko_GEF	1554	HALLMARK_OXIDATIVE_PHOSPHORYLATION	200	3.93E-04
58_Gecko_GEF	1554	HALLMARK_ANDROGEN_RESPONSE	101	8.48E-04
58_Gecko_GEF	1554	HALLMARK_MITOTIC_SPINDLE	200	8.48E-04
58_Gecko_GEF	1554	HALLMARK_P53_PATHWAY	200	8.48E-04
58_Gecko_GEF	1554	HALLMARK_ADIPOGENESIS	200	1.65E-03
58_Gecko_GEF	1554	HALLMARK_APICAL_JUNCTION	200	1.65E-03
58_Gecko_GEF	1554	HALLMARK_COMPLEMENT	200	1.65E-03
58_Gecko_GEF	1554	HALLMARK_ESTROGEN_RESPONSE_EARLY	200	1.65E-03
58_Gecko_GEF	1554	HALLMARK_GLYCOLYSIS	200	1.65E-03
58_Gecko_GEF	1554	HALLMARK_APICAL_SURFACE	44	2.00E-03
58_Gecko_GEF	1554	HALLMARK_COAGULATION	138	2.50E-03
58_Gecko_GEF	1554	HALLMARK_FATTY_ACID_METABOLISM	158	2.78E-03
58_Gecko_GEF	1554	HALLMARK_INFLAMMATORY_RESPONSE	200	3.39E-03
58_Gecko_GEF	1554	HALLMARK_KRAS_SIGNALING_DN	200	3.39E-03
58_Gecko_ERL	1656	HALLMARK_UV_RESPONSE_DN	144	5.74E-07
58_Gecko_ERL	1656	HALLMARK_ADIPOGENESIS	200	1.22E-06
58_Gecko_ERL	1656	HALLMARK_APICAL_JUNCTION	200	1.22E-06
58_Gecko_ERL	1656	HALLMARK_COAGULATION	138	2.71E-05
58_Gecko_ERL	1656	HALLMARK_G2M_CHECKPOINT	200	2.71E-05
58_Gecko_ERL	1656	HALLMARK_GLYCOLYSIS	200	2.71E-05

58_Gecko_ERL	1656	HALLMARK_IL2_STAT5_SIGNALING	200	2.71E-05
58_Gecko_ERL	1656	HALLMARK_PANCREAS_BETA_CELLS	40	6.24E-05
58_Gecko_ERL	1656	HALLMARK_HYPOXIA	200	6.41E-05
58_Gecko_ERL	1656	HALLMARK_KRAS_SIGNALING_DN	200	6.41E-05
58_Gecko_ERL	1656	HALLMARK_PI3K_AKT_MTOR_SIGNALING	105	1.15E-04
58_Gecko_ERL	1656	HALLMARK_E2F_TARGETS	200	1.59E-04
58_Gecko_ERL	1656	HALLMARK_ESTROGEN_RESPONSE_LATE	200	1.59E-04
58_Gecko_ERL	1656	HALLMARK_ANDROGEN_RESPONSE	101	2.52E-04
58_Gecko_ERL	1656	HALLMARK_COMPLEMENT	200	3.49E-04
58_Gecko_ERL	1656	HALLMARK_HEME_METABOLISM	200	3.49E-04
58_Gecko_ERL	1656	HALLMARK_MITOTIC_SPINDLE	200	3.49E-04
58_Gecko_ERL	1656	HALLMARK_MTORC1_SIGNALING	200	3.49E-04
58_Gecko_ERL	1656	HALLMARK_ESTROGEN_RESPONSE_EARLY	200	9.57E-04
58_Gecko_ERL	1656	HALLMARK_UNFOLDED_PROTEIN_RESPONSE	113	1.99E-03
49_Gecko_GEF	1579	HALLMARK_ADIPOGENESIS	200	1.03E-06
49_Gecko_GEF	1579	HALLMARK_SPERMATOGENESIS	135	1.03E-06
49_Gecko_GEF	1579	HALLMARK_UNFOLDED_PROTEIN_RESPONSE	113	1.03E-06
49_Gecko_GEF	1579	HALLMARK_UV_RESPONSE_UP	158	1.61E-06
49_Gecko_GEF	1579	HALLMARK_INTERFERON_GAMMA_RESPONSE	200	4.73E-06
49_Gecko_GEF	1579	HALLMARK_E2F_TARGETS	200	1.47E-05
49_Gecko_GEF	1579	HALLMARK_TNFA_SIGNALING_VIA_NFKB	200	4.48E-05
49_Gecko_GEF	1579	HALLMARK_COMPLEMENT	200	9.63E-05
49_Gecko_GEF	1579	HALLMARK_G2M_CHECKPOINT	200	9.63E-05
49_Gecko_GEF	1579	HALLMARK_HEME_METABOLISM	200	9.63E-05
49_Gecko_GEF	1579	HALLMARK_OXIDATIVE_PHOSPHORYLATION	200	9.63E-05
49_Gecko_GEF	1579	HALLMARK_PROTEIN_SECRETION	96	1.05E-04
49_Gecko_GEF	1579	HALLMARK_INTERFERON_ALPHA_RESPONSE	97	1.09E-04
49_Gecko_GEF	1579	HALLMARK_ALLOGRAFT_REJECTION	200	2.42E-04
49_Gecko_GEF	1579	HALLMARK_P53_PATHWAY	200	6.86E-04
49_Gecko_GEF	1579	HALLMARK_APOPTOSIS	161	1.46E-03
49_Gecko_GEF	1579	HALLMARK_INFLAMMATORY_RESPONSE	200	1.73E-03
49_Gecko_GEF	1579	HALLMARK_EPITHELIAL_MESENCHYMAL_TRANSITION	200	4.19E-03
49_Gecko_GEF	1579	HALLMARK_MITOTIC_SPINDLE	200	4.19E-03
49_Gecko_GEF	1579	HALLMARK_ANDROGEN_RESPONSE	101	6.31E-03
49_Gecko_ERL	806	HALLMARK_ADIPOGENESIS	200	2.94E-05
49_Gecko_ERL	806	HALLMARK_XENOBIOTIC_METABOLISM	200	7.34E-05
49_Gecko_ERL	806	HALLMARK_ALLOGRAFT_REJECTION	200	2.28E-04
49_Gecko_ERL	806	HALLMARK_IL2_STAT5_SIGNALING	200	5.94E-04
49_Gecko_ERL	806	HALLMARK_MYOGENESIS	200	5.94E-04
49_Gecko_ERL	806	HALLMARK_PEROXISOME	104	7.80E-04
49_Gecko_ERL	806	HALLMARK_ESTROGEN_RESPONSE_LATE	200	1.70E-03
49_Gecko_ERL	806	HALLMARK_MTORC1_SIGNALING	200	5.50E-03
49_Gecko_ERL	806	HALLMARK_APOPTOSIS	161	1.20E-02
49_Gecko_ERL	806	HALLMARK_G2M_CHECKPOINT	200	1.20E-02
49_Gecko_ERL	806	HALLMARK_MYC_TARGETS_V1	200	1.20E-02
49_Gecko_ERL	806	HALLMARK_P53_PATHWAY	200	1.20E-02
49_Gecko_ERL	806	HALLMARK_COAGULATION	138	1.20E-02
49_Gecko_ERL	806	HALLMARK_IL6_JAK_STAT3_SIGNALING	87	1.55E-02
49_Gecko_ERL	806	HALLMARK_DNA_REPAIR	150	1.72E-02
49_Gecko_ERL	806	HALLMARK_PROTEIN_SECRETION	96	1.91E-02
49_Gecko_ERL	806	HALLMARK_FATTY_ACID_METABOLISM	158	1.91E-02
49_Gecko_ERL	806	HALLMARK_APICAL_SURFACE	44	1.91E-02
49_Gecko_ERL	806	HALLMARK_COMPLEMENT	200	1.91E-02
49_Gecko_ERL	806	HALLMARK_E2F_TARGETS	200	1.91E-02
108_Gecko_GEF	1823	GGGCGGR_SP1_Q6	2940	2.03E-52
108_Gecko_GEF	1823	CAGGTG_E12_Q6	2485	5.58E-40
108_Gecko_GEF	1823	TTGTTT_FOXO4_01	2061	5.45E-34
108_Gecko_GEF	1823	GGGAGGRR_MAZ_Q6	2274	1.29E-31
108_Gecko_GEF	1823	AACTTT_UNKNOWN	1890	2.01E-30
108_Gecko_GEF	1823	TGGAAA_NFAT_Q4_01	1896	1.77E-28
108_Gecko_GEF	1823	CTTTGT_LEF1_Q2	1972	9.51E-28
108_Gecko_GEF	1823	SCGGAAGY_ELK1_02	1199	3.8E-26
108_Gecko_GEF	1823	TATAAA_TATA_01	1296	1.85E-22
108_Gecko_GEF	1823	GGGTGGRR_PAX4_03	1294	1.07E-20
108_Gecko_GEF	1823	RCGCANGCGY_NRF1_Q6	918	2.49E-18
108_Gecko_GEF	1823	YTATTTTNR_MEF2_02	697	1.6E-16

108_Gecko_GEF	1823	CAGCTG_AP4_Q5	1524	2.06E-16
108_Gecko_GEF	1823	CTTTGA_LEF1_Q2	1232	2.2E-16
108_Gecko_GEF	1823	CACGTG_MYC_Q2	1032	2.73E-16
108_Gecko_GEF	1823	RYTTCCTG_ETS2_B	1085	2.96E-15
108_Gecko_GEF	1823	TAATTA_CHX10_01	810	3.01E-15
108_Gecko_GEF	1823	GATA4_Q3	249	5.39E-13
108_Gecko_GEF	1823	WTGAAAT_UNKNOWN	616	5.87E-13
108_Gecko_GEF	1823	GCANCTGNY_MYOD_Q6	924	7.75E-13
108_Gecko_ERL	1587	CAGGTG_E12_Q6	2485	1.16E-39
108_Gecko_ERL	1587	GGGCGGR_SP1_Q6	2940	6.36E-39
108_Gecko_ERL	1587	CTTTGT_LEF1_Q2	1972	5.21E-27
108_Gecko_ERL	1587	GGGAGGRR_MAZ_Q6	2274	4.64E-23
108_Gecko_ERL	1587	TGGAAA_NFAT_Q4_01	1896	5.73E-19
108_Gecko_ERL	1587	AACTTT_UNKNOWN	1890	5.85E-18
108_Gecko_ERL	1587	GGGTGGRR_PAX4_03	1294	3.15E-17
108_Gecko_ERL	1587	RCGCANGCGY_NRF1_Q6	918	1.06E-16
108_Gecko_ERL	1587	CTTTAAR_UNKNOWN	972	3.46E-15
108_Gecko_ERL	1587	GCANCTGNY_MYOD_Q6	924	1.17E-14
108_Gecko_ERL	1587	CTTTGA_LEF1_Q2	1232	1.57E-14
108_Gecko_ERL	1587	TATAAA_TATA_01	1296	2.29E-14
108_Gecko_ERL	1587	TTGTTT_FOXO4_01	2061	2.78E-14
108_Gecko_ERL	1587	TGANTCA_AP1_C	1121	2.98E-14
108_Gecko_ERL	1587	RYTTCCTG_ETS2_B	1085	2.10E-13
108_Gecko_ERL	1587	TGCCAAR_NF1_Q6	722	2.19E-13
108_Gecko_ERL	1587	SCGGAAGY_ELK1_02	1199	2.31E-13
108_Gecko_ERL	1587	CAGCTG_AP4_Q5	1524	2.45E-13
108_Gecko_ERL	1587	TGACCTY_ERR1_Q2	1043	3.26E-13
108_Gecko_ERL	1587	GCACTTT_MIR175P_MIR20A_MIR106A_MIR106B_MIR20B_MIR519D	595	2.59E-11
58_Gecko_GEF	1554	GGGCGGR_SP1_Q6	2940	1.20E-43
58_Gecko_GEF	1554	CAGGTG_E12_Q6	2485	1.75E-29
58_Gecko_GEF	1554	GGGAGGRR_MAZ_Q6	2274	2.65E-29
58_Gecko_GEF	1554	CTTTGT_LEF1_Q2	1972	3.22E-28
58_Gecko_GEF	1554	TTGTTT_FOXO4_01	2061	1.91E-27
58_Gecko_GEF	1554	AACTTT_UNKNOWN	1890	3.22E-27
58_Gecko_GEF	1554	CAGCTG_AP4_Q5	1524	1.08E-22
58_Gecko_GEF	1554	SCGGAAGY_ELK1_02	1199	4.57E-20
58_Gecko_GEF	1554	GATTGGY_NFY_Q6_01	1160	2.96E-19
58_Gecko_GEF	1554	TGGAAA_NFAT_Q4_01	1896	6.78E-19
58_Gecko_GEF	1554	RYTTCCTG_ETS2_B	1085	1.60E-18
58_Gecko_GEF	1554	TGANTCA_AP1_C	1121	4.95E-18
58_Gecko_GEF	1554	GGGYGTGNY_UNKNOWN	664	6.38E-18
58_Gecko_GEF	1554	RNGTGGGC_UNKNOWN	766	1.14E-17
58_Gecko_GEF	1554	CTTTAAR_UNKNOWN	972	1.84E-16
58_Gecko_GEF	1554	TATAAA_TATA_01	1296	5.62E-16
58_Gecko_GEF	1554	TTANTCA_UNKNOWN	952	1.30E-15
58_Gecko_GEF	1554	TTTGCAC_MIR19A_MIR19B	516	1.44E-15
58_Gecko_GEF	1554	GCCATNTTG_YY1_Q6	427	4.93E-15
58_Gecko_GEF	1554	GTGACGY_E4F1_Q6	658	6.02E-15
58_Gecko_ERL	1656	GGGCGGR_SP1_Q6	2940	1.86E-40
58_Gecko_ERL	1656	CTTTGT_LEF1_Q2	1972	3.73E-36
58_Gecko_ERL	1656	TTGTTT_FOXO4_01	2061	3.08E-31
58_Gecko_ERL	1656	CAGGTG_E12_Q6	2485	6.34E-30
58_Gecko_ERL	1656	TGGAAA_NFAT_Q4_01	1896	6.31E-29
58_Gecko_ERL	1656	GGGAGGRR_MAZ_Q6	2274	3.04E-28
58_Gecko_ERL	1656	AACTTT_UNKNOWN	1890	2.32E-27
58_Gecko_ERL	1656	CACGTG_MYC_Q2	1032	2.60E-25
58_Gecko_ERL	1656	TATAAA_TATA_01	1296	2.32E-24
58_Gecko_ERL	1656	TTANTCA_UNKNOWN	952	2.94E-22
58_Gecko_ERL	1656	GGGTGGRR_PAX4_03	1294	4.99E-22
58_Gecko_ERL	1656	CTTTGA_LEF1_Q2	1232	1.81E-21
58_Gecko_ERL	1656	CAGCTG_AP4_Q5	1524	5.47E-20
58_Gecko_ERL	1656	RCGCANGCGY_NRF1_Q6	918	2.59E-19
58_Gecko_ERL	1656	SCGGAAGY_ELK1_02	1199	9.05E-18
58_Gecko_ERL	1656	TAATTA_CHX10_01	810	9.05E-18
58_Gecko_ERL	1656	CTTTAAR_UNKNOWN	972	3.51E-17
58_Gecko_ERL	1656	TGACATY_UNKNOWN	665	6.11E-16

58_Gecko_ERL	1656	GCANCTGNY_MYOD_Q6	924	9.57E-16
58_Gecko_ERL	1656	TGANTCA_AP1_C	1121	1.98E-15
49_Gecko_GEF	1579	CAGGTG_E12_Q6	2485	4.03E-35
49_Gecko_GEF	1579	CTTTGT_LEF1_Q2	1972	1.98E-34
49_Gecko_GEF	1579	GGGAGGRR_MAZ_Q6	2274	4.72E-33
49_Gecko_GEF	1579	GGGCGGR_SP1_Q6	2940	6.26E-32
49_Gecko_GEF	1579	TTGTTT_FOXO4_01	2061	6.32E-29
49_Gecko_GEF	1579	AACTTT_UNKNOWN	1890	1.99E-26
49_Gecko_GEF	1579	TGGAAA_NFAT_Q4_01	1896	2.04E-25
49_Gecko_GEF	1579	TATAAA_TATA_01	1296	3.33E-25
49_Gecko_GEF	1579	RTAAACA_FREAC2_01	919	9.33E-23
49_Gecko_GEF	1579	RYTTCCTG_ETS2_B	1085	5.57E-20
49_Gecko_GEF	1579	CAGCTG_AP4_Q5	1524	1.28E-18
49_Gecko_GEF	1579	GGGTGGRR_PAX4_03	1294	3.55E-17
49_Gecko_GEF	1579	TGANTCA_AP1_C	1121	1.24E-16
49_Gecko_GEF	1579	CTTTGA_LEF1_Q2	1232	4.25E-16
49_Gecko_GEF	1579	GATTGGY_NFY_Q6_01	1160	1.10E-15
49_Gecko_GEF	1579	TTANTCA_UNKNOWN	952	1.19E-15
49_Gecko_GEF	1579	TGACCTY_ERR1_Q2	1043	3.51E-14
49_Gecko_GEF	1579	TGAYRTCA_ATF3_Q6	538	8.08E-14
49_Gecko_GEF	1579	CACGTG_MYC_Q2	1032	1.31E-13
49_Gecko_GEF	1579	TAATTA_CHX10_01	810	1.77E-13
49_Gecko_ERL	806	CAGGTG_E12_Q6	2485	2.04E-19
49_Gecko_ERL	806	GGGAGGRR_MAZ_Q6	2274	2.74E-18
49_Gecko_ERL	806	GGGCGGR_SP1_Q6	2940	3.70E-18
49_Gecko_ERL	806	CAGCTG_AP4_Q5	1524	2.69E-16
49_Gecko_ERL	806	RYTTCCTG_ETS2_B	1085	5.44E-16
49_Gecko_ERL	806	CTTTGT_LEF1_Q2	1972	8.94E-15
49_Gecko_ERL	806	AACTTT_UNKNOWN	1890	1.54E-14
49_Gecko_ERL	806	CTTTGA_LEF1_Q2	1232	5.04E-14
49_Gecko_ERL	806	TGANTCA_AP1_C	1121	9.13E-13
49_Gecko_ERL	806	TGGAAA_NFAT_Q4_01	1896	9.13E-13
49_Gecko_ERL	806	TGACAGNY_MEIS1_01	827	6.03E-11
49_Gecko_ERL	806	TTGTTT_FOXO4_01	2061	1.72E-10
49_Gecko_ERL	806	TGTTTGY_HNF3_Q6	738	1.93E-10
49_Gecko_ERL	806	TGACCTY_ERR1_Q2	1043	4.87E-10
49_Gecko_ERL	806	RNGTGGGC_UNKNOWN	766	5.69E-10
49_Gecko_ERL	806	GGGYGTGNY_UNKNOWN	664	1.13E-09
49_Gecko_ERL	806	GCANCTGNY_MYOD_Q6	924	1.88E-09
49_Gecko_ERL	806	TGCCAAR_NF1_Q6	722	3.43E-09
49_Gecko_ERL	806	TCANNTGAY_SREBP1_01	475	6.06E-09
49_Gecko_ERL	806	YTATTTTNR_MEF2_02	697	1.38E-08
108_Gecko_GEF	1823	TBK1.DF_DN	287	4.11E-08
108_Gecko_GEF	1823	KRAS.600_UP.V1_DN	289	4.11E-08
108_Gecko_GEF	1823	CYCLIN_D1_KE_.V1_DN	194	5.65E-08
108_Gecko_GEF	1823	RPS14_DN.V1_UP	192	1.45E-07
108_Gecko_GEF	1823	CYCLIN_D1_UP.V1_DN	191	4.35E-07
108_Gecko_GEF	1823	KRAS.600.LUNG.BREAST_UP.V1_DN	289	5.81E-07
108_Gecko_GEF	1823	AKT_UP_MTOR_DN.V1_UP	184	5.81E-07
108_Gecko_GEF	1823	GCNP_SHH_UP_EARLY.V1_DN	169	1.59E-06
108_Gecko_GEF	1823	NRL_DN.V1_DN	134	1.64E-06
108_Gecko_GEF	1823	STK33_UP	293	1.64E-06
108_Gecko_GEF	1823	ESC_V6.5_UP_LATE.V1_DN	186	1.86E-06
108_Gecko_GEF	1823	E2F1_UP.V1_UP	189	2.33E-06
108_Gecko_GEF	1823	PIGF_UP.V1_UP	191	2.53E-06
108_Gecko_GEF	1823	STK33_DN	289	2.53E-06
108_Gecko_GEF	1823	P53_DN.V1_DN	192	2.53E-06
108_Gecko_GEF	1823	STK33_NOMO_DN	292	2.99E-06
108_Gecko_GEF	1823	ESC_V6.5_UP_EARLY.V1_DN	172	4.19E-06
108_Gecko_GEF	1823	ESC_J1_UP_LATE.V1_UP	191	7.09E-06
108_Gecko_GEF	1823	ATF2_S_UP.V1_UP	193	8.12E-06
108_Gecko_GEF	1823	STK33_NOMO_UP	294	8.45E-06
108_Gecko_ERL	1587	KRAS.PROSTATE_UP.V1_DN	144	3.31E-08
108_Gecko_ERL	1587	CSR_EARLY_UP.V1_UP	164	4.93E-08
108_Gecko_ERL	1587	PRC2_EED_UP.V1_DN	193	2.26E-07
108_Gecko_ERL	1587	RPS14_DN.V1_DN	187	3.93E-07

108_Gecko_ERL	1587	PRC1_BMI_UP.V1_UP	192	5.40E-07
108_Gecko_ERL	1587	TBK1.DF_DN	287	8.09E-07
108_Gecko_ERL	1587	BMI1_DN.V1_UP	147	1.07E-06
108_Gecko_ERL	1587	ESC_J1_UP_EARLY.V1_DN	179	1.61E-06
108_Gecko_ERL	1587	MTOR_UP.N4.V1_UP	196	1.71E-06
108_Gecko_ERL	1587	VEGF_A_UP.V1_UP	196	1.71E-06
108_Gecko_ERL	1587	ATM_DN.V1_DN	149	4.03E-06
108_Gecko_ERL	1587	E2F1_UP.V1_DN	193	4.29E-06
108_Gecko_ERL	1587	CYCLIN_D1_KE_.V1_DN	194	4.35E-06
108_Gecko_ERL	1587	STK33_DN	289	4.65E-06
108_Gecko_ERL	1587	CRX_DN.V1_DN	134	1.15E-05
108_Gecko_ERL	1587	KRAS.600.LUNG.BREAST_UP.V1_DN	289	1.30E-05
108_Gecko_ERL	1587	RAF_UP.V1_UP	196	1.52E-05
108_Gecko_ERL	1587	ERB2_UP.V1_DN	197	1.56E-05
108_Gecko_ERL	1587	ESC_V6.5_UP_EARLY.V1_DN	172	2.34E-05
108_Gecko_ERL	1587	NFE2L2.V2	481	2.37E-05
58_Gecko_GEF	1554	ATF2_UP.V1_DN	187	1.62E-09
58_Gecko_GEF	1554	TBK1.DF_DN	287	1.62E-09
58_Gecko_GEF	1554	ATF2_S_UP.V1_DN	187	3.46E-07
58_Gecko_GEF	1554	ESC_J1_UP_EARLY.V1_DN	179	4.92E-07
58_Gecko_GEF	1554	ESC_V6.5_UP_LATE.V1_DN	186	8.40E-07
58_Gecko_GEF	1554	STK33_NOMO_UP	294	8.82E-07
58_Gecko_GEF	1554	STK33_SKM_UP	290	1.93E-06
58_Gecko_GEF	1554	STK33_NOMO_DN	292	1.96E-06
58_Gecko_GEF	1554	VEGF_A_UP.V1_UP	196	5.25E-06
58_Gecko_GEF	1554	RB_P107_DN.V1_DN	128	6.41E-06
58_Gecko_GEF	1554	ESC_J1_UP_LATE.V1_DN	186	6.77E-06
58_Gecko_GEF	1554	LEF1_UP.V1_UP	195	1.40E-05
58_Gecko_GEF	1554	EGFR_UP.V1_DN	196	1.41E-05
58_Gecko_GEF	1554	CAMP_UP.V1_UP	200	1.84E-05
58_Gecko_GEF	1554	TBK1.DF_UP	290	2.94E-05
58_Gecko_GEF	1554	PDGF_ERK_DN.V1_UP	147	2.94E-05
58_Gecko_GEF	1554	KRAS.DF.V1_UP	193	2.94E-05
58_Gecko_GEF	1554	VEGF_A_UP.V1_DN	193	2.94E-05
58_Gecko_GEF	1554	HOXA9_DN.V1_UP	194	2.97E-05
58_Gecko_GEF	1554	HOXA9_DN.V1_DN	195	2.97E-05
58_Gecko_ERL	1656	MEK_UP.V1_DN	196	2.39E-08
58_Gecko_ERL	1656	ESC_V6.5_UP_EARLY.V1_DN	172	2.00E-07
58_Gecko_ERL	1656	ALK_DN.V1_DN	148	2.00E-07
58_Gecko_ERL	1656	CAMP_UP.V1_DN	200	2.00E-07
58_Gecko_ERL	1656	PIGF_UP.V1_UP	191	2.58E-07
58_Gecko_ERL	1656	TBK1.DF_DN	287	6.09E-07
58_Gecko_ERL	1656	RAPA_EARLY_UP.V1_UP	183	1.43E-06
58_Gecko_ERL	1656	CSR_LATE_UP.V1_UP	172	1.64E-06
58_Gecko_ERL	1656	STK33_SKM_UP	290	1.77E-06
58_Gecko_ERL	1656	RB_P107_DN.V1_DN	128	3.37E-06
58_Gecko_ERL	1656	MTOR_UP.N4.V1_UP	196	3.37E-06
58_Gecko_ERL	1656	IL15_UP.V1_DN	190	6.77E-06
58_Gecko_ERL	1656	KRAS.DF.V1_UP	193	6.91E-06
58_Gecko_ERL	1656	CAHOY_NEURONAL	100	6.91E-06
58_Gecko_ERL	1656	EIF4E_DN	100	6.91E-06
58_Gecko_ERL	1656	SRC_UP.V1_DN	179	6.91E-06
58_Gecko_ERL	1656	CRX_NRL_DN.V1_UP	140	8.22E-06
58_Gecko_ERL	1656	ERB2_UP.V1_DN	197	8.59E-06
58_Gecko_ERL	1656	PDGF_UP.V1_UP	146	1.41E-05
58_Gecko_GEF	1656	ATF2_UP.V1_UP	192	1.82E-05
49_Gecko_GEF	1579	WNT_UP.V1_DN	170	2.09E-10
49_Gecko_GEF	1579	SRC_UP.V1_DN	179	1.33E-06
49_Gecko_GEF	1579	STK33_DN	289	1.70E-06
49_Gecko_GEF	1579	SNF5_DN.V1_UP	177	2.10E-06
49_Gecko_GEF	1579	ATF2_UP.V1_UP	192	2.10E-06
49_Gecko_GEF	1579	PKCA_DN.V1_DN	167	2.23E-06
49_Gecko_GEF	1579	IL2_UP.V1_DN	196	2.23E-06
49_Gecko_GEF	1579	CSR_LATE_UP.V1_UP	172	3.07E-06
49_Gecko_GEF	1579	DCA_UP.V1_UP	191	4.34E-06
49_Gecko_GEF	1579	STK33_NOMO_DN	292	7.28E-06

49_Gecko_GEF	1579	PRC1_BMI_UP.V1_DN	190	1.27E-05
49_Gecko_GEF	1579	NOTCH_DN.V1_UP	193	1.44E-05
49_Gecko_GEF	1579	KRAS.600.LUNG.BREAST_UP.V1_DN	289	1.44E-05
49_Gecko_GEF	1579	TBK1.DF_UP	290	1.44E-05
49_Gecko_GEF	1579	IL15_UP.V1_DN	190	3.37E-05
49_Gecko_GEF	1579	PIGF_UP.V1_UP	191	3.37E-05
49_Gecko_GEF	1579	PTEN_DN.V1_UP	191	3.37E-05
49_Gecko_GEF	1579	MTOR_UP.N4.V1_DN	193	3.56E-05
49_Gecko_GEF	1579	VEGF_A_UP.V1_DN	193	3.56E-05
49_Gecko_GEF	1579	ESC_J1_UP_EARLY.V1_DN	179	3.81E-05
49_Gecko_ERL	806	GCNP_SHH_UP_EARLY.V1_UP	174	1.66E-05
49_Gecko_ERL	806	KRAS.600.LUNG.BREAST_UP.V1_UP	288	8.83E-05
49_Gecko_ERL	806	JNK_DN.V1_DN	191	8.83E-05
49_Gecko_ERL	806	P53_DN.V2_DN	145	8.83E-05
49_Gecko_ERL	806	CAMP_UP.V1_DN	200	1.11E-04
49_Gecko_ERL	806	RAPA_EARLY_UP.V1_DN	191	2.47E-04
49_Gecko_ERL	806	PRC2_EED_UP.V1_DN	193	2.47E-04
49_Gecko_ERL	806	VEGF_A_UP.V1_UP	196	2.57E-04
49_Gecko_ERL	806	CAMP_UP.V1_UP	200	2.88E-04
49_Gecko_ERL	806	NFE2L2.V2	481	3.41E-04
49_Gecko_ERL	806	STK33_NOMO_UP	294	3.63E-04
49_Gecko_ERL	806	PTEN_DN.V1_UP	191	5.67E-04
49_Gecko_ERL	806	PRC1_BMI_UP.V1_UP	192	5.67E-04
49_Gecko_ERL	806	STK33_SKM_DN	288	7.73E-04
49_Gecko_ERL	806	STK33_DN	289	7.73E-04
49_Gecko_ERL	806	JNK_DN.V1_UP	192	1.93E-03
49_Gecko_ERL	806	RAF_UP.V1_DN	194	1.97E-03
49_Gecko_ERL	806	KRAS.600_UP.V1_UP	287	1.97E-03
49_Gecko_ERL	806	IL2_UP.V1_DN	196	1.97E-03
49_Gecko_ERL	806	CSR_LATE_UP.V1_DN	170	2.02E-03

Table 3-7. Gene sets enriched in individual GeCKO library screens

Gene set enrichment analysis was performed with significant genes from each GeCKO screen to identify significant overlap with gene sets in the “Hallmark”, “Motif”, “Go-Biological Process” and “Oncogene” databases with the molecular signatures database v5.1. Pivotal input variables used for network analysis in Cytoscape are shown. Node is the sample in the following format: ‘cell line_library_drug’. Node Size is the number of input genes from the sample. Gene Set Name is the pathway enriched, with # of Genes in Gene Set being the number of genes in the GSEA pathway being tested.

Bibliography

1. Leemans CR, Braakhuis BJ, Brakenhoff RH. The molecular biology of head and neck cancer. Nat Rev Cancer. 2011;11(1):9-22. Epub 2010/12/17. doi: 10.1038/nrc2982. PubMed PMID: 21160525.
2. Seiwert TY, Burtness B, Mehra R, Weiss J, Berger R, Eder JP, Heath K, McClanahan T, Lunceford J, Gause C, Cheng JD, Chow LQ. Safety and clinical activity of pembrolizumab for treatment of recurrent or metastatic squamous cell carcinoma of the head and neck (KEYNOTE-012): an open-label, multicentre, phase 1b trial. The Lancet Oncology. 2016;17(7):956-65. Epub 2016/06/02. doi: 10.1016/s1470-2045(16)30066-3. PubMed PMID: 27247226.
3. Economopoulou P, Kotsantis I, Psyrri A. The promise of immunotherapy in head and neck squamous cell carcinoma: combinatorial immunotherapy approaches. ESMO Open. 2016;1(6):e000122. doi: 10.1136/esmoopen-2016-000122.
4. Bayat Mokhtari R, Homayouni TS, Baluch N, Morgatskaya E, Kumar S, Das B, Yeger H. Combination therapy in combating cancer. Oncotarget. 2017;8(23):38022-43. doi: 10.18632/oncotarget.16723. PubMed PMID: 28410237.
5. Wang T, Wei JJ, Sabatini DM, Lander ES. Genetic screens in human cells using the CRISPR-Cas9 system. Science. 2014;343(6166):80-4. Epub 2013/12/18. doi: 10.1126/science.1246981. PubMed PMID: 24336569; PMCID: 3972032.
6. Shalem O, Sanjana NE, Hartenian E, Shi X, Scott DA, Mikkelsen TS, Heckl D, Ebert BL, Root DE, Doench JG, Zhang F. Genome-scale CRISPR-Cas9 knockout screening in human cells. Science. 2014;343(6166):84-7. Epub 2013/12/18. doi: 10.1126/science.1247005. PubMed PMID: 24336571; PMCID: 4089965.
7. Shalem O, Sanjana NE, Zhang F. High-throughput functional genomics using CRISPR-Cas9. Nat Rev Genet. 2015;16(5):299-311. Epub 2015/04/10. doi: 10.1038/nrg3899. PubMed PMID: 25854182; PMCID: Pmc4503232.
8. Pendleton KP, Grandis JR. Cisplatin-Based Chemotherapy Options for Recurrent and/or Metastatic Squamous Cell Cancer of the Head and Neck. Clinical medicine insights Therapeutics. 2013;2013(5):10.4137/CMT.S10409. doi: 10.4137/CMT.S10409. PubMed PMID: 24273416.
9. Jennette KW, Lippard SJ, Vassiliades GA, Bauer WR. Metallointercalation reagents. 2-hydroxyethanethiolato(2,2',2'-terpyridine)-platinum(II) monocation binds strongly to DNA by intercalation. Proc Natl Acad Sci U S A. 1974;71(10):3839-43. Epub 1974/10/01. PubMed PMID: 4530265; PMCID: PMC434279.
10. Brockstein BE. Management of Recurrent Head and Neck Cancer. Drugs. 2011;71(12):1551-9. doi: 10.2165/11592540-000000000-00000.
11. Almeida LO, Abrahao AC, Rosselli-Murai LK, Giudice FS, Zagni C, Leopoldino AM, Squarize CH, Castilho RM. NFκB mediates cisplatin resistance through histone modifications in head and neck squamous cell carcinoma (HNSCC). FEBS Open Bio. 2014;4:96-104. doi: https://doi.org/10.1016/j.fob.2013.12.003.
12. Bonner JA, Harari PM, Giralt J, Azarnia N, Shin DM, Cohen RB, Jones CU, Sur R, Raben D, Jassem J, Ove R, Kies MS, Baselga J, Youssoufian H, Amellal N, Rowinsky EK, Ang KK. Radiotherapy plus cetuximab for squamous-cell carcinoma of the head and neck. N Engl J Med. 2006;354(6):567-78. Epub 2006/02/10. doi: 10.1056/NEJMoa053422. PubMed PMID: 16467544.

13. Vermorken JB, Trigo J, Hitt R, Koralewski P, Diaz-Rubio E, Rolland F, Knecht R, Amellal N, Schueler A, Baselga J. Open-label, uncontrolled, multicenter phase II study to evaluate the efficacy and toxicity of cetuximab as a single agent in patients with recurrent and/or metastatic squamous cell carcinoma of the head and neck who failed to respond to platinum-based therapy. J Clin Oncol. 2007;25(16):2171-7. Epub 2007/06/01. doi: 10.1200/jco.2006.06.7447. PubMed PMID: 17538161.
14. Ozanne B, Richards CS, Hendler F, Burns D, Gusterson B. Over-expression of the EGF receptor is a hallmark of squamous cell carcinomas. J Pathol. 1986;149(1):9-14. Epub 1986/05/01. doi: 10.1002/path.1711490104. PubMed PMID: 2425067.
15. Grandis JR, Tweardy DJ. Elevated levels of transforming growth factor alpha and epidermal growth factor receptor messenger RNA are early markers of carcinogenesis in head and neck cancer. Cancer Res. 1993;53(15):3579-84. Epub 1993/08/01. PubMed PMID: 8339264.
16. Madoz-Gurpide J, Zazo S, Chamizo C, Casado V, Carames C, Gavin E, Cristobal I, Garcia-Foncillas J, Rojo F. Activation of MET pathway predicts poor outcome to cetuximab in patients with recurrent or metastatic head and neck cancer. Journal of translational medicine. 2015;13:282. Epub 2015/09/01. doi: 10.1186/s12967-015-0633-7. PubMed PMID: 26319934; PMCID: PMC4552997.
17. Engelman JA, Zejnullahu K, Mitsudomi T, Song Y, Hyland C, Park JO, Lindeman N, Gale CM, Zhao X, Christensen J, Kosaka T, Holmes AJ, Rogers AM, Cappuzzo F, Mok T, Lee C, Johnson BE, Cantley LC, Janne PA. MET amplification leads to gefitinib resistance in lung cancer by activating ERBB3 signaling. Science. 2007;316(5827):1039-43. Epub 2007/04/28. doi: 10.1126/science.1141478. PubMed PMID: 17463250.
18. The Cancer Genome Atlas N. Comprehensive genomic characterization of head and neck squamous cell carcinomas. Nature. 2015;517(7536):576-82. doi: 10.1038/nature14129 http://www.nature.com/nature/journal/v517/n7536/abs/nature14129.html#supplementary-information.
19. Jimeno A, Shirai K, Choi M, Laskin J, Kochenderfer M, Spira A, Cline-Burkhardt V, Winquist E, Hausman D, Walker L, Cohen RB. A randomized, phase II trial of cetuximab with or without PX-866, an irreversible oral phosphatidylinositol 3-kinase inhibitor, in patients with relapsed or metastatic head and neck squamous cell cancer. Ann Oncol. 2015;26(3):556-61. Epub 2014/12/20. doi: 10.1093/annonc/mdu574. PubMed PMID: 25524478.
20. Ciardiello F, Tortora G. A Novel Approach in the Treatment of Cancer: Targeting the Epidermal Growth Factor Receptor. Clinical Cancer Research. 2001;7(10):2958.
21. Maemondo M, Inoue A, Kobayashi K, Sugawara S, Oizumi S, Isobe H, Gemma A, Harada M, Yoshizawa H, Kinoshita I, Fujita Y, Okinaga S, Hirano H, Yoshimori K, Harada T, Ogura T, Ando M, Miyazawa H, Tanaka T, Saijo Y, Hagiwara K, Morita S, Nukiwa T. Gefitinib or Chemotherapy for Non–Small-Cell Lung Cancer with Mutated EGFR. New England Journal of Medicine. 2010;362(25):2380-8. doi: 10.1056/NEJMoa0909530.
22. Hirsch FR, Sequist LV, Gore I, Mooradian M, Simon G, Croft EF, DeVincenzo D, Munley J, Stein D, Freivogel K, Sifakis F, Bunn PA, Jr. Long-term safety and survival with gefitinib in select patients with advanced non-small cell lung cancer: Results from the US IRESSA Clinical Access Program (ICAP). Cancer. 2018;124(11):2407-14. Epub 2018/03/27. doi: 10.1002/cncr.31313. PubMed PMID: 29579334.
23. Troiani T, Napolitano S, Della Corte CM, Martini G, Martinelli E, Morgillo F, Ciardiello F. Therapeutic value of EGFR inhibition in CRC and NSCLC: 15 years of clinical evidence. ESMO Open. 2016;1(5):e000088. doi: 10.1136/esmoopen-2016-000088.

24. Li W, Xu H, Xiao T, Cong L, Love MI, Zhang F, Irizarry RA, Liu JS, Brown M, Liu XS. MAGeCK enables robust identification of essential genes from genome-scale CRISPR/Cas9 knockout screens. Genome biology. 2014;15(12):554. Epub 2014/12/06. doi: 10.1186/s13059-014-0554-4. PubMed PMID: 25476604; PMCID: 4290824.
25. Benes C, Haber DA, Beare D, Edelman EJ, Lightfoot H, Thompson IR, Smith JA, Soares J, Stratton MR, Bindal N, Futreal PA, Greninger P, Forbes S, Ramaswamy S, Yang W, McDermott U, Garnett MJ. Genomics of Drug Sensitivity in Cancer (GDSC): a resource for therapeutic biomarker discovery in cancer cells. Nucleic Acids Research. 2012;41(D1):D955-D61. doi: 10.1093/nar/gks1111.
26. Garnett MJ, Edelman EJ, Heidorn SJ, Greenman CD, Dastur A, Lau KW, Greninger P, Thompson IR, Luo X, Soares J, Liu Q, Iorio F, Surdez D, Chen L, Milano RJ, Bignell GR, Tam AT, Davies H, Stevenson JA, Barthorpe S, Lutz SR, Kogera F, Lawrence K, McLaren-Douglas A, Mitropoulos X, Mironenko T, Thi H, Richardson L, Zhou W, Jewitt F, Zhang T, O'Brien P, Boisvert JL, Price S, Hur W, Yang W, Deng X, Butler A, Choi HG, Chang JW, Baselga J, Stamenkovic I, Engelman JA, Sharma SV, Delattre O, Saez-Rodriguez J, Gray NS, Settleman J, Futreal PA, Haber DA, Stratton MR, Ramaswamy S, McDermott U, Benes CH. Systematic identification of genomic markers of drug sensitivity in cancer cells. Nature. 2012;483(7391):570-5. Epub 2012/03/31. doi: 10.1038/nature11005. PubMed PMID: 22460902; PMCID: 3349233.
27. Iorio F, Knijnenburg TA, Vis DJ, Bignell GR, Menden MP, Schubert M, Aben N, Gonçalves E, Barthorpe S, Lightfoot H, Cokelaer T, Greninger P, van Dyk E, Chang H, de Silva H, Heyn H, Deng X, Egan RK, Liu Q, Mironenko T, Mitropoulos X, Richardson L, Wang J, Zhang T, Moran S, Sayols S, Soleimani M, Tamborero D, Lopez-Bigas N, Ross-Macdonald P, Esteller M, Gray NS, Haber DA, Stratton MR, Benes CH, Wessels LFA, Saez-Rodriguez J, McDermott U, Garnett MJ. A Landscape of Pharmacogenomic Interactions in Cancer. Cell. 2016;166(3):740-54. doi: https://doi.org/10.1016/j.cell.2016.06.017.
28. Cock PJA, Grüning BA, Paszkiewicz K, Pritchard L. Galaxy tools and workflows for sequence analysis with applications in molecular plant pathology. PeerJ. 2013;1:e167-e. doi: 10.7717/peerj.167. PubMed PMID: 24109552.
29. Tillman BN, Yanik M, Birkeland AC, Liu CJ, Hovelson DH, Cani AK, Palanisamy N, Carskadon S, Carey TE, Bradford CR, Tomlins SA, McHugh JB, Spector ME, Chad Brenner J. Fibroblast growth factor family aberrations as a putative driver of head and neck squamous cell carcinoma in an epidemiologically low-risk patient as defined by targeted sequencing. Head Neck. 2016;38 Suppl 1:E1646-52. doi: 10.1002/hed.24292. PubMed PMID: 26849095; PMCID: 4844767.
30. Ludwig ML, Kulkarni A, Birkeland AC, Michmerhuizen NL, Foltin SK, Mann JE, Hoesli RC, Devenport SN, Jewell BM, Shuman AG, Spector ME, Carey TE, Jiang H, Brenner JC. The genomic landscape of UM-SCC oral cavity squamous cell carcinoma cell lines. Oral Oncol. 2018;87:144-51. Epub 2018/12/12. doi: 10.1016/j.oraloncology.2018.10.031. PubMed PMID: 30527230; PMCID: PMC6349383.
31. Michmerhuizen N.M. LE, Kulkarni A., Brenner J.C. Differential Compensation mechanisms Define Resistance to PI3K inhibitors in PIK3CA amplified HNSCC. Oto Head and Neck Surgery. 2016(NIHMS799178).
32. McAuliffe SM, Morgan SL, Wyant GA, Tran LT, Muto KW, Chen YS, Chin KT, Partridge JC, Poole BB, Cheng K-H, Daggett J, Cullen K, Kantoff E, Hasselbatt K, Berkowitz J, Muto MG, Berkowitz RS, Aster JC, Matulonis UA, Dinulescu DM. Targeting Notch, a key

pathway for ovarian cancer stem cells, sensitizes tumors to platinum therapy. Proceedings of the National Academy of Sciences. 2012;109(43):E2939. doi: 10.1073/pnas.1206400109.
33. Aleksic T, Feller SM. Gamma-secretase inhibition combined with platinum compounds enhances cell death in a large subset of colorectal cancer cells. Cell communication and signaling : CCS. 2008;6:8-. doi: 10.1186/1478-811X-6-8. PubMed PMID: 18950493.
34. Anisuzzaman AS, Haque A, Wang D, Rahman MA, Zhang C, Chen Z, Chen ZG, Shin DM, Amin AR. In Vitro and In Vivo Synergistic Antitumor Activity of the Combination of BKM120 and Erlotinib in Head and Neck Cancer: Mechanism of Apoptosis and Resistance. Mol Cancer Ther. 2017;16(4):729-38. Epub 2017/01/26. doi: 10.1158/1535-7163.Mct-16-0683. PubMed PMID: 28119490.
35. Michmerhuizen NL, Leonard E, Matovina C, Harris M, Herbst G, Kulkarni A, Zhai J, Jiang H, Carey TE, Brenner C. Rationale for using irreversible EGFR Inhibitors in combination with PI3K inhibitors for advanced Head and Neck Squamous Cell Carcinoma. Molecular Pharmacology. 2019:mol.118.115162. doi: 10.1124/mol.118.115162.
36. D'Amato V, Rosa R, D'Amato C, Formisano L, Marciano R, Nappi L, Raimondo L, Di Mauro C, Servetto A, Fusciello C, Veneziani BM, De Placido S, Bianco R. The dual PI3K/mTOR inhibitor PKI-587 enhances sensitivity to cetuximab in EGFR-resistant human head and neck cancer models. British journal of cancer. 2014;110(12):2887-95. Epub 2014/05/16. doi: 10.1038/bjc.2014.241. PubMed PMID: 24823695; PMCID: PMC4056056.
37. Koole K, Brunen D, van Kempen PM, Noorlag R, de Bree R, Lieftink C, van Es RJ, Bernards R, Willems SM. FGFR1 Is a Potential Prognostic Biomarker and Therapeutic Target in Head and Neck Squamous Cell Carcinoma. Clinical cancer research : an official journal of the American Association for Cancer Research. 2016;22(15):3884-93. doi: 10.1158/1078-0432.CCR-15-1874. PubMed PMID: 26936917.
38. Ileana Dumbrava E, Alfattal R, Miller VA, Tsimberidou AM. Complete Response to a Fibroblast Growth Factor Receptor Inhibitor in a Patient With Head and Neck Squamous Cell Carcinoma Harboring FGF Amplifications. JCO Precision Oncology. 2018(2):1-7. doi: 10.1200/PO.18.00100.
39. Agrawal N, Frederick MJ, Pickering CR, Bettegowda C, Chang K, Li RJ, Fakhry C, Xie TX, Zhang J, Wang J, Zhang N, El-Naggar AK, Jasser SA, Weinstein JN, Trevino L, Drummond JA, Muzny DM, Wu Y, Wood LD, Hruban RH, Westra WH, Koch WM, Califano JA, Gibbs RA, Sidransky D, Vogelstein B, Velculescu VE, Papadopoulos N, Wheeler DA, Kinzler KW, Myers JN. Exome sequencing of head and neck squamous cell carcinoma reveals inactivating mutations in NOTCH1. Science. 2011;333(6046):1154-7. Epub 2011/07/30. doi: 10.1126/science.1206923. PubMed PMID: 21798897; PMCID: 3162986.
40. Pickering CR, Zhang J, Yoo SY, Bengtsson L, Moorthy S, Neskey DM, Zhao M, Ortega Alves MV, Chang K, Drummond J, Cortez E, Xie TX, Zhang D, Chung W, Issa JP, Zweidler-McKay PA, Wu X, El-Naggar AK, Weinstein JN, Wang J, Muzny DM, Gibbs RA, Wheeler DA, Myers JN, Frederick MJ. Integrative genomic characterization of oral squamous cell carcinoma identifies frequent somatic drivers. Cancer Discov. 2013;3(7):770-81. Epub 2013/04/27. doi: 10.1158/2159-8290.cd-12-0537. PubMed PMID: 23619168; PMCID: 3858325.
41. Gu F, Ma Y, Zhang Z, Zhao J, Kobayashi H, Zhang L, Fu L. Expression of Stat3 and Notch1 is associated with cisplatin resistance in head and neck squamous cell carcinoma. Oncology reports. 2010;23(3):671-6. Epub 2010/02/04. PubMed PMID: 20127005.
42. Zhang ZP, Sun YL, Fu L, Gu F, Zhang L, Hao XS. Correlation of Notch1 expression and activation to cisplatin-sensitivity of head and neck squamous cell carcinoma. Ai zheng =

Aizheng = Chinese journal of cancer. 2009;28(2):100-3. Epub 2009/06/25. PubMed PMID: 19550121.
43. Lee SH, Do SI, Lee HJ, Kang HJ, Koo BS, Lim YC. Notch1 signaling contributes to stemness in head and neck squamous cell carcinoma. Laboratory investigation; a journal of technical methods and pathology. 2016;96(5):508-16. Epub 2016/03/02. doi: 10.1038/labinvest.2015.163. PubMed PMID: 26927514.
44. Weng AP, Ferrando AA, Lee W, Morris JPt, Silverman LB, Sanchez-Irizarry C, Blacklow SC, Look AT, Aster JC. Activating mutations of NOTCH1 in human T cell acute lymphoblastic leukemia. Science. 2004;306(5694):269-71. Epub 2004/10/09. doi: 10.1126/science.1102160. PubMed PMID: 15472075.
45. Palomero T, Ferrando A. Therapeutic targeting of NOTCH1 signaling in T-cell acute lymphoblastic leukemia. Clinical lymphoma & myeloma. 2009;9 Suppl 3(Suppl 3):S205-S10. doi: 10.3816/CLM.2009.s.013. PubMed PMID: 19778842.
46. Takebe N, Nguyen D, Yang SX. Targeting notch signaling pathway in cancer: clinical development advances and challenges. Pharmacology & therapeutics. 2014;141(2):140-9. Epub 2013/10/01. doi: 10.1016/j.pharmthera.2013.09.005. PubMed PMID: 24076266; PMCID: PMC3982918.
47. Doody RS, Raman R, Farlow M, Iwatsubo T, Vellas B, Joffe S, Kieburtz K, He F, Sun X, Thomas RG, Aisen PS, Siemers E, Sethuraman G, Mohs R. A phase 3 trial of semagacestat for treatment of Alzheimer's disease. N Engl J Med. 2013;369(4):341-50. Epub 2013/07/26. doi: 10.1056/NEJMoa1210951. PubMed PMID: 23883379.
48. Zhao B, Wang L, Qiu H, Zhang M, Sun L, Peng P, Yu Q, Yuan X. Mechanisms of resistance to anti-EGFR therapy in colorectal cancer. Oncotarget. 2016;8(3):3980-4000. doi: 10.18632/oncotarget.14012. PubMed PMID: 28002810.
49. Pao W, Wang TY, Riely GJ, Miller VA, Pan Q, Ladanyi M, Zakowski MF, Heelan RT, Kris MG, Varmus HE. KRAS mutations and primary resistance of lung adenocarcinomas to gefitinib or erlotinib. PLoS medicine. 2005;2(1):e17. Epub 2005/02/08. doi: 10.1371/journal.pmed.0020017. PubMed PMID: 15696205; PMCID: PMC545207.
50. Massarelli E, Varella-Garcia M, Tang X, Xavier AC, Ozburn NC, Liu DD, Bekele BN, Herbst RS, Wistuba, II. KRAS mutation is an important predictor of resistance to therapy with epidermal growth factor receptor tyrosine kinase inhibitors in non-small-cell lung cancer. Clinical cancer research : an official journal of the American Association for Cancer Research. 2007;13(10):2890-6. Epub 2007/05/17. doi: 10.1158/1078-0432.Ccr-06-3043. PubMed PMID: 17504988.

Chapter 4: Investigating FGFR as a Common Resistance Mechanism to EGFR Inhibition in HNSCC

Abstract

In this chapter, we expand on our results from chapter three that nominated the FGF pathway as a compensatory mechanism to EGFR inhibition, and show that FGF is a more common compensatory pathway across 14/22 (63%) of UM-SCC cell lines across oral cavity and larynx subsites. Surprisingly, neither copy number or expression of FGFRs predict responsiveness to dual EGFR and FGFR inhibition. However, our generation of an EGFR knockout model using CRISPR/Cas9 demonstrated that FGFRs can compensate for the complete loss of EGFR. Additionally, dual inhibition of EGFR and FGFR significantly suppressed tumor growth in our mouse xenograft model, suggesting *in vivo* relevance of this combination for HNSCC. To further evaluate potential clinical relevance, we analyzed expression profiles of tumors from patients who received the EGFR inhibitor cetuximab. We observed changes in the FGFR receptors, KRAS signaling, and PI3K-mTOR signaling mid-treatment, similar to our *in vitro* work.

Introduction

The epidermal growth factor receptor (EGFR) is a known driver of cancer cell growth and proliferation in head and neck squamous cell carcinoma (HNSCC) as well as other cancer types. As such, several pathways have already been identified as contributing to resistance to EGFR inhibition such as ERBB family members(1-4), RAS/RAF signaling(5-9), FGFR (10-12),

MET (13, 14), and IGF1R(15-18). However, there are still no biomarkers to predict which pathway is driving compensation in a specific model, and as such makes it difficult to successfully advance combination therapies.

Here, we further investigate the results of our last chapter that nominated the FGFR pathway as a potential compensatory mechanism to EGFR inhibition in a UM-SCC cell line. The FGF pathway consists of four cell-surface receptors, FGFR1-4, that contain tyrosine kinase domains that are activated upon ligand binding, and can in turn activate downstream effectors such as PI3K and MAPKs (19-21). FGFR signaling has been proposed before as a compensatory mechanism to EGFR inhibition in both HNSCC and lung cancer, but specifically for cases of *FGFR1* amplification(10, 22-24). Cases with *FGFR1* amplification are thought to be reliant on FGFR1 and FGF signals, identifying these cases as potentially sensitive to dual inhibition of EGFR and FGFR. Interestingly, the UM-SCC cell line that nominated FGFR signaling as a compensatory mechanism, UM-SCC-49, has an *FGFR1* deletion(25). As FGFRs activate similar downstream pathways (19), we believe this suggests that FGFR may be a more common compensatory mechanism to EGFR inhibition than only in models with *FGFR1* amplification.

In this chapter, we expand on our results from chapter three and investigate the extent that FGFR may be a common compensatory pathway in more HNSCC models. We also sought to identify a biomarker that would predict FGFR as a compensatory pathway given our genetic characterization of these models in chapter two. We then further explored the mechanism of FGFR compensation, including short-term inhibition of EGFR by small molecule inhibitors and long-term loss of EGFR by CRISPR knockout. Additionally, we sought to evaluate the *in vivo* relevance FGFR as a compensatory pathway to EGFR inhibition through the creation of mouse models and analysis of patient samples pre- and mid-cetuximab treatment.

Methods

Cell Culture. Cell lines were cultured in Dulbecco's Modified Eagle's Medium (DMEM) (Invitrogen #11965) containing 10% fetal bovine serum (FBS, Sigma), 1% NEAA (Invitrogen 15140122) and 7 µL/mL penicillin-streptomycin (Invitrogen 15140122) in a humidified atmosphere of 5% CO_2 at 37°C. Cells were tested for mycoplasma contamination using the MycoAlert detection kit (Lonza).

Cell Viability assays. 2,000 cells per well were seeded in 384-well microplates using a Multiflo liquid handling dispensing system. After 24 hours, cells were treated with compound or DMSO in a 10-point two-fold dilution series in quadruplicate. 96-well plates were prepared with compounds in 200X concentration and then diluted to 10X concentration in media in a second 96-well plate using the Agilent Bravo Automated Liquid Handling Platform and VWorks Automation Control Software. These compounds were then used to treat the cells with the desired drug concentration, again using liquid handling robotics. Cells were stained with resazurin (Sigma) in PBS for 12-24 hours before fluorescent signal intensity was quantified 72 hours after treatment using the Cytation3 fluorescence plate reader enabled with automatic stacking at excitation and emission wavelengths of 540 and 612 nm, respectively. All compounds were purchased from Selleck Chemicals. 10mM aliquots were stored -80 °C. Each compound was subjected to no more than 5 freeze-thaw cycles.

Trypan Blue assays. Cells were seeded in 24-well plates. After 24 hours, cells were treated with compound or DMSO. After 72 hours, cells were harvested and counted with trypan blue reagent (Invitrogen) using the Countess II Automated Cell Counter (ThermoFisher).

Annexin V+ assay and statistics. Cells were seeded into 6-well plates. After 24 hours, cells were treated with compound or DMSO. After 48 hours, cells were prepared for Annexin V staining according to manufacturer recommendations (Invitrogen). Briefly, cells were harvested and then stained with propidium iodide and Alexa Fluor 488 annexin V before being analyzed on the Ze5 (Bio-Rad) at the University of Michigan Flow Cytometry core. Statistical significance was calculated on log-transformed data fitted with linear regression and interaction term. P-values were adjusted with Bonferroni method.

Immunoblotting. Western blot analysis was performed as previously described (25, 26). Briefly, UM-SCC cell lines at 70-80% confluency were rinsed with PBS and lysed in buffer (150 mM NaCl, 10% Glycerol, 1% NP40, 0.1% Triton X-100, 1 mM PIPES, 1 mM MgCl, 50 mM Tris) containing protease and phosphatase inhibitors (Thermo 186129, 1861277) as described (27). See **Table 4-1** for primary and secondary antibodies used.

Transcript analysis by qPCR. Cells were rinsed with PBS and then preserved in Qiazol (Qiagen) at -80°C until RNA extraction was performed using RNeasy Spin Kit (Qiagen) according to manufacturer recommendations. cDNA templates were then synthesized using random primers and SuperScript III Reverse Transcriptase (Invitrogen) according to manufacturer recommendations. Primers used for qPCR analysis are listed in **Table 4-2**.

Amplification by qPCR was performed with Quantitech Sybr Green (Qiagen) on QuantStudio5 (Applied Biosystems) under the cycling conditions recommended by manufacturer.

Generation of Clonal Knockout Lines. UM-SCC-92 was transduced with a lentiviral CRISPR construct targeting *EGFR (*Sigma Aldrich) and after antibiotic and GFP selection, individual clones were isolated. Individual clones were screened for knockout by sanger sequencing. DNA was extracted from clones (Qiagen, Gentra Puregene Cell Kit) and the gRNA region amplified by PCR using Platinum HiFi Taq (Invitrogen). Primers for amplification are in **Table 4-2**. PCR products were then ligated into pCR8 vector (ThermoFisher, K250020), transformed, and plasmid DNA extracted from individual colonies (Qiagen, QIAprep Spin Miniprep Kit) and submitted for sanger sequencing at the University of Michigan DNA Sequencing Core. Sequences were aligned using the DNASTAR Lasergene software suite.

Exome Sequencing and Variant Calling. Genomic DNA from UM-SCC-92 and EGFR K/O cell line was extracted according to Gentra PureGene Handbook (Qiagen) and genotyped. Exome Capture Library Construction was done using the Roche NimbleGen V3, and paired-end sequencing (2x150 bp) of the captured exons was carried out on an Illumina HiSeq 2500 High-Output at the University of Michigan DNA sequencing core according to standard protocol. Variant calling was performed as previously described (25). Variants reported were required to have at least 5 reads supporting the variant allele, and variants reported as intergenic or intronic were filtered out.

RNA Sequencing and Bioinformatic Analysis. RNA was isolated with the Qiagen RNeasy Spin Prep Kit and submitted to the University of Michigan DNA sequencing core. Sequencing libraries were prepared according to manufacturer's protocols with the Illumina TruSeq stranded mRNA kit and sequenced by paired end sequencing on the Illumina HiSeq 2500-Rapid. Read quality, alignment, and FPKM calculations were performed as previously described (25).

Mouse Xenografts. UM-SCC-108 cells in log-phase growth were trypsinized and re-suspended in a 1:1 ratio of DMEM and Matrigel (Corning #354234). Nude athymic mice (Charles River Laboratories) were subcutaneously injected with 2 million cells per flank. When the average tumor size measured around $100mm^3$, mice were treated with either vehicle (0.5% methylcellulose, 0.2% Tween-80), 150mg/kg gefitinib, 30mg/kg BGJ398, or the combination of 150mg/kg gefitinib and 30mg/kg BGJ398. Drugs were delivered by oral gavage.

Changes to cell signaling were evaluated on tumors staged to approximately $350mm^3$ and treated in the four different groups indicated above for 6 hours, tumors were then homogenized by pestle in protein lysis buffer with inhibitors and protein lysates were evaluated by immunoblotting as described above.

To monitor tumor growth, cell line xenografts were established and then treated over the course of twenty-one days using 16 tumors per treatment group in bilateral flanks, except for the combination arm which had 14 tumors due to the necessary euthanization of one mouse during treatment. During treatment, mice were dosed by oral gavage daily for five days then allowed to recover for two days. Tumors were measured twice weekly using calipers. Volume of tumor was calculated by $(\pi/6)$*(width x length x length) where length is defined by the longest measurement (28, 29).

Because tumors were in bilateral flanks which could cause a dependence of the two tumors within the same mouse, significance was calculated using the linear mixed model with random intercept only on log2 scaled data. This model considers the dependence of the measurements of the tumors on the same mouse and was therefore the most appropriate test. Two outliers were identified in FGFR group for the log2 scaled data, the highest of which was removed from the analysis.

Clinical specimens and clinical data. Formalin fixed paraffin embedded (FFPE) blocks were collected from a retrospective cohort of patients under an IRB-approved protocol for next generation sequencing of DNA and RNA (HUM00080561) from our recent clinical trial, "A Phase II Study of RT Concurrent with Cetuximab in Patients with Locally Advanced Head and Neck Squamous Cell Carcinoma Who Do Not Qualify For Standard Chemotherapy Due To Age>70 Or Co-Morbidities", University identification number: UMCC 2009.009, clinicialtrials.gov identification number: NCT00904345. Clinical variables of the cohort were previously described in (30). As previously noted, clinical, histologic, and outcome data was collected from medical records and death was documented from electronic medical record notes. Following hematoxylin and eosin staining of sections from each block, our HN pathologist J.B.M. identified blocks with >60% tumor content for coring and DNA/RNA isolation. In total, we identified 13 tumors and 4 adjacent normal tissues with sufficient material from both pre- and mid-cetuximab loading dose biopsy specimens for molecular analysis. DNA and RNA were simultaneously isolated using the Qiagen AllPrep kit as described (31) and advanced for NGS if it met our previously defined quality standards defined by Qubit and Bioanalyzer analysis (26, 32).

Clinical specimen transcriptome sequencing. Total RNA isolated using Allprep Kit (Qiagen) was submitted for library preparation and sequencing to the University of Michigan DNA sequencing core. Briefly, we used 500ng of RNA for library preparations or as much RNA as available with the Illumina TruSeq Stranded Total RNA library prep kit (Cat#: RS-122-2201/2). The protocol was followed according to the manufacturer's recommendations, with a single modification in which we used 14 cycles of PCR to amplify the library prior to the final bead purification. The samples were then pooled and loaded on an Illumina HiSEQ4000 across 5 lanes and paired end sequenced to 75nt length. A summary of sequencing quality statistics including total unique mapped reads for each sample is provided in **Table 4-3**.

Transcript Quantification and Statistical Analysis. Read quality was assessed using FastQC (v0.11.5). No quality issues were detected. The two-step STAR workflow was used to map the reads. In step 1, STAR (v2.5.3a) was used to generate the genome index database with the help of the reference human genome and annotated transcriptome files. In step 2, read mapping was guided by this generated genome index database generated in step 1. Only reads that map uniquely were retained by using samtools (v1.2). To compute FPKM, cufflinks (v2.2.1) was used with default parameters except for "--max-bundle-frags" which was changed to 100000000 to avoid raising of the HIDATA flag at loci that have more fragments than the pre-set threshold for every locus.

Differential transcripts with greater or less than 2-log2 fold change between mid- and pre-treatment samples were used to create up and down-regulated gene signature rank-lists for each tumor or normal pair. We then loaded gene set rank lists into the GSEA3.0.JAR module and

assessed statistical enrichment over 1000 permutations with four different gene set databases: 'Hallmark', 'Motif', 'Go-Biological Process' and 'Oncogene'. Enrichments with FDR < 0.05, up to a maximum of 20 significant pathways per database, were then used to create statistically significant enrichment networks for each Cetuximab-regulated tumor gene set. Networks were then filtered for concepts enriched in greater than one tumor. We then loaded tumor networks into the Cytoscape3.7.1 desktop module, using the FDR P-value as edge weight and number of genes in a gene set as node diameter. Network concepts were clustered and highlighted based on similarity to significant Hallmark gene sets.

Results

Our results from chapter three nominated the FGFR signaling pathway as a potential compensatory mechanism to EGFR inhibition in UM-SCC-49. In this chapter, we wanted to test the hypothesis that FGFR signaling could be a more common compensatory mechanism and therefore challenged multiple UM-SCC cell lines from the oral cavity and larynx subsites with the combination of the EGFR and pan-FGFR inhibition. We observed that a subset of cell lines had decreased viability after three days of treatment with the drug combination in comparison to either monotherapy both by resaurzin (**Fig 4-1A**) and trypan blue (**Fig 4-1B**) assays. We observed that a total of 14/22 (63%) of UM-SCC cell lines had decreased viability when challenged with the combination of EGFR and FGFR inhibitors but not to the monotherapy treatments. Of the lines tested, 10/13 (77%) of the responders to the combination were derived from the oral cavity subsite and 4/9 (44%) of the responders were derived from the larynx. We also included the human oral keratinocyte cell line HOK16B to test if dual EGFR and FGFR inhibition might be broadly toxic to non-cancer models. However, the HOK16B cell line did not

undergo cell death when treated with EGFR and FGFR inhibitors alone or in combination (**Fig 4-1B**), suggesting that there was specificity in the HNSCC cancer models.

We next wanted to test the mechanism of cell death and focused on using oral cavity cell line models due to the high response rate of this subsite. We choose the cell lines UM-SCC-49 and UM-SCC-108 which responded to the combination of EGFR and FGFR inhibition through decreased viability, as well as the non-responsive oral cavity cell line UM-SCC-97. We chose to analyze the amount of annexin V staining by flow cytometry, as annexin V is indicative of apoptosis(33) and a common mechanism of cell death. We observed that UM-SCC-49 and UM-SCC-108 had significantly higher annexin V staining in the combination treatment (p-value $\leq$ 0.05) as compared to the vehicle control or monotherapy treatments, while UM-SCC-97 did not (**Fig 4-2**). Accordingly, UM-SCC-49 and UM-SCC-108 had elevated levels of cleaved caspase-3 in the combination treatment at 24 hours, while UM-SCC-97 did not (**Fig 4-3**). We also evaluated a panel of other proteins that play a role in cell death, such as BCL-2, MCL1, and BAD, but did not observe any distinguishing differences between the responsive and non-responsive lines in their response to drug treatment.

We then hypothesized that there might be a biomarker that could predict which cell lines would respond and undergo cell death when treated with dual EGFR and FGFR inhibition. We first evaluated the copy number status of a panel of cell lines, as we postulated that perhaps amplifications of FGFRs would predict response. However, the UM-SCC models had a range of amplifications and deletions across all FGFR receptors for both subsets and was not a distinguishing factor for either responsive or non-responsive models (**Fig 4-4**). The copy number of *EGFR* was high across UM-SCC models with the exception of UM-SCC-55, a responder. As we thought it possible to identify FGFR signaling as the compensatory pathway from the lack of

other known resistance mechanisms, we evaluated copy numbers of *ERBB2* and *IGF1R*. Copy numbers of both *ERBB2* and *IGF1R* varied between subsets, suggesting that we can't identify FGFR is the compensatory mechanism to EGFR inhibition because of a lack of *ERBB2* or *IGF1R* amplification. We next evaluated the transcriptome to test if RNA expression could be a biomarker that predicts response to EGFR and FGFR inhibition. We observed that for the FGF receptors, expression varied for each receptor and did not distinguish between responsive and non-responsive models (**Fig 4-5**). Expression of EGFR remained high across all cell lines, and expression of ERBB2 and IGF1R varied.

We next evaluated downstream signaling mechanisms in response to EGFR and FGFR inhibition alone and in combination to determine if activation of a downstream effector might differentiate between responsive and non-responsive models. In a panel of oral cavity models, we observed decreases in phosphorylation of notable downstream effectors such as AKT, ERK1/2, and MEK1/2 in response to the inhibitors regardless of a responsive or non-responsive model (**Fig 4-6**). We also noted limited changes in phosphorylation of STAT1 or STAT3 across treatments, suggesting that STATs have a limited role in the effect of the EGFR and FGFR response. Notably, the phosphorylation of MET, another known resistance pathway to EGFR inhibition, did not change in response to EGFR inhibition for either the models that respond to the EGFR and FGFR combination, or UM-SCC-97. The lack of induction of MET phosphorylation in response may indicate that MET is not a compensatory pathway in these models. Overall, we did not observe any distinguishing factor that differentiated a responsive cell line model from a non-responsive model.

We hypothesized that the responsive cell lines might display a greater reliance on FGF signaling when EGFR signaling is inhibited, even though we do not see this reliance at the

genetic level or through FGFR expression during normal cell growth. Unfortunately, due to technical issues with specificity of phospho-antibodies, we were unable to directly assess the phosphorylation status of the FGF receptors. As we were unable to evaluate any induction of the FGF pathway by immunoblotting, we turned to assess the transcript levels of the receptors. After treatment of EGFR inhibitor, we observed no upregulation of FGF receptors in the responsive model UM-SCC-92 as compared to vehicle control (**Fig 4-7**). However, the responsive model UM-SCC-49 did have an upregulation of FGFR3 transcript at 12 hours.

These modest changes in FGFR transcript levels due to short-term inhibition of EGFR led us to postulate that long-term loss of EGFR signaling might give significant clues to compensatory pathways in the cell lines. We hypothesized that a complete loss of EGFR signaling may lead to reliance on FGF signaling if the FGF signaling pathway was a primary compensatory pathway for the cell line. To test this hypothesis, we used CRISPR/Cas9 to generate a knockout of EGFR in UM-SCC cell lines. We successfully derived a clonal cell line in UM-SCC-92 for which all three alleles of *EGFR* contained deletions leading to deleterious frame-shifts (**Fig 4-8A**), and for which we observed no expression of EGFR by immunoblot (**Fig 4-8B**). This EGFR knockout (EGFR K/O) cell line has a significantly slower proliferation rate than the parental UM-SCC-92 cell line (p-value ≤ 0.0001) (**Fig 4-9A**), which was not surprising given the known role of EGFR in cell growth and proliferation. We also observed morphological differences in the EGFR K/O cell line as compared to the parental UM-SCC-92 cell line, where the EGFR K/O cell line has a broader, stretched out cell body perhaps indicative of a more mesenchymal phenotype (**Fig 4-9B**).

As the EGFR K/O cell line, while slower growing, was capable of surviving without EGFR, we next wanted to address the question of what gene or pathway might be compensating

for this loss of EGFR signaling. We first postulated that a gain of function mutation might have occurred during the CRISPR/Cas9 and cloning process which helped the EGFR K/O cell line survive. We submitted the EGFR K/O cell line for exome sequencing and found an additional 18 synonymous mutations and 89 non-synonymous mutations not in parental UM-SCC-92 cell line (25). The non-synonymous mutations are categorized by effect in **Table 4-4**. Importantly, we did not see any gain of function mutations in notable kinases such as Ras, PIK3CA, or even the FGF receptors. We then analyzed the transcriptome of the EGFR K/O cell line, hypothesizing that a compensatory pathway may be upregulated in response to the loss of EGFR. We focused on kinases and receptors that were upregulated in the EGFR K/O as compared to UM-SCC-92 wildtype cell line, as we thought these genes would be more likely to have small molecule inhibitors available for further experimentation. There were 23 kinases and receptors that had >3 differential expression in the EGFR K/O as compared to UM-SCC-92 wildtype cell line and are listed in **Table 4-5**. We saw that FGFR1 was ranked 8th highest of the upregulated kinases in the EGFR K/O cell line, and so we also assessed if there were changes in the expression of FGFR2 and FGFR3. Interestingly, while FGFR1 was highly upregulated, FGFR2 and FGFR3 were downregulated (**Fig 4-10A**). PIK3CA, a known compensatory signaling mechanism to loss of EGFR, showed no transcriptome changes, while we saw the expected decrease of EGFR transcripts. We then confirmed the upregulation of FGFR1 and downregulation of FGFR2 by qPCR, though we saw a slight upregulation of FGFR3 (**Fig 4-10B**). We also confirmed the decrease in EGFR transcript with primers that were upstream or downstream of the gRNA cut site. Next, we used immunoblotting to evaluate any changes in cell signaling between UM-SCC-92 and the EGFR K/O cell lines. We observed that downstream activation of effectors such as AKT and ERK1/2 were still present in the EGFR K/O, despite the lack of EGFR (**Fig 4-11**). We

also saw an increase in FGFR1 protein expression in the EGFR K/O, corroborating the upregulated transcription of FGFR1, while we did not see any significant changes in either phospho or total MET protein.

While the parental UM-SCC-92 cell line is responsive to EGFR and FGFR inhibitors, UM-SCC-92 undergoes cell death only when treated with the combination and not the monotherapies. Given the upregulation of FGFR1 in the EGFR K/O cell line, we hypothesized that if FGFR signaling is compensating for the lack of EGFR, then FGFR inhibitors as a monotherapy should be able to cause cell death in the EGFR K/O cell line. Additionally, the EGFR K/O cell line should not respond to EGFR inhibition. To test this, we challenged the EGFR K/O cell line with the EGFR inhibitor gefitinib, multiple FGFR inhibitors, and a MET inhibitor. We postulated that if the EGFR K/O cell line relied specifically on FGF signaling as compensation, then the cell line should not undergo cell death by inhibiting MET. In our results, we saw no decrease in viability in the EGFR K/O cell line in response to EGFR inhibition or MET inhibition. However, when used as monotherapies, both pan-FGFR inhibitors BGJ398 and AZD4547 as well as the FGFR1 selective inhibitor PD173074 resulted in decreased viability in the EGFR K/O cell line (**Fig 4-12**).

We also wanted to further evaluate the response of the EGFR K/O cell line to the EGFR inhibitor gefitinib. As the EGFR inhibitor does not result in cell death in the wildtype cell line, we would not expect a decrease in viability in the EGFR K/O cell line regardless of EGFR expression. However, EGFR inhibition does result in decreased cell growth in UM-SCC-92, and so we analyzed cell growth of the EGFR K/O cell line after being challenged with the EGFR inhibitor. We observed that while UM-SCC-92 does see a decrease in cell growth with EGFR

inhibition, the EGFR K/O cell line does not (**Fig 4-13**) confirming that the EGFR K/O cell line does not respond to EGFR inhibition.

As our data nominated FGFR signaling as a robust compensatory pathway to EGFR inhibition, we hypothesized that the combination of EGFR and FGFR inhibition could be effective *in vivo*. As neither UM-SCC-92 nor UM-SCC-49 formed cell line xenograft models, we chose UM-SCC-108 to implant subcutaneously into the bilateral flanks of nude athymic mice. After establishing the cell line xenografts, we first wanted to determine that the EGFR inhibitor gefitinib and pan-FGFR inhibitor BGJ398 would affect cell signaling of the tumor. After dosing mice with vehicle, gefitinib, BGJ398, or the combination, we harvested tumors six hours post-treatment. We analyzed the protein content of the tumor by immunoblotting and observed decreased phosphorylation of EGFR and other downstream effectors in the mice receiving drug (**Fig 4-14**).

Given the success of the drugs to affect cell signaling of the tumors, we established additional xenograft models and monitored tumor size over the course of 21 days for each treatment. At the end of treatment, we observed no significant effect of the EGFR or FGFR inhibitor as a monotherapy. The tumor volumes in the mice receiving the combination of EGFR and FGFR inhibitors were significantly decreased in size as compared to the vehicle control and FGFR monotherapy (p-values ≤ 0.01), and EGFR monotherapy (p-value ≤ 0.05) (**Fig 4-15**). Additionally, at the end of treatment we visually observed that the tumors from the mice receiving the combination had less vascularization (**Fig 4-16**). To monitor for potential toxicity, we also measured the weight of the mice during the course of treatment. Towards the end of the treatment course, we did observe a dip in weight for mice in the combination arm while the mice receiving vehicle or monotherapy treatment gained weight (**Fig 4-17**).

To test the clinical relevance of FGFR as a compensatory mechanism to EGFR inhibition, through collaboration with Dr. Nyati we obtained tissue blocks from a recent clinical study of patients with locally advanced HNSCC that were treated with cetuximab for one week prior to moving on to a more complex clinical care regimen. Importantly, this study included biopsies that were taken before and after the single cetuximab treatment for each patient, creating a unique opportunity to study the molecular compensation mechanisms in human tumors. Thus, we performed comprehensive transcriptome sequencing on 14 formalin fixed paraffin embedded (FFPE) HNSCC tissue pairs and 4 FFPE normal tissues pre- and mid-cetuximab treatment.

Overall, we generated an average of 74,709,217 reads per sample of which an average of 71% uniquely mapped to the reference (**Table 4-3**). On average, we identified 19,913 genes per sample with an FPKM >1 indicating high quality RNAseq libraries. Thus, following FPKM analysis, we performed gene set enrichment analysis (GSEA) and network analysis to look for gene set concepts that were differentially regulated following cetuximab treatment in multiple tumors. Consistent with previous *in vitro* studies from our work and others, gene set concepts associated with PI3K/mTOR signaling, cell survival, cell cycle and angiogenesis were strongly upregulated in the tumors, supporting that the analysis defined relevant gene set concepts (**Fig 4-18**). Surprisingly, however, the data also showed a strong enrichment of gene sets associated with KRAS signaling. Comparison of gene sets identified in our UM-SCC-92 EGFR K/O model showed similar significant gene set enrichments, including KRAS signaling, epithelial to mesenchymal transition, and TNFalpha signaling through NFKB, supporting the postulate that KRAS adaption in HNSCC tumors occurs in tumor cells. GSEA outputs for the individual HNSCC tumors and EGFR K/O cell are in **Table 4-6, 4-7**. We then de-constructed the network analysis to look at changes in expression in the individual tumors, and we observed varying

responses per sample. Notably, HNSCC-10 exhibited marked decreases in expression for FGFR1, PIK3CA, and MAP3K8 while HNSCC-11 had marked increases in expression (**Fig 4-19**). HNSCC-3 had a specific marked increase in PI3KCA, while overall changes in FGFR1 and FGF3 expression varied per sample. Collectively, this analysis highlights the continued need to monitor individual samples during response to treatment.

Discussion

In HNSCC, monotherapies have been broadly ineffective. While inhibition of EGFR with cetuximab treatment has been effective, resistance and recurrence are still common. We investigated the hypothesis that there are signaling pathways compensating when EGFR is inhibited, and that co-targeting EGFR and this compensatory pathway will be more effective. In this chapter we present the results of investigating the FGF signaling pathway as a common compensatory mechanism to EGFR inhibition, where we expanded this finding to nominate >50% of cells lines having FGFR signaling as a compensatory response. Our results suggest that FGFR may be a more common compensatory mechanism than previously realized, and not limited to cases with *FGFR1* amplification.

Unfortunately, we were unable to find a biomarker that predicted which UM-SCC cell lines would respond and undergo cell death when challenged with the combination of EGFR and FGFR inhibitors. We expected that copy number amplifications or expression of the FGF receptors would identify models that may be reliant on FGF signaling in the absence of EGFR, such as the case for this combination in lung cancer (22, 23). Additionally, our interrogation of the downstream signaling pathways was unable to find a differential marker between cell lines that respond to the EGFR and FGFR combination and cell lines that do not. A more global look

in using elastic net analysis (34) to identify differential genetic mutations, copy number changes, or transcriptome markers between responsive and non-responsive models would be useful. However, for this global analysis to be robust, ideally hundreds of more lines would be tested to identify a biomarker of sensitivity or resistance (35), which was not possible for this thesis work. Instead, we did a preliminary investigation to identify compensatory pathways based on the response of a cell line to EGFR inhibition. As we had difficulty interrogating the activation of FGFRs by immunoblotting, we assessed transcript levels of FGFRs after EGFR inhibition. Our results were conflicting. We expected that responsive cell lines either would not change, suggesting that we could not use transcript expression of FGFRs to identify responsive models, or that both cell lines would see an increase in at least one of the FGF receptors. Further investigation is warranted to evaluate if response to EGFR inhibition, such as upregulating the FGFRs, may predict response to dual EGFR and FGFR inhibition. We then postulated that perhaps the short-term inhibition of EGFR by gefitinib made it difficult to observe any changes in FGFR signaling, and we hypothesized that long-term inhibition or complete loss of EGFR signaling might highlight the reliance on the compensatory pathway. Thus, we used CRISPR/Cas9 to successfully engineer an EGFR K/O cell line. This complete loss of EGFR expression led to an upregulation of FGFR1 expression and sensitivity to FGFR inhibition as a monotherapy, supporting the hypothesis that FGFR is a compensatory mechanism when EGFR is inhibited or completely lost.

Excitingly, our mouse model supports the translational potential of dual EGFR and FGFR inhibition. The tumors from mice receiving the combination arm were significantly smaller and containing less visible vasculature, potentially due to inhibiting FGFRs' role in vascularization (36). However, the weights of the mice receiving the combination treatment suggest possible

toxicity issues for this combination that were not observed in either monotherapy arm. Indeed, a clinical trial testing the combination of the EGFR inhibitor erlotinib and the pan-FGFR inhibitor dovitinib was halted early due to toxicity (37).

Of interest is the significant changes in KRAS signaling mid-cetuximab treatment for HNSCC patients. While genetic disruption of *KRAS* is a well-known driver of cetuximab-resistance in colorectal and other cancers (5, 38-40), compensatory KRAS signaling has not previously been described to play a significant role in HNSCC. This compensatory activation of KRAS signaling was supported in our EGFR K/O model, as the EGFR K/O model showed increased KRAS signaling but had no acquired or inherent Ras mutations. Importantly, the discovery of compensatory KRAS signaling is also consistent with our CRISPR genome and CRISPR kinome network analysis from chapter three that also identified KRAS-related gene knockouts as EGFR inhibitor sensitizers in HNSCC cell line. Thus, we believe that this is the first evidence that strongly indicates a role for KRAS signaling in cetuximab-response in HNSCC.

Acknowledgements

Thank you to Dr. Mukesh Nyati and lab for the collaboration on the patient samples pre- and mid-cetuximab treatment. Thank you to N. Michmerhuizen and S. Foltin on the resazurin cell viability assays. Thank you to N. Michmerhuizen, J. Wang, S. Nimmagadda, D. Genouw, and L. Remer for assistance in the immunoblotting results. Thank you to A. Birkeland for assistance in generating the EGFR K/O model, and thank you to B. Marinelli and Dr. A. Birkeland for assistance with mouse xenograft experiments. Thank you to A. Kulkarni for the bioinformatics analysis, and thank you to C. Brenner for the GSEA analysis. Thank you to J. Zhai and H. Jiang for statistical analysis.

Figures

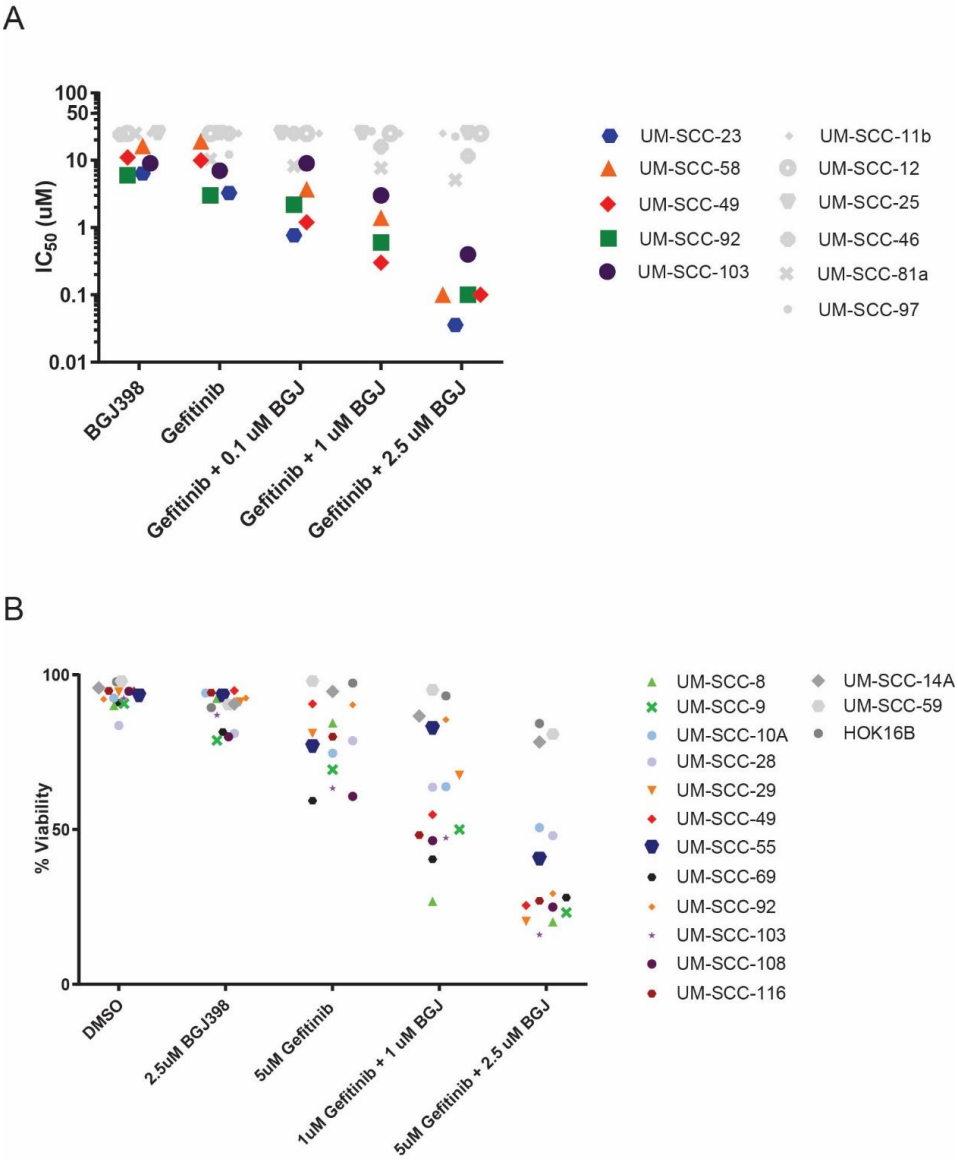

Figure 4-1. Cell line responses to EGFR and FGFR combination treatment

A) Each dot indicates an IC_{50} value for each drug listed on x-axis, for each cell line as indicated in the legend, plotted on a log-scale. Cell lines that respond to EGFR and FGFR combination treatment have decreased IC_{50} values in the presence of both inhibitors, and are highlighted by color. Cell lines that do not respond to the combination are greyed out. B) Each dot indicates a percent cell viability for each drug on the x-axis, for each cell line as indicated in the legend. Cell lines that respond to EGFR and FGFR combination treatment have decreased cell viability in the presence of both inhibitors, and are highlighted by color. Cell lines that do not respond to the combination are greyed out.

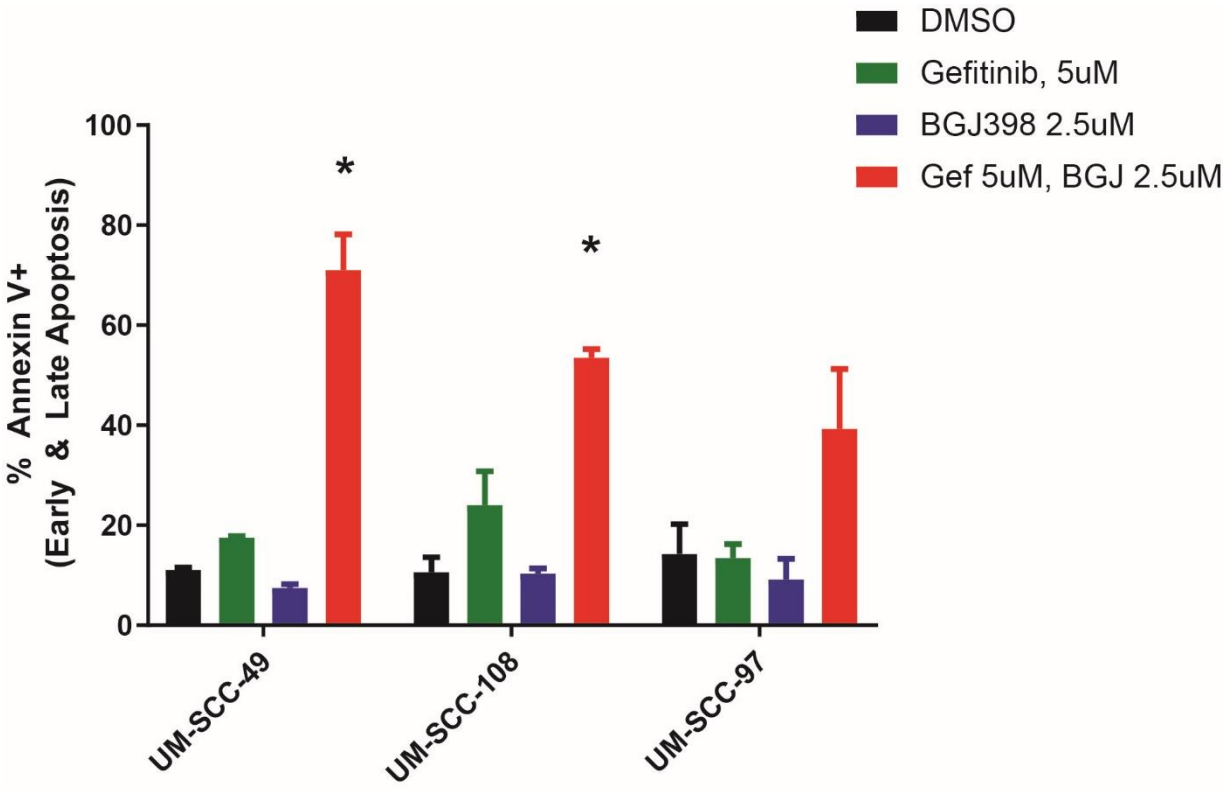

Figure 4-2. Cell death by annexin V+ staining

Graph represents the percentage of cells positive for annexin V staining, which is indicative of early or late state apoptosis. Cell lines were treated with DMSO (black), 5 μM gefitinib (green), 2.5 μM BGJ398 (blue), or the combination of 5 μM gefitinib and 2.5 μM BGJ398 (red). For UM-SCC-49 and UM-SCC-108, the combination treatment had significantly higher cell death than the DMSO or monotherapies, as tested by linear regression with interaction term.

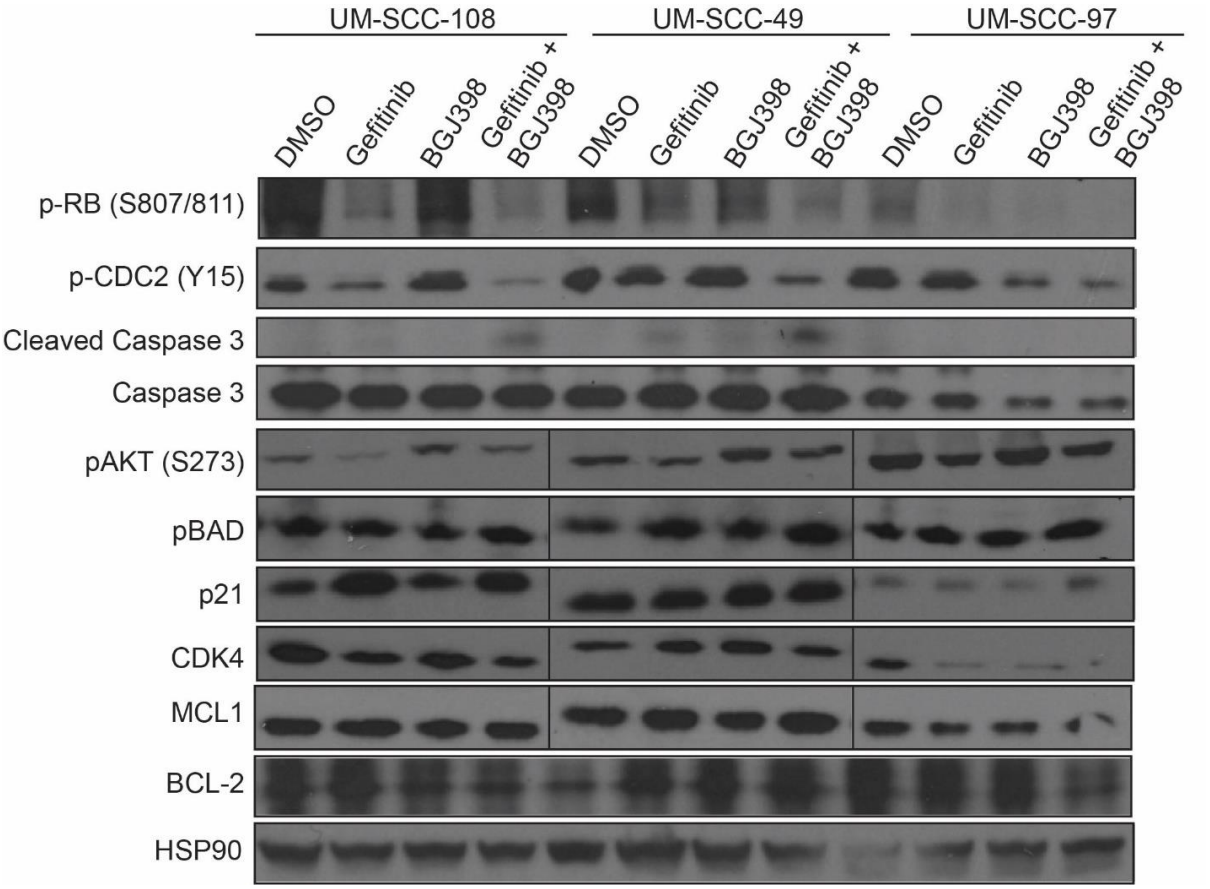

Figure 4-3. Immunoblot of UM-SCC lines, 24 hour post-treatment

UM-SCC cell lines were treated with 1 μM of each compound listed above with lysates harvested 24 hours after treatment.

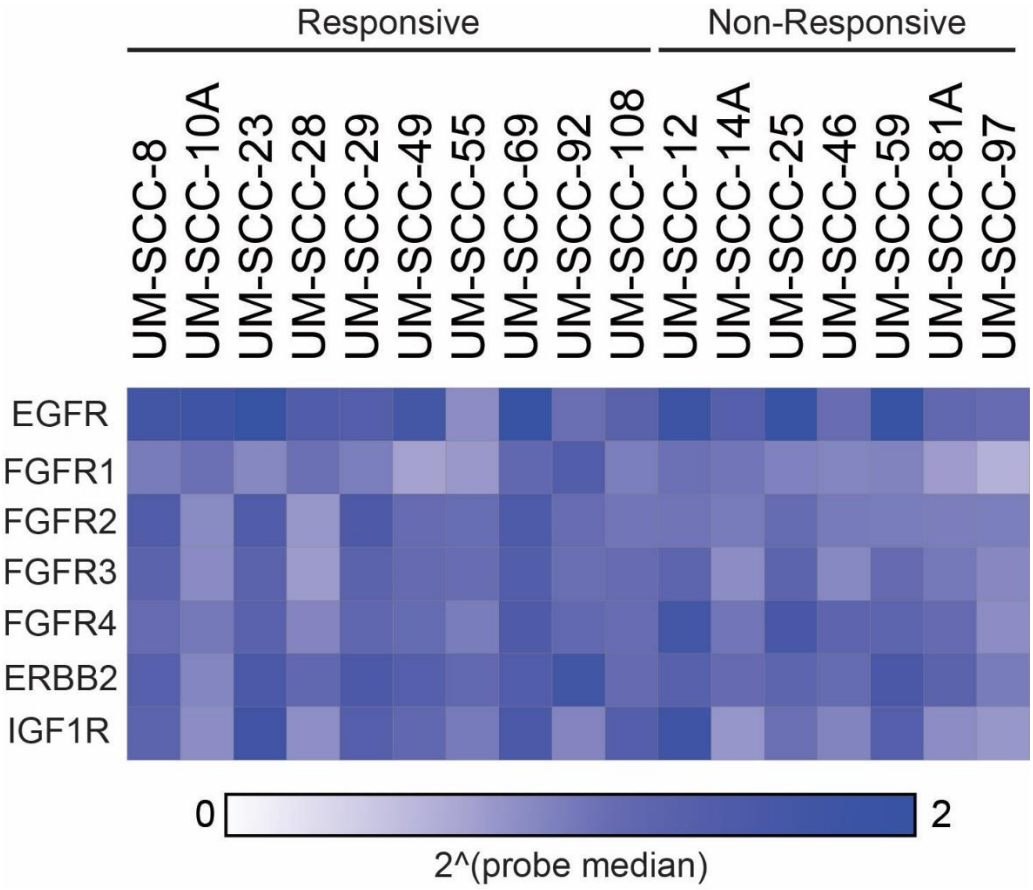

Figure 4-4. Copy number analysis of UM-SCC lines

Heatmap of relative copy number of genes as listed. Values plotted are two raised to the power of the probe median of the gene. Heatmap was generated using the Morpheus webtool available from Broad Institute (https://software.broadinstitute.org/morpheus).

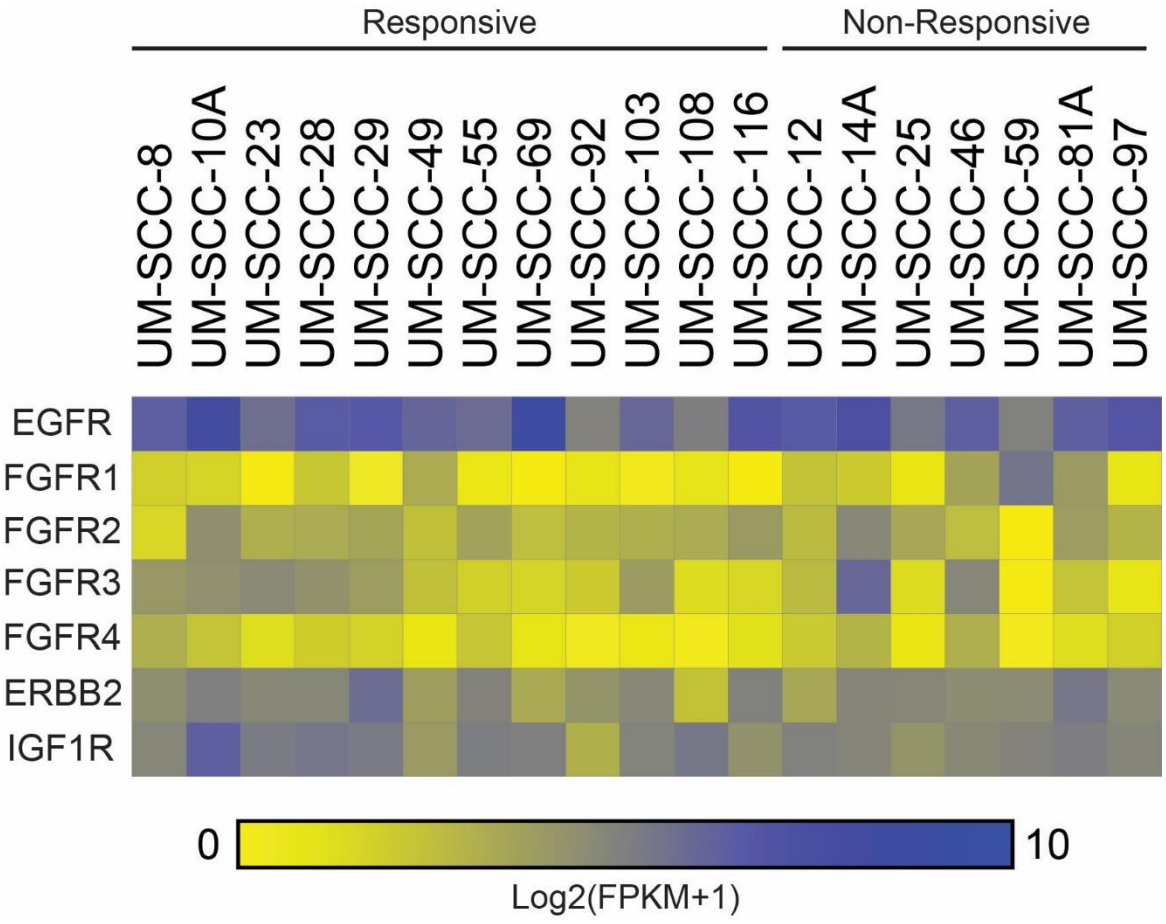

Figure 4-5. Expression analysis of UM-SCC lines

Heatmap depicting expression values of each gene listed, plotted as FPKM +1 on a log2 scale. Yellow indicates low expression, and blue indicates higher expression. Heatmap was generated using the Morpheus webtool available from Broad Institute (https://software.broadinstitute.org/morpheus).

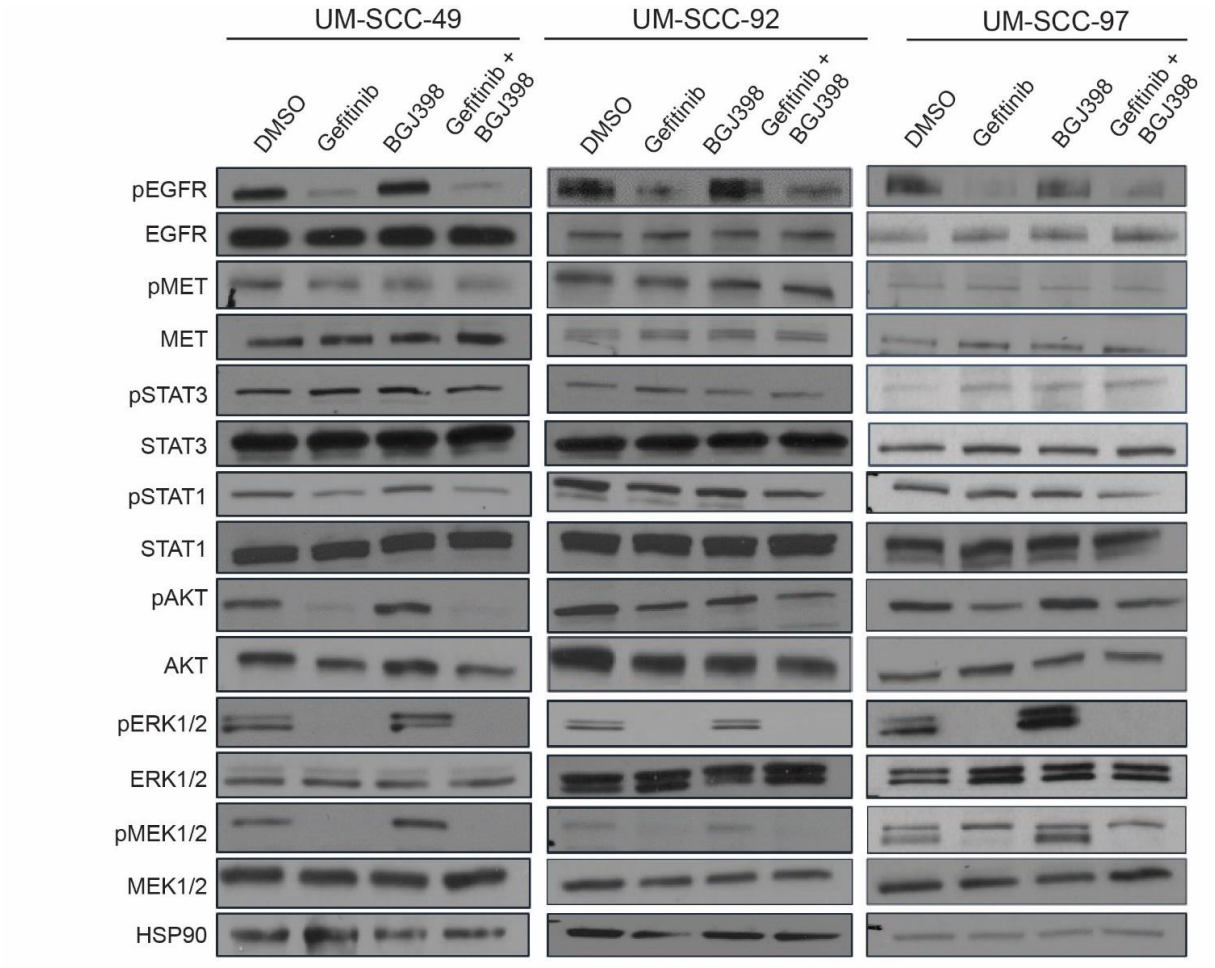

Figure 4-6. Immunoblot of UM-SCC cell lines, 1 hour post-treatment

UM-SCC cell lines were treated with 1 μM of each compound listed above with lysates harvested 1 hour after treatment.

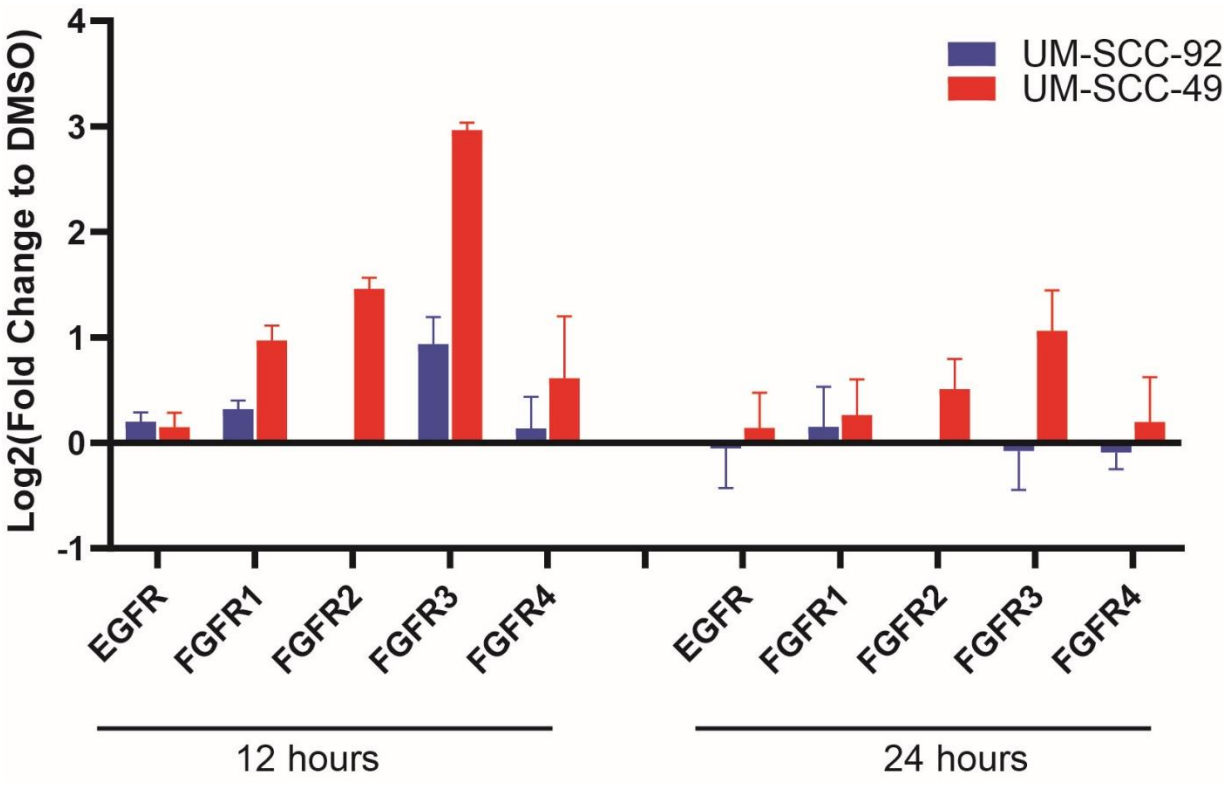

Figure 4-7. FGFR transcript analysis during EGFR inhibition

Graph plots the changes in transcript expression for each gene listed after treatment with 5 μM gefitinib. Values were determined by fold change to the DMSO vehicle control treatment. Lysates were collected and analyzed at 12 or 24 hours post-treatment with gefitinib for UM-SCC-92 (blue) and UM-SCC-49 (red). Note, FGFR2 transcript was undetectable for UM-SCC-92 in DMSO and gefitinib treatments at both timepoints.

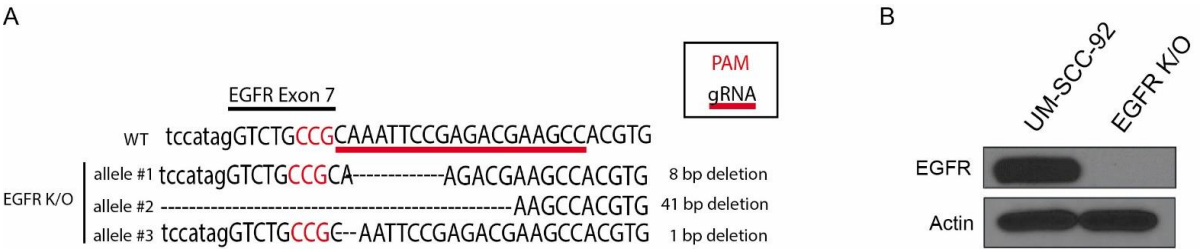

Figure 4-8. Genetic and protein confirmation of EGFR K/O cell line

A) Schematic of sanger sequencing results of the EGFR K/O cell line as compared to wildtype sequence. The gRNA targeted exon 7 of *EGFR* is underlined in red, and PAM sequence colored red. Three allelic deletions are depicted, with 8bp, 41bp, or 1bp deletion. B) Immunoblot of parental UM-SCC-92 cell line and EGFR K/O line evaluating EGFR protein expression and loading control.

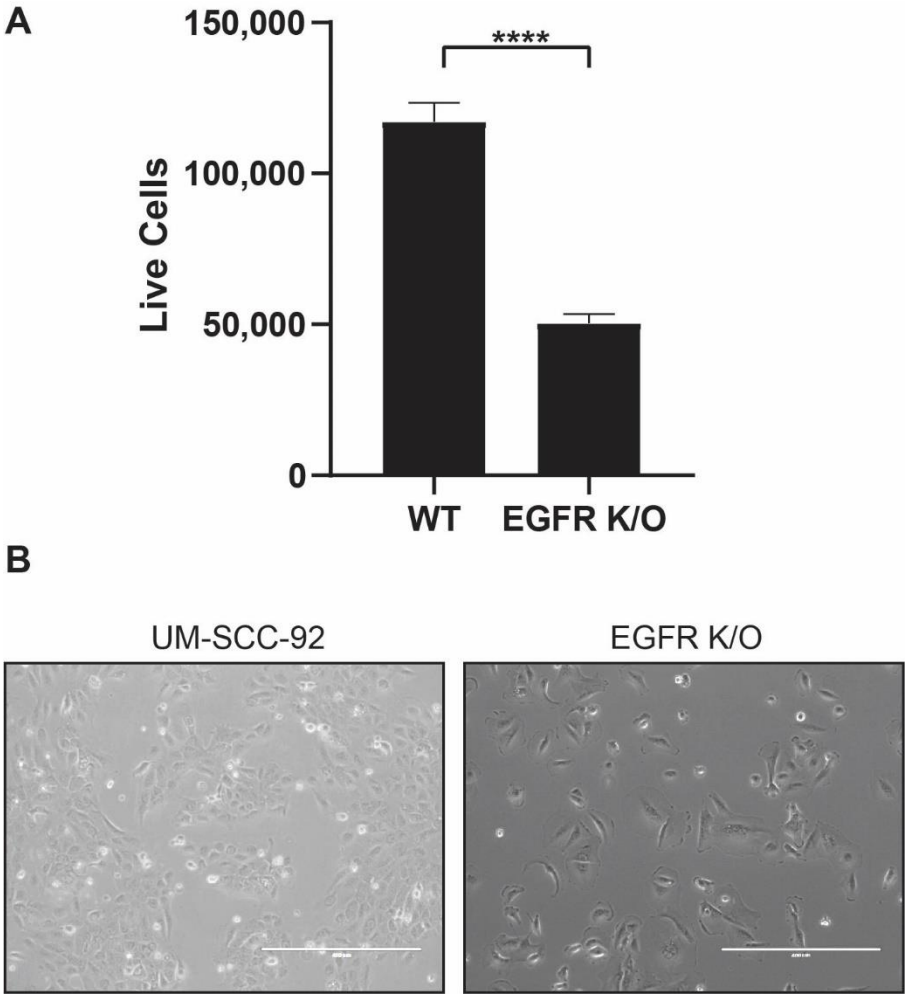

Figure 4-9. Phenotype of EGFR K/O cell line

A) Graph representative of number of lives cells after 4 day's growth. Cells were counted and seeded for 16,000 cells on day zero. Asteriscks depict a significant difference between UM-SCC-92 parental line (WT) and EGFR K/O (p-value ≤ 0.0001). B) Representative images taken at 40X on Nikon Eclipse TS100. Scale bar is shown.

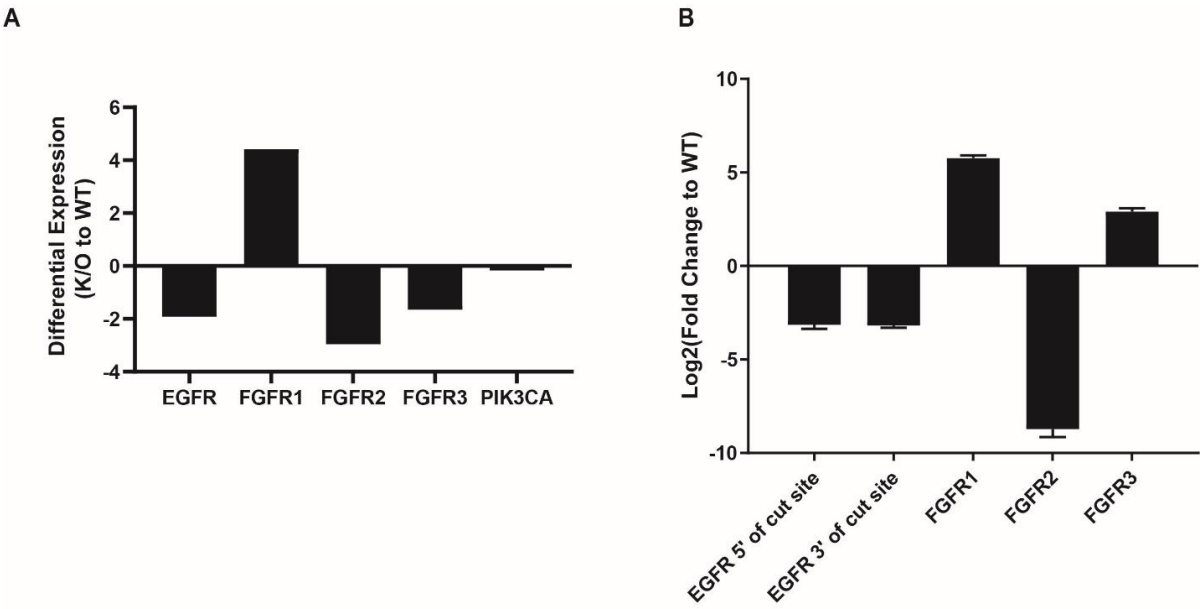

Figure 4-10. Transcript analysis of EGFR K/O compared to WT

A) Bar graph showing transcriptional changes in the EGFR K/O model. Value shown is differential expression in the EGFR K/O compared to UM-SCC-92 (WT) for EGFR, FGFRs 1-3, and PIK3CA. B) Bar graph showing qPCR confirmation of transcriptional changes in the EGFR K/O model. Value shown is the fold change of the EGFR K/O cell line as compared to UM-SCC-92 (WT) shown on a log2 scale. There were two primer sets used to evaluate EGFR transcription, targeted either upstream (5') or downstream (3') of the gRNA cut site.

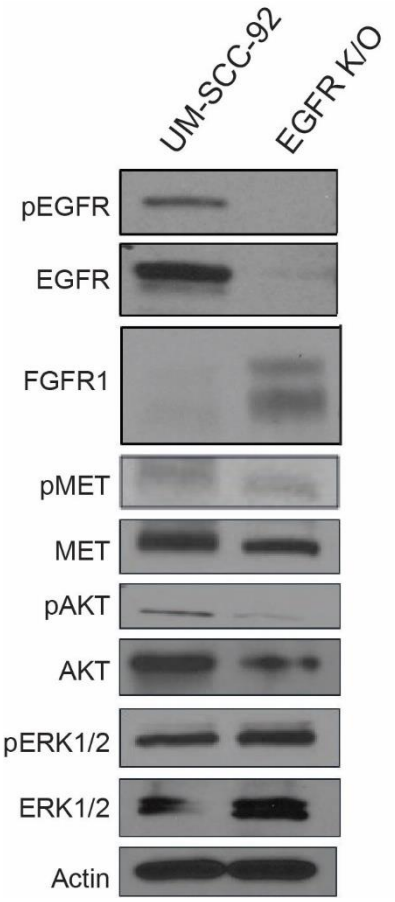

Figure 4-11. Signaling changes in EGFR K/O model by immunoblot

Lysates harvested during log-phase growth for UM-SCC-92 and EGFR K/O cell line and evaluated for protein expression by immunoblot.

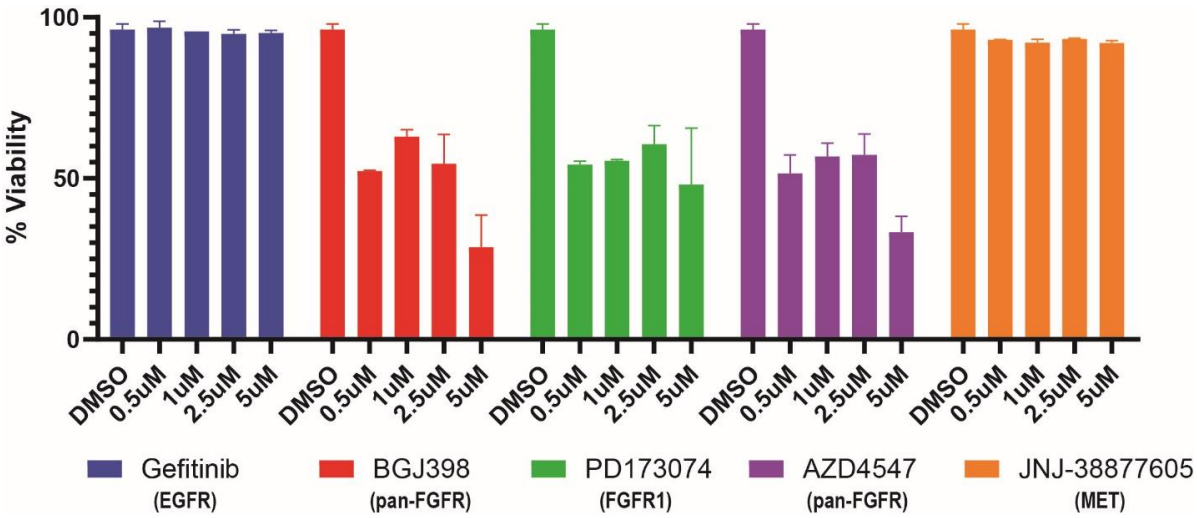

Figure 4-12. Response of EGFR K/O cell line to FGFR monotherapy

Cell viability of the EGFR K/O cell line after challenge with inhibitors, as tested by trypan blue assay. Inhibitors are the gefitinib (blue), BGJ398 (red), PD173074 (green), AZD4547 (purple), or JNJ-38877605 (orange).

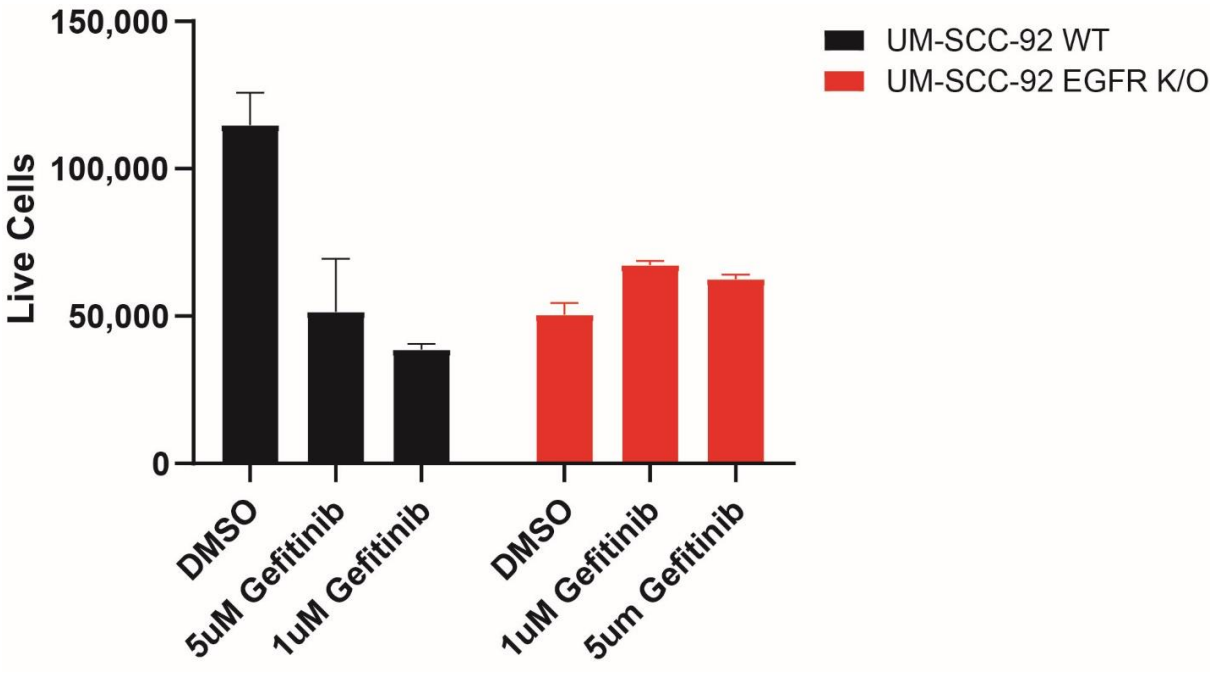

Figure 4-13. No response of EGFR K/O to EGFR inhibition

Graph of live cell counts after 3 days of treatment listed on x-axis for UM-SCC-92 (black) or EGFR K/O (red).

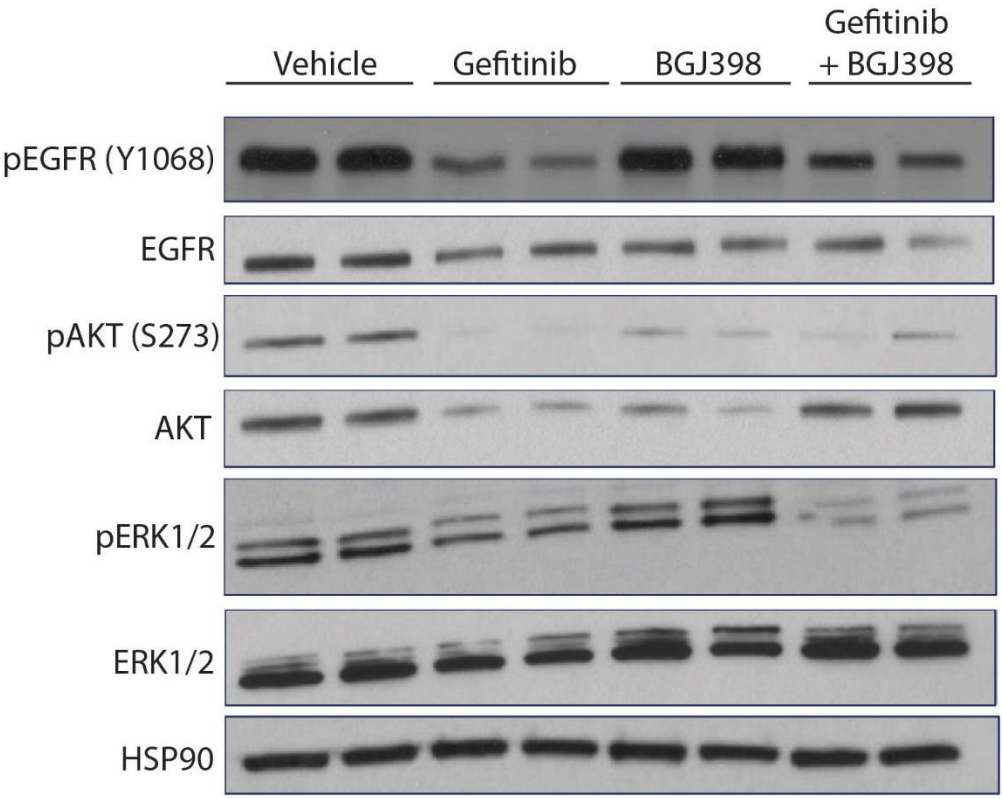

Figure 4-14. Cell signaling effects of inhibitors in mouse xenograft model

Western blot results of xenograft tumors that were harvested six hours after mice were dosed with vehicle, 150mg/kg gefitinib, 30mg/kg BGJ398, or 150mg/kg gefitinib and 30mg/kg BGJ398. Effects on phosphorylated EGFR and other downstream effectors are shown.

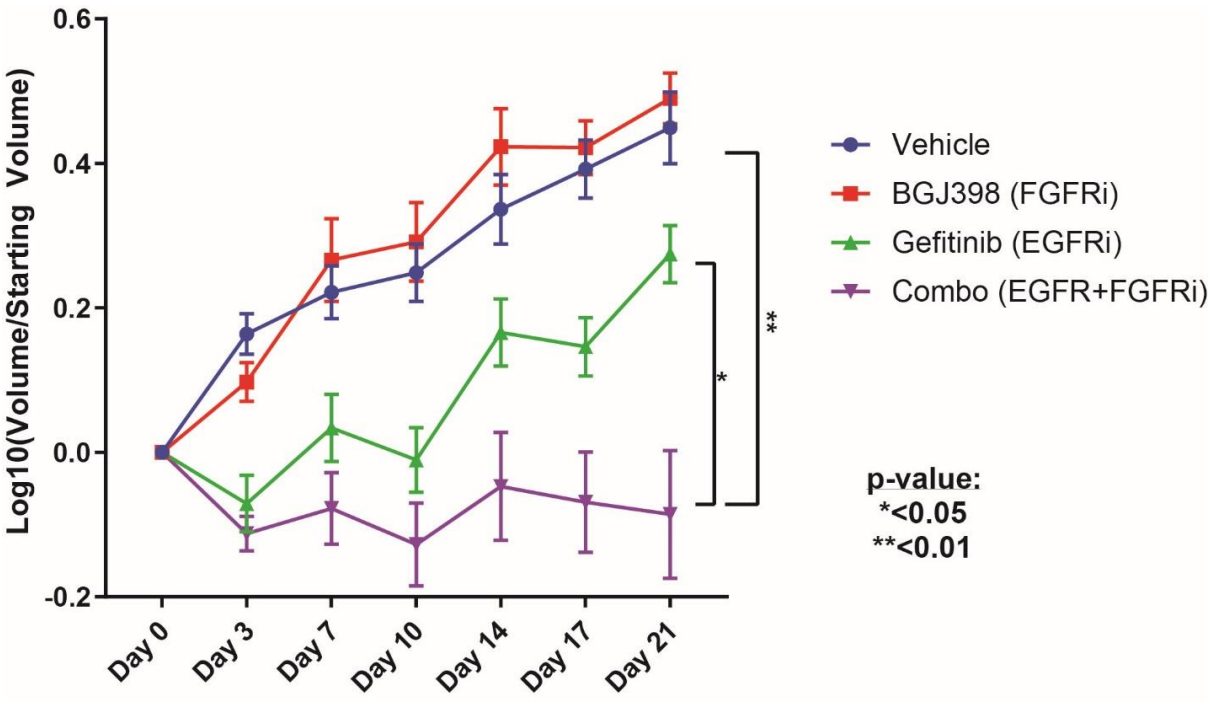

Figure 4-15. Tumor volumes of mouse xenografts

Tumor volumes were normalized to starting tumor growth on Day 0 of treatment, and then put on a log-scale go accommodate the linear mixed model that was used to analyze significance. Data points represent average tumor volume of the cohort, while the bars represent standard error. Significance is indicated.

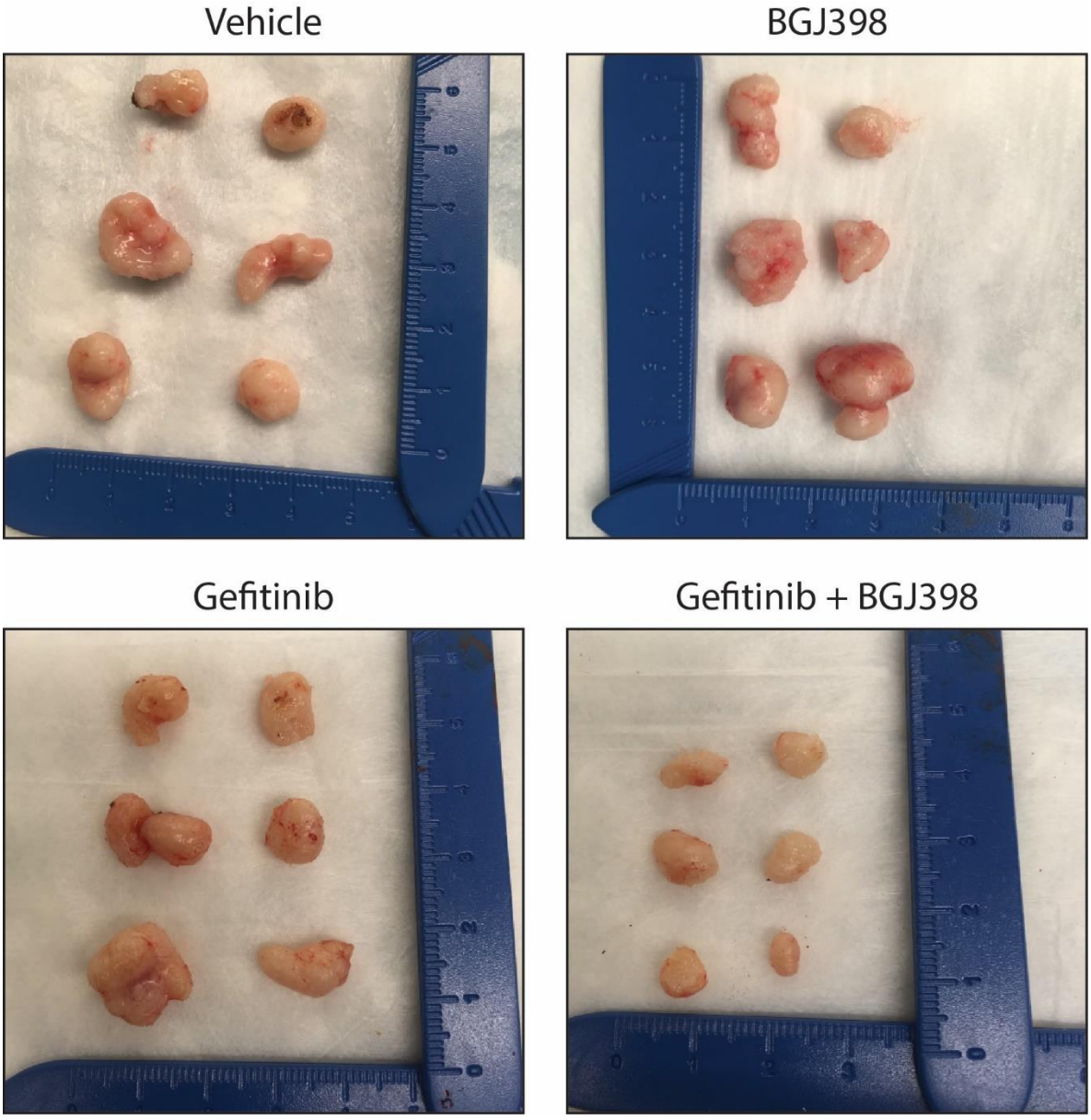

Figure 4-16. Representative pictures of mouse xenograft tumors harvested at 21 days

Images were taken of six tumors from each cohort as indicated, with ruler shown for scale. Tumors were harvested at the end of 21-day treatment.

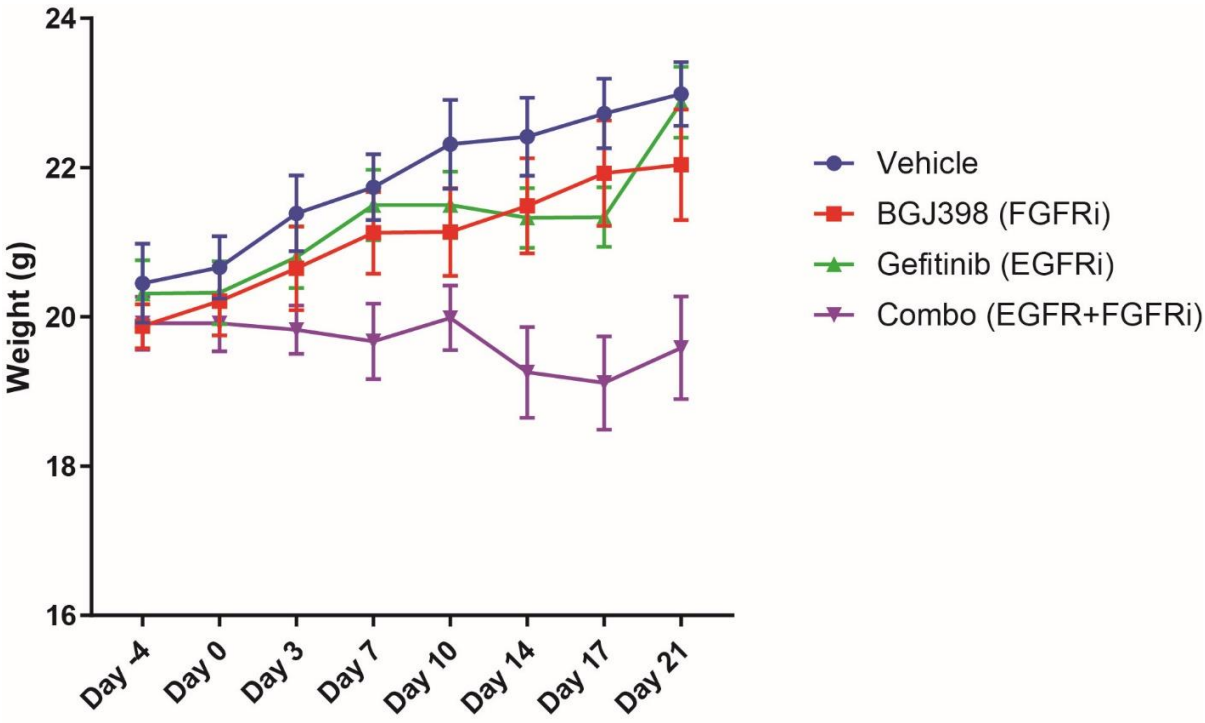

Figure 4-17. Mouse weights during xenograft experiment

The average weight of the cohort is plotted over the course of treatment, while bars indicate standard error. Treatments are indicated by the color in the legend.

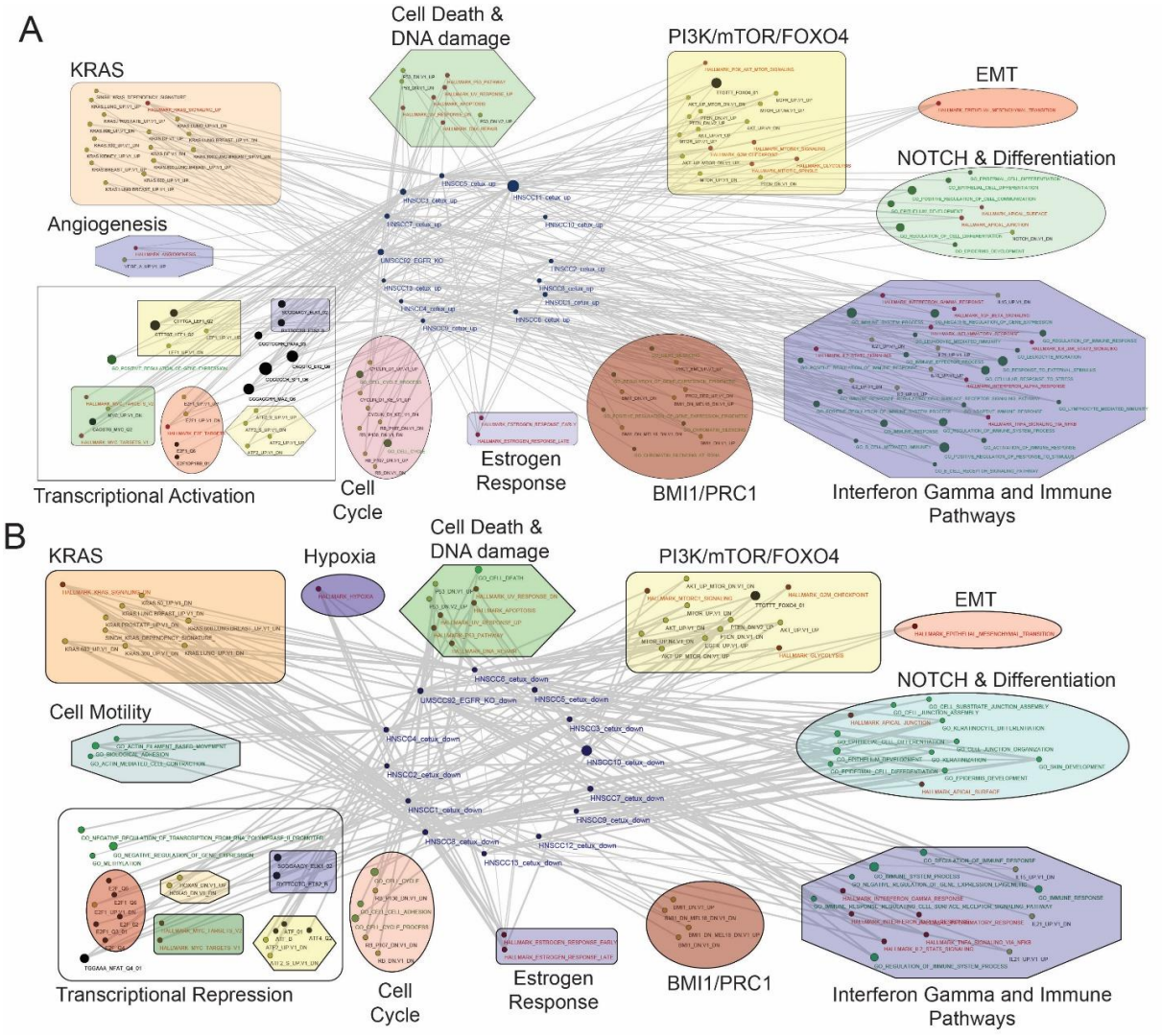

Figure 4-18. Gene set enrichment analysis of 13 HNSCC tumors treated with cetuximab and EGFR K/O cell line

Cytoscape network plot shows significant enrichments of gene sets significantly upregulated (**A**) or downregulated (**B**) following cetuximab treatment in each of the 13 HNSCC tumors as well as the genes upregulated in UM-SCC-92_EGFR knockout compared to control (each gene set is represented by labeled blue circular nodes in the center of the plot) with annotated gene sets downloaded from the molecular signatures data bases v5.1 (red nodes = "Hallmark" gene sets, black nodes = "Motif" gene sets, green nodes = "Go-biological process" gene sets and yellow nodes = "Oncogene" gene sets). The size of each node is proportional to the number of genes in the gene set. Lines connecting each node are proportional to the significance of overlap between the gene sets, determined by false discovery rate (FDR), with more significant interactions represented by thicker edge weights. All interactions shown have FDR < 0.05. Recurrent and selected concepts are grouped within the transparent geometric shapes to highlight network concepts identified by the analysis.

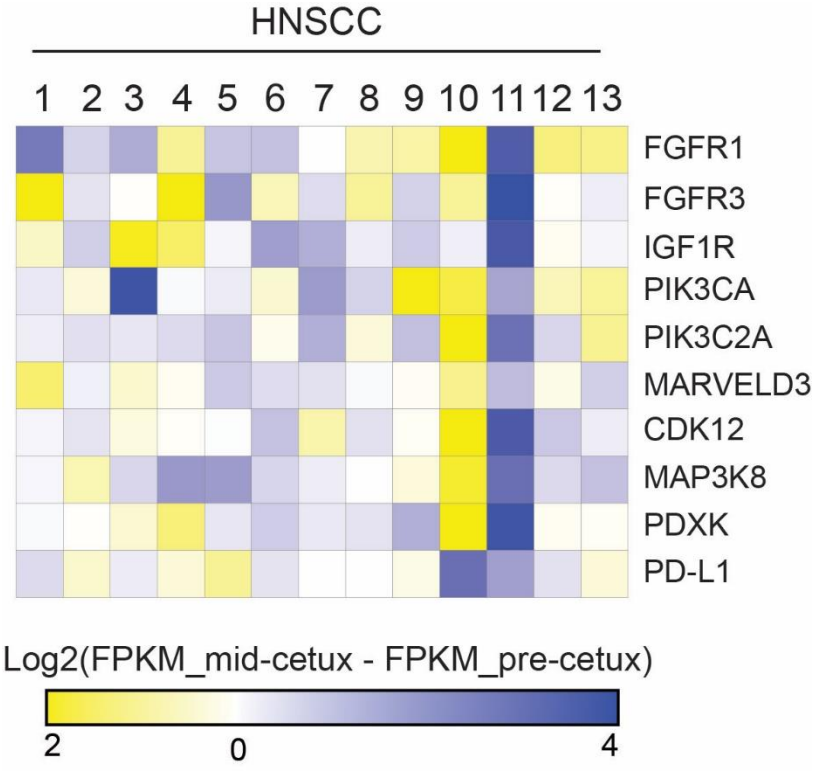

Figure 4-19. Heatmap of expression changes in cetuximab-treated samples

Heatmap shows the changes in expression mid-cetuximab treatment, where blue indicates an increase in expression and yellow indicates a decrease. Values were calculated by subtracting the pre-cetuximab treatment FPKM value from the mid-cetuximab treatment and plotted on a log2 scale, using the Morpheus webtool available from Broad Institute (https://software.broadinstitute.org/morpheus).

Tables

Antibody	Catalog #
p-EGFR Y1068	CST 3777
EGFR	CST 8504
p-AKT	CST 4060
AKT	CST 4685
p-ERK1/2 T202/Y204	CST4370
ERK1/2	CST 4695
p-MEK 1/2	CST 9121
MEK 1/2	CST 8727
HSP90	CST 4877
BCL 2	CST 4223
Cleaved Caspase 3	CST 9664
Total Caspase 3	CST 9665
CDK4	CST 12790
p21	CST 2947
p-CDC2 Y15	CST 4539
pBAD S136	CST 4366
pRb S807/811	CST 8516
MCL1	CST 5453
STAT1	CST 14994
pSTAT1	CST 8826
MET	CST 8198
pMET (Tyr1234/1235)	CST 3077
pSTAT3	CST p145
STAT3	CST 30835
FGFR1	CST 9740
Actin	CST 4970
Anti-Rabbit Secondary	Jackson Research 111-035-045
Anti-Mouse Secondary	Jackson Research 715-035-151

Table 4-1. Antibodies used for immunoblotting

Gene	Direction	Sequence (5'-3')
EGFR	Fwd	TGTGCCCACTACATTGACGG
	Rev	CGGGATCTTAGGCCCATTCG
FGFR1	Fwd	AAAGGAGGATCGAGCTCACTG
	Rev	CCAGGGCTGGGCTTGTTCA
FGFR2	Fwd	TTGCCCAGTGTCAGCTTATCT
	Rev	AACAGTTTCGGCTGAGTCCA
FGFR3	Fwd	GCGCTAACACCACCGACA
	Rev	AGCTCCTCTCGGCTGG
HPRT	Fwd	AGATGGTCAAGGTCGCAAGC
	Rev	ATGACACAAACATGATTCAAATCCC
RPL19	Fwd	AAATCGCCAATGCCAACTCC
	Rev	CCGCTTACCTATGCCCATGT
ACTIN	Fwd	GCCGCCAGCTCACCAT
	Rev	AATCCTTCTGACCCATGCCC
EGFR 5' of gRNA cut site, qPCR	Fwd	AGTTTGCCAAGGCACGAGTA
	Rev	CCACCTCCTGGATGGTCTTTA
EGFR 3' of gRNA cut site, qPCR	Fwd	TGTGCCCACTACATTGACGG
	Rev	CGGGATCTTAGGCCCATTCG
EGFR, genomic region of gRNA	Fwd	GGCTTTCTGACGGGAGTCAA
	Rev	CTGTATTTGCCCTCGGGGTT

Table 4-2. Primers used for qPCR and genomic amplification

Sample	Total Reads	% Uniquely Mapped	Non-Zero FPKMs
HNSCC1_PreCetux	59,437,572	74.8	18,570
HNSCC1_MidCetux	70,180,145	73.8	23,233
HNSCC2_PreCetux	73,637,010	76.2	22,027
HNSCC2_MidCetux	85,593,958	74.3	23,081
HNSCC3_PreCetux	67,433,628	69.3	15,188
HNSCC4_MidCetux	69,187,588	70.1	16,006
HNSCC4_PreCetux	60,105,607	70	22,357
HNSCC4_MidCetux	66,802,892	78.3	22,619
HNSCC5_PreCetux	102,630,698	77.5	18,356
HNSCC5_MidCetux	67,844,060	69.4	18,351
HNSCC6_PreCetux	80,559,807	73.9	19,920
HNSCC6_MidCetux	62,010,165	78.1	20,359
HNSCC7_PreCetux	92,414,717	70.2	15,500
HNSCC7_MidCetux	69,861,669	65.9	16,081
HNSCC8_PreCetux	82,439,705	72.8	25,287
HNSCC8_MidCetux	108,845,855	67.3	27,069
HNSCC9_PreCetux	61,249,773	72.7	19,526
HNSCC9_MidCetux	62,636,343	76.1	23,890
HNSCC10_PreCetux	85,138,732	60.3	19,236
HNSCC10_MidCetux	62,163,895	56.6	10,527
HNSCC11_PreCetux	73,325,291	62.6	8,029
HNSCC11_MidCetux	74,545,093	67.5	19,522
HNSCC12_PreCetux	83,414,271	69.6	21,841
HNSCC12_MidCetux	57,730,761	74.2	18,024
HNSCC13_PreCetux	90,893,707	63.9	21,667
HNSCC13_MidCetux	74,441,825	78.5	25,184

Table 4-3. Sequencing statistics for samples from patients receiving cetuximab

Total reads generated by RNAseq per sample, with percent of reads uniquely mapped shown. Non-zero FPKMs is the number of transcripts with > 0 value, indicative of diversity.

	Gene Name	Chr:Pos	Ref/Alt
Stop Gain	NT5C1B-RDH14,NT5C1B	2:18765924	G/C
	ZNF804A	2:185801336	G/T
	FAM71B	5:156589997	C/A
	CNGB3	8:87683195	G/T
	SERPINA11	14:94914990	G/T
Splice Variant	SORCS2	4:7706012	G/C
	SLIT2	4:20259487	T/C
	PRKG2	4:82027093	G/A
	FBXW7	4:153271186	A/C
	FLNC	7:128483013	C/A
UTR Variant	C1orf158	1:12806253	C/G
	PAFAH2	1:26288379	G/T
	LRP8	1:53711735	G/C
	KCNA2	1:111136289	T/C
	LAD1	1:201350285	G/A
	EPAS1	2:46612626	C/G
	CCDC88A	2:55517271	T/C
	CTNNA2,LRRTM1	2:80529217	T/C
	SI	3:164697131	C/T
	KCNMB3	3:178984521	G/A
	TMPRSS11A	4:68776852	A/T
	SMAP1,B3GAT2	6:71571694	T/A
	VOPP1	7:55540132	G/A
	GRM8	7:126078821	G/A
	LZTS1	8:20106576	C/A
	MAK16,TTI2	8:33358270	G/A
	CLVS1	8:62212374	G/T
	IL33	9:6257454	T/C
	GKAP1	9:86421470	T/C
	DFNB31	9:117164510	G/A
	PRKG1	10:54053983	T/G
	NPAP1	15:24927196	G/T
	FAM174B	15:93162549	G/A
	HSPB6	19:36246418	C/G
	TMEM230	20:5093724	C/A
	MAP7D2	X:20025422	A/C
	TAB3	X:30846292	C/T
	USP27X	X:49646487	A/C
Missense	HTATSF1	X:135593004	G/A
	HCFC1	X:153217337	T/A
	HCFC1	X:153222905	G/A
	SERPINB13	18:61264276	G/T
	FLJ22184	19:7935863	G/T
	APOC1	19:45419485	G/C
	LIG1	19:48637261	G/A

	Gene Name	Chr:Pos	Ref/Alt
Missense	ZSCAN20	1:33957209	G/T
	LOC100288142	1:148312431	A/G
	NUP210L	1:154061969	C/T
	EFNA1	1:155103912	A/T
	DNAH14	1:225586277	C/A
	SLC30A3	2:27480837	C/T
	HOXD9	2:176988779	G/T
	DNAH7	2:196801403	T/G
	VWC2L	2:215301391	T/A
	COL4A4	2:227942723	C/T
	LTF	3:46480969	T/A
	ACAD11	3:132294638	A/G
	MUC4	3:195506747	C/T
	MUC4	3:195506750	G/C
	GABRA1	5:161317947	G/T
	AKAP9	7:91730186	T/G
	CFTR	7:117232191	G/C
	KIAA1967	8:22464533	A/G
	CCDC171	9:15784553	A/C
	SURF6	9:136198772	C/G
	DBH	9:136523451	T/A
	KIF20B	10:91492669	G/A
	PDE3B	11:14665679	G/A
	PDE3B	11:14665680	C/T
	FAT3	11:92257971	C/A
	PUS7L	12:44139903	T/C
	KRT75	12:52818456	C/T
	FAM222A	12:110207009	G/T
	GOLGA3	12:133360800	T/C
	TPP2	13:103326642	C/G
	TDRD9	14:104498355	C/A
	ADAMTS7	15:79059746	G/T
	WDR90	16:699835	G/A
	MMP2	16:55522595	C/T
	CNOT1	16:58568254	A/T
	NF1	17:29652938	A/G
	KANSL1	17:44110456	G/A
	PRR11	17:57270962	C/T
	ZNF665	19:53668122	G/T
	ZNF837	19:58880235	G/T
	ID1	20:30193215	G/A
	DGCR2	22:19076897	G/C
	SSX2	X:52734778	C/A
	SSX2B	X:52781779	G/T

Table 4-4. Non-synonymous mutations in EGFR K/O cell line

Non-synonymous mutations found in the EGFR K/O cell line that are not present in UM-SCC-92 parental cell line, categorized by effect of mutation.

Rank	Gene	FPKM_WT	FPKM_K/O	DE
1	PGK1	0	312.318	8.29
2	NCOA4	0	108.671	6.78
3	CSNK2B	0	88.6994	6.49
4	IRAK1	0	80.1222	6.34
5	CDK7	0	51.4813	5.71
6	PPIP5K2	0	37.4859	5.27
7	CDK16	0	29.5537	4.93
8	**FGFR1**	**1.57785**	**54.1979**	**4.42**
9	TK2	0	19.0733	4.33
10	IFNGR2	0	18.915	4.32
11	MAPKAPK2	0	14.9457	4
12	LIMK1	0	13.4991	3.86
13	FYN	2.88515	47.403	3.64
14	RXRB	0	11.0631	3.59
15	GPR107	0	9.72812	3.42
16	DCLK1	0.305365	12.8606	3.41
17	TNIK	0.467579	14.2765	3.38
18	DDR1	0	8.84388	3.3
19	AGK	0	8.45822	3.24
20	TLR4	0.0960775	8.6858	3.14
21	ALPK2	0.214953	9.39677	3.1
22	DYRK3	0	7.35272	3.06
23	STK19	0	7.18523	3.03

Table 4-5. Kinases and receptors upregulated in the EGFR K/O cell line

Table of kinases and receptors that are upregulated in the EGFR K/O cell line as compared to wildtype, with a differential expression of at least three. Genes are ranked by upregulation, and show the FPKM of UM-SCC-92 (FPKM_WT), FPKM in the EGFR K/O (FPKM_K/O), and differential expression (DE).

Node	Node Size	Gene Set Name	# Genes in Gene Set (K)	FDR q-value
HNSCC1_cetux_up	337	HALLMARK_MYOGENESIS	200	1.68E-16
HNSCC1_cetux_up	337	HALLMARK_ESTROGEN_RESPONSE_LATE	200	9.10E-08
HNSCC1_cetux_up	337	HALLMARK_ESTROGEN_RESPONSE_EARLY	200	5.91E-07
HNSCC1_cetux_up	337	HALLMARK_KRAS_SIGNALING_UP	200	3.23E-05
HNSCC1_cetux_up	337	HALLMARK_COAGULATION	138	7.64E-04
HNSCC1_cetux_up	337	HALLMARK_HYPOXIA	200	8.96E-04
HNSCC1_cetux_up	337	HALLMARK_XENOBIOTIC_METABOLISM	200	8.96E-04
HNSCC1_cetux_up	337	HALLMARK_COMPLEMENT	200	4.07E-03
HNSCC1_cetux_up	337	HALLMARK_EPITHELIAL_MESENCHYMAL_TRANSITION	200	4.07E-03
HNSCC1_cetux_up	337	HALLMARK_ANDROGEN_RESPONSE	101	4.59E-03
HNSCC1_cetux_up	337	HALLMARK_FATTY_ACID_METABOLISM	158	5.22E-03
HNSCC1_cetux_up	337	TGCCAAR_NF1_Q6	722	1.10E-07
HNSCC1_cetux_up	337	TTGTTT_FOXO4_01	2061	1.10E-07
HNSCC1_cetux_up	337	CAGGTG_E12_Q6	2485	2.82E-07
HNSCC1_cetux_up	337	TATAAA_TATA_01	1296	6.18E-07
HNSCC1_cetux_up	337	CAGCTG_AP4_Q5	1524	1.92E-06
HNSCC1_cetux_up	337	SOX9_B1	237	3.14E-06
HNSCC1_cetux_up	337	MEF2_03	238	3.14E-06
HNSCC1_cetux_up	337	GCANCTGNY_MYOD_Q6	924	3.14E-06
HNSCC1_cetux_up	337	TGACCTY_ERR1_Q2	1043	7.37E-06
HNSCC1_cetux_up	337	GGGAGGRR_MAZ_Q6	2274	1.03E-05
HNSCC1_cetux_up	337	WTGAAAT_UNKNOWN	616	1.52E-05
HNSCC1_cetux_up	337	CAGGTA_AREB6_01	792	3.70E-05
HNSCC1_cetux_up	337	CTAWWWATA_RSRFC4_Q2	361	3.70E-05
HNSCC1_cetux_up	337	TGGAAA_NFAT_Q4_01	1896	3.88E-05
HNSCC1_cetux_up	337	TGATTTRY_GFI1_01	294	1.22E-04
HNSCC1_cetux_up	337	FOXO3_01	245	1.22E-04
HNSCC1_cetux_up	337	TFIIA_Q6	251	1.44E-04
HNSCC1_cetux_up	337	OCT1_05	254	1.50E-04
HNSCC1_cetux_up	337	SRY_02	255	1.50E-04
HNSCC1_cetux_up	337	GGGTGGRR_PAX4_03	1294	1.83E-04
HNSCC1_cetux_up	337	GO_COMPLEMENT_ACTIVATION	76	3.02E-29
HNSCC1_cetux_up	337	GO_HUMORAL_IMMUNE_RESPONSE_MEDIATED_BY_CIRCULATING_IMMUNOGLOBULIN	69	7.33E-29
HNSCC1_cetux_up	337	GO_PROTEIN_ACTIVATION_CASCADE	99	2.87E-28
HNSCC1_cetux_up	337	GO_HUMORAL_IMMUNE_RESPONSE	187	1.26E-26
HNSCC1_cetux_up	337	GO_B_CELL_MEDIATED_IMMUNITY	99	3.83E-25
HNSCC1_cetux_up	337	GO_PHAGOCYTOSIS_RECOGNITION	34	7.07E-23
HNSCC1_cetux_up	337	GO_LYMPHOCYTE_MEDIATED_IMMUNITY	147	4.63E-21
HNSCC1_cetux_up	337	GO_ADAPTIVE_IMMUNE_RESPONSE_BASED_ON_SOMATIC_RECOMBINATION_OF_IMMUNE_RECEPTORS_BUILT_FROM_IMMUNOGLOBULIN_SUPERFAMILY_DOMAINS	154	1.23E-20
HNSCC1_cetux_up	337	GO_LEUKOCYTE_MEDIATED_IMMUNITY	189	6.42E-20
HNSCC1_cetux_up	337	GO_REGULATION_OF_IMMUNE_SYSTEM_PROCESS	1403	2.09E-18
HNSCC1_cetux_up	337	GO_PHAGOCYTOSIS_ENGULFMENT	38	3.30E-18
HNSCC1_cetux_up	337	GO_DEFENSE_RESPONSE_TO_BACTERIUM	237	1.10E-17
HNSCC1_cetux_up	337	GO_REGULATION_OF_IMMUNE_RESPONSE	858	5.24E-17
HNSCC1_cetux_up	337	GO_DEFENSE_RESPONSE	1231	5.24E-17
HNSCC1_cetux_up	337	GO_ACTIVATION_OF_IMMUNE_RESPONSE	427	6.54E-17
HNSCC1_cetux_up	337	GO_MEMBRANE_INVAGINATION	48	1.06E-16
HNSCC1_cetux_up	337	GO_IMMUNE_RESPONSE	1100	1.40E-16
HNSCC1_cetux_up	337	GO_PHAGOCYTOSIS	190	2.83E-16
HNSCC1_cetux_up	337	GO_POSITIVE_REGULATION_OF_IMMUNE_SYSTEM_PROCESS	867	3.76E-16
HNSCC1_cetux_up	337	GO_B_CELL_RECEPTOR_SIGNALING_PATHWAY	54	5.48E-16
HNSCC1_cetux_up	337	BMI1_DN_MEL18_DN.V1_DN	147	1.34E-08
HNSCC1_cetux_up	337	ATF2_UP.V1_DN	187	1.34E-08
HNSCC1_cetux_up	337	MEL18_DN.V1_DN	148	9.23E-07
HNSCC1_cetux_up	337	ATF2_S_UP.V1_DN	187	7.64E-06
HNSCC1_cetux_up	337	BMI1_DN.V1_DN	144	4.97E-05
HNSCC1_cetux_up	337	P53_DN.V1_UP	194	6.19E-05

HNSCC1_cetux_up	337	AKT_UP_MTOR_DN.V1_DN	183	2.53E-04
HNSCC1_cetux_up	337	PTEN_DN.V1_UP	191	3.12E-04
HNSCC1_cetux_up	337	PKCA_DN.V1_UP	170	8.45E-04
HNSCC1_cetux_up	337	SNF5_DN.V1_UP	177	9.84E-04
HNSCC1_cetux_up	337	KRAS.600.LUNG.BREAST_UP.V1_DN	289	9.84E-04
HNSCC1_cetux_up	337	ESC_J1_UP_EARLY.V1_UP	183	9.84E-04
HNSCC1_cetux_up	337	MTOR_UP.V1_DN	184	9.84E-04
HNSCC1_cetux_up	337	AKT_UP.V1_DN	187	9.84E-04
HNSCC1_cetux_up	337	IL15_UP.V1_DN	190	9.84E-04
HNSCC1_cetux_up	337	PRC1_BMI_UP.V1_UP	192	9.84E-04
HNSCC1_cetux_up	337	E2F1_UP.V1_DN	193	9.84E-04
HNSCC1_cetux_up	337	CAHOY_ASTROGLIAL	100	9.84E-04
HNSCC1_cetux_up	337	KRAS.KIDNEY_UP.V1_UP	145	9.84E-04
HNSCC1_cetux_up	337	KRAS.LUNG.BREAST_UP.V1_DN	145	9.84E-04
HNSCC2_cetux_up	152	HALLMARK_INTERFERON_ALPHA_RESPONSE	97	1.89E-06
HNSCC2_cetux_up	152	HALLMARK_E2F_TARGETS	200	1.26E-04
HNSCC2_cetux_up	152	HALLMARK_INTERFERON_GAMMA_RESPONSE	200	9.61E-04
HNSCC2_cetux_up	152	HALLMARK_G2M_CHECKPOINT	200	7.00E-03
HNSCC2_cetux_up	152	HALLMARK_KRAS_SIGNALING_DN	200	3.61E-02
HNSCC2_cetux_up	152	HALLMARK_ANDROGEN_RESPONSE	101	3.61E-02
HNSCC2_cetux_up	152	HALLMARK_PEROXISOME	104	3.61E-02
HNSCC2_cetux_up	152	ISRE_01	247	1.30E-04
HNSCC2_cetux_up	152	MAZR_01	220	3.29E-04
HNSCC2_cetux_up	152	AREB6_01	271	1.04E-03
HNSCC2_cetux_up	152	CAGGTG_E12_Q6	2485	1.62E-03
HNSCC2_cetux_up	152	IRF_Q6	242	2.91E-03
HNSCC2_cetux_up	152	GGGCGGR_SP1_Q6	2940	5.22E-03
HNSCC2_cetux_up	152	KRCTCNNNNMANAGC_UNKNOWN	66	7.47E-03
HNSCC2_cetux_up	152	CAGGTA_AREB6_01	792	7.47E-03
HNSCC2_cetux_up	152	E2F1DP1RB_01	231	1.18E-02
HNSCC2_cetux_up	152	GGGAGGRR_MAZ_Q6	2274	1.63E-02
HNSCC2_cetux_up	152	DR4_Q2	260	1.71E-02
HNSCC2_cetux_up	152	CTTTGA_LEF1_Q2	1232	1.71E-02
HNSCC2_cetux_up	152	STTTCRNTTT_IRF_Q6	188	2.72E-02
HNSCC2_cetux_up	152	AACTTT_UNKNOWN	1890	3.32E-02
HNSCC2_cetux_up	152	COMP1_01	115	3.33E-02
HNSCC2_cetux_up	152	RP58_01	207	3.42E-02
HNSCC2_cetux_up	152	MEF2_02	228	3.79E-02
HNSCC2_cetux_up	152	TTTNNANAGCYR_UNKNOWN	133	3.79E-02
HNSCC2_cetux_up	152	E2F1_Q6	232	3.79E-02
HNSCC2_cetux_up	152	E2F_Q6	232	3.79E-02
HNSCC2_cetux_up	152	GO_CELL_CYCLE	1316	3.76E-03
HNSCC2_cetux_up	152	GO_NEGATIVE_REGULATION_OF_GENE_EXPRESSION	1493	3.76E-03
HNSCC2_cetux_up	152	GO_NEGATIVE_REGULATION_OF_NITROGEN_COMPOUND_METABOLIC_PROCESS	1517	3.76E-03
HNSCC2_cetux_up	152	GO_CELL_CYCLE_PROCESS	1081	3.76E-03
HNSCC2_cetux_up	152	GO_CHROMOSOME_ORGANIZATION	1009	6.48E-03
HNSCC2_cetux_up	152	GO_REGULATION_OF_MULTICELLULAR_ORGANISMAL_DEVELOPMENT	1672	8.54E-03
HNSCC2_cetux_up	152	GO_RESPONSE_TO_EXTERNAL_STIMULUS	1821	1.85E-02
HNSCC2_cetux_up	152	GO_NEGATIVE_REGULATION_OF_GENE_EXPRESSION_EPIGENETIC	112	1.85E-02
HNSCC2_cetux_up	152	GO_DNA_CONFORMATION_CHANGE	273	1.85E-02
HNSCC2_cetux_up	152	GO_REGULATION_OF_NERVOUS_SYSTEM_DEVELOPMENT	750	1.95E-02
HNSCC2_cetux_up	152	GO_REGULATION_OF_NOTCH_SIGNALING_PATHWAY	67	2.67E-02
HNSCC2_cetux_up	152	GO_RESPONSE_TO_TYPE_I_INTERFERON	68	2.67E-02
HNSCC2_cetux_up	152	GO_GENE_SILENCING	212	2.67E-02
HNSCC2_cetux_up	152	GO_HUMORAL_IMMUNE_RESPONSE_MEDIATED_BY_CIRCULATING_IMMUNOGLOBULIN	69	2.67E-02
HNSCC2_cetux_up	152	GO_REGULATION_OF_GENE_EXPRESSION_EPIGENETIC	229	3.38E-02
HNSCC2_cetux_up	152	GO_COMPLEMENT_ACTIVATION	76	3.38E-02
HNSCC2_cetux_up	152	GO_RENAL_TUBULE_DEVELOPMENT	78	3.38E-02
HNSCC2_cetux_up	152	GO_REGULATION_OF_CELL_DIFFERENTIATION	1492	3.38E-02
HNSCC2_cetux_up	152	GO_KIDNEY_MORPHOGENESIS	82	3.84E-02
HNSCC2_cetux_up	152	GO_RESPONSE_TO_BIOTIC_STIMULUS	886	4.12E-02
HNSCC2_cetux_up	152	PIGF_UP.V1_DN	194	7.81E-04
HNSCC2_cetux_up	152	KRAS.PROSTATE_UP.V1_UP	143	8.24E-04

HNSCC2_cetux_up	152	CSR_LATE_UP.V1_DN	170	1.47E-03
HNSCC2_cetux_up	152	IL15_UP.V1_DN	190	1.89E-03
HNSCC2_cetux_up	152	HOXA9_DN.V1_DN	195	1.89E-03
HNSCC2_cetux_up	152	ATM_DN.V1_UP	146	4.14E-03
HNSCC2_cetux_up	152	IL21_UP.V1_DN	187	8.05E-03
HNSCC2_cetux_up	152	PRC2_EED_UP.V1_DN	193	8.05E-03
HNSCC2_cetux_up	152	LEF1_UP.V1_UP	195	8.05E-03
HNSCC2_cetux_up	152	E2F3_UP.V1_UP	196	8.05E-03
HNSCC2_cetux_up	152	EGFR_UP.V1_DN	196	8.05E-03
HNSCC2_cetux_up	152	MEK_UP.V1_DN	196	8.05E-03
HNSCC2_cetux_up	152	KRAS.300_UP.V1_DN	143	1.96E-02
HNSCC2_cetux_up	152	KRAS.600_UP.V1_DN	289	3.45E-02
HNSCC2_cetux_up	152	SRC_UP.V1_DN	179	3.45E-02
HNSCC2_cetux_up	152	GCNP_SHH_UP_LATE.V1_DN	180	3.45E-02
HNSCC2_cetux_up	152	RAPA_EARLY_UP.V1_UP	183	3.45E-02
HNSCC2_cetux_up	152	ATF2_UP.V1_UP	192	3.45E-02
HNSCC2_cetux_up	152	JNK_DN.V1_UP	192	3.45E-02
HNSCC2_cetux_up	152	KRAS.DF.V1_UP	193	3.45E-02
HNSCC3_cetux_up	729	HALLMARK_MYC_TARGETS_V1	200	7.77E-06
HNSCC3_cetux_up	729	HALLMARK_OXIDATIVE_PHOSPHORYLATION	200	1.11E-04
HNSCC3_cetux_up	729	HALLMARK_G2M_CHECKPOINT	200	2.87E-04
HNSCC3_cetux_up	729	HALLMARK_PROTEIN_SECRETION	96	2.87E-04
HNSCC3_cetux_up	729	HALLMARK_DNA_REPAIR	150	3.01E-04
HNSCC3_cetux_up	729	HALLMARK_GLYCOLYSIS	200	6.75E-04
HNSCC3_cetux_up	729	HALLMARK_XENOBIOTIC_METABOLISM	200	6.75E-04
HNSCC3_cetux_up	729	HALLMARK_APOPTOSIS	161	1.68E-03
HNSCC3_cetux_up	729	HALLMARK_TNFA_SIGNALING_VIA_NFKB	200	2.15E-03
HNSCC3_cetux_up	729	HALLMARK_UV_RESPONSE_DN	144	2.58E-03
HNSCC3_cetux_up	729	HALLMARK_UV_RESPONSE_UP	158	4.55E-03
HNSCC3_cetux_up	729	HALLMARK_COMPLEMENT	200	4.81E-03
HNSCC3_cetux_up	729	HALLMARK_E2F_TARGETS	200	4.81E-03
HNSCC3_cetux_up	729	HALLMARK_IL2_STAT5_SIGNALING	200	4.81E-03
HNSCC3_cetux_up	729	HALLMARK_KRAS_SIGNALING_UP	200	4.81E-03
HNSCC3_cetux_up	729	HALLMARK_TGF_BETA_SIGNALING	54	5.16E-03
HNSCC3_cetux_up	729	HALLMARK_UNFOLDED_PROTEIN_RESPONSE	113	6.54E-03
HNSCC3_cetux_up	729	HALLMARK_HEME_METABOLISM	200	1.17E-02
HNSCC3_cetux_up	729	HALLMARK_MITOTIC_SPINDLE	200	1.17E-02
HNSCC3_cetux_up	729	HALLMARK_MYOGENESIS	200	1.17E-02
HNSCC3_cetux_up	729	GGGCGGR_SP1_Q6	2940	2.98E-31
HNSCC3_cetux_up	729	TGANTCA_AP1_C	1121	1.12E-14
HNSCC3_cetux_up	729	CAGGTG_E12_Q6	2485	3.33E-14
HNSCC3_cetux_up	729	TGGAAA_NFAT_Q4_01	1896	3.21E-10
HNSCC3_cetux_up	729	SCGGAAGY_ELK1_02	1199	5.67E-10
HNSCC3_cetux_up	729	CTTTGT_LEF1_Q2	1972	1.36E-09
HNSCC3_cetux_up	729	TTGCCAA_MIR182	327	3.04E-09
HNSCC3_cetux_up	729	TTGTTT_FOXO4_01	2061	3.06E-09
HNSCC3_cetux_up	729	TGACCTY_ERR1_Q2	1043	6.37E-09
HNSCC3_cetux_up	729	GGGAGGRR_MAZ_Q6	2274	6.37E-09
HNSCC3_cetux_up	729	GATTGGY_NFY_Q6_01	1160	7.28E-09
HNSCC3_cetux_up	729	TAATTA_CHX10_01	810	9.87E-07
HNSCC3_cetux_up	729	CAGCTG_AP4_Q5	1524	1.25E-06
HNSCC3_cetux_up	729	TGTTTAC_MIR30A5P_MIR30C_MIR30D_MIR30B_MIR30E5P	579	1.30E-06
HNSCC3_cetux_up	729	TGAATGT_MIR181A_MIR181B_MIR181C_MIR181D	484	1.37E-06
HNSCC3_cetux_up	729	CACGTG_MYC_Q2	1032	2.04E-06
HNSCC3_cetux_up	729	CTTTGA_LEF1_Q2	1232	2.04E-06
HNSCC3_cetux_up	729	ERR1_Q2	259	2.04E-06
HNSCC3_cetux_up	729	RYTTCCTG_ETS2_B	1085	2.51E-06
HNSCC3_cetux_up	729	CTTTAAR_UNKNOWN	972	2.60E-06
HNSCC3_cetux_up	729	GO_PROTEIN_LOCALIZATION	1805	1.60E-21
HNSCC3_cetux_up	729	GO_REGULATION_OF_INTRACELLULAR_SIGNAL_TRANSDUCTION	1656	3.85E-19
HNSCC3_cetux_up	729	GO_POSITIVE_REGULATION_OF_RESPONSE_TO_STIMULUS	1929	8.12E-19
HNSCC3_cetux_up	729	GO_CELLULAR_MACROMOLECULE_LOCALIZATION	1234	8.12E-19
HNSCC3_cetux_up	729	GO_ESTABLISHMENT_OF_PROTEIN_LOCALIZATION	1423	2.32E-18
HNSCC3_cetux_up	729	GO_ESTABLISHMENT_OF_LOCALIZATION_IN_CELL	1676	1.40E-17
HNSCC3_cetux_up	729	GO_POSITIVE_REGULATION_OF_CELL_COMMUNICATION	1532	1.26E-16

HNSCC3_cetux_up	729	GO_PHOSPHATE_CONTAINING_COMPOUND_METABOLIC_PROCESS	1977	2.07E-16
HNSCC3_cetux_up	729	GO_REGULATION_OF_PROTEIN_MODIFICATION_PROCESS	1710	1.33E-15
HNSCC3_cetux_up	729	GO_REGULATION_OF_ORGANELLE_ORGANIZATION	1178	2.16E-15
HNSCC3_cetux_up	729	GO_ORGANONITROGEN_COMPOUND_METABOLIC_PROCESS	1796	5.67E-15
HNSCC3_cetux_up	729	GO_TISSUE_DEVELOPMENT	1518	7.05E-15
HNSCC3_cetux_up	729	GO_INTRACELLULAR_PROTEIN_TRANSPORT	781	8.81E-15
HNSCC3_cetux_up	729	GO_POSITIVE_REGULATION_OF_CELLULAR_COMPONENT_ORGANIZATION	1152	1.16E-13
HNSCC3_cetux_up	729	GO_CATABOLIC_PROCESS	1773	6.43E-13
HNSCC3_cetux_up	729	GO_CELLULAR_RESPONSE_TO_STRESS	1565	9.47E-13
HNSCC3_cetux_up	729	GO_INTRACELLULAR_SIGNAL_TRANSDUCTION	1572	1.11E-12
HNSCC3_cetux_up	729	GO_CELLULAR_RESPONSE_TO_ORGANIC_SUBSTANCE	1848	1.58E-12
HNSCC3_cetux_up	729	GO_SINGLE_ORGANISM_CELLULAR_LOCALIZATION	898	1.65E-12
HNSCC3_cetux_up	729	GO_REGULATION_OF_CELL_PROLIFERATION	1496	2.76E-12
HNSCC3_cetux_up	729	E2F1_UP.V1_DN	193	4.48E-07
HNSCC3_cetux_up	729	RPS14_DN.V1_UP	192	8.37E-06
HNSCC3_cetux_up	729	MEK_UP.V1_DN	196	2.52E-05
HNSCC3_cetux_up	729	MEK_UP.V1_UP	196	2.52E-05
HNSCC3_cetux_up	729	MTOR_UP.N4.V1_UP	196	2.52E-05
HNSCC3_cetux_up	729	TBK1.DF_UP	290	3.62E-05
HNSCC3_cetux_up	729	E2F1_UP.V1_UP	189	6.19E-05
HNSCC3_cetux_up	729	RAF_UP.V1_UP	196	4.07E-04
HNSCC3_cetux_up	729	STK33_UP	293	4.63E-04
HNSCC3_cetux_up	729	PDGF_ERK_DN.V1_UP	147	4.72E-04
HNSCC3_cetux_up	729	MYC_UP.V1_DN	182	6.55E-04
HNSCC3_cetux_up	729	AKT_UP.V1_DN	187	7.81E-04
HNSCC3_cetux_up	729	LTE2_UP.V1_UP	190	8.41E-04
HNSCC3_cetux_up	729	LEF1_UP.V1_UP	195	1.00E-03
HNSCC3_cetux_up	729	STK33_NOMO_UP	294	1.07E-03
HNSCC3_cetux_up	729	ESC_V6.5_UP_LATE.V1_DN	186	2.25E-03
HNSCC3_cetux_up	729	ATF2_UP.V1_DN	187	2.25E-03
HNSCC3_cetux_up	729	SINGH_KRAS_DEPENDENCY_SIGNATURE_	20	2.25E-03
HNSCC3_cetux_up	729	LEF1_UP.V1_DN	190	2.25E-03
HNSCC3_cetux_up	729	ERB2_UP.V1_UP	191	2.25E-03
HNSCC4_cetux_up	129	HALLMARK_INFLAMMATORY_RESPONSE	200	4.25E-05
HNSCC4_cetux_up	129	HALLMARK_TNFA_SIGNALING_VIA_NFKB	200	4.25E-05
HNSCC4_cetux_up	129	HALLMARK_APOPTOSIS	161	1.90E-02
HNSCC4_cetux_up	129	HALLMARK_ALLOGRAFT_REJECTION	200	2.09E-02
HNSCC4_cetux_up	129	HALLMARK_COMPLEMENT	200	2.09E-02
HNSCC4_cetux_up	129	HALLMARK_INTERFERON_GAMMA_RESPONSE	200	2.09E-02
HNSCC4_cetux_up	129	PEA3_Q6	255	5.75E-04
HNSCC4_cetux_up	129	AML_Q6	266	4.66E-02
HNSCC4_cetux_up	129	GO_POSITIVE_REGULATION_OF_IMMUNE_SYSTEM_PROCESS	867	1.54E-13
HNSCC4_cetux_up	129	GO_REGULATION_OF_CELL_ACTIVATION	484	2.85E-13
HNSCC4_cetux_up	129	GO_ADAPTIVE_IMMUNE_RESPONSE	288	2.85E-13
HNSCC4_cetux_up	129	GO_REGULATION_OF_IMMUNE_SYSTEM_PROCESS	1403	2.85E-13
HNSCC4_cetux_up	129	GO_REGULATION_OF_IMMUNE_RESPONSE	858	2.98E-13
HNSCC4_cetux_up	129	GO_IMMUNE_SYSTEM_PROCESS	1984	4.10E-13
HNSCC4_cetux_up	129	GO_PHAGOCYTOSIS_ENGULFMENT	38	7.10E-13
HNSCC4_cetux_up	129	GO_REGULATION_OF_B_CELL_ACTIVATION	121	7.10E-13
HNSCC4_cetux_up	129	GO_IMMUNE_RESPONSE	1100	3.29E-12
HNSCC4_cetux_up	129	GO_MEMBRANE_INVAGINATION	48	5.52E-12
HNSCC4_cetux_up	129	GO_POSITIVE_REGULATION_OF_CELL_ACTIVATION	311	6.15E-12
HNSCC4_cetux_up	129	GO_ADAPTIVE_IMMUNE_RESPONSE_BASED_ON_SOMATIC_RECOMBINATION_OF_IMMUNE_RECEPTORS_BUILT_FROM_IMMUNOGLOBULIN_SUPERFAMILY_DOMAINS	154	8.96E-12
HNSCC4_cetux_up	129	GO_B_CELL_RECEPTOR_SIGNALING_PATHWAY	54	1.33E-11
HNSCC4_cetux_up	129	GO_PHAGOCYTOSIS_RECOGNITION	34	1.67E-11
HNSCC4_cetux_up	129	GO_POSITIVE_REGULATION_OF_B_CELL_ACTIVATION	86	1.86E-11
HNSCC4_cetux_up	129	GO_PHAGOCYTOSIS	190	8.36E-11
HNSCC4_cetux_up	129	GO_HUMORAL_IMMUNE_RESPONSE_MEDIATED_BY_CIRCULATING_IMMUNOGLOBULIN	69	1.01E-10
HNSCC4_cetux_up	129	GO_ANTIGEN_RECEPTOR_MEDIATED_SIGNALING_PATHWAY	195	1.01E-10
HNSCC4_cetux_up	129	GO_POSITIVE_REGULATION_OF_IMMUNE_RESPONSE	563	1.13E-10

HNSCC4_cetux_up	1532	GO_IMMUNE_RESPONSE_REGULATING_CELL_SURFACE_RECEPTOR_SIGNALING_PATHWAY	323	1.13E-10
HNSCC4_cetux_up	129	BMI1_DN_MEL18_DN.V1_UP	145	1.11E-02
HNSCC4_cetux_up	129	NOTCH_DN.V1_DN	189	1.14E-02
HNSCC4_cetux_up	129	PRC1_BMI_UP.V1_UP	192	1.14E-02
HNSCC4_cetux_up	129	IL2_UP.V1_DN	196	1.14E-02
HNSCC4_cetux_up	129	BRCA1_DN.V1_UP	141	2.36E-02
HNSCC4_cetux_up	129	P53_DN.V2_UP	148	2.36E-02
HNSCC4_cetux_up	129	HINATA_NFKB_IMMU_INF	17	2.36E-02
HNSCC4_cetux_up	129	KRAS.600.LUNG.BREAST_UP.V1_DN	289	2.36E-02
HNSCC4_cetux_up	129	AKT_UP.V1_UP	172	2.36E-02
HNSCC4_cetux_up	129	AKT_UP_MTOR_DN.V1_UP	184	2.36E-02
HNSCC4_cetux_up	129	LEF1_UP.V1_DN	190	2.36E-02
HNSCC4_cetux_up	129	ERB2_UP.V1_UP	191	2.36E-02
HNSCC4_cetux_up	129	IL15_UP.V1_UP	192	2.36E-02
HNSCC4_cetux_up	129	IL2_UP.V1_UP	192	2.36E-02
HNSCC4_cetux_up	129	JNK_DN.V1_UP	192	2.36E-02
HNSCC4_cetux_up	129	RPS14_DN.V1_UP	192	2.36E-02
HNSCC4_cetux_up	129	DCA_UP.V1_DN	193	2.36E-02
HNSCC4_cetux_up	129	CYCLIN_D1_KE_.V1_DN	194	2.36E-02
HNSCC4_cetux_up	129	CAMP_UP.V1_DN	200	2.50E-02
HNSCC5_cetux_up	384	HALLMARK_ESTROGEN_RESPONSE_LATE	200	9.29E-09
HNSCC5_cetux_up	384	HALLMARK_P53_PATHWAY	200	4.63E-08
HNSCC5_cetux_up	384	HALLMARK_APICAL_JUNCTION	200	2.85E-07
HNSCC5_cetux_up	384	HALLMARK_KRAS_SIGNALING_DN	200	1.22E-06
HNSCC5_cetux_up	384	HALLMARK_MYOGENESIS	200	1.22E-06
HNSCC5_cetux_up	384	HALLMARK_XENOBIOTIC_METABOLISM	200	1.22E-06
HNSCC5_cetux_up	384	HALLMARK_KRAS_SIGNALING_UP	200	8.15E-06
HNSCC5_cetux_up	384	HALLMARK_G2M_CHECKPOINT	200	3.28E-04
HNSCC5_cetux_up	384	HALLMARK_EPITHELIAL_MESENCHYMAL_TRANSITION	200	1.68E-03
HNSCC5_cetux_up	384	HALLMARK_ESTROGEN_RESPONSE_EARLY	200	5.97E-03
HNSCC5_cetux_up	384	HALLMARK_GLYCOLYSIS	200	5.97E-03
HNSCC5_cetux_up	384	HALLMARK_HYPOXIA	200	5.97E-03
HNSCC5_cetux_up	384	HALLMARK_TNFA_SIGNALING_VIA_NFKB	200	5.97E-03
HNSCC5_cetux_up	384	HALLMARK_PI3K_AKT_MTOR_SIGNALING	105	6.91E-03
HNSCC5_cetux_up	384	HALLMARK_APICAL_SURFACE	44	1.98E-02
HNSCC5_cetux_up	384	HALLMARK_E2F_TARGETS	200	2.05E-02
HNSCC5_cetux_up	384	HALLMARK_HEME_METABOLISM	200	2.05E-02
HNSCC5_cetux_up	384	CAGGTG_E12_Q6	2485	2.91E-16
HNSCC5_cetux_up	384	CTTTGT_LEF1_Q2	1972	3.75E-14
HNSCC5_cetux_up	384	TGANTCA_AP1_C	1121	2.29E-09
HNSCC5_cetux_up	384	GGGCGGR_SP1_Q6	2940	1.11E-08
HNSCC5_cetux_up	384	GGGTGGRR_PAX4_03	1294	2.19E-07
HNSCC5_cetux_up	384	GGGAGGRR_MAZ_Q6	2274	2.19E-07
HNSCC5_cetux_up	384	CAGCTG_AP4_Q5	1524	3.31E-07
HNSCC5_cetux_up	384	RYTTCCTG_ETS2_B	1085	1.55E-06
HNSCC5_cetux_up	384	TATAAA_TATA_01	1296	6.12E-06
HNSCC5_cetux_up	384	KRCTCNNNNMANAGC_UNKNOWN	66	6.95E-06
HNSCC5_cetux_up	384	WGGAATGY_TEF1_Q6	378	6.70E-05
HNSCC5_cetux_up	384	WTGAAAT_UNKNOWN	616	9.94E-05
HNSCC5_cetux_up	384	TTANTCA_UNKNOWN	952	1.36E-04
HNSCC5_cetux_up	384	TGACAGNY_MEIS1_01	827	1.44E-04
HNSCC5_cetux_up	384	TGGAAA_NFAT_Q4_01	1896	2.74E-04
HNSCC5_cetux_up	384	TGGTGCT_MIR29A_MIR29B_MIR29C	521	5.32E-04
HNSCC5_cetux_up	384	SOX5_01	265	7.98E-04
HNSCC5_cetux_up	384	CTTTGA_LEF1_Q2	1232	7.98E-04
HNSCC5_cetux_up	384	CCCNNGGGAR_OLF1_01	320	7.98E-04
HNSCC5_cetux_up	384	GATTGGY_NFY_Q6_01	1160	7.98E-04
HNSCC5_cetux_up	384	GO_EPIDERMIS_DEVELOPMENT	253	1.61E-20
HNSCC5_cetux_up	384	GO_TISSUE_DEVELOPMENT	1518	1.06E-18
HNSCC5_cetux_up	384	GO_EPITHELIUM_DEVELOPMENT	945	1.48E-18
HNSCC5_cetux_up	384	GO_MOVEMENT_OF_CELL_OR_SUBCELLULAR_COMPONENT	1275	3.02E-17
HNSCC5_cetux_up	384	GO_BIOLOGICAL_ADHESION	1032	2.02E-13
HNSCC5_cetux_up	384	GO_CELL_MOTILITY	835	6.15E-12
HNSCC5_cetux_up	384	GO_LOCOMOTION	1114	9.53E-12
HNSCC5_cetux_up	384	GO_SKIN_DEVELOPMENT	211	1.73E-10

HNSCC5_cetux_up	384	GO_REGULATION_OF_INTRACELLULAR_SIGNAL_TRANSDUCTION	1656	1.76E-10
HNSCC5_cetux_up	384	GO_POSITIVE_REGULATION_OF_GENE_EXPRESSION	1733	2.08E-10
HNSCC5_cetux_up	384	GO_EPITHELIAL_CELL_DIFFERENTIATION	495	4.73E-10
HNSCC5_cetux_up	384	GO_POSITIVE_REGULATION_OF_RESPONSE_TO_STIMULUS	1929	6.20E-10
HNSCC5_cetux_up	384	GO_REGULATION_OF_MULTICELLULAR_ORGANISMAL_DEVELOPMENT	1672	2.40E-09
HNSCC5_cetux_up	384	GO_RESPONSE_TO_EXTERNAL_STIMULUS	1821	2.96E-09
HNSCC5_cetux_up	384	GO_REGULATION_OF_CELL_PROLIFERATION	1496	2.96E-09
HNSCC5_cetux_up	384	GO_CELLULAR_RESPONSE_TO_STRESS	1565	3.08E-09
HNSCC5_cetux_up	384	GO_REGULATION_OF_HYDROLASE_ACTIVITY	1327	3.94E-09
HNSCC5_cetux_up	384	GO_EPIDERMAL_CELL_DIFFERENTIATION	142	4.67E-09
HNSCC5_cetux_up	384	GO_SINGLE_ORGANISM_BIOSYNTHETIC_PROCESS	1340	4.67E-09
HNSCC5_cetux_up	384	GO_POSITIVE_REGULATION_OF_CELL_COMMUNICATION	1532	4.67E-09
HNSCC5_cetux_up	384	KRAS.LUNG_UP.V1_DN	145	2.15E-16
HNSCC5_cetux_up	384	KRAS.600.LUNG.BREAST_UP.V1_DN	289	4.74E-08
HNSCC5_cetux_up	384	KRAS.600_UP.V1_DN	289	2.45E-07
HNSCC5_cetux_up	384	CSR_LATE_UP.V1_UP	172	1.31E-06
HNSCC5_cetux_up	384	KRAS.LUNG.BREAST_UP.V1_DN	145	1.69E-06
HNSCC5_cetux_up	384	AKT_UP.V1_DN	187	1.89E-06
HNSCC5_cetux_up	384	RPS14_DN.V1_DN	187	1.89E-06
HNSCC5_cetux_up	384	CYCLIN_D1_KE_.V1_UP	190	1.63E-05
HNSCC5_cetux_up	384	KRAS.DF.V1_DN	194	1.68E-05
HNSCC5_cetux_up	384	LEF1_UP.V1_UP	195	1.68E-05
HNSCC5_cetux_up	384	ATF2_UP.V1_DN	187	7.72E-05
HNSCC5_cetux_up	384	STK33_DN	289	1.09E-04
HNSCC5_cetux_up	384	SNF5_DN.V1_DN	164	1.59E-04
HNSCC5_cetux_up	384	SNF5_DN.V1_UP	177	2.72E-04
HNSCC5_cetux_up	384	AKT_UP_MTOR_DN.V1_DN	183	3.26E-04
HNSCC5_cetux_up	384	ATF2_S_UP.V1_DN	187	3.26E-04
HNSCC5_cetux_up	384	JAK2_DN.V1_UP	188	3.26E-04
HNSCC5_cetux_up	384	IL15_UP.V1_DN	190	3.26E-04
HNSCC5_cetux_up	384	STK33_SKM_DN	288	3.26E-04
HNSCC5_cetux_up	384	DCA_UP.V1_DN	193	3.26E-04
HNSCC6_cetux_up	242	HALLMARK_COMPLEMENT	200	4.97E-03
HNSCC6_cetux_up	242	KRCTCNNNNMANAGC_UNKNOWN	66	4.78E-11
HNSCC6_cetux_up	242	TTTNNANAGCYR_UNKNOWN	133	1.09E-06
HNSCC6_cetux_up	242	TTCYNRGAA_STAT5B_01	335	2.23E-02
HNSCC6_cetux_up	242	TGANTCA_AP1_C	1121	4.98E-02
HNSCC6_cetux_up	242	CIZ_01	246	4.98E-02
HNSCC6_cetux_up	242	ETS_Q4	247	4.98E-02
HNSCC6_cetux_up	242	STAT_01	253	4.98E-02
HNSCC6_cetux_up	242	GO_IMMUNE_RESPONSE	1100	1.73E-10
HNSCC6_cetux_up	242	GO_REGULATION_OF_IMMUNE_SYSTEM_PROCESS	1403	1.78E-09
HNSCC6_cetux_up	242	GO_IMMUNE_SYSTEM_PROCESS	1984	9.16E-09
HNSCC6_cetux_up	242	GO_REGULATION_OF_IMMUNE_RESPONSE	858	2.70E-07
HNSCC6_cetux_up	242	GO_NEGATIVE_REGULATION_OF_GENE_EXPRESSION_EPIGENETIC	112	4.27E-07
HNSCC6_cetux_up	242	GO_POSITIVE_REGULATION_OF_IMMUNE_SYSTEM_PROCESS	867	1.24E-06
HNSCC6_cetux_up	242	GO_CHROMATIN_SILENCING	95	1.35E-06
HNSCC6_cetux_up	242	GO_DEFENSE_RESPONSE	1231	1.35E-06
HNSCC6_cetux_up	242	GO_HUMORAL_IMMUNE_RESPONSE_MEDIATED_BY_CIRCULATING_IMMUNOGLOBULIN	69	1.65E-06
HNSCC6_cetux_up	242	GO_ADAPTIVE_IMMUNE_RESPONSE	288	2.23E-06
HNSCC6_cetux_up	242	GO_HUMORAL_IMMUNE_RESPONSE	187	2.23E-06
HNSCC6_cetux_up	242	GO_COMPLEMENT_ACTIVATION	76	2.70E-06
HNSCC6_cetux_up	242	GO_RESPONSE_TO_BIOTIC_STIMULUS	886	4.42E-06
HNSCC6_cetux_up	242	GO_CHROMOSOME_ORGANIZATION	1009	8.02E-06
HNSCC6_cetux_up	242	GO_POSITIVE_REGULATION_OF_RESPONSE_TO_STIMULUS	1929	1.15E-05
HNSCC6_cetux_up	242	GO_REGULATION_OF_GENE_EXPRESSION_EPIGENETIC	229	1.24E-05
HNSCC6_cetux_up	242	GO_B_CELL_MEDIATED_IMMUNITY	99	1.47E-05
HNSCC6_cetux_up	242	GO_PROTEIN_ACTIVATION_CASCADE	99	1.47E-05
HNSCC6_cetux_up	242	GO_LYMPHOCYTE_MEDIATED_IMMUNITY	147	2.29E-05
HNSCC6_cetux_up	242	GO_GENE_SILENCING	212	4.86E-05
HNSCC6_cetux_up	242	LEF1_UP.V1_UP	195	5.52E-03
HNSCC6_cetux_up	242	EGFR_UP.V1_DN	196	5.52E-03
HNSCC6_cetux_up	242	MEK_UP.V1_DN	196	5.52E-03
HNSCC6_cetux_up	242	ESC_J1_UP_EARLY.V1_UP	183	2.00E-02

HNSCC6_cetux_up	242	PRC2_EED_UP.V1_DN	193	2.00E-02
HNSCC6_cetux_up	242	LTE2_UP.V1_DN	196	2.00E-02
HNSCC7_cetux_up	412	HALLMARK_E2F_TARGETS	200	9.75E-07
HNSCC7_cetux_up	412	HALLMARK_INTERFERON_GAMMA_RESPONSE	200	9.75E-07
HNSCC7_cetux_up	412	HALLMARK_ADIPOGENESIS	200	2.81E-05
HNSCC7_cetux_up	412	HALLMARK_EPITHELIAL_MESENCHYMAL_TRANSITION	200	2.81E-05
HNSCC7_cetux_up	412	HALLMARK_INTERFERON_ALPHA_RESPONSE	97	2.84E-04
HNSCC7_cetux_up	412	HALLMARK_MYC_TARGETS_V1	200	7.46E-04
HNSCC7_cetux_up	412	HALLMARK_MYC_TARGETS_V2	58	1.25E-03
HNSCC7_cetux_up	412	HALLMARK_UV_RESPONSE_DN	144	1.05E-02
HNSCC7_cetux_up	412	HALLMARK_APICAL_JUNCTION	200	1.05E-02
HNSCC7_cetux_up	412	HALLMARK_G2M_CHECKPOINT	200	1.05E-02
HNSCC7_cetux_up	412	HALLMARK_P53_PATHWAY	200	1.05E-02
HNSCC7_cetux_up	412	HALLMARK_ANGIOGENESIS	36	1.71E-02
HNSCC7_cetux_up	412	HALLMARK_IL6_JAK_STAT3_SIGNALING	87	2.84E-02
HNSCC7_cetux_up	412	HALLMARK_ALLOGRAFT_REJECTION	200	2.84E-02
HNSCC7_cetux_up	412	HALLMARK_KRAS_SIGNALING_UP	200	2.84E-02
HNSCC7_cetux_up	412	HALLMARK_OXIDATIVE_PHOSPHORYLATION	200	2.84E-02
HNSCC7_cetux_up	412	HALLMARK_TNFA_SIGNALING_VIA_NFKB	200	2.84E-02
HNSCC7_cetux_up	412	HALLMARK_TGF_BETA_SIGNALING	54	3.46E-02
HNSCC7_cetux_up	412	HALLMARK_ANDROGEN_RESPONSE	101	3.46E-02
HNSCC7_cetux_up	412	HALLMARK_PEROXISOME	104	3.63E-02
HNSCC7_cetux_up	412	GGGCGGR_SP1_Q6	2940	5.48E-14
HNSCC7_cetux_up	412	GATTGGY_NFY_Q6_01	1160	2.81E-06
HNSCC7_cetux_up	412	AACTTT_UNKNOWN	1890	2.81E-06
HNSCC7_cetux_up	412	GGGAGGRR_MAZ_Q6	2274	3.33E-06
HNSCC7_cetux_up	412	CACGTG_MYC_Q2	1032	1.34E-05
HNSCC7_cetux_up	412	RCGCANGCGY_NRF1_Q6	918	1.34E-05
HNSCC7_cetux_up	412	CTTTGT_LEF1_Q2	1972	7.76E-05
HNSCC7_cetux_up	412	SCGGAAGY_ELK1_02	1199	1.84E-04
HNSCC7_cetux_up	412	TGANTCA_AP1_C	1121	4.03E-04
HNSCC7_cetux_up	412	CAGGTG_E12_Q6	2485	5.83E-04
HNSCC7_cetux_up	412	TGGAAA_NFAT_Q4_01	1896	7.01E-04
HNSCC7_cetux_up	412	GTGACGY_E4F1_Q6	658	7.01E-04
HNSCC7_cetux_up	412	POU3F2_02	260	1.72E-03
HNSCC7_cetux_up	412	HNF4_Q6	263	1.77E-03
HNSCC7_cetux_up	412	EFC_Q6	268	1.96E-03
HNSCC7_cetux_up	412	CHX10_01	225	2.13E-03
HNSCC7_cetux_up	412	USF_C	279	2.49E-03
HNSCC7_cetux_up	412	TATAAA_TATA_01	1296	2.53E-03
HNSCC7_cetux_up	412	SP1_01	237	2.77E-03
HNSCC7_cetux_up	412	GGGYGTGNY_UNKNOWN	664	4.91E-03
HNSCC7_cetux_up	412	GO_IMMUNE_SYSTEM_PROCESS	1984	8.90E-13
HNSCC7_cetux_up	412	GO_DEFENSE_RESPONSE	1231	1.02E-12
HNSCC7_cetux_up	412	GO_RESPONSE_TO_BIOTIC_STIMULUS	886	2.09E-11
HNSCC7_cetux_up	412	GO_REGULATION_OF_IMMUNE_SYSTEM_PROCESS	1403	5.86E-11
HNSCC7_cetux_up	412	GO_CELLULAR_RESPONSE_TO_ORGANIC_SUBSTANCE	1848	9.96E-11
HNSCC7_cetux_up	412	GO_DEFENSE_RESPONSE_TO_OTHER_ORGANISM	505	1.48E-10
HNSCC7_cetux_up	412	GO_REGULATION_OF_PROTEIN_MODIFICATION_PROCESS	1710	2.44E-09
HNSCC7_cetux_up	412	GO_RESPONSE_TO_EXTERNAL_STIMULUS	1821	5.57E-09
HNSCC7_cetux_up	412	GO_LOCOMOTION	1114	6.16E-09
HNSCC7_cetux_up	412	GO_CELLULAR_RESPONSE_TO_STRESS	1565	1.38E-08
HNSCC7_cetux_up	412	GO_REGULATION_OF_CELLULAR_COMPONENT_MOVEMENT	771	5.21E-08
HNSCC7_cetux_up	412	GO_IMMUNE_EFFECTOR_PROCESS	486	5.21E-08
HNSCC7_cetux_up	412	GO_PHOSPHATE_CONTAINING_COMPOUND_METABOLIC_PROCESS	1977	5.79E-08
HNSCC7_cetux_up	412	GO_REGULATION_OF_RESPONSE_TO_STRESS	1468	5.92E-08
HNSCC7_cetux_up	412	GO_REGULATION_OF_CELL_DIFFERENTIATION	1492	8.92E-08
HNSCC7_cetux_up	412	GO_POSITIVE_REGULATION_OF_LOCOMOTION	420	9.29E-08
HNSCC7_cetux_up	412	GO_REGULATION_OF_RESPONSE_TO_EXTERNAL_STIMULUS	926	1.33E-07
HNSCC7_cetux_up	412	GO_MACROMOLECULAR_COMPLEX_ASSEMBLY	1398	1.36E-07
HNSCC7_cetux_up	412	GO_PROTEIN_LOCALIZATION	1805	1.96E-07
HNSCC7_cetux_up	412	GO_RESPONSE_TO_OXYGEN_CONTAINING_COMPOUND	1381	3.00E-07
HNSCC7_cetux_up	412	STK33_NOMO_UP	294	1.66E-05
HNSCC7_cetux_up	412	BMI1_DN.V1_DN	144	4.94E-04
HNSCC7_cetux_up	412	BMI1_DN_MEL18_DN.V1_DN	147	4.94E-04

HNSCC7_cetux_up	412	RPS14_DN.V1_UP	192	4.94E-04
HNSCC7_cetux_up	412	KRAS.600.LUNG.BREAST_UP.V1_DN	289	5.04E-04
HNSCC7_cetux_up	412	STK33_UP	293	5.04E-04
HNSCC7_cetux_up	412	PKCA_DN.V1_UP	170	6.58E-04
HNSCC7_cetux_up	412	CSR_LATE_UP.V1_UP	172	6.58E-04
HNSCC7_cetux_up	412	RB_P107_DN.V1_UP	140	8.73E-04
HNSCC7_cetux_up	412	LEF1_UP.V1_UP	195	1.32E-03
HNSCC7_cetux_up	412	LTE2_UP.V1_DN	196	1.32E-03
HNSCC7_cetux_up	412	MTOR_UP.V1_UP	170	2.54E-03
HNSCC7_cetux_up	412	AKT_UP.V1_UP	172	2.54E-03
HNSCC7_cetux_up	412	SNF5_DN.V1_UP	177	2.87E-03
HNSCC7_cetux_up	412	AKT_UP_MTOR_DN.V1_UP	184	3.49E-03
HNSCC7_cetux_up	412	KRAS.LUNG_UP.V1_DN	145	3.60E-03
HNSCC7_cetux_up	412	EGFR_UP.V1_UP	193	3.60E-03
HNSCC7_cetux_up	412	KRAS.DF.V1_UP	193	3.60E-03
HNSCC7_cetux_up	412	P53_DN.V1_UP	194	3.60E-03
HNSCC7_cetux_up	412	ALK_DN.V1_DN	148	3.60E-03
HNSCC8_cetux_up	201	HALLMARK_KRAS_SIGNALING_UP	200	1.40E-05
HNSCC8_cetux_up	201	HALLMARK_ALLOGRAFT_REJECTION	200	6.14E-03
HNSCC8_cetux_up	201	HALLMARK_COAGULATION	138	6.14E-03
HNSCC8_cetux_up	201	HALLMARK_EPITHELIAL_MESENCHYMAL_TRANSITION	200	1.94E-02
HNSCC8_cetux_up	201	HALLMARK_IL2_STAT5_SIGNALING	200	1.94E-02
HNSCC8_cetux_up	201	GO_ADAPTIVE_IMMUNE_RESPONSE_BASED_ON_SOMATIC_RECOMBINATION_OF_IMMUNE_RECEPTORS_BUILT_FROM_IMMUNOGLOBULIN_SUPERFAMILY_DOMAINS	154	2.43E-35
HNSCC8_cetux_up	201	GO_ADAPTIVE_IMMUNE_RESPONSE	288	5.39E-35
HNSCC8_cetux_up	201	GO_HUMORAL_IMMUNE_RESPONSE_MEDIATED_BY_CIRCULATING_IMMUNOGLOBULIN	69	2.24E-34
HNSCC8_cetux_up	201	GO_COMPLEMENT_ACTIVATION	76	2.32E-33
HNSCC8_cetux_up	201	GO_B_CELL_RECEPTOR_SIGNALING_PATHWAY	54	3.99E-33
HNSCC8_cetux_up	201	GO_B_CELL_MEDIATED_IMMUNITY	99	1.36E-30
HNSCC8_cetux_up	201	GO_PROTEIN_ACTIVATION_CASCADE	99	1.36E-30
HNSCC8_cetux_up	201	GO_HUMORAL_IMMUNE_RESPONSE	187	2.80E-30
HNSCC8_cetux_up	201	GO_PHAGOCYTOSIS	190	3.91E-30
HNSCC8_cetux_up	201	GO_REGULATION_OF_IMMUNE_RESPONSE	858	5.92E-30
HNSCC8_cetux_up	201	GO_IMMUNE_RESPONSE	1100	5.92E-30
HNSCC8_cetux_up	201	GO_LYMPHOCYTE_MEDIATED_IMMUNITY	147	5.92E-30
HNSCC8_cetux_up	201	GO_POSITIVE_REGULATION_OF_IMMUNE_SYSTEM_PROCESS	867	7.44E-30
HNSCC8_cetux_up	201	GO_IMMUNE_SYSTEM_PROCESS	1984	4.15E-29
HNSCC8_cetux_up	201	GO_POSITIVE_REGULATION_OF_IMMUNE_RESPONSE	563	1.75E-28
HNSCC8_cetux_up	201	GO_IMMUNE_RESPONSE_REGULATING_CELL_SURFACE_RECEPTOR_SIGNALING_PATHWAY	323	2.96E-28
HNSCC8_cetux_up	201	GO_ACTIVATION_OF_IMMUNE_RESPONSE	427	2.61E-27
HNSCC8_cetux_up	201	GO_LEUKOCYTE_MEDIATED_IMMUNITY	189	2.99E-27
HNSCC8_cetux_up	201	GO_REGULATION_OF_IMMUNE_SYSTEM_PROCESS	1403	1.40E-26
HNSCC8_cetux_up	201	GO_FC_GAMMA_RECEPTOR_SIGNALING_PATHWAY	95	7.10E-26
HNSCC8_cetux_up	201	KRAS.600.LUNG.BREAST_UP.V1_UP	288	4.31E-03
HNSCC8_cetux_up	201	KRAS.LUNG.BREAST_UP.V1_UP	145	4.31E-03
HNSCC8_cetux_up	201	PKCA_DN.V1_DN	167	6.28E-03
HNSCC8_cetux_up	201	ALK_DN.V1_UP	145	2.18E-02
HNSCC8_cetux_up	201	HINATA_NFKB_MATRIX	10	3.16E-02
HNSCC8_cetux_up	201	IL21_UP.V1_UP	193	4.68E-02
HNSCC8_cetux_up	201	KRAS.600_UP.V1_UP	287	4.68E-02
HNSCC9_cetux_up	176	HALLMARK_EPITHELIAL_MESENCHYMAL_TRANSITION	200	3.29E-04
HNSCC9_cetux_up	176	HALLMARK_ESTROGEN_RESPONSE_EARLY	200	3.29E-04
HNSCC9_cetux_up	176	HALLMARK_ESTROGEN_RESPONSE_LATE	200	1.29E-03
HNSCC9_cetux_up	176	HALLMARK_KRAS_SIGNALING_UP	200	1.29E-03
HNSCC9_cetux_up	176	HALLMARK_TNFA_SIGNALING_VIA_NFKB	200	1.29E-03
HNSCC9_cetux_up	176	HALLMARK_APOPTOSIS	161	2.93E-02
HNSCC9_cetux_up	176	HALLMARK_IL6_JAK_STAT3_SIGNALING	87	3.30E-02
HNSCC9_cetux_up	176	HALLMARK_MYOGENESIS	200	3.83E-02
HNSCC9_cetux_up	176	HALLMARK_OXIDATIVE_PHOSPHORYLATION	200	3.83E-02
HNSCC9_cetux_up	176	HALLMARK_PI3K_AKT_MTOR_SIGNALING	105	3.83E-02
HNSCC9_cetux_up	176	HALLMARK_ANGIOGENESIS	36	3.83E-02
HNSCC9_cetux_up	176	KRCTCNNNNMANAGC_UNKNOWN	66	5.77E-06
HNSCC9_cetux_up	176	TATAAA_TATA_01	1296	2.48E-04

HNSCC9_cetux_up	176	TTTNNANAGCYR_UNKNOWN	133	2.48E-04
HNSCC9_cetux_up	176	NGFIC_01	255	1.28E-03
HNSCC9_cetux_up	176	AREB6_03	258	1.28E-03
HNSCC9_cetux_up	176	CTTTGT_LEF1_Q2	1972	3.34E-03
HNSCC9_cetux_up	176	TGGAAA_NFAT_Q4_01	1896	5.17E-03
HNSCC9_cetux_up	176	CAGGTG_E12_Q6	2485	8.71E-03
HNSCC9_cetux_up	176	TGANTCA_AP1_C	1121	3.50E-02
HNSCC9_cetux_up	176	GATA4_Q3	249	3.50E-02
HNSCC9_cetux_up	176	CATTGTYY_SOX9_B1	358	3.73E-02
HNSCC9_cetux_up	176	SOX5_01	265	4.05E-02
HNSCC9_cetux_up	176	GO_REGULATION_OF_CELL_DIFFERENTIATION	1492	1.04E-07
HNSCC9_cetux_up	176	GO_REGULATION_OF_MULTICELLULAR_ORGANISMAL_DEVELOPMENT	1672	1.27E-07
HNSCC9_cetux_up	176	GO_CHROMATIN_SILENCING_AT_RDNA	37	1.42E-07
HNSCC9_cetux_up	176	GO_CHROMATIN_SILENCING	95	1.42E-07
HNSCC9_cetux_up	176	GO_RESPONSE_TO_EXTERNAL_STIMULUS	1821	3.51E-07
HNSCC9_cetux_up	176	GO_NEGATIVE_REGULATION_OF_GENE_EXPRESSION_EPIGENETIC	112	4.18E-07
HNSCC9_cetux_up	176	GO_DNA_REPLICATION_DEPENDENT_NUCLEOSOME_ORGANIZATION	32	1.53E-06
HNSCC9_cetux_up	176	GO_REGULATION_OF_NERVOUS_SYSTEM_DEVELOPMENT	750	3.07E-06
HNSCC9_cetux_up	176	GO_POSITIVE_REGULATION_OF_RESPONSE_TO_STIMULUS	1929	3.07E-06
HNSCC9_cetux_up	176	GO_PROTEIN_HETEROTETRAMERIZATION	38	3.20E-06
HNSCC9_cetux_up	176	GO_REGULATION_OF_CELLULAR_COMPONENT_MOVEMENT	771	3.55E-06
HNSCC9_cetux_up	176	GO_POSITIVE_REGULATION_OF_GENE_EXPRESSION_EPIGENETIC	78	8.32E-06
HNSCC9_cetux_up	176	GO_REGULATION_OF_CELL_DEVELOPMENT	836	9.72E-06
HNSCC9_cetux_up	176	GO_CHROMATIN_ASSEMBLY_OR_DISASSEMBLY	177	1.01E-05
HNSCC9_cetux_up	176	GO_REGULATION_OF_NEURON_DIFFERENTIATION	554	1.07E-05
HNSCC9_cetux_up	176	GO_PROTEIN_TETRAMERIZATION	135	1.60E-05
HNSCC9_cetux_up	176	GO_DNA_PACKAGING	194	1.82E-05
HNSCC9_cetux_up	176	GO_PROTEIN_COMPLEX_BIOGENESIS	1132	2.12E-05
HNSCC9_cetux_up	176	GO_POSITIVE_REGULATION_OF_CELL_COMMUNICATION	1532	2.59E-05
HNSCC9_cetux_up	176	GO_REGULATION_OF_IMMUNE_SYSTEM_PROCESS	1403	2.59E-05
HNSCC9_cetux_up	176	KRAS.LUNG.BREAST_UP.V1_UP	145	1.06E-06
HNSCC9_cetux_up	176	KRAS.600.LUNG.BREAST_UP.V1_UP	288	1.83E-05
HNSCC9_cetux_up	176	RB_DN.V1_DN	126	3.89E-05
HNSCC9_cetux_up	176	BMI1_DN.V1_UP	147	8.21E-05
HNSCC9_cetux_up	176	ATF2_S_UP.V1_UP	193	2.92E-04
HNSCC9_cetux_up	176	KRAS.DF.V1_UP	193	2.92E-04
HNSCC9_cetux_up	176	RAF_UP.V1_DN	194	2.92E-04
HNSCC9_cetux_up	176	ALK_DN.V1_UP	145	4.73E-04
HNSCC9_cetux_up	176	KRAS.BREAST_UP.V1_UP	146	4.73E-04
HNSCC9_cetux_up	176	HINATA_NFKB_IMMU_INF	17	6.82E-04
HNSCC9_cetux_up	176	ESC_V6.5_UP_LATE.V1_UP	190	1.52E-03
HNSCC9_cetux_up	176	P53_DN.V1_DN	192	1.52E-03
HNSCC9_cetux_up	176	KRAS.DF.V1_DN	194	1.52E-03
HNSCC9_cetux_up	176	HOXA9_DN.V1_DN	195	1.52E-03
HNSCC9_cetux_up	176	STK33_SKM_UP	290	1.73E-03
HNSCC9_cetux_up	176	CRX_DN.V1_UP	136	2.20E-03
HNSCC9_cetux_up	176	CTIP_DN.V1_UP	138	2.20E-03
HNSCC9_cetux_up	176	RB_P107_DN.V1_UP	140	2.20E-03
HNSCC9_cetux_up	176	KRAS.LUNG_UP.V1_UP	141	2.20E-03
HNSCC9_cetux_up	176	BMI1_DN_MEL18_DN.V1_UP	145	2.38E-03
HNSCC10_cetux_up	146	TGGAAA_NFAT_Q4_01	1896	5.02E-03
HNSCC10_cetux_up	146	ELF1_Q6	244	5.02E-03
HNSCC10_cetux_up	146	TEF_Q6	255	5.02E-03
HNSCC10_cetux_up	146	TTAYRTAA_E4BP4_01	265	5.02E-03
HNSCC10_cetux_up	146	CAGGTG_E12_Q6	2485	1.70E-02
HNSCC10_cetux_up	146	E2A_Q2	243	1.70E-02
HNSCC10_cetux_up	146	NFAT_Q6	246	1.70E-02
HNSCC10_cetux_up	146	CTTTGA_LEF1_Q2	1232	1.70E-02
HNSCC10_cetux_up	146	RTAAACA_FREAC2_01	919	1.70E-02
HNSCC10_cetux_up	146	YGACNNYACAR_UNKNOWN	96	2.16E-02
HNSCC10_cetux_up	146	CTTTAAR_UNKNOWN	972	2.24E-02
HNSCC10_cetux_up	146	GATTGGY_NFY_Q6_01	1160	2.45E-02
HNSCC10_cetux_up	146	GGGCGGR_SP1_Q6	2940	2.68E-02
HNSCC10_cetux_up	146	CACGTG_MYC_Q2	1032	2.90E-02

HNSCC10_cetux_up	146	RYTTCCTG_ETS2_B	1085	4.08E-02
HNSCC10_cetux_up	146	PU1_Q6	234	4.81E-02
HNSCC10_cetux_up	146	TTANTCA_UNKNOWN	952	4.81E-02
HNSCC10_cetux_up	146	HNF1_01	245	4.81E-02
HNSCC10_cetux_up	146	CAGCTG_AP4_Q5	1524	4.81E-02
HNSCC10_cetux_up	146	AP2_Q3	251	4.81E-02
HNSCC10_cetux_up	146	GO_SINGLE_ORGANISM_BIOSYNTHETIC_PROCESS	1340	5.13E-03
HNSCC10_cetux_up	146	GO_VESICLE_MEDIATED_TRANSPORT	1239	5.13E-03
HNSCC10_cetux_up	146	GO_MITOCHONDRION_ORGANIZATION	594	5.15E-03
HNSCC10_cetux_up	146	GO_EXOCYTOSIS	310	8.18E-03
HNSCC10_cetux_up	146	GO_ION_HOMEOSTASIS	576	1.27E-02
HNSCC10_cetux_up	146	GO_ORGANONITROGEN_COMPOUND_METABOLIC_PROCESS	1796	1.27E-02
HNSCC10_cetux_up	146	GO_CHEMICAL_HOMEOSTASIS	874	1.58E-02
HNSCC10_cetux_up	146	GO_CARBOHYDRATE_DERIVATIVE_METABOLIC_PROCESS	1047	1.79E-02
HNSCC10_cetux_up	146	GO_SMALL_MOLECULE_METABOLIC_PROCESS	1767	2.45E-02
HNSCC10_cetux_up	146	GO_ORGANIC_ACID_METABOLIC_PROCESS	953	2.55E-02
HNSCC10_cetux_up	146	GO_LIPID_METABOLIC_PROCESS	1158	3.60E-02
HNSCC10_cetux_up	146	GO_SECRETION	588	4.38E-02
HNSCC10_cetux_up	146	GO_WNT_SIGNALING_PATHWAY	351	4.77E-02
HNSCC10_cetux_up	146	GO_NUCLEIC_ACID_PHOSPHODIESTER_BOND_HYDROLYSIS	254	4.83E-02
HNSCC10_cetux_up	146	GO_CELLULAR_LIPID_METABOLIC_PROCESS	913	4.83E-02
HNSCC10_cetux_up	146	GO_SECRETION_BY_CELL	486	4.83E-02
HNSCC10_cetux_up	146	CSR_EARLY_UP.V1_UP	164	2.86E-03
HNSCC11_cetux_up	2568	HALLMARK_MYC_TARGETS_V1	200	8.13E-87
HNSCC11_cetux_up	2568	HALLMARK_OXIDATIVE_PHOSPHORYLATION	200	1.34E-43
HNSCC11_cetux_up	2568	HALLMARK_E2F_TARGETS	200	7.08E-39
HNSCC11_cetux_up	2568	HALLMARK_G2M_CHECKPOINT	200	7.08E-39
HNSCC11_cetux_up	2568	HALLMARK_INTERFERON_GAMMA_RESPONSE	200	7.08E-39
HNSCC11_cetux_up	2568	HALLMARK_MTORC1_SIGNALING	200	5.67E-37
HNSCC11_cetux_up	2568	HALLMARK_P53_PATHWAY	200	4.27E-35
HNSCC11_cetux_up	2568	HALLMARK_MITOTIC_SPINDLE	200	1.48E-29
HNSCC11_cetux_up	2568	HALLMARK_TNFA_SIGNALING_VIA_NFKB	200	2.25E-24
HNSCC11_cetux_up	2568	HALLMARK_PROTEIN_SECRETION	96	2.26E-24
HNSCC11_cetux_up	2568	HALLMARK_INTERFERON_ALPHA_RESPONSE	97	3.93E-23
HNSCC11_cetux_up	2568	HALLMARK_PI3K_AKT_MTOR_SIGNALING	105	1.08E-22
HNSCC11_cetux_up	2568	HALLMARK_APOPTOSIS	161	1.33E-22
HNSCC11_cetux_up	2568	HALLMARK_UNFOLDED_PROTEIN_RESPONSE	113	2.34E-22
HNSCC11_cetux_up	2568	HALLMARK_ESTROGEN_RESPONSE_EARLY	200	2.30E-21
HNSCC11_cetux_up	2568	HALLMARK_ESTROGEN_RESPONSE_LATE	200	2.30E-21
HNSCC11_cetux_up	2568	HALLMARK_UV_RESPONSE_UP	158	2.30E-21
HNSCC11_cetux_up	2568	HALLMARK_APICAL_JUNCTION	200	7.90E-20
HNSCC11_cetux_up	2568	HALLMARK_HEME_METABOLISM	200	4.17E-19
HNSCC11_cetux_up	2568	HALLMARK_HYPOXIA	200	4.17E-19
HNSCC11_cetux_up	2568	GGGCGGR_SP1_Q6	2940	6.71E-172
HNSCC11_cetux_up	2568	GGGAGGRR_MAZ_Q6	2274	4.60E-106
HNSCC11_cetux_up	2568	CTTTGT_LEF1_Q2	1972	1.17E-90
HNSCC11_cetux_up	2568	GCCATNTTG_YY1_Q6	427	7.83E-83
HNSCC11_cetux_up	2568	SCGGAAGY_ELK1_02	1199	9.30E-82
HNSCC11_cetux_up	2568	CAGGTG_E12_Q6	2485	1.70E-76
HNSCC11_cetux_up	2568	GATTGGY_NFY_Q6_01	1160	7.27E-74
HNSCC11_cetux_up	2568	GGGTGGRR_PAX4_03	1294	8.15E-68
HNSCC11_cetux_up	2568	RCGCANGCGY_NRF1_Q6	918	2.09E-67
HNSCC11_cetux_up	2568	CACGTG_MYC_Q2	1032	2.50E-66
HNSCC11_cetux_up	2568	TGANTCA_AP1_C	1121	3.47E-64
HNSCC11_cetux_up	2568	TTGTTT_FOXO4_01	2061	4.09E-59
HNSCC11_cetux_up	2568	TGGAAA_NFAT_Q4_01	1896	1.02E-54
HNSCC11_cetux_up	2568	GTGACGY_E4F1_Q6	658	1.51E-54
HNSCC11_cetux_up	2568	AACTTT_UNKNOWN	1890	1.84E-51
HNSCC11_cetux_up	2568	RYTTCCTG_ETS2_B	1085	4.86E-49
HNSCC11_cetux_up	2568	NFMUE1_Q6	245	1.93E-46
HNSCC11_cetux_up	2568	MGGAAGTG_GABP_B	757	1.93E-45
HNSCC11_cetux_up	2568	CTTTGTA_MIR524	433	2.82E-44
HNSCC11_cetux_up	2568	GGGYGTGNY_UNKNOWN	664	1.19E-40
HNSCC11_cetux_up	2568	GO_ESTABLISHMENT_OF_LOCALIZATION_IN_CELL	1676	4.72E-175
HNSCC11_cetux_up	2568	GO_PROTEIN_LOCALIZATION	1805	1.27E-146
HNSCC11_cetux_up	2568	GO_INTERSPECIES_INTERACTION_BETWEEN_ORGANISMS	662	1.06E-145

HNSCC11_cetux_up	2568	GO_ESTABLISHMENT_OF_PROTEIN_LOCALIZATION	1423	2.70E-141
HNSCC11_cetux_up	2568	GO_CELLULAR_MACROMOLECULE_LOCALIZATION	1234	1.51E-130
HNSCC11_cetux_up	2568	GO_MACROMOLECULE_CATABOLIC_PROCESS	926	3.71E-130
HNSCC11_cetux_up	2568	GO_CATABOLIC_PROCESS	1773	2.84E-127
HNSCC11_cetux_up	2568	GO_CELLULAR_CATABOLIC_PROCESS	1322	6.78E-123
HNSCC11_cetux_up	2568	GO_MRNA_METABOLIC_PROCESS	611	7.69E-123
HNSCC11_cetux_up	2568	GO_INTRACELLULAR_PROTEIN_TRANSPORT	781	1.46E-113
HNSCC11_cetux_up	2568	GO_SINGLE_ORGANISM_CELLULAR_LOCALIZATION	898	8.50E-110
HNSCC11_cetux_up	2568	GO_MEMBRANE_ORGANIZATION	899	5.78E-108
HNSCC11_cetux_up	2568	GO_POSITIVE_REGULATION_OF_RESPONSE_TO_STIMULUS	1929	6.24E-108
HNSCC11_cetux_up	2568	GO_IMMUNE_SYSTEM_PROCESS	1984	2.68E-107
HNSCC11_cetux_up	2568	GO_MACROMOLECULAR_COMPLEX_ASSEMBLY	1398	2.95E-107
HNSCC11_cetux_up	2568	GO_NEGATIVE_REGULATION_OF_GENE_EXPRESSION	1493	1.54E-105
HNSCC11_cetux_up	2568	GO_CELLULAR_RESPONSE_TO_STRESS	1565	4.13E-103
HNSCC11_cetux_up	2568	GO_CELL_CYCLE	1316	8.28E-103
HNSCC11_cetux_up	2568	GO_RNA_PROCESSING	835	3.71E-102
HNSCC11_cetux_up	2568	GO_CELLULAR_RESPONSE_TO_ORGANIC_SUBSTANCE	1848	5.98E-100
HNSCC11_cetux_up	2568	CAMP_UP.V1_UP	200	4.48E-28
HNSCC11_cetux_up	2568	SIRNA_EIF4GI_UP	95	3.81E-21
HNSCC11_cetux_up	2568	TBK1.DF_DN	287	1.34E-18
HNSCC11_cetux_up	2568	CAMP_UP.V1_DN	200	1.34E-18
HNSCC11_cetux_up	2568	STK33_SKM_UP	290	3.78E-17
HNSCC11_cetux_up	2568	MEK_UP.V1_UP	196	6.89E-17
HNSCC11_cetux_up	2568	CYCLIN_D1_KE_.V1_UP	190	8.61E-17
HNSCC11_cetux_up	2568	EGFR_UP.V1_UP	193	1.40E-16
HNSCC11_cetux_up	2568	RB_P107_DN.V1_DN	128	1.40E-16
HNSCC11_cetux_up	2568	P53_DN.V1_UP	194	1.48E-16
HNSCC11_cetux_up	2568	LTE2_UP.V1_DN	196	2.09E-16
HNSCC11_cetux_up	2568	GCNP_SHH_UP_LATE.V1_UP	183	3.31E-16
HNSCC11_cetux_up	2568	E2F1_UP.V1_DN	193	5.03E-16
HNSCC11_cetux_up	2568	MEK_UP.V1_DN	196	8.87E-16
HNSCC11_cetux_up	2568	RB_DN.V1_DN	126	2.40E-15
HNSCC11_cetux_up	2568	EGFR_UP.V1_DN	196	2.08E-14
HNSCC11_cetux_up	2568	CSR_LATE_UP.V1_UP	172	1.04E-13
HNSCC11_cetux_up	2568	STK33_UP	293	1.45E-12
HNSCC11_cetux_up	2568	RB_P130_DN.V1_DN	139	1.93E-12
HNSCC11_cetux_up	2568	ERB2_UP.V1_UP	191	3.50E-12
HNSCC13_cetux_up	81	HALLMARK_INFLAMMATORY_RESPONSE	200	3.40E-26
HNSCC13_cetux_up	81	HALLMARK_TNFA_SIGNALING_VIA_NFKB	200	4.50E-14
HNSCC13_cetux_up	81	HALLMARK_ALLOGRAFT_REJECTION	200	4.57E-08
HNSCC13_cetux_up	81	HALLMARK_COMPLEMENT	200	5.87E-07
HNSCC13_cetux_up	81	HALLMARK_EPITHELIAL_MESENCHYMAL_TRANSITION	200	5.87E-07
HNSCC13_cetux_up	81	HALLMARK_KRAS_SIGNALING_UP	200	5.87E-07
HNSCC13_cetux_up	81	HALLMARK_IL6_JAK_STAT3_SIGNALING	87	1.27E-04
HNSCC13_cetux_up	81	HALLMARK_INTERFERON_GAMMA_RESPONSE	200	1.82E-04
HNSCC13_cetux_up	81	HALLMARK_ANGIOGENESIS	36	2.01E-04
HNSCC13_cetux_up	81	HALLMARK_COAGULATION	138	9.52E-03
HNSCC13_cetux_up	81	HALLMARK_APOPTOSIS	161	1.34E-02
HNSCC13_cetux_up	81	HALLMARK_HYPOXIA	200	2.25E-02
HNSCC13_cetux_up	81	GO_DEFENSE_RESPONSE	1231	1.27E-17
HNSCC13_cetux_up	81	GO_IMMUNE_SYSTEM_PROCESS	1984	3.38E-17
HNSCC13_cetux_up	81	GO_IMMUNE_RESPONSE	1100	1.57E-15
HNSCC13_cetux_up	81	GO_INFLAMMATORY_RESPONSE	454	4.81E-15
HNSCC13_cetux_up	81	GO_LOCOMOTION	1114	2.00E-14
HNSCC13_cetux_up	81	GO_TAXIS	464	6.85E-11
HNSCC13_cetux_up	81	GO_POSITIVE_REGULATION_OF_RESPONSE_TO_STIMULUS	1929	1.08E-10
HNSCC13_cetux_up	81	GO_CELL_CHEMOTAXIS	162	1.88E-10
HNSCC13_cetux_up	81	GO_REGULATION_OF_RESPONSE_TO_WOUNDING	413	2.20E-10
HNSCC13_cetux_up	81	GO_REGULATION_OF_RESPONSE_TO_EXTERNAL_STIMULUS	926	2.20E-10
HNSCC13_cetux_up	81	GO_MOVEMENT_OF_CELL_OR_SUBCELLULAR_COMPONENT	1275	2.72E-10
HNSCC13_cetux_up	81	GO_LEUKOCYTE_CHEMOTAXIS	117	2.72E-10
HNSCC13_cetux_up	81	GO_LEUKOCYTE_MIGRATION	259	4.30E-10
HNSCC13_cetux_up	81	GO_CELL_MOTILITY	835	4.34E-10
HNSCC13_cetux_up	81	GO_RESPONSE_TO_EXTERNAL_STIMULUS	1821	1.33E-09
HNSCC13_cetux_up	81	GO_MYELOID_LEUKOCYTE_MIGRATION	99	2.72E-09
HNSCC13_cetux_up	81	GO_REGULATION_OF_CYTOKINE_PRODUCTION	563	5.59E-09

HNSCC13_cetux_up	81	GO_RESPONSE_TO_OXYGEN_CONTAINING_COMPOUND	1381	6.72E-09
HNSCC13_cetux_up	81	GO_POSITIVE_REGULATION_OF_IMMUNE_SYSTEM_PROCESS	867	7.25E-09
HNSCC13_cetux_up	81	GO_REGULATION_OF_IMMUNE_SYSTEM_PROCESS	1403	7.82E-09
HNSCC13_cetux_up	81	STK33_NOMO_UP	294	3.52E-10
HNSCC13_cetux_up	81	STK33_UP	293	5.40E-08
HNSCC13_cetux_up	81	STK33_SKM_UP	290	8.94E-05
HNSCC13_cetux_up	81	ESC_V6.5_UP_EARLY.V1_DN	172	3.86E-04
HNSCC13_cetux_up	81	P53_DN.V1_UP	194	6.12E-04
HNSCC13_cetux_up	81	PTEN_DN.V2_UP	143	1.49E-03
HNSCC13_cetux_up	81	KRAS.DF.V1_UP	193	4.36E-03
HNSCC13_cetux_up	81	MEK_UP.V1_UP	196	4.36E-03
HNSCC13_cetux_up	81	RAF_UP.V1_UP	196	4.36E-03
HNSCC13_cetux_up	81	RELA_DN.V1_DN	141	1.17E-02
HNSCC13_cetux_up	81	BMI1_DN.V1_UP	147	1.24E-02
HNSCC13_cetux_up	81	KRAS.600_UP.V1_UP	287	1.78E-02
HNSCC13_cetux_up	81	TBK1.DF_UP	290	1.78E-02
HNSCC13_cetux_up	81	ESC_V6.5_UP_LATE.V1_DN	186	1.86E-02
HNSCC13_cetux_up	81	CYCLIN_D1_KE_.V1_UP	190	1.86E-02
HNSCC13_cetux_up	81	ESC_V6.5_UP_LATE.V1_UP	190	1.86E-02
HNSCC13_cetux_up	81	LEF1_UP.V1_DN	190	1.86E-02
HNSCC13_cetux_up	81	ESC_J1_UP_LATE.V1_UP	191	1.86E-02
HNSCC13_cetux_up	81	EGFR_UP.V1_UP	193	1.86E-02
HNSCC13_cetux_up	81	VEGF_A_UP.V1_DN	193	1.86E-02
UMSCC92_EGFR_KO	766	HALLMARK_EPITHELIAL_MESENCHYMAL_TRANSITION	200	1.16E-40
UMSCC92_EGFR_KO	766	HALLMARK_UV_RESPONSE_DN	144	8.91E-23
UMSCC92_EGFR_KO	766	HALLMARK_COAGULATION	138	2.62E-09
UMSCC92_EGFR_KO	766	HALLMARK_APICAL_JUNCTION	200	2.62E-09
UMSCC92_EGFR_KO	766	HALLMARK_COMPLEMENT	200	6.40E-08
UMSCC92_EGFR_KO	766	HALLMARK_HYPOXIA	200	6.40E-08
UMSCC92_EGFR_KO	766	HALLMARK_KRAS_SIGNALING_UP	200	6.40E-08
UMSCC92_EGFR_KO	766	HALLMARK_GLYCOLYSIS	200	1.88E-06
UMSCC92_EGFR_KO	766	HALLMARK_TNFA_SIGNALING_VIA_NFKB	200	7.91E-06
UMSCC92_EGFR_KO	766	HALLMARK_XENOBIOTIC_METABOLISM	200	7.91E-06
UMSCC92_EGFR_KO	766	HALLMARK_ANGIOGENESIS	36	8.67E-06
UMSCC92_EGFR_KO	766	HALLMARK_ADIPOGENESIS	200	2.77E-05
UMSCC92_EGFR_KO	766	HALLMARK_INTERFERON_GAMMA_RESPONSE	200	2.77E-05
UMSCC92_EGFR_KO	766	HALLMARK_OXIDATIVE_PHOSPHORYLATION	200	2.77E-05
UMSCC92_EGFR_KO	766	HALLMARK_IL2_STAT5_SIGNALING	200	1.18E-04
UMSCC92_EGFR_KO	766	HALLMARK_APOPTOSIS	161	2.79E-04
UMSCC92_EGFR_KO	766	HALLMARK_ALLOGRAFT_REJECTION	200	4.40E-04
UMSCC92_EGFR_KO	766	HALLMARK_PROTEIN_SECRETION	96	5.64E-04
UMSCC92_EGFR_KO	766	HALLMARK_INTERFERON_ALPHA_RESPONSE	97	5.64E-04
UMSCC92_EGFR_KO	766	HALLMARK_DNA_REPAIR	150	5.64E-04
UMSCC92_EGFR_KO	766	GGGCGGR_SP1_Q6	2940	2.67E-39
UMSCC92_EGFR_KO	766	TGGAAA_NFAT_Q4_01	1896	6.04E-32
UMSCC92_EGFR_KO	766	GGGAGGRR_MAZ_Q6	2274	1.20E-29
UMSCC92_EGFR_KO	766	CTTTGT_LEF1_Q2	1972	3.04E-21
UMSCC92_EGFR_KO	766	CAGGTG_E12_Q6	2485	5.83E-20
UMSCC92_EGFR_KO	766	GATTGGY_NFY_Q6_01	1160	2.24E-19
UMSCC92_EGFR_KO	766	GGGTGGRR_PAX4_03	1294	2.15E-17
UMSCC92_EGFR_KO	766	TATAAA_TATA_01	1296	1.07E-15
UMSCC92_EGFR_KO	766	TTGTTT_FOXO4_01	2061	3.65E-15
UMSCC92_EGFR_KO	766	TGANTCA_AP1_C	1121	2.33E-14
UMSCC92_EGFR_KO	766	GGGYGTGNY_UNKNOWN	664	2.41E-13
UMSCC92_EGFR_KO	766	AACTTT_UNKNOWN	1890	8.71E-13
UMSCC92_EGFR_KO	766	SCGGAAGY_ELK1_02	1199	4.49E-12
UMSCC92_EGFR_KO	766	GCCATNTTG_YY1_Q6	427	5.18E-12
UMSCC92_EGFR_KO	766	CACGTG_MYC_Q2	1032	1.28E-11
UMSCC92_EGFR_KO	766	CAGCTG_AP4_Q5	1524	1.63E-11
UMSCC92_EGFR_KO	766	TAATTA_CHX10_01	810	4.32E-11
UMSCC92_EGFR_KO	766	CAGTATT_MIR200B_MIR200C_MIR429	469	2.75E-10
UMSCC92_EGFR_KO	766	CTTTAAR_UNKNOWN	972	5.02E-10
UMSCC92_EGFR_KO	766	RTAAACA_FREAC2_01	919	2.61E-09
UMSCC92_EGFR_KO	766	GO_CELLULAR_RESPONSE_TO_ORGANIC_SUBSTANCE	1848	3.38E-19
UMSCC92_EGFR_KO	766	GO_REGULATION_OF_MULTICELLULAR_ORGANISMAL_DEVELOPMENT	1672	1.47E-18

UMSCC92_EGFR_KO	766	GO_POSITIVE_REGULATION_OF_RESPONSE_TO_STIMULUS	1929	2.27E-18
UMSCC92_EGFR_KO	766	GO_REGULATION_OF_INTRACELLULAR_SIGNAL_TRANSDUCTION	1656	5.17E-18
UMSCC92_EGFR_KO	766	GO_PROTEIN_LOCALIZATION	1805	6.18E-18
UMSCC92_EGFR_KO	766	GO_PHOSPHATE_CONTAINING_COMPOUND_METABOLIC_PROCESS	1977	6.18E-18
UMSCC92_EGFR_KO	766	GO_ESTABLISHMENT_OF_LOCALIZATION_IN_CELL	1676	6.37E-18
UMSCC92_EGFR_KO	766	GO_MACROMOLECULAR_COMPLEX_ASSEMBLY	1398	1.01E-17
UMSCC92_EGFR_KO	766	GO_REGULATION_OF_CELL_DIFFERENTIATION	1492	2.80E-17
UMSCC92_EGFR_KO	766	GO_PROTEIN_COMPLEX_SUBUNIT_ORGANIZATION	1527	2.80E-17
UMSCC92_EGFR_KO	766	GO_ORGANONITROGEN_COMPOUND_METABOLIC_PROCESS	1796	2.80E-17
UMSCC92_EGFR_KO	766	GO_TISSUE_DEVELOPMENT	1518	6.28E-17
UMSCC92_EGFR_KO	766	GO_NEGATIVE_REGULATION_OF_RESPONSE_TO_STIMULUS	1360	6.84E-17
UMSCC92_EGFR_KO	766	GO_REGULATION_OF_RESPONSE_TO_STRESS	1468	9.90E-17
UMSCC92_EGFR_KO	766	GO_EXTRACELLULAR_STRUCTURE_ORGANIZATION	304	1.20E-16
UMSCC92_EGFR_KO	766	GO_CATABOLIC_PROCESS	1773	3.20E-16
UMSCC92_EGFR_KO	766	GO_IMMUNE_SYSTEM_PROCESS	1984	9.55E-16
UMSCC92_EGFR_KO	766	GO_BIOLOGICAL_ADHESION	1032	1.39E-15
UMSCC92_EGFR_KO	766	GO_POSITIVE_REGULATION_OF_BIOSYNTHETIC_PROCESS	1805	2.57E-15
UMSCC92_EGFR_KO	766	GO_POSITIVE_REGULATION_OF_GENE_EXPRESSION	1733	7.37E-15
UMSCC92_EGFR_KO	766	BMI1_DN.V1_UP	147	5.81E-17
UMSCC92_EGFR_KO	766	BMI1_DN_MEL18_DN.V1_UP	145	2.68E-16
UMSCC92_EGFR_KO	766	MEL18_DN.V1_UP	141	1.15E-15
UMSCC92_EGFR_KO	766	TBK1.DF_UP	290	8.74E-13
UMSCC92_EGFR_KO	766	LEF1_UP.V1_UP	195	6.90E-10
UMSCC92_EGFR_KO	766	ESC_V6.5_UP_EARLY.V1_DN	172	2.52E-08
UMSCC92_EGFR_KO	766	RB_P107_DN.V1_UP	140	4.00E-07
UMSCC92_EGFR_KO	766	KRAS.DF.V1_UP	193	7.49E-07
UMSCC92_EGFR_KO	766	CAMP_UP.V1_DN	200	1.12E-06
UMSCC92_EGFR_KO	766	KRAS.600_UP.V1_UP	287	1.91E-06
UMSCC92_EGFR_KO	766	ESC_J1_UP_LATE.V1_UP	191	2.76E-06
UMSCC92_EGFR_KO	766	VEGF_A_UP.V1_UP	196	3.60E-06
UMSCC92_EGFR_KO	766	STK33_DN	289	7.45E-06
UMSCC92_EGFR_KO	766	STK33_NOMO_UP	294	8.96E-06
UMSCC92_EGFR_KO	766	CSR_EARLY_UP.V1_UP	164	9.47E-06
UMSCC92_EGFR_KO	766	P53_DN.V1_UP	194	1.28E-05
UMSCC92_EGFR_KO	766	KRAS.600.LUNG.BREAST_UP.V1_UP	288	2.32E-05
UMSCC92_EGFR_KO	766	PTEN_DN.V1_DN	187	3.75E-05
UMSCC92_EGFR_KO	766	CYCLIN_D1_UP.V1_UP	188	3.78E-05
UMSCC92_EGFR_KO	766	CORDENONSI_YAP_CONSERVED_SIGNATURE	57	4.06E-05

Table 4-6. Upregulated gene sets enriched in each of the 13 cetuximab-treated gene sets and EGFR K/O gene sets

Gene set enrichment analysis was performed with significantly upregulated genes from each of the 14 gene sets to identify significant overlap with gene sets in the “Hallmark”, “Motif”, “Go-Biological Process” and “Oncogene” databases with the molecular signatures database v5.1. Node is the sample, and Node Size is the number of input genes from the sample. Gene Set Name is the pathway enriched, with # of Genes in Gene Set being the number of genes in the GSEA pathway being tested.

Node	Node Size	Gene Set Name	# Genes in Gene Set (K)	FDR q-value
HNSCC1_cetux_down	120	HALLMARK_EPITHELIAL_MESENCHYMAL_TRANSITION	200	5.37E-08
HNSCC1_cetux_down	120	HALLMARK_ESTROGEN_RESPONSE_LATE	200	5.37E-08
HNSCC1_cetux_down	120	HALLMARK_P53_PATHWAY	200	5.37E-08
HNSCC1_cetux_down	120	HALLMARK_ESTROGEN_RESPONSE_EARLY	200	7.74E-07
HNSCC1_cetux_down	120	HALLMARK_APICAL_JUNCTION	200	8.71E-06
HNSCC1_cetux_down	120	HALLMARK_HYPOXIA	200	8.71E-06
HNSCC1_cetux_down	120	HALLMARK_KRAS_SIGNALING_DN	200	1.18E-03
HNSCC1_cetux_down	120	HALLMARK_TNFA_SIGNALING_VIA_NFKB	200	1.18E-03
HNSCC1_cetux_down	120	HALLMARK_KRAS_SIGNALING_UP	200	1.07E-02
HNSCC1_cetux_down	120	HALLMARK_COAGULATION	138	2.88E-02
HNSCC1_cetux_down	120	TGANTCA_AP1_C	1121	1.27E-14
HNSCC1_cetux_down	120	AP1_Q2_01	275	7.86E-08
HNSCC1_cetux_down	120	CAGGTG_E12_Q6	2485	3.00E-07
HNSCC1_cetux_down	120	BACH1_01	263	7.22E-06
HNSCC1_cetux_down	120	BACH2_01	271	7.46E-06
HNSCC1_cetux_down	120	TTANTCA_UNKNOWN	952	1.11E-03
HNSCC1_cetux_down	120	GGGCGGR_SP1_Q6	2940	2.82E-03
HNSCC1_cetux_down	120	P53_DECAMER_Q2	256	5.12E-03
HNSCC1_cetux_down	120	SREBP_Q3	258	5.12E-03
HNSCC1_cetux_down	120	GGGYGTGNY_UNKNOWN	664	5.12E-03
HNSCC1_cetux_down	120	AP1_Q4_01	261	5.12E-03
HNSCC1_cetux_down	120	AP1_Q4	271	5.75E-03
HNSCC1_cetux_down	120	GGGAGGRR_MAZ_Q6	2274	5.75E-03
HNSCC1_cetux_down	120	MZF1_01	236	2.41E-02
HNSCC1_cetux_down	120	WGGAATGY_TEF1_Q6	378	2.76E-02
HNSCC1_cetux_down	120	TATAAA_TATA_01	1296	3.10E-02
HNSCC1_cetux_down	120	YCATTAA_UNKNOWN	556	3.10E-02
HNSCC1_cetux_down	120	NFAT_Q4_01	266	3.10E-02
HNSCC1_cetux_down	120	AP1_01	267	3.10E-02
HNSCC1_cetux_down	120	GO_TISSUE_DEVELOPMENT	1518	1.20E-14
HNSCC1_cetux_down	120	GO_EPIDERMIS_DEVELOPMENT	253	5.34E-13
HNSCC1_cetux_down	120	GO_BIOLOGICAL_ADHESION	1032	5.01E-11
HNSCC1_cetux_down	120	GO_EPITHELIUM_DEVELOPMENT	945	6.90E-11
HNSCC1_cetux_down	120	GO_INTERMEDIATE_FILAMENT_BASED_PROCESS	43	1.88E-10
HNSCC1_cetux_down	120	GO_HEMIDESMOSOME_ASSEMBLY	12	1.88E-10
HNSCC1_cetux_down	120	GO_CELL_JUNCTION_ORGANIZATION	185	1.68E-09
HNSCC1_cetux_down	120	GO_CELL_SUBSTRATE_JUNCTION_ASSEMBLY	41	8.03E-09
HNSCC1_cetux_down	120	GO_CELL_JUNCTION_ASSEMBLY	129	3.23E-08
HNSCC1_cetux_down	120	GO_EXTRACELLULAR_STRUCTURE_ORGANIZATION	304	2.41E-07
HNSCC1_cetux_down	120	GO_EXTRACELLULAR_MATRIX_DISASSEMBLY	76	2.12E-05
HNSCC1_cetux_down	120	GO_RESPONSE_TO_INORGANIC_SUBSTANCE	479	2.18E-05
HNSCC1_cetux_down	120	GO_INTERMEDIATE_FILAMENT_ORGANIZATION	20	7.08E-05
HNSCC1_cetux_down	120	GO_RESPONSE_TO_WOUNDING	563	9.32E-05
HNSCC1_cetux_down	120	GO_CELL_MOTILITY	835	9.32E-05
HNSCC1_cetux_down	120	GO_RESPONSE_TO_ZINC_ION	55	9.70E-05
HNSCC1_cetux_down	120	GO_CELL_CELL_ADHESION	608	1.64E-04
HNSCC1_cetux_down	120	GO_MULTICELLULAR_ORGANISMAL_MACROMOLECULE_METABOLIC_PROCESS	79	5.31E-04
HNSCC1_cetux_down	120	GO_RESPONSE_TO_TRANSITION_METAL_NANOPARTICLE	148	6.35E-04
HNSCC1_cetux_down	120	GO_RESPONSE_TO_METAL_ION	333	6.44E-04
HNSCC1_cetux_down	120	RB_DN.V1_DN	126	2.84E-10
HNSCC1_cetux_down	120	KRAS.LUNG.BREAST_UP.V1_DN	145	1.77E-08
HNSCC1_cetux_down	120	KRAS.600_UP.V1_DN	289	3.29E-07
HNSCC1_cetux_down	120	ESC_V6.5_UP_EARLY.V1_DN	172	9.09E-07
HNSCC1_cetux_down	120	P53_DN.V1_UP	194	1.85E-06
HNSCC1_cetux_down	120	KRAS.600.LUNG.BREAST_UP.V1_DN	289	2.43E-06
HNSCC1_cetux_down	120	KRAS.LUNG_UP.V1_DN	145	3.21E-06
HNSCC1_cetux_down	120	AKT_UP.V1_DN	187	1.57E-05
HNSCC1_cetux_down	120	KRAS.300_UP.V1_DN	143	4.68E-05
HNSCC1_cetux_down	120	BMI1_DN.V1_UP	147	4.94E-05

HNSCC1_cetux_down	120	SINGH_KRAS_DEPENDENCY_SIGNATURE_	20	3.29E-04
HNSCC1_cetux_down	120	RB_P130_DN.V1_DN	139	5.28E-04
HNSCC1_cetux_down	120	MEL18_DN.V1_UP	141	5.28E-04
HNSCC1_cetux_down	120	BMI1_DN_MEL18_DN.V1_UP	145	5.61E-04
HNSCC1_cetux_down	120	SNF5_DN.V1_DN	164	9.39E-04
HNSCC1_cetux_down	120	WNT_UP.V1_UP	180	1.36E-03
HNSCC1_cetux_down	120	AKT_UP_MTOR_DN.V1_DN	183	1.39E-03
HNSCC1_cetux_down	120	EGFR_UP.V1_UP	193	1.68E-03
HNSCC1_cetux_down	120	MEK_UP.V1_UP	196	1.71E-03
HNSCC1_cetux_down	120	KRAS.50_UP.V1_DN	49	2.77E-03
HNSCC2_cetux_down	77	HALLMARK_TNFA_SIGNALING_VIA_NFKB	200	1.82E-17
HNSCC2_cetux_down	77	HALLMARK_HYPOXIA	200	1.24E-06
HNSCC2_cetux_down	77	HALLMARK_ESTROGEN_RESPONSE_LATE	200	1.93E-05
HNSCC2_cetux_down	77	HALLMARK_UV_RESPONSE_UP	158	9.12E-05
HNSCC2_cetux_down	77	HALLMARK_ESTROGEN_RESPONSE_EARLY	200	3.06E-03
HNSCC2_cetux_down	77	HALLMARK_P53_PATHWAY	200	3.06E-03
HNSCC2_cetux_down	77	HALLMARK_COMPLEMENT	200	2.60E-02
HNSCC2_cetux_down	77	HALLMARK_EPITHELIAL_MESENCHYMAL_TRANSITION	200	2.60E-02
HNSCC2_cetux_down	77	HALLMARK_KRAS_SIGNALING_DN	200	2.60E-02
HNSCC2_cetux_down	77	CREBP1_Q2	254	6.93E-09
HNSCC2_cetux_down	77	ATF_01	259	6.93E-09
HNSCC2_cetux_down	77	CREB_Q2	263	6.93E-09
HNSCC2_cetux_down	77	SRF_01	50	5.68E-08
HNSCC2_cetux_down	77	E4F1_Q6	289	2.52E-07
HNSCC2_cetux_down	77	SRF_C	211	3.86E-07
HNSCC2_cetux_down	77	CREB_Q2_01	220	4.59E-07
HNSCC2_cetux_down	77	GGGAGGRR_MAZ_Q6	2274	4.89E-07
HNSCC2_cetux_down	77	SRF_Q6	241	7.29E-07
HNSCC2_cetux_down	77	GTGACGY_E4F1_Q6	658	1.13E-06
HNSCC2_cetux_down	77	CREB_01	262	1.14E-06
HNSCC2_cetux_down	77	CREB_Q4	268	1.25E-06
HNSCC2_cetux_down	77	ATF_B	187	2.01E-06
HNSCC2_cetux_down	77	CREB_Q4_01	211	4.26E-06
HNSCC2_cetux_down	77	SRF_Q4	221	5.45E-06
HNSCC2_cetux_down	77	TAXCREB_01	137	6.54E-06
HNSCC2_cetux_down	77	TATAAA_TATA_01	1296	1.14E-05
HNSCC2_cetux_down	77	ATF4_Q2	258	1.26E-05
HNSCC2_cetux_down	77	CREBP1CJUN_01	259	1.26E-05
HNSCC2_cetux_down	77	AML_Q6	266	1.43E-05
HNSCC2_cetux_down	77	GO_REGULATION_OF_PROTEOLYSIS	711	6.02E-08
HNSCC2_cetux_down	77	GO_RESPONSE_TO_REACTIVE_OXYGEN_SPECIES	191	8.58E-08
HNSCC2_cetux_down	77	GO_REGULATION_OF_CELL_DEATH	1472	4.06E-07
HNSCC2_cetux_down	77	GO_RESPONSE_TO_OXIDATIVE_STRESS	352	4.06E-07
HNSCC2_cetux_down	77	GO_TISSUE_DEVELOPMENT	1518	4.06E-07
HNSCC2_cetux_down	77	GO_RESPONSE_TO_OXYGEN_CONTAINING_COMPOUND	1381	7.31E-07
HNSCC2_cetux_down	77	GO_REGULATION_OF_PEPTIDASE_ACTIVITY	392	7.61E-07
HNSCC2_cetux_down	77	GO_NEGATIVE_REGULATION_OF_PROTEOLYSIS	329	2.58E-06
HNSCC2_cetux_down	77	GO_POSITIVE_REGULATION_OF_CELL_DEATH	605	2.82E-06
HNSCC2_cetux_down	77	GO_NEGATIVE_REGULATION_OF_PEPTIDASE_ACTIVITY	245	3.96E-06
HNSCC2_cetux_down	77	GO_NEGATIVE_REGULATION_OF_HYDROLASE_ACTIVITY	397	8.70E-06
HNSCC2_cetux_down	77	GO_NEGATIVE_REGULATION_OF_GENE_EXPRESSION	1493	8.70E-06
HNSCC2_cetux_down	77	GO_NEGATIVE_REGULATION_OF_PROTEIN_METABOLIC_PROCESS	1087	1.01E-05
HNSCC2_cetux_down	77	GO_RESPONSE_TO_HYDROGEN_PEROXIDE	109	1.01E-05
HNSCC2_cetux_down	77	GO_PEPTIDE_CROSS_LINKING	56	1.22E-05
HNSCC2_cetux_down	77	GO_NEGATIVE_REGULATION_OF_TRANSCRIPTION_FROM_RNA_POLYMERASE_II_PROMOTER	740	1.24E-05
HNSCC2_cetux_down	77	GO_SKIN_DEVELOPMENT	211	1.86E-05
HNSCC2_cetux_down	77	GO_RESPONSE_TO_INORGANIC_SUBSTANCE	479	2.86E-05
HNSCC2_cetux_down	77	GO_RESPONSE_TO_ABIOTIC_STIMULUS	1024	3.19E-05
HNSCC2_cetux_down	77	GO_RESPONSE_TO_STEROID_HORMONE	497	3.44E-05
HNSCC2_cetux_down	77	RELA_DN.V1_UP	149	3.89E-05
HNSCC2_cetux_down	77	CORDENONSI_YAP_CONSERVED_SIGNATURE	57	2.54E-04
HNSCC2_cetux_down	77	PDGF_UP.V1_UP	146	3.13E-04
HNSCC2_cetux_down	77	ESC_J1_UP_LATE.V1_UP	191	8.62E-04
HNSCC2_cetux_down	77	BMI1_DN.V1_DN	144	2.90E-03
HNSCC2_cetux_down	77	KRAS.PROSTATE_UP.V1_DN	144	2.90E-03

HNSCC2_cetux_down	77	MEL18_DN.V1_DN	148	2.90E-03
HNSCC2_cetux_down	77	STK33_SKM_UP	290	2.90E-03
HNSCC2_cetux_down	77	STK33_UP	293	2.90E-03
HNSCC2_cetux_down	77	MTOR_UP.V1_DN	184	4.85E-03
HNSCC2_cetux_down	77	CYCLIN_D1_UP.V1_UP	188	4.85E-03
HNSCC2_cetux_down	77	EGFR_UP.V1_UP	193	4.85E-03
HNSCC2_cetux_down	77	HOXA9_DN.V1_DN	195	4.85E-03
HNSCC2_cetux_down	77	CAMP_UP.V1_DN	200	4.96E-03
HNSCC2_cetux_down	77	BMI1_DN_MEL18_DN.V1_UP	145	2.28E-02
HNSCC2_cetux_down	77	BMI1_DN_MEL18_DN.V1_DN	147	2.28E-02
HNSCC2_cetux_down	77	PDGF_ERK_DN.V1_DN	149	2.28E-02
HNSCC2_cetux_down	77	ESC_V6.5_UP_EARLY.V1_DN	172	2.81E-02
HNSCC2_cetux_down	77	ESC_J1_UP_EARLY.V1_DN	179	2.81E-02
HNSCC2_cetux_down	77	AKT_UP_MTOR_DN.V1_DN	183	2.81E-02
HNSCC3_cetux_down	242	HALLMARK_GLYCOLYSIS	200	1.77E-02
HNSCC3_cetux_down	242	HALLMARK_XENOBIOTIC_METABOLISM	200	1.77E-02
HNSCC3_cetux_down	242	HALLMARK_FATTY_ACID_METABOLISM	158	2.59E-02
HNSCC3_cetux_down	242	HALLMARK_MYC_TARGETS_V2	58	3.07E-02
HNSCC3_cetux_down	242	HALLMARK_ADIPOGENESIS	200	3.07E-02
HNSCC3_cetux_down	242	HALLMARK_G2M_CHECKPOINT	200	3.07E-02
HNSCC3_cetux_down	242	HALLMARK_OXIDATIVE_PHOSPHORYLATION	200	3.07E-02
HNSCC3_cetux_down	242	SCGGAAGY_ELK1_02	1199	7.09E-04
HNSCC3_cetux_down	242	GGGCGGR_SP1_Q6	2940	7.09E-04
HNSCC3_cetux_down	242	MGGAAGTG_GABP_B	757	7.09E-04
HNSCC3_cetux_down	242	SGCGSSAAA_E2F1DP2_01	168	7.09E-04
HNSCC3_cetux_down	242	TGGAAA_NFAT_Q4_01	1896	1.35E-03
HNSCC3_cetux_down	242	TGACAGNY_MEIS1_01	827	1.35E-03
HNSCC3_cetux_down	242	CYTAGCAAY_UNKNOWN	147	1.67E-03
HNSCC3_cetux_down	242	E2F1_Q6	232	2.31E-03
HNSCC3_cetux_down	242	TEL2_Q6	233	2.31E-03
HNSCC3_cetux_down	242	ATAAGCT_MIR21	116	2.31E-03
HNSCC3_cetux_down	242	E2F1DP1_01	235	2.31E-03
HNSCC3_cetux_down	242	E2F1DP2_01	235	2.31E-03
HNSCC3_cetux_down	242	E2F4DP2_01	235	2.31E-03
HNSCC3_cetux_down	242	E2F_02	235	2.31E-03
HNSCC3_cetux_down	242	E2F4DP1_01	239	2.42E-03
HNSCC3_cetux_down	242	YYCATTCAWW_UNKNOWN	191	3.89E-03
HNSCC3_cetux_down	242	ER_Q6_01	269	4.88E-03
HNSCC3_cetux_down	242	E2F_Q6	232	1.15E-02
HNSCC3_cetux_down	242	E2F_Q4	234	1.15E-02
HNSCC3_cetux_down	242	WTGAAAT_UNKNOWN	616	1.98E-02
HNSCC3_cetux_down	242	GO_MACROMOLECULAR_COMPLEX_ASSEMBLY	1398	4.27E-03
HNSCC3_cetux_down	242	GO_CHROMOSOME_ORGANIZATION	1009	4.27E-03
HNSCC3_cetux_down	242	GO_PROTEIN_COMPLEX_BIOGENESIS	1132	4.27E-03
HNSCC3_cetux_down	242	GO_RECEPTOR_MEDIATED_ENDOCYTOSIS	231	4.76E-03
HNSCC3_cetux_down	242	GO_ORGANELLE_FUSION	131	5.85E-03
HNSCC3_cetux_down	242	GO_CELLULAR_MACROMOLECULAR_COMPLEX_ASSEMBLY	727	6.42E-03
HNSCC3_cetux_down	242	GO_CARBOHYDRATE_DERIVATIVE_METABOLIC_PROCESS	1047	8.37E-03
HNSCC3_cetux_down	242	GO_POSITIVE_REGULATION_OF_IMMUNE_SYSTEM_PROCESS	867	9.54E-03
HNSCC3_cetux_down	242	GO_PROTEIN_COMPLEX_SUBUNIT_ORGANIZATION	1527	1.08E-02
HNSCC3_cetux_down	242	GO_SMALL_MOLECULE_METABOLIC_PROCESS	1767	1.08E-02
HNSCC3_cetux_down	242	GO_DEFENSE_RESPONSE	1231	1.34E-02
HNSCC3_cetux_down	242	GO_BIOLOGICAL_ADHESION	1032	1.34E-02
HNSCC3_cetux_down	242	GO_RESPONSE_TO_EXTERNAL_STIMULUS	1821	1.34E-02
HNSCC3_cetux_down	242	GO_CHROMATIN_ORGANIZATION	663	1.84E-02
HNSCC3_cetux_down	242	GO_SINGLE_ORGANISM_MEMBRANE_FUSION	128	1.88E-02
HNSCC3_cetux_down	242	GO_ORGANONITROGEN_COMPOUND_METABOLIC_PROCESS	1796	2.43E-02
HNSCC3_cetux_down	242	GO_CELLULAR_PROTEIN_COMPLEX_ASSEMBLY	346	2.66E-02
HNSCC3_cetux_down	242	GO_VESICLE_MEDIATED_TRANSPORT	1239	2.82E-02
HNSCC3_cetux_down	242	GO_METHYLATION	284	3.21E-02
HNSCC3_cetux_down	242	GO_IMMUNE_SYSTEM_PROCESS	1984	3.21E-02
HNSCC3_cetux_down	242	CRX_NRL_DN.V1_UP	140	1.93E-03
HNSCC3_cetux_down	242	ESC_V6.5_UP_LATE.V1_UP	190	5.54E-03
HNSCC3_cetux_down	242	NRL_DN.V1_UP	136	5.54E-03
HNSCC3_cetux_down	242	PTEN_DN.V2_UP	143	5.54E-03
HNSCC3_cetux_down	242	CYCLIN_D1_UP.V1_UP	188	1.67E-02

HNSCC3_cetux_down	242	E2F1_UP.V1_DN	193	1.67E-02
HNSCC3_cetux_down	242	HOXA9_DN.V1_DN	195	1.67E-02
HNSCC4_cetux_down	255	HALLMARK_MYOGENESIS	200	2.40E-72
HNSCC4_cetux_down	255	HALLMARK_KRAS_SIGNALING_DN	200	3.99E-08
HNSCC4_cetux_down	255	HALLMARK_APICAL_JUNCTION	200	2.59E-06
HNSCC4_cetux_down	255	HALLMARK_EPITHELIAL_MESENCHYMAL_TRANSITION	200	2.59E-06
HNSCC4_cetux_down	255	HALLMARK_ESTROGEN_RESPONSE_LATE	200	1.14E-03
HNSCC4_cetux_down	255	HALLMARK_HYPOXIA	200	1.14E-03
HNSCC4_cetux_down	255	HALLMARK_ESTROGEN_RESPONSE_EARLY	200	6.61E-03
HNSCC4_cetux_down	255	CAGCTG_AP4_Q5	1524	9.31E-41
HNSCC4_cetux_down	255	CAGGTG_E12_Q6	2485	8.18E-33
HNSCC4_cetux_down	255	YTATTTTNR_MEF2_02	697	2.71E-29
HNSCC4_cetux_down	255	CTAWWWATA_RSRFC4_Q2	361	5.61E-29
HNSCC4_cetux_down	255	GCANCTGNY_MYOD_Q6	924	1.14E-27
HNSCC4_cetux_down	255	MEF2_02	228	3.61E-24
HNSCC4_cetux_down	255	RSRFC4_01	245	4.61E-18
HNSCC4_cetux_down	255	RSRFC4_Q2	214	9.66E-17
HNSCC4_cetux_down	255	TGACCTY_ERR1_Q2	1043	1.87E-15
HNSCC4_cetux_down	255	TAAWWATAG_RSRFC4_Q2	165	6.29E-15
HNSCC4_cetux_down	255	MEF2_Q6_01	244	1.61E-14
HNSCC4_cetux_down	255	AMEF2_Q6	259	4.46E-14
HNSCC4_cetux_down	255	E12_Q6	262	5.09E-14
HNSCC4_cetux_down	255	TGGAAA_NFAT_Q4_01	1896	5.17E-14
HNSCC4_cetux_down	255	GGGTGGRR_PAX4_03	1294	1.16E-13
HNSCC4_cetux_down	255	MEF2_03	238	1.16E-13
HNSCC4_cetux_down	255	MEF2_01	144	2.14E-13
HNSCC4_cetux_down	255	TGANTCA_AP1_C	1121	3.46E-13
HNSCC4_cetux_down	255	HMEF2_Q6	138	2.31E-12
HNSCC4_cetux_down	255	TATAAA_TATA_01	1296	3.18E-12
HNSCC4_cetux_down	255	GO_MUSCLE_CONTRACTION	233	1.66E-45
HNSCC4_cetux_down	255	GO_MUSCLE_SYSTEM_PROCESS	282	2.33E-45
HNSCC4_cetux_down	255	GO_MUSCLE_STRUCTURE_DEVELOPMENT	432	5.94E-43
HNSCC4_cetux_down	255	GO_ACTIN_MYOSIN_FILAMENT_SLIDING	38	2.13E-37
HNSCC4_cetux_down	255	GO_ACTIN_FILAMENT_BASED_PROCESS	450	1.91E-35
HNSCC4_cetux_down	255	GO_MUSCLE_CELL_DEVELOPMENT	128	5.13E-32
HNSCC4_cetux_down	255	GO_MUSCLE_CELL_DIFFERENTIATION	237	8.67E-32
HNSCC4_cetux_down	255	GO_ACTIN_MEDIATED_CELL_CONTRACTION	74	1.46E-29
HNSCC4_cetux_down	255	GO_MUSCLE_ORGAN_DEVELOPMENT	277	3.01E-28
HNSCC4_cetux_down	255	GO_ACTIN_FILAMENT_BASED_MOVEMENT	93	3.54E-27
HNSCC4_cetux_down	255	GO_TISSUE_DEVELOPMENT	1518	3.64E-27
HNSCC4_cetux_down	255	GO_MYOFIBRIL_ASSEMBLY	48	3.15E-26
HNSCC4_cetux_down	255	GO_ACTOMYOSIN_STRUCTURE_ORGANIZATION	77	1.36E-25
HNSCC4_cetux_down	255	GO_STRIATED_MUSCLE_CELL_DIFFERENTIATION	173	1.73E-25
HNSCC4_cetux_down	255	GO_SYSTEM_PROCESS	1785	8.37E-24
HNSCC4_cetux_down	255	GO_STRIATED_MUSCLE_CONTRACTION	99	2.89E-23
HNSCC4_cetux_down	255	GO_MOVEMENT_OF_CELL_OR_SUBCELLULAR_COMPONENT	1275	1.06E-20
HNSCC4_cetux_down	255	GO_REGULATION_OF_SYSTEM_PROCESS	507	1.55E-20
HNSCC4_cetux_down	255	GO_MUSCLE_TISSUE_DEVELOPMENT	275	3.31E-19
HNSCC4_cetux_down	255	GO_CYTOSKELETON_ORGANIZATION	838	5.25E-19
HNSCC4_cetux_down	255	MTOR_UP.V1_DN	184	7.01E-08
HNSCC4_cetux_down	255	ATF2_S_UP.V1_DN	187	7.01E-08
HNSCC4_cetux_down	255	AKT_UP.V1_DN	187	5.99E-07
HNSCC4_cetux_down	255	KRAS.600.LUNG.BREAST_UP.V1_DN	289	4.01E-06
HNSCC4_cetux_down	255	ESC_J1_UP_LATE.V1_UP	191	4.01E-06
HNSCC4_cetux_down	255	KRAS.LUNG_UP.V1_DN	145	4.01E-06
HNSCC4_cetux_down	255	IL21_UP.V1_UP	193	4.01E-06
HNSCC4_cetux_down	255	SNF5_DN.V1_DN	164	9.16E-06
HNSCC4_cetux_down	255	ESC_V6.5_UP_EARLY.V1_DN	172	1.22E-05
HNSCC4_cetux_down	255	STK33_SKM_DN	288	1.41E-05
HNSCC4_cetux_down	255	KRAS.LUNG.BREAST_UP.V1_DN	145	2.86E-05
HNSCC4_cetux_down	255	ALK_DN.V1_DN	148	3.06E-05
HNSCC4_cetux_down	255	KRAS.600_UP.V1_DN	289	8.34E-05
HNSCC4_cetux_down	255	ATF2_UP.V1_DN	187	1.47E-04
HNSCC4_cetux_down	255	CYCLIN_D1_UP.V1_DN	191	1.50E-04
HNSCC4_cetux_down	255	ERB2_UP.V1_UP	191	1.50E-04
HNSCC4_cetux_down	255	PRC2_SUZ12_UP.V1_DN	194	1.55E-04

HNSCC4_cetux_down	255	LEF1_UP.V1_UP	195	1.55E-04
HNSCC4_cetux_down	255	PTEN_DN.V2_UP	143	1.63E-04
HNSCC4_cetux_down	255	NFE2L2.V2	481	1.69E-04
HNSCC5_cetux_down	352	HALLMARK_ALLOGRAFT_REJECTION	200	9.49E-05
HNSCC5_cetux_down	352	HALLMARK_KRAS_SIGNALING_UP	200	9.49E-05
HNSCC5_cetux_down	352	HALLMARK_COMPLEMENT	200	4.46E-04
HNSCC5_cetux_down	352	HALLMARK_ADIPOGENESIS	200	2.92E-02
HNSCC5_cetux_down	352	HALLMARK_ESTROGEN_RESPONSE_EARLY	200	2.92E-02
HNSCC5_cetux_down	352	HALLMARK_ESTROGEN_RESPONSE_LATE	200	2.92E-02
HNSCC5_cetux_down	352	HALLMARK_MYOGENESIS	200	2.92E-02
HNSCC5_cetux_down	352	HALLMARK_APICAL_SURFACE	44	2.92E-02
HNSCC5_cetux_down	352	HALLMARK_REACTIVE_OXIGEN_SPECIES_PATHWAY	49	3.51E-02
HNSCC5_cetux_down	352	HALLMARK_APOPTOSIS	161	4.11E-02
HNSCC5_cetux_down	352	RGAGGAARY_PU1_Q6	502	4.51E-05
HNSCC5_cetux_down	352	PEA3_Q6	255	4.51E-05
HNSCC5_cetux_down	352	CAGGTG_E12_Q6	2485	9.11E-04
HNSCC5_cetux_down	352	RYTTCCTG_ETS2_B	1085	9.11E-04
HNSCC5_cetux_down	352	ETS1_B	259	1.00E-03
HNSCC5_cetux_down	352	ELK1_01	269	1.19E-03
HNSCC5_cetux_down	352	RTAAACA_FREAC2_01	919	1.26E-02
HNSCC5_cetux_down	352	ELF1_Q6	244	1.26E-02
HNSCC5_cetux_down	352	NERF_Q2	247	1.26E-02
HNSCC5_cetux_down	352	GGGTGGRR_PAX4_03	1294	1.60E-02
HNSCC5_cetux_down	352	TEL2_Q6	233	3.37E-02
HNSCC5_cetux_down	352	PU1_Q6	234	3.37E-02
HNSCC5_cetux_down	352	ETS_Q4	247	4.43E-02
HNSCC5_cetux_down	352	GO_IMMUNE_SYSTEM_PROCESS	1984	2.18E-26
HNSCC5_cetux_down	352	GO_IMMUNE_RESPONSE	1100	4.01E-18
HNSCC5_cetux_down	352	GO_REGULATION_OF_IMMUNE_SYSTEM_PROCESS	1403	4.95E-17
HNSCC5_cetux_down	352	GO_ADAPTIVE_IMMUNE_RESPONSE	288	6.55E-16
HNSCC5_cetux_down	352	GO_REGULATION_OF_CELL_ACTIVATION	484	2.01E-15
HNSCC5_cetux_down	352	GO_ACTIVATION_OF_IMMUNE_RESPONSE	427	5.36E-14
HNSCC5_cetux_down	352	GO_IMMUNE_RESPONSE_REGULATING_CELL_SURFACE_RECEPTOR_SIGNALING_PATHWAY	323	6.76E-14
HNSCC5_cetux_down	352	GO_POSITIVE_REGULATION_OF_IMMUNE_RESPONSE	563	7.76E-14
HNSCC5_cetux_down	352	GO_B_CELL_RECEPTOR_SIGNALING_PATHWAY	54	1.03E-13
HNSCC5_cetux_down	352	GO_LEUKOCYTE_ACTIVATION	414	1.44E-13
HNSCC5_cetux_down	352	GO_HUMORAL_IMMUNE_RESPONSE	187	2.27E-13
HNSCC5_cetux_down	352	GO_ANTIGEN_RECEPTOR_MEDIATED_SIGNALING_PATHWAY	195	4.55E-13
HNSCC5_cetux_down	352	GO_B_CELL_MEDIATED_IMMUNITY	99	5.59E-13
HNSCC5_cetux_down	352	GO_POSITIVE_REGULATION_OF_IMMUNE_SYSTEM_PROCESS	867	5.75E-13
HNSCC5_cetux_down	352	GO_LYMPHOCYTE_ACTIVATION	342	1.19E-12
HNSCC5_cetux_down	352	GO_REGULATION_OF_IMMUNE_RESPONSE	858	2.22E-12
HNSCC5_cetux_down	352	GO_CELL_ACTIVATION	568	2.72E-12
HNSCC5_cetux_down	352	GO_ADAPTIVE_IMMUNE_RESPONSE_BASED_ON_SOMATIC_RECOMBINATION_OF_IMMUNE_RECEPTORS_BUILT_FROM_IMMUNOGLOBULIN_SUPERFAMILY_DOMAINS	154	2.02E-11
HNSCC5_cetux_down	352	GO_IMMUNE_EFFECTOR_PROCESS	486	2.64E-11
HNSCC5_cetux_down	352	GO_LEUKOCYTE_MEDIATED_IMMUNITY	189	3.30E-11
HNSCC5_cetux_down	352	CYCLIN_D1_KE_.V1_DN	194	6.81E-05
HNSCC5_cetux_down	352	KRAS.600.LUNG.BREAST_UP.V1_DN	289	1.38E-03
HNSCC5_cetux_down	352	LEF1_UP.V1_UP	195	1.38E-03
HNSCC5_cetux_down	352	SNF5_DN.V1_UP	177	3.43E-03
HNSCC5_cetux_down	352	PTEN_DN.V2_UP	143	3.68E-03
HNSCC5_cetux_down	352	ATF2_UP.V1_UP	192	3.68E-03
HNSCC5_cetux_down	352	KRAS.LUNG.BREAST_UP.V1_UP	145	3.68E-03
HNSCC5_cetux_down	352	KRAS.600.LUNG.BREAST_UP.V1_UP	288	8.81E-03
HNSCC5_cetux_down	352	STK33_SKM_DN	288	8.81E-03
HNSCC5_cetux_down	352	AKT_UP_MTOR_DN.V1_UP	184	1.00E-02
HNSCC5_cetux_down	352	CYCLIN_D1_UP.V1_DN	191	1.00E-02
HNSCC5_cetux_down	352	JNK_DN.V1_UP	192	1.00E-02
HNSCC5_cetux_down	352	PRC1_BMI_UP.V1_UP	192	1.00E-02
HNSCC5_cetux_down	352	RPS14_DN.V1_UP	192	1.00E-02
HNSCC5_cetux_down	352	VEGF_A_UP.V1_UP	196	1.06E-02
HNSCC5_cetux_down	352	KRAS.LUNG_UP.V1_DN	145	1.09E-02
HNSCC5_cetux_down	352	STK33_SKM_UP	290	2.12E-02

HNSCC5_cetux_down	352	CSR_LATE_UP.V1_DN	170	2.18E-02
HNSCC5_cetux_down	352	PTEN_DN.V1_DN	187	3.13E-02
HNSCC5_cetux_down	352	ESC_V6.5_UP_LATE.V1_UP	190	3.13E-02
HNSCC6_cetux_down	157	HALLMARK_APICAL_SURFACE	44	8.71E-03
HNSCC6_cetux_down	157	HALLMARK_IL2_STAT5_SIGNALING	200	8.71E-03
HNSCC6_cetux_down	157	HALLMARK_ESTROGEN_RESPONSE_LATE	200	3.89E-02
HNSCC6_cetux_down	157	HALLMARK_KRAS_SIGNALING_DN	200	3.89E-02
HNSCC6_cetux_down	157	TGANTCA_AP1_C	1121	3.85E-05
HNSCC6_cetux_down	157	TATAAA_TATA_01	1296	7.38E-04
HNSCC6_cetux_down	157	GO_KERATINOCYTE_DIFFERENTIATION	101	2.37E-14
HNSCC6_cetux_down	157	GO_KERATINIZATION	50	7.61E-13
HNSCC6_cetux_down	157	GO_EPIDERMAL_CELL_DIFFERENTIATION	142	7.61E-13
HNSCC6_cetux_down	157	GO_PEPTIDE_CROSS_LINKING	56	1.39E-12
HNSCC6_cetux_down	157	GO_EPIDERMIS_DEVELOPMENT	253	1.61E-12
HNSCC6_cetux_down	157	GO_SKIN_DEVELOPMENT	211	6.65E-11
HNSCC6_cetux_down	157	GO_EPITHELIAL_CELL_DIFFERENTIATION	495	1.10E-10
HNSCC6_cetux_down	157	GO_TISSUE_DEVELOPMENT	1518	1.34E-08
HNSCC6_cetux_down	157	GO_EPITHELIUM_DEVELOPMENT	945	3.31E-08
HNSCC6_cetux_down	157	GO_SEQUESTERING_OF_METAL_ION	11	1.86E-03
HNSCC6_cetux_down	157	GO_PROTEOLYSIS	1208	6.63E-03
HNSCC6_cetux_down	157	GO_IMMUNE_SYSTEM_PROCESS	1984	9.84E-03
HNSCC6_cetux_down	157	GO_ZINC_ION_HOMEOSTASIS	21	1.13E-02
HNSCC6_cetux_down	157	GO_CELLULAR_TRANSITION_METAL_ION_HOMEOSTASIS	77	2.74E-02
HNSCC6_cetux_down	157	GO_IMMUNE_RESPONSE	1100	3.54E-02
HNSCC6_cetux_down	157	KRAS.PROSTATE_UP.V1_DN	144	2.20E-09
HNSCC6_cetux_down	157	KRAS.LUNG_UP.V1_DN	145	2.20E-09
HNSCC6_cetux_down	157	KRAS.50_UP.V1_DN	49	4.98E-07
HNSCC6_cetux_down	157	KRAS.600_UP.V1_DN	289	1.30E-04
HNSCC6_cetux_down	157	KRAS.300_UP.V1_DN	143	1.58E-04
HNSCC6_cetux_down	157	KRAS.BREAST_UP.V1_UP	146	1.58E-04
HNSCC6_cetux_down	157	P53_DN.V2_UP	148	1.58E-04
HNSCC6_cetux_down	157	EGFR_UP.V1_UP	193	6.24E-04
HNSCC6_cetux_down	157	AKT_UP.V1_UP	172	3.65E-03
HNSCC6_cetux_down	157	RAPA_EARLY_UP.V1_UP	183	4.03E-03
HNSCC6_cetux_down	157	AKT_UP_MTOR_DN.V1_UP	184	4.03E-03
HNSCC6_cetux_down	157	PTEN_DN.V1_DN	187	4.03E-03
HNSCC6_cetux_down	157	ERB2_UP.V1_UP	191	4.09E-03
HNSCC6_cetux_down	157	P53_DN.V1_UP	194	4.09E-03
HNSCC6_cetux_down	157	RB_P130_DN.V1_DN	139	1.01E-02
HNSCC6_cetux_down	157	RELA_DN.V1_DN	141	1.01E-02
HNSCC6_cetux_down	157	PTEN_DN.V2_UP	143	1.01E-02
HNSCC6_cetux_down	157	KRAS.LUNG.BREAST_UP.V1_DN	145	1.01E-02
HNSCC6_cetux_down	157	KRAS.600.LUNG.BREAST_UP.V1_DN	289	1.73E-02
HNSCC6_cetux_down	157	TBK1.DF_UP	290	1.73E-02
HNSCC7_cetux_down	404	HALLMARK_OXIDATIVE_PHOSPHORYLATION	200	9.31E-05
HNSCC7_cetux_down	404	HALLMARK_E2F_TARGETS	200	4.24E-03
HNSCC7_cetux_down	404	HALLMARK_MYC_TARGETS_V1	200	4.24E-03
HNSCC7_cetux_down	404	HALLMARK_MYOGENESIS	200	4.24E-03
HNSCC7_cetux_down	404	HALLMARK_P53_PATHWAY	200	4.24E-03
HNSCC7_cetux_down	404	HALLMARK_REACTIVE_OXIGEN_SPECIES_PATHWAY	49	7.60E-03
HNSCC7_cetux_down	404	HALLMARK_ADIPOGENESIS	200	1.48E-02
HNSCC7_cetux_down	404	HALLMARK_APOPTOSIS	161	1.77E-02
HNSCC7_cetux_down	404	HALLMARK_BILE_ACID_METABOLISM	112	1.77E-02
HNSCC7_cetux_down	404	HALLMARK_APICAL_JUNCTION	200	4.01E-02
HNSCC7_cetux_down	404	HALLMARK_COMPLEMENT	200	4.01E-02
HNSCC7_cetux_down	404	GGGCGGR_SP1_Q6	2940	3.60E-07
HNSCC7_cetux_down	404	MGGAAGTG_GABP_B	757	3.59E-05
HNSCC7_cetux_down	404	CAGGTG_E12_Q6	2485	3.59E-05
HNSCC7_cetux_down	404	AACTTT_UNKNOWN	1890	5.56E-05
HNSCC7_cetux_down	404	ETS_Q4	247	5.56E-05
HNSCC7_cetux_down	404	GGGAGGRR_MAZ_Q6	2274	5.56E-05
HNSCC7_cetux_down	404	STAT6_02	258	6.88E-05
HNSCC7_cetux_down	404	CTTTGA_LEF1_Q2	1232	6.88E-05
HNSCC7_cetux_down	404	TTGCACT_MIR130A_MIR301_MIR130B	403	6.88E-05
HNSCC7_cetux_down	404	CAGCTG_AP4_Q5	1524	7.26E-05
HNSCC7_cetux_down	404	SCGGAAGY_ELK1_02	1199	2.69E-04

HNSCC7_cetux_down	404	STAT_Q6	260	2.75E-04
HNSCC7_cetux_down	404	RORA1_01	242	7.38E-04
HNSCC7_cetux_down	404	CTGCAGY_UNKNOWN	765	1.11E-03
HNSCC7_cetux_down	404	RCGCANGCGY_NRF1_Q6	918	1.50E-03
HNSCC7_cetux_down	404	GATTGGY_NFY_Q6_01	1160	2.30E-03
HNSCC7_cetux_down	404	TGACAGNY_MEIS1_01	827	2.70E-03
HNSCC7_cetux_down	404	TTTGCAC_MIR19A_MIR19B	516	2.96E-03
HNSCC7_cetux_down	404	E2F1_Q3_01	247	3.16E-03
HNSCC7_cetux_down	404	TAL1BETAE47_01	248	3.16E-03
HNSCC7_cetux_down	404	GO_REGULATION_OF_IMMUNE_SYSTEM_PROCESS	1403	6.00E-12
HNSCC7_cetux_down	404	GO_POSITIVE_REGULATION_OF_MOLECULAR_FUNCTION	1791	2.37E-11
HNSCC7_cetux_down	404	GO_ORGANONITROGEN_COMPOUND_METABOLIC_PROCESS	1796	2.37E-11
HNSCC7_cetux_down	404	GO_POSITIVE_REGULATION_OF_IMMUNE_SYSTEM_PROCESS	867	2.37E-11
HNSCC7_cetux_down	404	GO_OXIDATION_REDUCTION_PROCESS	898	2.74E-10
HNSCC7_cetux_down	404	GO_REGULATION_OF_IMMUNE_RESPONSE	858	3.19E-10
HNSCC7_cetux_down	404	GO_IMMUNE_SYSTEM_PROCESS	1984	5.80E-09
HNSCC7_cetux_down	404	GO_PROTEIN_LOCALIZATION	1805	6.91E-09
HNSCC7_cetux_down	404	GO_POSITIVE_REGULATION_OF_CATALYTIC_ACTIVITY	1518	1.09E-08
HNSCC7_cetux_down	404	GO_POSITIVE_REGULATION_OF_IMMUNE_RESPONSE	563	2.48E-08
HNSCC7_cetux_down	404	GO_POSITIVE_REGULATION_OF_RESPONSE_TO_STIMULUS	1929	4.79E-08
HNSCC7_cetux_down	404	GO_ACTIVATION_OF_IMMUNE_RESPONSE	427	1.16E-07
HNSCC7_cetux_down	404	GO_IMMUNE_RESPONSE	1100	1.16E-07
HNSCC7_cetux_down	404	GO_RNA_PROCESSING	835	7.14E-07
HNSCC7_cetux_down	404	GO_CATABOLIC_PROCESS	1773	7.56E-07
HNSCC7_cetux_down	404	GO_IMMUNE_RESPONSE_REGULATING_CELL_SURFACE_RECEPTOR_SIGNALING_PATHWAY	323	1.54E-06
HNSCC7_cetux_down	404	GO_ESTABLISHMENT_OF_PROTEIN_LOCALIZATION	1423	1.54E-06
HNSCC7_cetux_down	404	GO_PHOSPHATE_CONTAINING_COMPOUND_METABOLIC_PROCESS	1977	1.79E-06
HNSCC7_cetux_down	404	GO_CELLULAR_CATABOLIC_PROCESS	1322	2.32E-06
HNSCC7_cetux_down	404	GO_SMALL_MOLECULE_METABOLIC_PROCESS	1767	4.26E-06
HNSCC7_cetux_down	404	KRAS.600.LUNG.BREAST_UP.V1_DN	289	1.10E-02
HNSCC7_cetux_down	404	TBK1.DF_DN	287	1.14E-02
HNSCC7_cetux_down	404	IL21_UP.V1_DN	187	1.14E-02
HNSCC7_cetux_down	404	PTEN_DN.V1_DN	187	1.14E-02
HNSCC7_cetux_down	404	CYCLIN_D1_KE_.V1_UP	190	1.14E-02
HNSCC7_cetux_down	404	WNT_UP.V1_DN	170	2.56E-02
HNSCC7_cetux_down	404	STK33_SKM_UP	290	2.87E-02
HNSCC7_cetux_down	404	STK33_UP	293	2.87E-02
HNSCC7_cetux_down	404	ESC_J1_UP_LATE.V1_DN	186	2.87E-02
HNSCC7_cetux_down	404	IL15_UP.V1_DN	190	2.90E-02
HNSCC7_cetux_down	404	KRAS.DF.V1_UP	193	2.90E-02
HNSCC7_cetux_down	404	RAF_UP.V1_UP	196	2.90E-02
HNSCC8_cetux_down	334	HALLMARK_ESTROGEN_RESPONSE_EARLY	200	3.78E-14
HNSCC8_cetux_down	334	HALLMARK_ESTROGEN_RESPONSE_LATE	200	7.66E-09
HNSCC8_cetux_down	334	HALLMARK_P53_PATHWAY	200	5.45E-08
HNSCC8_cetux_down	334	HALLMARK_APOPTOSIS	161	4.13E-06
HNSCC8_cetux_down	334	HALLMARK_APICAL_SURFACE	44	9.85E-05
HNSCC8_cetux_down	334	HALLMARK_IL2_STAT5_SIGNALING	200	9.85E-05
HNSCC8_cetux_down	334	HALLMARK_KRAS_SIGNALING_DN	200	9.85E-05
HNSCC8_cetux_down	334	HALLMARK_KRAS_SIGNALING_UP	200	9.85E-05
HNSCC8_cetux_down	334	HALLMARK_MYOGENESIS	200	9.85E-05
HNSCC8_cetux_down	334	HALLMARK_COMPLEMENT	200	5.36E-04
HNSCC8_cetux_down	334	HALLMARK_HYPOXIA	200	5.36E-04
HNSCC8_cetux_down	334	HALLMARK_TNFA_SIGNALING_VIA_NFKB	200	2.90E-03
HNSCC8_cetux_down	334	HALLMARK_COAGULATION	138	1.28E-02
HNSCC8_cetux_down	334	HALLMARK_APICAL_JUNCTION	200	1.28E-02
HNSCC8_cetux_down	334	HALLMARK_ANDROGEN_RESPONSE	101	2.15E-02
HNSCC8_cetux_down	334	HALLMARK_GLYCOLYSIS	200	4.40E-02
HNSCC8_cetux_down	334	HALLMARK_INTERFERON_GAMMA_RESPONSE	200	4.40E-02
HNSCC8_cetux_down	334	HALLMARK_XENOBIOTIC_METABOLISM	200	4.40E-02
HNSCC8_cetux_down	334	TGANTCA_AP1_C	1121	1.28E-22
HNSCC8_cetux_down	334	CAGGTG_E12_Q6	2485	3.95E-13
HNSCC8_cetux_down	334	GGGAGGRR_MAZ_Q6	2274	1.34E-12
HNSCC8_cetux_down	334	GGGTGGRR_PAX4_03	1294	8.58E-11
HNSCC8_cetux_down	334	TATAAA_TATA_01	1296	1.01E-07
HNSCC8_cetux_down	334	CAGCTG_AP4_Q5	1524	1.01E-07

HNSCC8_cetux_down	334	RYTTCCTG_ETS2_B	1085	1.01E-06
HNSCC8_cetux_down	334	BACH1_01	263	1.01E-06
HNSCC8_cetux_down	334	TTANTCA_UNKNOWN	952	1.01E-06
HNSCC8_cetux_down	334	AP1_01	267	1.06E-06
HNSCC8_cetux_down	334	TTGTTT_FOXO4_01	2061	1.51E-06
HNSCC8_cetux_down	334	WGGAATGY_TEF1_Q6	378	1.05E-05
HNSCC8_cetux_down	334	CAGGTA_AREB6_01	792	3.02E-05
HNSCC8_cetux_down	334	AP1_Q4_01	261	3.42E-05
HNSCC8_cetux_down	334	BACH2_01	271	4.75E-05
HNSCC8_cetux_down	334	AP1_Q2_01	275	5.19E-05
HNSCC8_cetux_down	334	TGCCAAR_NF1_Q6	722	9.13E-05
HNSCC8_cetux_down	334	MYOGENIN_Q6	255	1.46E-04
HNSCC8_cetux_down	334	TGGAAA_NFAT_Q4_01	1896	1.75E-04
HNSCC8_cetux_down	334	TEF1_Q6	226	2.95E-04
HNSCC8_cetux_down	334	GO_EPIDERMIS_DEVELOPMENT	253	1.49E-27
HNSCC8_cetux_down	334	GO_EPITHELIUM_DEVELOPMENT	945	1.34E-25
HNSCC8_cetux_down	334	GO_TISSUE_DEVELOPMENT	1518	1.77E-24
HNSCC8_cetux_down	334	GO_EPITHELIAL_CELL_DIFFERENTIATION	495	4.19E-24
HNSCC8_cetux_down	334	GO_KERATINOCYTE_DIFFERENTIATION	101	2.20E-23
HNSCC8_cetux_down	334	GO_EPIDERMAL_CELL_DIFFERENTIATION	142	1.92E-21
HNSCC8_cetux_down	334	GO_SKIN_DEVELOPMENT	211	9.59E-19
HNSCC8_cetux_down	334	GO_KERATINIZATION	50	6.03E-18
HNSCC8_cetux_down	334	GO_PEPTIDE_CROSS_LINKING	56	3.72E-17
HNSCC8_cetux_down	334	GO_RESPONSE_TO_OXYGEN_CONTAINING_COMPOUND	1381	1.31E-06
HNSCC8_cetux_down	334	GO_REGULATION_OF_HYDROLASE_ACTIVITY	1327	1.68E-06
HNSCC8_cetux_down	334	GO_REGULATION_OF_INTRACELLULAR_SIGNAL_TRANSDUCTION	1656	2.31E-06
HNSCC8_cetux_down	334	GO_PROTEOLYSIS	1208	2.31E-06
HNSCC8_cetux_down	334	GO_CELL_DEATH	1001	2.31E-06
HNSCC8_cetux_down	334	GO_POSITIVE_REGULATION_OF_RESPONSE_TO_STIMULUS	1929	3.03E-06
HNSCC8_cetux_down	334	GO_CELL_JUNCTION_ORGANIZATION	185	3.58E-06
HNSCC8_cetux_down	334	GO_BIOLOGICAL_ADHESION	1032	3.58E-06
HNSCC8_cetux_down	334	GO_CELL_JUNCTION_ASSEMBLY	129	1.01E-05
HNSCC8_cetux_down	334	GO_REGULATION_OF_RESPONSE_TO_STRESS	1468	1.02E-05
HNSCC8_cetux_down	334	GO_REGULATION_OF_CELL_ADHESION	629	1.12E-05
HNSCC8_cetux_down	334	KRAS.LUNG_UP.V1_DN	145	5.72E-19
HNSCC8_cetux_down	334	P53_DN.V1_UP	194	6.32E-13
HNSCC8_cetux_down	334	KRAS.600_UP.V1_DN	289	3.83E-11
HNSCC8_cetux_down	334	MYC_UP.V1_DN	182	3.25E-10
HNSCC8_cetux_down	334	AKT_UP.V1_UP	172	1.56E-09
HNSCC8_cetux_down	334	ERB2_UP.V1_UP	191	5.25E-09
HNSCC8_cetux_down	334	KRAS.PROSTATE_UP.V1_DN	144	2.12E-08
HNSCC8_cetux_down	334	KRAS.300_UP.V1_DN	143	2.20E-07
HNSCC8_cetux_down	334	RAF_UP.V1_DN	194	4.82E-07
HNSCC8_cetux_down	334	RB_P107_DN.V1_DN	128	7.22E-07
HNSCC8_cetux_down	334	KRAS.50_UP.V1_DN	49	1.14E-06
HNSCC8_cetux_down	334	PTEN_DN.V2_UP	143	1.72E-06
HNSCC8_cetux_down	334	KRAS.BREAST_UP.V1_UP	146	1.89E-06
HNSCC8_cetux_down	334	ESC_V6.5_UP_LATE.V1_DN	186	1.89E-06
HNSCC8_cetux_down	334	ALK_DN.V1_DN	148	1.90E-06
HNSCC8_cetux_down	334	LTE2_UP.V1_UP	190	2.05E-06
HNSCC8_cetux_down	334	EGFR_UP.V1_UP	193	2.13E-06
HNSCC8_cetux_down	334	IL21_UP.V1_UP	193	2.13E-06
HNSCC8_cetux_down	334	PRC2_EZH2_UP.V1_UP	194	2.13E-06
HNSCC8_cetux_down	334	MEK_UP.V1_UP	196	2.15E-06
HNSCC9_cetux_down	53	GO_PEPTIDE_CROSS_LINKING	56	2.72E-05
HNSCC9_cetux_down	53	GO_KERATINOCYTE_DIFFERENTIATION	101	2.72E-04
HNSCC9_cetux_down	53	GO_KERATINIZATION	50	5.16E-04
HNSCC9_cetux_down	53	GO_EPIDERMAL_CELL_DIFFERENTIATION	142	7.41E-04
HNSCC9_cetux_down	53	GO_SKIN_DEVELOPMENT	211	4.14E-03
HNSCC9_cetux_down	53	GO_EPIDERMIS_DEVELOPMENT	253	8.31E-03
HNSCC9_cetux_down	53	KRAS.BREAST_UP.V1_UP	146	4.79E-03
HNSCC10_cetux_down	2476	HALLMARK_OXIDATIVE_PHOSPHORYLATION	200	2.96E-19
HNSCC10_cetux_down	2476	HALLMARK_MYC_TARGETS_V1	200	9.02E-19
HNSCC10_cetux_down	2476	HALLMARK_E2F_TARGETS	200	1.76E-14
HNSCC10_cetux_down	2476	HALLMARK_ADIPOGENESIS	200	2.15E-13
HNSCC10_cetux_down	2476	HALLMARK_G2M_CHECKPOINT	200	2.15E-13

HNSCC10_cetux_down	2476	HALLMARK_MTORC1_SIGNALING	200	2.15E-13
HNSCC10_cetux_down	2476	HALLMARK_DNA_REPAIR	150	9.65E-13
HNSCC10_cetux_down	2476	HALLMARK_UNFOLDED_PROTEIN_RESPONSE	113	1.23E-12
HNSCC10_cetux_down	2476	HALLMARK_HEME_METABOLISM	200	1.39E-11
HNSCC10_cetux_down	2476	HALLMARK_UV_RESPONSE_DN	144	1.52E-10
HNSCC10_cetux_down	2476	HALLMARK_MITOTIC_SPINDLE	200	2.06E-10
HNSCC10_cetux_down	2476	HALLMARK_APOPTOSIS	161	5.55E-10
HNSCC10_cetux_down	2476	HALLMARK_PROTEIN_SECRETION	96	4.35E-09
HNSCC10_cetux_down	2476	HALLMARK_UV_RESPONSE_UP	158	2.33E-08
HNSCC10_cetux_down	2476	HALLMARK_HYPOXIA	200	3.30E-08
HNSCC10_cetux_down	2476	HALLMARK_FATTY_ACID_METABOLISM	158	8.17E-08
HNSCC10_cetux_down	2476	HALLMARK_XENOBIOTIC_METABOLISM	200	1.03E-07
HNSCC10_cetux_down	2476	HALLMARK_ANDROGEN_RESPONSE	101	2.33E-07
HNSCC10_cetux_down	2476	HALLMARK_ESTROGEN_RESPONSE_LATE	200	2.84E-07
HNSCC10_cetux_down	2476	HALLMARK_IL2_STAT5_SIGNALING	200	2.84E-07
HNSCC10_cetux_down	2476	GGGCGGR_SP1_Q6	2940	1.49E-113
HNSCC10_cetux_down	2476	SCGGAAGY_ELK1_02	1199	5.72E-82
HNSCC10_cetux_down	2476	CTTTGT_LEF1_Q2	1972	5.43E-64
HNSCC10_cetux_down	2476	TTGTTT_FOXO4_01	2061	2.10E-63
HNSCC10_cetux_down	2476	RCGCANGCGY_NRF1_Q6	918	6.23E-62
HNSCC10_cetux_down	2476	TGGAAA_NFAT_Q4_01	1896	1.66E-53
HNSCC10_cetux_down	2476	AACTTT_UNKNOWN	1890	3.38E-48
HNSCC10_cetux_down	2476	GGGAGGRR_MAZ_Q6	2274	3.39E-45
HNSCC10_cetux_down	2476	MGGAAGTG_GABP_B	757	9.05E-44
HNSCC10_cetux_down	2476	GATTGGY_NFY_Q6_01	1160	9.07E-40
HNSCC10_cetux_down	2476	CAGGTG_E12_Q6	2485	2.08E-39
HNSCC10_cetux_down	2476	TTGCACT_MIR130A_MIR301_MIR130B	403	3.62E-39
HNSCC10_cetux_down	2476	TTTGCAC_MIR19A_MIR19B	516	2.77E-38
HNSCC10_cetux_down	2476	CTTTAAR_UNKNOWN	972	4.37E-35
HNSCC10_cetux_down	2476	TGCCTTA_MIR124A	552	2.66E-33
HNSCC10_cetux_down	2476	CACGTG_MYC_Q2	1032	5.57E-32
HNSCC10_cetux_down	2476	TGACCTY_ERR1_Q2	1043	5.57E-32
HNSCC10_cetux_down	2476	GCCATNTTG_YY1_Q6	427	1.43E-29
HNSCC10_cetux_down	2476	ACCAAAG_MIR9	499	2.22E-29
HNSCC10_cetux_down	2476	GCACTTT_MIR175P_MIR20A_MIR106A_MIR106B_MIR20B_MIR519D	595	4.63E-29
HNSCC10_cetux_down	2476	GO_PROTEIN_LOCALIZATION	1805	1.21E-82
HNSCC10_cetux_down	2476	GO_ESTABLISHMENT_OF_LOCALIZATION_IN_CELL	1676	7.40E-82
HNSCC10_cetux_down	2476	GO_PHOSPHATE_CONTAINING_COMPOUND_METABOLIC_PROCESS	1977	1.83E-74
HNSCC10_cetux_down	2476	GO_ESTABLISHMENT_OF_PROTEIN_LOCALIZATION	1423	3.44E-70
HNSCC10_cetux_down	2476	GO_CATABOLIC_PROCESS	1773	3.99E-68
HNSCC10_cetux_down	2476	GO_CELLULAR_RESPONSE_TO_STRESS	1565	5.40E-65
HNSCC10_cetux_down	2476	GO_CELLULAR_CATABOLIC_PROCESS	1322	2.07E-64
HNSCC10_cetux_down	2476	GO_RNA_PROCESSING	835	3.37E-64
HNSCC10_cetux_down	2476	GO_CELLULAR_MACROMOLECULE_LOCALIZATION	1234	3.82E-62
HNSCC10_cetux_down	2476	GO_ORGANONITROGEN_COMPOUND_METABOLIC_PROCESS	1796	2.36E-61
HNSCC10_cetux_down	2476	GO_CELL_CYCLE	1316	1.41E-60
HNSCC10_cetux_down	2476	GO_CHROMOSOME_ORGANIZATION	1009	6.00E-60
HNSCC10_cetux_down	2476	GO_MACROMOLECULAR_COMPLEX_ASSEMBLY	1398	1.45E-58
HNSCC10_cetux_down	2476	GO_SMALL_MOLECULE_METABOLIC_PROCESS	1767	1.91E-57
HNSCC10_cetux_down	2476	GO_SINGLE_ORGANISM_BIOSYNTHETIC_PROCESS	1340	2.43E-57
HNSCC10_cetux_down	2476	GO_PROTEIN_COMPLEX_SUBUNIT_ORGANIZATION	1527	5.66E-53
HNSCC10_cetux_down	2476	GO_CELL_CYCLE_PROCESS	1081	5.78E-53
HNSCC10_cetux_down	2476	GO_POSITIVE_REGULATION_OF_GENE_EXPRESSION	1733	3.91E-51
HNSCC10_cetux_down	2476	GO_REGULATION_OF_TRANSCRIPTION_FROM_RNA_POLYMERASE_II_PROMOTER	1784	2.91E-50
HNSCC10_cetux_down	2476	GO_MACROMOLECULE_CATABOLIC_PROCESS	926	3.06E-50
HNSCC10_cetux_down	2476	TBK1.DF_DN	287	3.65E-23
HNSCC10_cetux_down	2476	ERB2_UP.V1_DN	197	4.22E-20
HNSCC10_cetux_down	2476	MEK_UP.V1_DN	196	1.68E-16
HNSCC10_cetux_down	2476	E2F1_UP.V1_UP	189	1.68E-16
HNSCC10_cetux_down	2476	TBK1.DF_UP	290	6.37E-16
HNSCC10_cetux_down	2476	PIGF_UP.V1_UP	191	2.89E-14
HNSCC10_cetux_down	2476	LTE2_UP.V1_DN	196	6.65E-14
HNSCC10_cetux_down	2476	STK33_SKM_UP	290	1.28E-13
HNSCC10_cetux_down	2476	HOXA9_DN.V1_UP	194	1.78E-13
HNSCC10_cetux_down	2476	E2F1_UP.V1_DN	193	5.95E-13

HNSCC10_cetux_down	2476	VEGF_A_UP.V1_DN	193	5.95E-13
HNSCC10_cetux_down	2476	STK33_NOMO_UP	294	2.33E-12
HNSCC10_cetux_down	2476	STK33_UP	293	7.07E-12
HNSCC10_cetux_down	2476	ERB2_UP.V1_UP	191	3.38E-11
HNSCC10_cetux_down	2476	GCNP_SHH_UP_LATE.V1_UP	183	3.67E-11
HNSCC10_cetux_down	2476	SIRNA_EIF4GI_UP	95	4.30E-11
HNSCC10_cetux_down	2476	CAMP_UP.V1_DN	200	1.20E-10
HNSCC10_cetux_down	2476	EGFR_UP.V1_DN	196	2.57E-10
HNSCC10_cetux_down	2476	CYCLIN_D1_KE_.V1_UP	190	4.03E-10
HNSCC10_cetux_down	2476	MTOR_UP.N4.V1_DN	193	6.09E-10
HNSCC12_cetux_down	133	HALLMARK_DNA_REPAIR	150	4.90E-02
HNSCC12_cetux_down	133	KRCTCNNNNMANAGC_UNKNOWN	66	8.19E-07
HNSCC12_cetux_down	133	TTTNNANAGCYR_UNKNOWN	133	1.11E-03
HNSCC12_cetux_down	133	WTTGKCTG_UNKNOWN	516	5.86E-03
HNSCC12_cetux_down	133	GO_KERATINOCYTE_DIFFERENTIATION	101	8.83E-13
HNSCC12_cetux_down	133	GO_EPIDERMAL_CELL_DIFFERENTIATION	142	2.92E-11
HNSCC12_cetux_down	133	GO_KERATINIZATION	50	3.62E-11
HNSCC12_cetux_down	133	GO_SKIN_DEVELOPMENT	211	1.67E-09
HNSCC12_cetux_down	133	GO_PEPTIDE_CROSS_LINKING	56	4.46E-09
HNSCC12_cetux_down	133	GO_EPIDERMIS_DEVELOPMENT	253	9.39E-09
HNSCC12_cetux_down	133	GO_EPITHELIAL_CELL_DIFFERENTIATION	495	1.60E-05
HNSCC12_cetux_down	133	GO_CHROMATIN_ASSEMBLY_OR_DISASSEMBLY	177	2.98E-05
HNSCC12_cetux_down	133	GO_DNA_PACKAGING	194	5.13E-05
HNSCC12_cetux_down	133	GO_DNA_CONFORMATION_CHANGE	273	5.13E-05
HNSCC12_cetux_down	133	GO_CHROMOSOME_ORGANIZATION	1009	1.06E-04
HNSCC12_cetux_down	133	GO_CHROMATIN_SILENCING	95	1.32E-04
HNSCC12_cetux_down	133	GO_PROTEIN_DNA_COMPLEX_SUBUNIT_ORGANIZATION	229	1.32E-04
HNSCC12_cetux_down	133	GO_NEGATIVE_REGULATION_OF_GENE_EXPRESSION_EPIGENETIC	112	3.09E-04
HNSCC12_cetux_down	133	GO_PROTEIN_COMPLEX_BIOGENESIS	1132	3.26E-04
HNSCC12_cetux_down	133	GO_REGULATION_OF_MEGAKARYOCYTE_DIFFERENTIATION	28	3.61E-04
HNSCC12_cetux_down	133	GO_TELOMERE_CAPPING	29	3.93E-04
HNSCC12_cetux_down	133	GO_ANATOMICAL_STRUCTURE_HOMEOSTASIS	285	4.90E-04
HNSCC12_cetux_down	133	GO_PROTEIN_COMPLEX_SUBUNIT_ORGANIZATION	1527	5.09E-04
HNSCC12_cetux_down	133	GO_DEFENSE_RESPONSE_TO_OTHER_ORGANISM	505	5.27E-04
HNSCC13_cetux_down	151	HALLMARK_KRAS_SIGNALING_DN	200	2.42E-04
HNSCC13_cetux_down	151	TGANTCA_AP1_C	1121	4.04E-03
HNSCC13_cetux_down	151	GO_HUMORAL_IMMUNE_RESPONSE_MEDIATED_BY_CIRCULATING_IMMUNOGLOBULIN	69	5.95E-22
HNSCC13_cetux_down	151	GO_COMPLEMENT_ACTIVATION	76	1.55E-21
HNSCC13_cetux_down	151	GO_PROTEIN_ACTIVATION_CASCADE	99	1.55E-21
HNSCC13_cetux_down	151	GO_B_CELL_MEDIATED_IMMUNITY	99	8.09E-20
HNSCC13_cetux_down	151	GO_PHAGOCYTOSIS_RECOGNITION	34	4.63E-19
HNSCC13_cetux_down	151	GO_PHAGOCYTOSIS_ENGULFMENT	38	1.80E-18
HNSCC13_cetux_down	151	GO_ADAPTIVE_IMMUNE_RESPONSE_BASED_ON_SOMATIC_RECOMBINATION_OF_IMMUNE_RECEPTORS_BUILT_FROM_IMMUNOGLOBULIN_SUPERFAMILY_DOMAINS	154	1.80E-18
HNSCC13_cetux_down	151	GO_LYMPHOCYTE_MEDIATED_IMMUNITY	147	3.05E-17
HNSCC13_cetux_down	151	GO_MEMBRANE_INVAGINATION	48	3.14E-17
HNSCC13_cetux_down	151	GO_HUMORAL_IMMUNE_RESPONSE	187	3.68E-17
HNSCC13_cetux_down	151	GO_B_CELL_RECEPTOR_SIGNALING_PATHWAY	54	1.25E-16
HNSCC13_cetux_down	151	GO_LEUKOCYTE_MEDIATED_IMMUNITY	189	1.23E-15
HNSCC13_cetux_down	151	GO_PHAGOCYTOSIS	190	1.23E-15
HNSCC13_cetux_down	151	GO_ADAPTIVE_IMMUNE_RESPONSE	288	1.77E-15
HNSCC13_cetux_down	151	GO_FC_GAMMA_RECEPTOR_SIGNALING_PATHWAY	95	2.51E-15
HNSCC13_cetux_down	151	GO_POSITIVE_REGULATION_OF_B_CELL_ACTIVATION	86	3.49E-14
HNSCC13_cetux_down	151	GO_KERATINOCYTE_DIFFERENTIATION	101	2.45E-13
HNSCC13_cetux_down	151	GO_KERATINIZATION	50	2.45E-13
HNSCC13_cetux_down	151	GO_DEFENSE_RESPONSE_TO_BACTERIUM	237	7.02E-13
HNSCC13_cetux_down	151	GO_EPIDERMIS_DEVELOPMENT	253	1.75E-12
HNSCC13_cetux_down	151	KRAS.PROSTATE_UP.V1_DN	144	1.08E-08
HNSCC13_cetux_down	151	KRAS.LUNG_UP.V1_DN	145	1.37E-07
HNSCC13_cetux_down	151	KRAS.600_UP.V1_DN	289	2.33E-07
HNSCC13_cetux_down	151	KRAS.50_UP.V1_DN	49	6.70E-07
HNSCC13_cetux_down	151	KRAS.300_UP.V1_DN	143	1.95E-05
HNSCC13_cetux_down	151	ESC_V6.5_UP_EARLY.V1_DN	172	5.62E-05
HNSCC13_cetux_down	151	KRAS.BREAST_UP.V1_UP	146	3.44E-03

HNSCC13_cetux_down	151	PTEN_DN.V2_UP	143	2.56E-02
HNSCC13_cetux_down	151	KRAS.LUNG.BREAST_UP.V1_DN	145	2.56E-02
HNSCC13_cetux_down	151	MEL18_DN.V1_DN	148	2.56E-02
HNSCC13_cetux_down	151	P53_DN.V2_UP	148	2.56E-02
HNSCC13_cetux_down	151	PKCA_DN.V1_DN	167	3.64E-02
HNSCC13_cetux_down	151	KRAS.600_UP.V1_UP	287	3.89E-02
HNSCC13_cetux_down	151	PTEN_DN.V1_DN	187	4.00E-02
HNSCC13_cetux_down	151	IL15_UP.V1_DN	190	4.00E-02
HNSCC13_cetux_down	151	RAPA_EARLY_UP.V1_DN	191	4.00E-02
HNSCC13_cetux_down	151	P53_DN.V1_DN	192	4.00E-02
HNSCC13_cetux_down	151	RPS14_DN.V1_UP	192	4.00E-02
HNSCC13_cetux_down	151	LEF1_UP.V1_UP	195	4.01E-02
UMSCC92_EGFR_KO_down	516	HALLMARK_ESTROGEN_RESPONSE_LATE	200	8.84E-27
UMSCC92_EGFR_KO_down	516	HALLMARK_ESTROGEN_RESPONSE_EARLY	200	2.45E-16
UMSCC92_EGFR_KO_down	516	HALLMARK_APICAL_JUNCTION	200	1.82E-14
UMSCC92_EGFR_KO_down	516	HALLMARK_P53_PATHWAY	200	1.82E-14
UMSCC92_EGFR_KO_down	516	HALLMARK_KRAS_SIGNALING_UP	200	1.29E-08
UMSCC92_EGFR_KO_down	516	HALLMARK_INFLAMMATORY_RESPONSE	200	8.48E-08
UMSCC92_EGFR_KO_down	516	HALLMARK_APOPTOSIS	161	2.92E-07
UMSCC92_EGFR_KO_down	516	HALLMARK_GLYCOLYSIS	200	4.68E-07
UMSCC92_EGFR_KO_down	516	HALLMARK_INTERFERON_ALPHA_RESPONSE	97	8.52E-07
UMSCC92_EGFR_KO_down	516	HALLMARK_IL2_STAT5_SIGNALING	200	2.32E-06
UMSCC92_EGFR_KO_down	516	HALLMARK_INTERFERON_GAMMA_RESPONSE	200	2.32E-06
UMSCC92_EGFR_KO_down	516	HALLMARK_ALLOGRAFT_REJECTION	200	1.34E-05
UMSCC92_EGFR_KO_down	516	HALLMARK_TNFA_SIGNALING_VIA_NFKB	200	7.15E-05
UMSCC92_EGFR_KO_down	516	HALLMARK_KRAS_SIGNALING_DN	200	3.51E-04
UMSCC92_EGFR_KO_down	516	HALLMARK_ANDROGEN_RESPONSE	101	4.99E-04
UMSCC92_EGFR_KO_down	516	HALLMARK_UV_RESPONSE_UP	158	1.31E-03
UMSCC92_EGFR_KO_down	516	HALLMARK_HYPOXIA	200	1.31E-03
UMSCC92_EGFR_KO_down	516	HALLMARK_MTORC1_SIGNALING	200	1.31E-03
UMSCC92_EGFR_KO_down	516	HALLMARK_MYOGENESIS	200	5.32E-03
UMSCC92_EGFR_KO_down	516	HALLMARK_REACTIVE_OXIGEN_SPECIES_PATHWAY	49	5.58E-03
UMSCC92_EGFR_KO_down	516	CAGGTG_E12_Q6	2485	9.57E-38
UMSCC92_EGFR_KO_down	516	TGANTCA_AP1_C	1121	4.66E-27
UMSCC92_EGFR_KO_down	516	GGGAGGRR_MAZ_Q6	2274	7.32E-19
UMSCC92_EGFR_KO_down	516	TTGTTT_FOXO4_01	2061	9.66E-16
UMSCC92_EGFR_KO_down	516	CAGGTA_AREB6_01	792	6.81E-13
UMSCC92_EGFR_KO_down	516	TGTTTGY_HNF3_Q6	738	1.69E-10
UMSCC92_EGFR_KO_down	516	RYTTCCTG_ETS2_B	1085	1.69E-10

UMSCC92_EGFR_KO_down	516	AACTTT_UNKNOWN	1890	2.10E-10
UMSCC92_EGFR_KO_down	516	AREB6_01	271	5.80E-10
UMSCC92_EGFR_KO_down	516	TGGNNNNNNKCCAR_UNKNOWN	424	2.06E-09
UMSCC92_EGFR_KO_down	516	TATAAA_TATA_01	1296	2.61E-09
UMSCC92_EGFR_KO_down	516	AP1_Q2_01	275	4.06E-09
UMSCC92_EGFR_KO_down	516	CAGCTG_AP4_Q5	1524	4.06E-09
UMSCC92_EGFR_KO_down	516	GGGTGGRR_PAX4_03	1294	6.48E-09
UMSCC92_EGFR_KO_down	516	AREB6_02	254	6.48E-09
UMSCC92_EGFR_KO_down	516	TGGAAA_NFAT_Q4_01	1896	9.60E-09
UMSCC92_EGFR_KO_down	516	HNF4_Q6	263	1.03E-08
UMSCC92_EGFR_KO_down	516	TTANTCA_UNKNOWN	952	1.66E-08
UMSCC92_EGFR_KO_down	516	WGGAATGY_TEF1_Q6	378	2.19E-08
UMSCC92_EGFR_KO_down	516	CTTTGT_LEF1_Q2	1972	3.16E-08
UMSCC92_EGFR_KO_down	516	GO_TISSUE_DEVELOPMENT	1518	3.81E-30
UMSCC92_EGFR_KO_down	516	GO_EPIDERMIS_DEVELOPMENT	253	6.28E-29
UMSCC92_EGFR_KO_down	516	GO_IMMUNE_SYSTEM_PROCESS	1984	2.72E-27
UMSCC92_EGFR_KO_down	516	GO_EPITHELIUM_DEVELOPMENT	945	6.77E-26
UMSCC92_EGFR_KO_down	516	GO_BIOLOGICAL_ADHESION	1032	2.46E-22
UMSCC92_EGFR_KO_down	516	GO_CELL_JUNCTION_ORGANIZATION	185	1.20E-21
UMSCC92_EGFR_KO_down	516	GO_RESPONSE_TO_EXTERNAL_STIMULUS	1821	1.77E-19
UMSCC92_EGFR_KO_down	516	GO_DEFENSE_RESPONSE	1231	2.16E-19
UMSCC92_EGFR_KO_down	516	GO_POSITIVE_REGULATION_OF_RESPONSE_TO_STIMULUS	1929	3.90E-18
UMSCC92_EGFR_KO_down	516	GO_IMMUNE_RESPONSE	1100	1.47E-17
UMSCC92_EGFR_KO_down	516	GO_POSITIVE_REGULATION_OF_CELL_COMMUNICATION	1532	1.88E-17
UMSCC92_EGFR_KO_down	516	GO_REGULATION_OF_CELLULAR_COMPONENT_MOVEMENT	771	1.88E-17
UMSCC92_EGFR_KO_down	516	GO_REGULATION_OF_CELL_PROLIFERATION	1496	9.90E-17
UMSCC92_EGFR_KO_down	516	GO_CELL_JUNCTION_ASSEMBLY	129	5.77E-16
UMSCC92_EGFR_KO_down	516	GO_SKIN_DEVELOPMENT	211	8.19E-16
UMSCC92_EGFR_KO_down	516	GO_REGULATION_OF_IMMUNE_SYSTEM_PROCESS	1403	5.50E-15
UMSCC92_EGFR_KO_down	516	GO_REGULATION_OF_HYDROLASE_ACTIVITY	1327	7.87E-15
UMSCC92_EGFR_KO_down	516	GO_REGULATION_OF_PEPTIDASE_ACTIVITY	392	6.18E-14
UMSCC92_EGFR_KO_down	516	GO_CELL_DEATH	1001	2.56E-13
UMSCC92_EGFR_KO_down	516	GO_ORGAN_MORPHOGENESIS	841	2.67E-13
UMSCC92_EGFR_KO_down	516	P53_DN.V1_UP	194	7.34E-23

UMSCC92_EGFR_KO_down	516	MEK_UP.V1_UP	196	3.06E-18
UMSCC92_EGFR_KO_down	516	ERB2_UP.V1_UP	191	1.51E-17
UMSCC92_EGFR_KO_down	516	SINGH_KRAS_DEPENDENCY_SIGNATURE_	20	1.94E-17
UMSCC92_EGFR_KO_down	516	LEF1_UP.V1_DN	190	1.11E-16
UMSCC92_EGFR_KO_down	516	AKT_UP_MTOR_DN.V1_UP	184	7.76E-15
UMSCC92_EGFR_KO_down	516	AKT_UP.V1_UP	172	1.82E-14
UMSCC92_EGFR_KO_down	516	ESC_V6.5_UP_EARLY.V1_DN	172	1.82E-14
UMSCC92_EGFR_KO_down	516	MEL18_DN.V1_DN	148	1.52E-13
UMSCC92_EGFR_KO_down	516	ESC_J1_UP_LATE.V1_UP	191	1.48E-10
UMSCC92_EGFR_KO_down	516	KRAS.LUNG_UP.V1_DN	145	1.78E-10
UMSCC92_EGFR_KO_down	516	RAF_UP.V1_UP	196	1.86E-10
UMSCC92_EGFR_KO_down	516	BMI1_DN_MEL18_DN.V1_DN	147	1.86E-10
UMSCC92_EGFR_KO_down	516	RB_P107_DN.V1_DN	128	2.60E-10
UMSCC92_EGFR_KO_down	516	EGFR_UP.V1_UP	193	1.10E-09
UMSCC92_EGFR_KO_down	516	STK33_SKM_DN	288	1.68E-09
UMSCC92_EGFR_KO_down	516	TBK1.DF_UP	290	1.78E-09
UMSCC92_EGFR_KO_down	516	ATF2_UP.V1_DN	187	5.06E-09
UMSCC92_EGFR_KO_down	516	ATF2_S_UP.V1_DN	187	4.06E-08
UMSCC92_EGFR_KO_down	516	LTE2_UP.V1_UP	190	4.80E-08

Table 4-7. Downregulated gene sets enriched in each of the 13 cetuximab-treated gene sets and EGFR K/O gene sets

Gene set enrichment analysis was performed with significantly downregulated genes from each of the 14 gene sets to identify significant overlap with gene sets in the “Hallmark”, “Motif”, “Go-Biological Process” and “Oncogene” databases with the molecular signatures database v5.1. Node is the sample, and Node Size is the number of input genes from the sample. Gene Set Name is the pathway enriched, with # of Genes in Gene Set being the number of genes in the GSEA pathway being tested.

Bibliography

1. De Pauw I, Lardon F, Van den Bossche J, Baysal H, Fransen E, Deschoolmeester V, Pauwels P, Peeters M, Vermorken JB, Wouters A. Simultaneous targeting of EGFR, HER2, and HER4 by afatinib overcomes intrinsic and acquired cetuximab resistance in head and neck squamous cell carcinoma cell lines. Molecular oncology. 2018;12(6):830-54. doi: 10.1002/1878-0261.12197. PubMed PMID: 29603584; PMCID: 5983215.
2. De Pauw I, Wouters A, Van den Bossche J, Deschoolmeester V, Baysal H, Pauwels P, Peeters M, Vermorken JB, Lardon F. Dual Targeting of Epidermal Growth Factor Receptor and HER3 by MEHD7945A as Monotherapy or in Combination with Cisplatin Partially Overcomes Cetuximab Resistance in Head and Neck Squamous Cell Carcinoma Cell Lines. Cancer biotherapy & radiopharmaceuticals. 2017;32(7):229-38. PubMed PMID: 28910149.
3. Martinelli E, Troiani T, Sforza V, Martini G, Cardone C, Vitiello PP, Ciardiello D, Rachiglio AM, Normanno N, Sartore-Bianchi A, Marsoni S, Bardelli A, Siena S, Ciardiello F. Sequential HER2 blockade as effective therapy in chemorefractory, HER2 gene-amplified, RAS wild-type, metastatic colorectal cancer: learning from a clinical case. ESMO Open. 2018;3(1):e000299. doi: 10.1136/esmoopen-2017-000299. PubMed PMID: 29387480; PMCID: 5786925.
4. Wang D, Qian G, Zhang H, Magliocca KR, Nannapaneni S, Amin AR, Rossi M, Patel M, El-Deiry M, Wadsworth JT, Chen Z, Khuri FR, Shin DM, Saba NF, Chen ZG. HER3 Targeting Sensitizes HNSCC to Cetuximab by Reducing HER3 Activity and HER2/HER3 Dimerization: Evidence from Cell Line and Patient-Derived Xenograft Models. Clinical cancer research : an official journal of the American Association for Cancer Research. 2017;23(3):677-86. doi: 10.1158/1078-0432.CCR-16-0558. PubMed PMID: 27358485; PMCID: 5199640.
5. De Pauw I, Lardon F, Van den Bossche J, Baysal H, Pauwels P, Peeters M, Vermorken JB, Wouters A. Overcoming Intrinsic and Acquired Cetuximab Resistance in RAS Wild-Type Colorectal Cancer: An In Vitro Study on the Expression of HER Receptors and the Potential of Afatinib. Cancers (Basel). 2019;11(1). doi: 10.3390/cancers11010098. PubMed PMID: 30650638.
6. Cremolini C, Rossini D, Dell'Aquila E, Lonardi S, Conca E, Del Re M, Busico A, Pietrantonio F, Danesi R, Aprile G, Tamburini E, Barone C, Masi G, Pantano F, Pucci F, Corsi DC, Pella N, Bergamo F, Rofi E, Barbara C, Falcone A, Santini D. Rechallenge for Patients With RAS and BRAF Wild-Type Metastatic Colorectal Cancer With Acquired Resistance to First-line Cetuximab and Irinotecan: A Phase 2 Single-Arm Clinical Trial. JAMA Oncol. 2018. doi: 10.1001/jamaoncol.2018.5080. PubMed PMID: 30476968.
7. Yu Y, Guo M, Wei Y, Yu S, Li H, Wang Y, Xu X, Cui Y, Tian J, Liang L, Peng K, Liu T. FoxO3a confers cetuximab resistance in RAS wild-type metastatic colorectal cancer through c-Myc. Oncotarget. 2016;7(49):80888-900. doi: 10.18632/oncotarget.13105. PubMed PMID: 27825133; PMCID: 5348362.
8. Zuo Q, Shi M, Chen J, Liao W. The Ras signaling pathway mediates cetuximab resistance in nasopharyngeal carcinoma. Biomedicine & pharmacotherapy = Biomedecine & pharmacotherapie. 2011;65(3):168-74. doi: 10.1016/j.biopha.2011.02.005. PubMed PMID: 21602020.
9. Luwor RB, Lu Y, Li X, Liang K, Fan Z. Constitutively active Harvey Ras confers resistance to epidermal growth factor receptor-targeted therapy with cetuximab and gefitinib.

Cancer letters. 2011;306(1):85-91. doi: 10.1016/j.canlet.2011.02.035. PubMed PMID: 21411223; PMCID: 3102794.
10. Koole K, Brunen D, van Kempen PM, Noorlag R, de Bree R, Lieftink C, van Es RJ, Bernards R, Willems SM. FGFR1 Is a Potential Prognostic Biomarker and Therapeutic Target in Head and Neck Squamous Cell Carcinoma. Clinical cancer research : an official journal of the American Association for Cancer Research. 2016;22(15):3884-93. doi: 10.1158/1078-0432.CCR-15-1874. PubMed PMID: 26936917.
11. Herrera-Abreu MT, Pearson A, Campbell J, Shnyder SD, Knowles MA, Ashworth A, Turner NC. Parallel RNA interference screens identify EGFR activation as an escape mechanism in FGFR3-mutant cancer. Cancer Discov. 2013;3(9):1058-71. doi: 10.1158/2159-8290.CD-12-0569. PubMed PMID: 23744832; PMCID: 3770512.
12. Ware KE, Marshall ME, Heasley LR, Marek L, Hinz TK, Hercule P, Helfrich BA, Doebele RC, Heasley LE. Rapidly acquired resistance to EGFR tyrosine kinase inhibitors in NSCLC cell lines through de-repression of FGFR2 and FGFR3 expression. PLoS One. 2010;5(11):e14117. doi: 10.1371/journal.pone.0014117. PubMed PMID: 21152424; PMCID: 2994708.
13. Engelman JA, Zejnullahu K, Mitsudomi T, Song Y, Hyland C, Park JO, Lindeman N, Gale CM, Zhao X, Christensen J, Kosaka T, Holmes AJ, Rogers AM, Cappuzzo F, Mok T, Lee C, Johnson BE, Cantley LC, Janne PA. MET amplification leads to gefitinib resistance in lung cancer by activating ERBB3 signaling. Science. 2007;316(5827):1039-43. Epub 2007/04/28. doi: 10.1126/science.1141478. PubMed PMID: 17463250.
14. Madoz-Gurpide J, Zazo S, Chamizo C, Casado V, Carames C, Gavin E, Cristobal I, Garcia-Foncillas J, Rojo F. Activation of MET pathway predicts poor outcome to cetuximab in patients with recurrent or metastatic head and neck cancer. Journal of translational medicine. 2015;13:282. Epub 2015/09/01. doi: 10.1186/s12967-015-0633-7. PubMed PMID: 26319934; PMCID: PMC4552997.
15. Morgillo F, Kim WY, Kim ES, Ciardiello F, Hong WK, Lee HY. Implication of the insulin-like growth factor-IR pathway in the resistance of non-small cell lung cancer cells to treatment with gefitinib. Clinical cancer research : an official journal of the American Association for Cancer Research. 2007;13(9):2795-803. doi: 10.1158/1078-0432.CCR-06-2077. PubMed PMID: 17473213.
16. Alvarez-Teijeiro S, Garcia-Inclan C, Villaronga MA, Casado P, Hermida-Prado F, Granda-Diaz R, Rodrigo JP, Calvo F, Del-Rio-Ibisate N, Gandarillas A, Moris F, Hermsen M, Cutillas P, Garcia-Pedrero JM. Factors Secreted by Cancer-Associated Fibroblasts that Sustain Cancer Stem Properties in Head and Neck Squamous Carcinoma Cells as Potential Therapeutic Targets. Cancers (Basel). 2018;10(9). doi: 10.3390/cancers10090334. PubMed PMID: 30227608; PMCID: 6162704.
17. Husain H, Scur M, Murtuza A, Bui N, Woodward B, Kurzrock R. Strategies to Overcome Bypass Mechanisms Mediating Clinical Resistance to EGFR Tyrosine Kinase Inhibition in Lung Cancer. Mol Cancer Ther. 2017;16(2):265-72. doi: 10.1158/1535-7163.MCT-16-0105. PubMed PMID: 28159915.
18. Choi YJ, Park GM, Rho JK, Kim SY, So GS, Kim HR, Choi CM, Lee JC. Role of IGF-binding protein 3 in the resistance of EGFR mutant lung cancer cells to EGFR-tyrosine kinase inhibitors. PLoS One. 2013;8(12):e81393. doi: 10.1371/journal.pone.0081393. PubMed PMID: 24339922; PMCID: 3855319.

19. Turner N, Grose R. Fibroblast growth factor signalling: from development to cancer. Nature Reviews Cancer. 2010;10:116. doi: 10.1038/nrc2780.
20. Dieci MV, Arnedos M, Andre F, Soria JC. Fibroblast growth factor receptor inhibitors as a cancer treatment: from a biologic rationale to medical perspectives. Cancer Discov. 2013;3(3):264-79. Epub 2013/02/19. doi: 10.1158/2159-8290.Cd-12-0362. PubMed PMID: 23418312.
21. Katoh M, Nakagama H. FGF receptors: cancer biology and therapeutics. Medicinal research reviews. 2014;34(2):280-300. Epub 2013/05/23. doi: 10.1002/med.21288. PubMed PMID: 23696246.
22. Goke F, Franzen A, Hinz TK, Marek LA, Yoon P, Sharma R, Bode M, von Maessenhausen A, Lankat-Buttgereit B, Goke A, Golletz C, Kirsten R, Boehm D, Vogel W, Kleczko EK, Eagles JR, Hirsch FR, Van Bremen T, Bootz F, Schroeck A, Kim J, Tan AC, Jimeno A, Heasley LE, Perner S. FGFR1 Expression Levels Predict BGJ398 Sensitivity of FGFR1-Dependent Head and Neck Squamous Cell Cancers. Clinical cancer research : an official journal of the American Association for Cancer Research. 2015;21(19):4356-64. doi: 10.1158/1078-0432.CCR-14-3357. PubMed PMID: 26015511; PMCID: 4592392.
23. Quintanal-Villalonga A, Molina-Pinelo S, Cirauqui C, Ojeda-Márquez L, Marrugal Á, Suarez R, Conde E, Ponce-Aix S, Enguita AB, Carnero A, Ferrer I, Paz-Ares L. FGFR1 Cooperates with EGFR in Lung Cancer Oncogenesis, and Their Combined Inhibition Shows Improved Efficacy. Journal of Thoracic Oncology. 2019;14(4):641-55. doi: https://doi.org/10.1016/j.jtho.2018.12.021.
24. von Massenhausen A, Franzen A, Heasley L, Perner S. FGFR1 as a novel prognostic and predictive biomarker in squamous cell cancers of the lung and the head and neck area. Annals of translational medicine. 2013;1(3):23. doi: 10.3978/j.issn.2305-5839.2013.06.08. PubMed PMID: 25332967; PMCID: 4200677.
25. Ludwig ML, Kulkarni A, Birkeland AC, Michmerhuizen NL, Foltin SK, Mann JE, Hoesli RC, Devenport SN, Jewell BM, Shuman AG, Spector ME, Carey TE, Jiang H, Brenner JC. The genomic landscape of UM-SCC oral cavity squamous cell carcinoma cell lines. Oral Oncol. 2018;87:144-51. Epub 2018/12/12. doi: 10.1016/j.oraloncology.2018.10.031. PubMed PMID: 30527230; PMCID: PMC6349383.
26. Tillman BN, Yanik M, Birkeland AC, Liu CJ, Hovelson DH, Cani AK, Palanisamy N, Carskadon S, Carey TE, Bradford CR, Tomlins SA, McHugh JB, Spector ME, Brenner J. Fibroblast growth factor family aberrations as a putative driver of head and neck squamous cell carcinoma in an epidemiologically low-risk patient as defined by targeted sequencing. Head Neck. 2016;38 Suppl 1:E1646-52. doi: 10.1002/hed.24292. PubMed PMID: 26849095; PMCID: 4844767.
27. Michmerhuizen N.M. LE, Kulkarni A., Brenner J.C. Differential Compensation mechanisms Define Resistance to PI3K inhibitors in PIK3CA amplified HNSCC. Oto Head and Neck Surgery. 2016(NIHMS799178).
28. Jensen MM, Jørgensen JT, Binderup T, Kjaer A. Tumor volume in subcutaneous mouse xenografts measured by microCT is more accurate and reproducible than determined by 18F-FDG-microPET or external caliper. BMC medical imaging. 2008;8:16-. doi: 10.1186/1471-2342-8-16. PubMed PMID: 18925932.
29. Tomayko MM, Reynolds CP. Determination of subcutaneous tumor size in athymic (nude) mice. Cancer chemotherapy and pharmacology. 1989;24(3):148-54. Epub 1989/01/01. PubMed PMID: 2544306.

30. Swiecicki P, Schipper MJ, Malloy KM, Stucken C, Shuman AG, Spector ME, Chepeha DB, Casper K, McLean SA, Moyer J, Wolf GT, Prince ME, Bradford CR, Carey TE, Eisbruch A, Jolly S, Worden FP. Phase II prospective trial of cetuximab and radiotherapy for locally advanced, squamous cell carcinomas of the head and neck in patients >70 years old or with comorbidities not-eligible for platinum-based chemotherapy. Journal of Clinical Oncology. 2016;34(15_suppl):6071-. doi: 10.1200/JCO.2016.34.15_suppl.6071.
31. Birkeland AC, Foltin SK, Michmerhuizen NL, Hoesli RC, Rosko AJ, Byrd S, Yanik M, Nor JE, Bradford CR, Prince ME, Carey TE, McHugh JB, Spector ME, Brenner JC. Correlation of Crtc1/3-Maml2 fusion status, grade and survival in mucoepidermoid carcinoma. Oral oncology. 2017;68:5-8. doi: 10.1016/j.oraloncology.2017.02.025. PubMed PMID: 28438292; PMCID: 5433350.
32. Birkeland AC, Yanik M, Tillman BN, Scott MV, Foltin SK, Mann JE, Michmerhuizen NL, Ludwig ML, Sandelski MM, Komarck CM, Carey TE, Prince ME, Bradford CR, McHugh JB, Spector ME, Brenner JC. Identification of Targetable ERBB2 Aberrations in Head and Neck Squamous Cell Carcinoma. JAMA Otolaryngol Head Neck Surg. 2016. doi: 10.1001/jamaoto.2016.0335. PubMed PMID: 27077364.
33. Vermes I, Haanen C, Steffens-Nakken H, Reutellingsperger C. A novel assay for apoptosis Flow cytometric detection of phosphatidylserine expression on early apoptotic cells using fluorescein labelled Annexin V. Journal of Immunological Methods. 1995;184(1):39-51. doi: https://doi.org/10.1016/0022-1759(95)00072-I.
34. Zou H, Hastie T. Regularization and Variable Selection via the Elastic Net. Journal of the Royal Statistical Society Series B (Statistical Methodology). 2005;67(2):301-20.
35. Garnett MJ, Edelman EJ, Heidorn SJ, Greenman CD, Dastur A, Lau KW, Greninger P, Thompson IR, Luo X, Soares J, Liu Q, Iorio F, Surdez D, Chen L, Milano RJ, Bignell GR, Tam AT, Davies H, Stevenson JA, Barthorpe S, Lutz SR, Kogera F, Lawrence K, McLaren-Douglas A, Mitropoulos X, Mironenko T, Thi H, Richardson L, Zhou W, Jewitt F, Zhang T, O'Brien P, Boisvert JL, Price S, Hur W, Yang W, Deng X, Butler A, Choi HG, Chang JW, Baselga J, Stamenkovic I, Engelman JA, Sharma SV, Delattre O, Saez-Rodriguez J, Gray NS, Settleman J, Futreal PA, Haber DA, Stratton MR, Ramaswamy S, McDermott U, Benes CH. Systematic identification of genomic markers of drug sensitivity in cancer cells. Nature. 2012;483(7391):570-5. Epub 2012/03/31. doi: 10.1038/nature11005. PubMed PMID: 22460902; PMCID: 3349233.
36. Lieu C, Heymach J, Overman M, Tran H, Kopetz S. Beyond VEGF: inhibition of the fibroblast growth factor pathway and antiangiogenesis. Clinical cancer research : an official journal of the American Association for Cancer Research. 2011;17(19):6130-9. Epub 2011/09/29. doi: 10.1158/1078-0432.Ccr-11-0659. PubMed PMID: 21953501; PMCID: PMC5562355.
37. Das M, Padda SK, Frymoyer A, Zhou L, Riess JW, Neal JW, Wakelee HA. Dovitinib and erlotinib in patients with metastatic non-small cell lung cancer: A drug-drug interaction. Lung cancer (Amsterdam, Netherlands). 2015;89(3):280-6. Epub 2015/07/08. doi: 10.1016/j.lungcan.2015.06.011. PubMed PMID: 26149476; PMCID: PMC4613811.
38. Bertotti A, Papp E, Jones S, Adleff V, Anagnostou V, Lupo B, Sausen M, Phallen J, Hruban CA, Tokheim C, Niknafs N, Nesselbush M, Lytle K, Sassi F, Cottino F, Migliardi G, Zanella ER, Ribero D, Russolillo N, Mellano A, Muratore A, Paraluppi G, Salizzoni M, Marsoni S, Kragh M, Lantto J, Cassingena A, Li QK, Karchin R, Scharpf R, Sartore-Bianchi A, Siena S,

Diaz Jr LA, Trusolino L, Velculescu VE. The genomic landscape of response to EGFR blockade in colorectal cancer. Nature. 2015;526:263. doi: 10.1038/nature14969 https://www.nature.com/articles/nature14969#supplementary-information.
39. Braig F, Voigtlaender M, Schieferdecker A, Busch CJ, Laban S, Grob T, Kriegs M, Knecht R, Bokemeyer C, Binder M. Liquid biopsy monitoring uncovers acquired RAS-mediated resistance to cetuximab in a substantial proportion of patients with head and neck squamous cell carcinoma. Oncotarget. 2016;7(28):42988-95. doi: 10.18632/oncotarget.8943. PubMed PMID: 27119512; PMCID: 5190002.
40. Rampias T, Giagini A, Siolos S, Matsuzaki H, Sasaki C, Scorilas A, Psyrri A. RAS/PI3K crosstalk and cetuximab resistance in head and neck squamous cell carcinoma. Clinical cancer research : an official journal of the American Association for Cancer Research. 2014;20(11):2933-46. doi: 10.1158/1078-0432.CCR-13-2721. PubMed PMID: 24696319.

Chapter 5: Summary and Perspectives

Summary

My thesis examined the hypothesis that co-targeting the epidermal growth factor receptor (EGFR) and a compensatory pathway could be an effective combination to cause cell death in head and neck squamous cell carcinoma (HNSCC). My work first characterized the genetics of a panel of UM-SCC cell lines, which are frequently used models for HNSCC. I then used CRISPR libraries to identify genes and pathways that compensate during inhibition of EGFR, leading to the nomination of the fibroblast growth factor (FGF) pathway as a common compensatory mechanism in HNSCC. Further, I evaluated the mechanism of dual inhibition of EGFR and FGFR, and also tested this combination in a mouse xenograft model. Here, I review the main findings of my thesis, identify remaining questions, and discuss possible directions for future work.

Section 1: Challenges to precision medicine in HNSCC

Head and neck squamous cell carcinoma (HNSCC) remains a disease with poor outcomes (1). To generate new, effective strategies to improve patient survival, much work has been done to develop precision medicine protocols – protocols that use genetic understandings of the cancer to affect the course of treatment. Notably, The Cancer Genome Atlas (TCGA)(2) as well as others (3, 4) have made strides to identify genetic mutations and copy number alterations, offering genetic insight into HNSCC. In chapter one of this thesis, I reviewed genetic signatures in the larynx subsite of HNSCC and identified potential therapeutic options that may be effective

for that cohort. This genetic information, for HNSCC as well as other cancer types, has allowed for significant strides in designing and implementing effective precision medicine approaches. Several groups have enrolled patients with metastatic or recurrent cancer into clinical trials that use sequencing information to identify actionable mutations to inform treatment decisions (5-7). While the rate of success has not been overwhelming, with the highest rate being Gustave Roussy with 10/68 (15%)(5), the metastatic and recurrent setting makes turnaround time of sequencing results and maintaining health for clinical trial eligibility a challenge (5, 6). Still, this is a promising precedent that when biomarkers are found, they can be effectively leveraged even in metastatic and recurrent cancers.

The need for biomarkers is especially apparent given the results of the clinical trial RTOG 1016 which evaluated the possible de-escalation of oropharyngeal carcinoma that are positive for human papillomavirus (HPV). As HPV-positive cancers generally do well under treatment (8), this de-escalation evaluated if radiotherapy plus cetuximab would offer similar outcomes as the standard, but more toxic (9), treatment of radiotherapy plus cisplatin. Unfortunately, patients receiving radiotherapy plus cetuximab had worse overall survival and progression-free survival compared to patients who received radiotherapy plus cisplatin(10). The failure of this de-escalation trial illuminates a need to understand biomarkers of response and be able to match tumors to therapy to prevent failures from future trials. For example, if we had a biomarker of known response to cetuximab, then HPV+ cancers containing this biomarker would more likely respond to cetuximab plus radiotherapy than cisplatin plus radiotherapy. Alternatively, if the tumor had a biomarker for known sensitivity to cisplatin, then the most effective therapy may likely be cisplatin plus radiotherapy. In fact, in another trial that evaluated the effects of radiotherapy alongside either cetuximab or cisplatin, both arms had similar

efficacies (11). Notably, this trial is underpowered with 70 patients compared to the 987 patients enrolled in RTOG 1016, but there is potential for higher efficacy with both cetuximab and cisplatin in early stage HNSCC with the utilization of appropriate biomarkers, hence why I focused on EGFR inhibition and cisplatin therapy in my thesis work. My results from chapter three suggest that evaluating NOTCH1 genetic status, or the activity of the Notch signaling pathway, may be useful as a biomarker for cisplatin sensitivity. As previously discussed, advancement of a combination therapy of cisplatin and Notch inhibition is unlikely due to toxicity, but Notch status may prove an effective marker for response to cisplatin therapy.

In the quest to identify biomarkers and advance precision medicine strategies, the genetic complexity of most of HNSCC tumors has been a challenge. The high number of alterations spanning across multiple pathways in HNSCC (2-4, 12, 13) makes interpretation and prioritization of actionable alterations difficult. Therefore, to develop and advance biomarkers, we need to identify and use models that represent this genetic complexity of HNSCC. While the identification of genetic alterations from the TCGA as well as other cohorts have made great contributions to understanding the genetic landscape of HNSCC, we now need to combine this understanding with phenotypic responses. Thus, in chapter two of my thesis, I characterized the genetic landscape of 14 oral cavity UM-SCC cell lines. These UM-SCC cell lines have been used as models in HNSCC research for decades, and we now have the ability to combine the phenotypic information gathered with the underlining genetic processes in the cell lines. We now know that these UM-SCC cell lines have very similar genetic alterations to each other, such amplification of EGFR and PIK3CA and mutations in *TP53*. Surprisingly, the cell lines had multiple genetic events along the same pathway, and this redundancy means that overall the cell lines do not represent the diversity found in the TCGA data of primary HNSCC patients,

suggesting a need for developing additional models for study. However, although these cell lines are derived largely from primary untreated disease, they tend to represent the genetic composition of tumors from metastatic HNSCC with their high mutational burden, and therefore may be particularly useful in the study of resistance. As discussed in chapter two, other available HNSCC cell line models do not seem to have the diversity or number of mutations that are in the UM-SCC cell lines, such as frequent *NOTCH1* or *TP53* mutations. However, evaluating therapeutic resistance and advancement of biomarkers in this challenging setting of high, recurrent mutational loads within the UM-SCC cell lines is a relevant struggle to translating results for clinical benefit in HNSCC.

Section 2: Utilizing CRISPR screens to identify co-dependent genes and/or pathways

Advances in the CRISPR/Cas9 system, still new enough to be considered recent, have made CRISPR and genetic engineering a more widespread phenomenon. Along with the technological advances for CRISPR/Cas9 came CRISPR screening libraries, powerful alternatives to siRNA or shRNA libraries. 2014 saw the first of the CRISPR screening libraries in both mouse and human cell lines (14-17). These first papers represent both positive and negative selection screens, for example identifying genes that create resistance to thioguanine in a sensitive CML cell line(16) or vemurafenib in a BRAF mutant melanoma cell line(14).

For my thesis, I adapted new CRISPR screening strategies that had only just been developed to identify genes and pathways that were co-dependent with EGFR signaling and cisplatin therapy. I used these initial screens to set the parameters of my own CRISPR screening. Notably, that a vehicle control is run alongside the treatment group for comparison of loss or enrichment of gRNAs. Additionally, the 14-day timeline of my experiments was chosen given

previous setups of 12-14 days in the literature. In Shalem et al, they observed more distinctive shifts in gRNA representation at 14 days than after 7 days of treatment(14).

We chose to use the MAGeCK algorithm(18) as it was one of the first pipelines for CRISPR analysis that was publicly available, and that the MAGeCK algorithm can be used for negative selection screen comparisons of treatment versus control groups. For comparison, some analysis pipelines such as BAGEL(19) require comparison to an earlier passage of the library pre-treatment. Additionally, other publicly available tools such as caRpool (20) are not as well-cited (caRpool's <10 citations compared to >100 for MAGeCK). Additionally, MAGeCK is supposed to be robust and able to make accurate calls even when there are fewer gRNAs per gene in the screen, though as discussed in chapter three we still struggled with prioritizing targets in the genome-wide screens that had less gRNA coverage.

In looking to compare our data with the literature we modeled our screens after, it is important to note that the MAGeCK pipeline was not available for the initial published CRISPR screens. However, Li et al. re-analyzed both Wang et al. and Shalem et al.'s results to show the utility of MAGeCK (18). As such, it allows for comparison of the results of my CRISPR screens to these initial papers. In the original publication, Wang et al. used the Kolmogorov-Smirov test with p-value correction, and noted 2 genes of significance in their negative selection screen (16). Shalem et al. used the RNAi analysis method RIGER, and noted 6 genes of significance (14). Neither study mentioned the total number of genes, only the genes they highlighted for further validation. The MAGeCK algorithm identified >100 more significant genes with a p-value <0.05 for both studies (18). Unfortunately, the complete analysis was not published, only the top 100 genes, and so it is still unknown whether the MAGeCK algorithm identified >1000 genes for the

GeCKO library of ~3 gRNAs/gene as similar to my data, or ~100 significant genes for the library of 10gRNAs/gene like the kinome.

While analysis pipelines attempt to be robust and make accurate calls when there are few gRNAs per gene, it provides much more confidence in the results when multiple gRNAs exhibit the desired phenotype. We found the results of the kinome library easier to prioritize given the expected recurrence of genes across our EGFR inhibitors and cell lines, and we expect this is due to the relatively large number of gRNAs per gene. Although, the Cancer Dependency Map, which screened a large CRISPR library with an average of 4 gRNAs per gene across 342 cancer cell lines, has the depth of data for robust analysis (21). However, this scale of experiment was infeasible for my thesis, and so we found more utility out of the kinome library with 10 gRNAs per gene than the genome-wide library with 3 gRNAs, at least when considering each library on its own. Combined, we've generated a wealth of data that we have explored to answer our primary scientific question, which can be mined by many future researchers.

An additional, interesting direction would have been setting up a positive selection screen and identifying genetic knockouts that created resistance to EGFR inhibition. This approach would have offered the benefits of generating the mechanistic models of interest for subsequent validation. After treatment with EGFR inhibition, a portion of cells could have been preserved for cloning out and further mechanistic work. For the negative selection model, the knockouts of most interest are a small population among the majority or are missing entirely because the knockouts underwent cell death in response to EGFR inhibition. For my validation, it required remaking the individual genetic knockouts for further experimentation and mechanistic work. However, none of the UM-SCC models that we have evaluated so far have an acute sensitivity to

gefitinib or erlotinib and therefore were not the appropriate models to address this question of using a positive selection approach.

Section 3: Identifying & Validating Resistance Mechanisms

In using CRISPR screens to identify genes that, when lost, generate sensitivity to HNSCC therapies, we assume that one gene plays a major role in resistance. In some cases, this appears to be true. In our CRISPR screen to identify genetic knockouts that create sensitivity to cisplatin, we identified several genes in the Notch pathway as significantly depleted. We then went on to validate that *NOTCH1* loss specifically created sensitivity to cisplatin, and despite changes in expression of Notch2, the other Notch receptors were unable to compensate for the lack of Notch1. We also identified *FGFR3* alone as a sensitizer to EGFR inhibition. Like the Notch receptors, FGFR3 is a part of a family of receptors that are generally understood to activate similar downstream pathways. The genetic knockout of FGFR3 alone was enough to cause sensitivity to EGFR inhibition. However, in the case of FGFR3 knockouts, cell death was significantly higher when a pan-FGFR inhibitor was in combination with EGFR inhibition, and not simply EGFR inhibition and FGFR3 loss. While we did not observe any upregulation of the other FGFRs in response to the FGFR3 knockout, there does seem to be compensation from the other FGFRs when EGFR is inhibited.

As CRISPR screens designed to knockout a single gene have generated targets and validated hits, both ours and others, the data suggest that one gene can play a major role in resistance. Notably, the results of genetic knockouts that were clonally derived, such as in this work, may be caveated as representing only a subset of the heterogeneity in the cell line. However, the combinations identified in the CRISPR screen and validated in the individual

genetic knockouts also significantly affected the heterogenous wildtype model. Creating genetic knockouts in cell line models with heterogeneity may be a concern, but our work suggests that impactful results can still be generated. However, we can't ignore that additional compensation can and still happens. While we did not see compensation for the loss of *NOTCH1* when treated with cisplatin, we did see compensation from other FGFRs during EGFR inhibition when *FGFR3* was knocked out. Then, when we generated the *EGFR* knockout model and treated the cell line with FGFR inhibitors, we did not get complete cell death and kill every cell. Eventually, cells can compensate under inhibition and genetic loss, and resistance occurs. Perhaps then it is better to target pathways, and more broadly shut down cellular signals to prevent the chance for compensation. Our CRISPR screens identify individual genes, but we are able to collate that information into understanding pathways that play a role in resistance – such as KRAS signaling. Targeting pathways in attempts to circumvent compensation early may help improve efficacy of inhibitors and improve patient survival. Broader-based therapies targeting pathways rather than specific genes may be especially needed for patients with metastatic or recurrent cancer, which for HNSCC is a common presentation (22). The additional mutational burden in HNSCC cancers lend to giving tumors multiple options and opportunities for compensation. While our work in UM-SCC models - that we characterized with a large mutational load and still containing heterogeneity - supports that targeted therapy combinations can be effective, it is most likely that resistance and compensation will continue to be a challenge.

Some work on the dual inhibition of EGFR and FGFR has already been accomplished, mostly in lung cancer but also HNSCC (23-27). This inhibition was founded based on the noted frequent amplification of *FGFR1* in both cancer types. Amplification and overexpression of *FGFR1* has been thought to mark cases addicted to FGFR oncogenic signaling, and therefore

sensitive to FGFR inhibition (24, 27, 28). Multiple FGFR-targeted therapies are approved for treatment (23, 29), and it had been noted that EGFR signaling is a possible resistance mechanism to FGFR monotherapy (30). While none of the UM-SCC models that were tested for my thesis were sensitive to FGFR inhibition as a monotherapy, our results suggest that FGFR may be a more common compensatory mechanism than previously realized. Cell lines that responded to dual inhibition had a mix of amplifications and deletions of each FGFR receptor, as well as cell lines that remained resistant. Even expression profiles of the receptors did not predict sensitivity to combined EGFR and FGFR inhibition, though we did not evaluate different isoforms of the FGFRs that may be expressed. Our data suggest that *FGFR1* amplification is not the biomarker of FGFR compensation, and that this dual inhibition may be effective in a broader selection of patients.

However, the most limiting factor in translating this combination to the clinic is the toxicity of combining EGFR and FGFR inhibitors. A trial of the EGFR inhibitor erlotinib and pan-FGFR inhibitor dovitinib in metastatic non-small cell lung cancer was halted early given dose limiting toxicities (31), and no other combination of EGFR and FGFR inhibitors has been attempted in a trial since. However, no biomarker was used to restrict patient eligibility, and the status of the FGF receptors were unknown. One patient of the nine enrolled in the study had a partial response, indicating that the combination of EGFR and FGFR could be effective without the unexpected toxicity for this combination. Unfortunately, further investigation into the combination of EGFR and FGFR inhibitors may be halted for the time being. While multiple FGFR inhibitors are approved for use and cetuximab would have a different toxicity profile than erlotinib, it is unlikely for such a study to be attempted without additional work investigating potential toxicity issues.

Of potential future interest is anlotinib, a new inhibitor that targeted FGFR, vascular endothelial growth factor receptor (VEGFR), platelet-derived growth factor receptor (PDGFR), and c-kit (32). Given the signaling similarities of FGFR, VEGF, and PDGF (33), it is possible that VEGF and PDGF may be secondary or tertiary compensatory mechanisms to EGFR and FGFR dual inhibition. As discussed above, a broad-based tyrosine kinase inhibitor targeting multiple pathways may be especially beneficial in metastatic settings, though again toxicity will be a major concern. Several trials are recruiting or will be recruiting for the combination treatment of an EGFR inhibitor including gefitinib, erlotinib, or icotininb, along with anlotinib (NCT03736837, NCT03720873, NCT03766490, NCT03461185), and it will be interesting to see the results. These trials are for non-small cell lung cancer, and the biomarkers for eligibility include EGFR del19 or L858R, EGFR mutations known to be sensitive to EGFR inhibitors, and an absence of EGFR T790M, a known mutation that prevents first generation EGFR inhibitors from binding to EGFR.

It would be interesting to test our UM-SCC models with the combination of EGFR inhibition and anlotinib, and determine if lines respond. I would expect cell lines that respond to EGFR and FGFR inhibition to also respond to EGFR inhibition and anlotinib, perhaps with even greater sensitivity. If so, this could speak to a common downstream node from these receptors that would illuminate the mechanism behind this pathway compensation. Additionally, perhaps cell lines that do not respond to dual EGFR and FGFR inhibition may respond to EGFR, FGFR, VEGF, and PDGF inhibition, suggesting that VEGF and PDGF are compensating during EGFR and FGFR inhibition.

One possible mechanism for FGFR compensation during EGFR inhibition that was noted in lung cancer is reactivation of the Ras-MAPK pathway (34). This may be true in HNSCC

samples as well, with another group noticing loss of AKT and ERK inhibition under dual inhibition (25). Our investigation of the MAPK pathway, including AKT and ERK phosphorylation, showed decreases in activation of these downstream effectors, but the combination treatment did not have observable differences from EGFR inhibition alone. Additionally, UM-SCC cell lines that do not undergo cell death under dual inhibition of EGFR and FGFR also had decreased phosphorylation and activation of these downstream effectors in the combination treatment. If it is reactivation of the Ras-MAPK pathway that is a key player in the compensatory response, then perhaps additional timepoints to observe the reactivation in the non-responsive models will need to be investigated. Additionally, perhaps a more wide-spread approach, such as a phospho-proteomics screen, would help illuminate critical downstream effectors of this response.

An interesting mechanism of FGFR compensation to EGFR inhibition that was observed in lung adenocarcinoma is the physical interaction of EGFR and FGFR1 (26), suggesting that FGF ligands can then stimulate EGFR and EGF ligands can stimulate FGFR1. However, this mechanism does not seem applicable to my work in HNSCC. The EGFR K/O model, with the complete loss of EGFR, still upregulated FGFR1 expression and was sensitive to FGFR inhibition. If a physical interaction and co-activation of EGFR and FGFR1 was essential to compensation, then inhibition of FGFR should not have affected cell survival.

For colon and lung cancer, a frequent resistance mechanism to cetuximab treatment is the acquiring of somatic mutations (35), but these are infrequently seen in HNSCC (2, 12, 13). Instead, focus for HNSCC has been observing changes in expression, such as the frequent overexpression of MET, FGFR1, or AXL either intrinsic or in response to EGFR inhibition. As such, it makes comparisons difficult across cancer types as focus is on exome sequencing and

uncovering mutations. However, there are known Ras signaling expression signatures from work done in colon and breast cancer (36), and it would be interesting to compare the expression profile to the pre- and post- cetuximab treated transcriptomes in HNSCC. For samples that had a significant enrichment of up- or down-regulated Ras genes post-treatment, then it would suggest that other cancer treatments to circumvent Ras activation or suppress Ras signaling may also be effective in HNSCC. Additionally, the Ras expression profile could serve as a biomarker for adapting treatment for known Ras-mediated resistance.

Section 4. Future Directions

Future work that I think would be exciting to explore is an in-depth look at heterogeneity within a tumor or cell line and how this might factor into response. More specifically, an experimental approach that could address if differential compensation mechanisms arise from the same tumor due to heterogeneity. Given the mutational load in metastatic and recurrent HNSCC, as well as the multiple potential resistance mechanisms, it's possible that a tumor may contain 60% of cells that rely on FGFR signaling for compensation and 40% on MET signaling, for example. Single cell sequencing of a heterogenous population after EGFR inhibition would be one method to address this question. If a heterogenous population responds similarly to EGFR inhibition, then it would shift focus onto identifying and targeting the primary compensation pathway, with more focus on sequential resistance mechanisms. If there are differential populations after EGFR inhibition, then it's possible that multiple compensatory pathways will need to be targeted in combination such as EGFR, FGFR, and MET signaling as in the example discussed above. If only two of the three pathways are targeted, then the sub-population will remain resistant and most likely continue to proliferate.

I anticipate that work will continue on identifying and validating combination therapies for potential advancement into HNSCC. The data of my thesis supports the hypothesis that targeted therapies in combination can be more effective than monotherapies. Strides in clinical benefits are yet to be seen, however, and it will continue to be difficult to prove efficacy in metastatic and recurrent settings where combination therapies are usually tested. Biomarkers will be of particular importance to restrict enrollment and include patients that have a chance at responding to treatment.

Bibliography

1. Pulte D, Brenner H. Changes in survival in head and neck cancers in the late 20th and early 21st century: a period analysis. The oncologist. 2010;15(9):994-1001. Epub 2010/08/26. doi: 10.1634/theoncologist.2009-0289. PubMed PMID: 20798198.
2. Cancer Genome Atlas N. Comprehensive genomic characterization of head and neck squamous cell carcinomas. Nature. 2015;517(7536):576-82. doi: 10.1038/nature14129. PubMed PMID: 25631445; PMCID: 4311405.
3. Agrawal N, Frederick MJ, Pickering CR, Bettegowda C, Chang K, Li RJ, Fakhry C, Xie TX, Zhang J, Wang J, Zhang N, El-Naggar AK, Jasser SA, Weinstein JN, Trevino L, Drummond JA, Muzny DM, Wu Y, Wood LD, Hruban RH, Westra WH, Koch WM, Califano JA, Gibbs RA, Sidransky D, Vogelstein B, Velculescu VE, Papadopoulos N, Wheeler DA, Kinzler KW, Myers JN. Exome sequencing of head and neck squamous cell carcinoma reveals inactivating mutations in NOTCH1. Science. 2011;333(6046):1154-7. Epub 2011/07/30. doi: 10.1126/science.1206923. PubMed PMID: 21798897; PMCID: 3162986.
4. Stransky N, Egloff AM, Tward AD, Kostic AD, Cibulskis K, Sivachenko A, Kryukov GV, Lawrence MS, Sougnez C, McKenna A, Shefler E, Ramos AH, Stojanov P, Carter SL, Voet D, Cortes ML, Auclair D, Berger MF, Saksena G, Guiducci C, Onofrio RC, Parkin M, Romkes M, Weissfeld JL, Seethala RR, Wang L, Rangel-Escareno C, Fernandez-Lopez JC, Hidalgo-Miranda A, Melendez-Zajgla J, Winckler W, Ardlie K, Gabriel SB, Meyerson M, Lander ES, Getz G, Golub TR, Garraway LA, Grandis JR. The mutational landscape of head and neck squamous cell carcinoma. Science. 2011;333(6046):1157-60. Epub 2011/07/30. doi: 10.1126/science.1208130. PubMed PMID: 21798893; PMCID: 3415217.
5. Ingrid Breuskin CE, Ecaterina Ileana, Christophe Massard, Naima Lezghed, Ludovic Lacroix, Antoine Hollebecque, Rastislav Bahleda, Maud Ngo-Camus, Yohann Loriot, Nathalie Auger, Valerie Koubi-Pick, Thierry De Baere, Philippe Vielh, Vladimir Lazar, Marie-Cécile Le Deley, Catherine Richon, Joël Guigay, François Janot, Jean-Charles Soria, Charles Ferté, editor. MOLECULAR SCREENING FOR CANCER TREATMENT OPTIMIZATION IN HEAD AND NECK CANCER (MOSCATO 01): A PROSPECTIVE MOLECULAR TRIAGE TRIAL; INTERIM ANALYSIS OF 78 PATIENTS WITH RECURRENT OR METASTATIC HEAD AND NECK CANCERS American Head and Neck Society Translational Meeting; 2015 April 21-22, 2015; Boston, MA.
6. Beltran H, Eng K, Mosquera JM, Sigaras A, Romanel A, Rennert H, Kossai M, Pauli C, Faltas B, Fontugne J, Park K, Banfelder J, Prandi D, Madhukar N, Zhang T, Padilla J, Greco N, McNary TJ, Herrscher E, Wilkes D, MacDonald TY, Xue H, Vacic V, Emde AK, Oschwald D, Tan AY, Chen Z, Collins C, Gleave ME, Wang Y, Chakravarty D, Schiffman M, Kim R, Campagne F, Robinson BD, Nanus DM, Tagawa ST, Xiang JZ, Smogorzewska A, Demichelis F, Rickman DS, Sboner A, Elemento O, Rubin MA. Whole-Exome Sequencing of Metastatic Cancer and Biomarkers of Treatment Response. JAMA Oncol. 2015;1(4):466-74. Epub 2015/07/17. doi: 10.1001/jamaoncol.2015.1313. PubMed PMID: 26181256; PMCID: 4505739.
7. Roychowdhury S, Iyer MK, Robinson DR, Lonigro RJ, Wu YM, Cao X, Kalyana-Sundaram S, Sam L, Balbin OA, Quist MJ, Barrette T, Everett J, Siddiqui J, Kunju LP, Navone N, Araujo JC, Troncoso P, Logothetis CJ, Innis JW, Smith DC, Lao CD, Kim SY, Roberts JS, Gruber SB, Pienta KJ, Talpaz M, Chinnaiyan AM. Personalized oncology through integrative high-throughput sequencing: a pilot study. Sci Transl Med. 2011;3(111):111ra21. Epub 2011/12/03. doi: 10.1126/scitranslmed.3003161. PubMed PMID: 22133722; PMCID: 3476478.

8. Mehanna H. Update on De-intensification and Intensification Studies in HPV. In: Golusiński W, Leemans CR, Dietz A, editors. HPV Infection in Head and Neck Cancer. Cham: Springer International Publishing; 2017. p. 251-6.
9. Denis F, Garaud P, Bardet E, Alfonsi M, Sire C, Germain T, Bergerot P, Rhein B, Tortochaux J, Calais G. Final results of the 94-01 French Head and Neck Oncology and Radiotherapy Group randomized trial comparing radiotherapy alone with concomitant radiochemotherapy in advanced-stage oropharynx carcinoma. J Clin Oncol. 2004;22(1):69-76. Epub 2003/12/06. doi: 10.1200/jco.2004.08.021. PubMed PMID: 14657228.
10. Gillison ML, Trotti AM, Harris J, Eisbruch A, Harari PM, Adelstein DJ, Sturgis EM, Burtness B, Ridge JA, Ringash J, Galvin J, Yao M, Koyfman SA, Blakaj DM, Razaq MA, Colevas AD, Beitler JJ, Jones CU, Dunlap NE, Seaward SA, Spencer S, Galloway TJ, Phan J, Dignam JJ, Le QT. Radiotherapy plus cetuximab or cisplatin in human papillomavirus-positive oropharyngeal cancer (NRG Oncology RTOG 1016): a randomised, multicentre, non-inferiority trial. Lancet (London, England). 2019;393(10166):40-50. Epub 2018/11/20. doi: 10.1016/s0140-6736(18)32779-x. PubMed PMID: 30449625.
11. Magrini SM, Buglione M, Corvo R, Pirtoli L, Paiar F, Ponticelli P, Petrucci A, Bacigalupo A, Crociani M, Lastrucci L, Vecchio S, Bonomo P, Pasinetti N, Triggiani L, Cavagnini R, Costa L, Tonoli S, Maddalo M, Grisanti S. Cetuximab and Radiotherapy Versus Cisplatin and Radiotherapy for Locally Advanced Head and Neck Cancer: A Randomized Phase II Trial. J Clin Oncol. 2016;34(5):427-35. Epub 2015/12/09. doi: 10.1200/jco.2015.63.1671. PubMed PMID: 26644536.
12. Ludwig ML, Kulkarni A, Birkeland AC, Michmerhuizen NL, Foltin SK, Mann JE, Hoesli RC, Devenport SN, Jewell BM, Shuman AG, Spector ME, Carey TE, Jiang H, Brenner JC. The genomic landscape of UM-SCC oral cavity squamous cell carcinoma cell lines. Oral Oncol. 2018;87:144-51. Epub 2018/12/12. doi: 10.1016/j.oraloncology.2018.10.031. PubMed PMID: 30527230; PMCID: PMC6349383.
13. Pickering CR, Zhang J, Yoo SY, Bengtsson L, Moorthy S, Neskey DM, Zhao M, Ortega Alves MV, Chang K, Drummond J, Cortez E, Xie TX, Zhang D, Chung W, Issa JP, Zweidler-McKay PA, Wu X, El-Naggar AK, Weinstein JN, Wang J, Muzny DM, Gibbs RA, Wheeler DA, Myers JN, Frederick MJ. Integrative genomic characterization of oral squamous cell carcinoma identifies frequent somatic drivers. Cancer Discov. 2013;3(7):770-81. Epub 2013/04/27. doi: 10.1158/2159-8290.cd-12-0537. PubMed PMID: 23619168; PMCID: 3858325.
14. Shalem O, Sanjana NE, Hartenian E, Shi X, Scott DA, Mikkelsen TS, Heckl D, Ebert BL, Root DE, Doench JG, Zhang F. Genome-scale CRISPR-Cas9 knockout screening in human cells. Science. 2014;343(6166):84-7. Epub 2013/12/18. doi: 10.1126/science.1247005. PubMed PMID: 24336571; PMCID: 4089965.
15. Shalem O, Sanjana NE, Zhang F. High-throughput functional genomics using CRISPR-Cas9. Nat Rev Genet. 2015;16(5):299-311. Epub 2015/04/10. doi: 10.1038/nrg3899. PubMed PMID: 25854182; PMCID: Pmc4503232.
16. Wang T, Wei JJ, Sabatini DM, Lander ES. Genetic screens in human cells using the CRISPR-Cas9 system. Science. 2014;343(6166):80-4. Epub 2013/12/18. doi: 10.1126/science.1246981. PubMed PMID: 24336569; PMCID: 3972032.
17. Zhou Y, Zhu S, Cai C, Yuan P, Li C, Huang Y, Wei W. High-throughput screening of a CRISPR/Cas9 library for functional genomics in human cells. Nature. 2014;509(7501):487-91. Epub 2014/04/11. doi: 10.1038/nature13166. PubMed PMID: 24717434.

18. Li W, Xu H, Xiao T, Cong L, Love MI, Zhang F, Irizarry RA, Liu JS, Brown M, Liu XS. MAGeCK enables robust identification of essential genes from genome-scale CRISPR/Cas9 knockout screens. Genome biology. 2014;15(12):554. Epub 2014/12/06. doi: 10.1186/s13059-014-0554-4. PubMed PMID: 25476604; PMCID: 4290824.
19. Hart T, Moffat J. BAGEL: a computational framework for identifying essential genes from pooled library screens. BMC Bioinformatics. 2016;17(1):164. doi: 10.1186/s12859-016-1015-8.
20. Winter J, Breinig M, Heigwer F, Brugemann D, Leible S, Pelz O, Zhan T, Boutros M. caRpools: an R package for exploratory data analysis and documentation of pooled CRISPR/Cas9 screens. Bioinformatics. 2016;32(4):632-4. Epub 2015/10/29. doi: 10.1093/bioinformatics/btv617. PubMed PMID: 26508755.
21. Meyers RM, Bryan JG, McFarland JM, Weir BA, Sizemore AE, Xu H, Dharia NV, Montgomery PG, Cowley GS, Pantel S, Goodale A, Lee Y, Ali LD, Jiang G, Lubonja R, Harrington WF, Strickland M, Wu T, Hawes DC, Zhivich VA, Wyatt MR, Kalani Z, Chang JJ, Okamoto M, Stegmaier K, Golub TR, Boehm JS, Vazquez F, Root DE, Hahn WC, Tsherniak A. Computational correction of copy number effect improves specificity of CRISPR-Cas9 essentiality screens in cancer cells. Nat Genet. 2017;49(12):1779-84. Epub 2017/10/31. doi: 10.1038/ng.3984. PubMed PMID: 29083409; PMCID: PMC5709193.
22. Argiris A, Harrington KJ, Tahara M, Schulten J, Chomette P, Ferreira Castro A, Licitra L. Evidence-Based Treatment Options in Recurrent and/or Metastatic Squamous Cell Carcinoma of the Head and Neck. Frontiers in oncology. 2017;7:72-. doi: 10.3389/fonc.2017.00072. PubMed PMID: 28536670.
23. Dieci MV, Arnedos M, Andre F, Soria JC. Fibroblast growth factor receptor inhibitors as a cancer treatment: from a biologic rationale to medical perspectives. Cancer Discov. 2013;3(3):264-79. Epub 2013/02/19. doi: 10.1158/2159-8290.Cd-12-0362. PubMed PMID: 23418312.
24. Goke F, Franzen A, Hinz TK, Marek LA, Yoon P, Sharma R, Bode M, von Maessenhausen A, Lankat-Buttgereit B, Goke A, Golletz C, Kirsten R, Boehm D, Vogel W, Kleczko EK, Eagles JR, Hirsch FR, Van Bremen T, Bootz F, Schroeck A, Kim J, Tan AC, Jimeno A, Heasley LE, Perner S. FGFR1 Expression Levels Predict BGJ398 Sensitivity of FGFR1-Dependent Head and Neck Squamous Cell Cancers. Clinical cancer research : an official journal of the American Association for Cancer Research. 2015;21(19):4356-64. doi: 10.1158/1078-0432.CCR-14-3357. PubMed PMID: 26015511; PMCID: 4592392.
25. Koole K, Brunen D, van Kempen PM, Noorlag R, de Bree R, Lieftink C, van Es RJ, Bernards R, Willems SM. FGFR1 Is a Potential Prognostic Biomarker and Therapeutic Target in Head and Neck Squamous Cell Carcinoma. Clinical cancer research : an official journal of the American Association for Cancer Research. 2016;22(15):3884-93. doi: 10.1158/1078-0432.CCR-15-1874. PubMed PMID: 26936917.
26. Quintanal-Villalonga A, Molina-Pinelo S, Cirauqui C, Ojeda-Márquez L, Marrugal Á, Suarez R, Conde E, Ponce-Aix S, Enguita AB, Carnero A, Ferrer I, Paz-Ares L. FGFR1 Cooperates with EGFR in Lung Cancer Oncogenesis, and Their Combined Inhibition Shows Improved Efficacy. Journal of Thoracic Oncology. 2019;14(4):641-55. doi: https://doi.org/10.1016/j.jtho.2018.12.021.
27. von Massenhausen A, Franzen A, Heasley L, Perner S. FGFR1 as a novel prognostic and predictive biomarker in squamous cell cancers of the lung and the head and neck area. Annals of

translational medicine. 2013;1(3):23. doi: 10.3978/j.issn.2305-5839.2013.06.08. PubMed PMID: 25332967; PMCID: 4200677.
28. Ileana Dumbrava E, Alfattal R, Miller VA, Tsimberidou AM. Complete Response to a Fibroblast Growth Factor Receptor Inhibitor in a Patient With Head and Neck Squamous Cell Carcinoma Harboring FGF Amplifications. JCO Precision Oncology. 2018(2):1-7. doi: 10.1200/PO.18.00100.
29. Katoh M, Nakagama H. FGF receptors: cancer biology and therapeutics. Medicinal research reviews. 2014;34(2):280-300. Epub 2013/05/23. doi: 10.1002/med.21288. PubMed PMID: 23696246.
30. Herrera-Abreu MT, Pearson A, Campbell J, Shnyder SD, Knowles MA, Ashworth A, Turner NC. Parallel RNA interference screens identify EGFR activation as an escape mechanism in FGFR3-mutant cancer. Cancer Discov. 2013;3(9):1058-71. doi: 10.1158/2159-8290.CD-12-0569. PubMed PMID: 23744832; PMCID: 3770512.
31. Das M, Padda SK, Frymoyer A, Zhou L, Riess JW, Neal JW, Wakelee HA. Dovitinib and erlotinib in patients with metastatic non-small cell lung cancer: A drug-drug interaction. Lung cancer (Amsterdam, Netherlands). 2015;89(3):280-6. Epub 2015/07/08. doi: 10.1016/j.lungcan.2015.06.011. PubMed PMID: 26149476; PMCID: PMC4613811.
32. Shen G, Zheng F, Ren D, Du F, Dong Q, Wang Z, Zhao F, Ahmad R, Zhao J. Anlotinib: a novel multi-targeting tyrosine kinase inhibitor in clinical development. Journal of Hematology & Oncology. 2018;11(1):120. doi: 10.1186/s13045-018-0664-7.
33. Lieu C, Heymach J, Overman M, Tran H, Kopetz S. Beyond VEGF: inhibition of the fibroblast growth factor pathway and antiangiogenesis. Clinical cancer research : an official journal of the American Association for Cancer Research. 2011;17(19):6130-9. Epub 2011/09/29. doi: 10.1158/1078-0432.Ccr-11-0659. PubMed PMID: 21953501; PMCID: PMC5562355.
34. Bockorny B, Rusan M, Chen W, Liao RG, Li Y, Piccioni F, Wang J, Tan L, Thorner AR, Li T, Zhang Y, Miao C-H, Ovesen T, Shapiro GI, Kwiatkowski DJ, Gray NS, Meyerson M, Hammerman PS, Bass AJ. RAS-MAPK reactivation facilitates acquired resistance in FGFR1-amplified lung cancer and underlies a rationale for upfront FGFR-MEK blockade. Molecular Cancer Therapeutics. 2018:molcanther.0464.2017. doi: 10.1158/1535-7163.MCT-17-0464.
35. Bertotti A, Papp E, Jones S, Adleff V, Anagnostou V, Lupo B, Sausen M, Phallen J, Hruban CA, Tokheim C, Niknafs N, Nesselbush M, Lytle K, Sassi F, Cottino F, Migliardi G, Zanella ER, Ribero D, Russolillo N, Mellano A, Muratore A, Paraluppi G, Salizzoni M, Marsoni S, Kragh M, Lantto J, Cassingena A, Li QK, Karchin R, Scharpf R, Sartore-Bianchi A, Siena S, Diaz Jr LA, Trusolino L, Velculescu VE. The genomic landscape of response to EGFR blockade in colorectal cancer. Nature. 2015;526:263. doi: 10.1038/nature14969 https://www.nature.com/articles/nature14969#supplementary-information.
36. Loboda A, Nebozhyn M, Klinghoffer R, Frazier J, Chastain M, Arthur W, Roberts B, Zhang T, Chenard M, Haines B, Andersen J, Nagashima K, Paweletz C, Lynch B, Feldman I, Dai H, Huang P, Watters J. A gene expression signature of RAS pathway dependence predicts response to PI3K and RAS pathway inhibitors and expands the population of RAS pathway activated tumors. BMC medical genomics. 2010;3:26-. doi: 10.1186/1755-8794-3-26. PubMed PMID: 20591134.